APPLICATIONS OF CHIRAL ALUMINUM AND BORON CATALYSTS IN ASYMMETRIC SYNTHESIS

By

Li Zheng

A DISSERTATION

Submitted to
Michigan State University
in partial fulfillment of the requirements
for the degree of

Chemistry – Doctor of Philosophy

2020

ABSTRACT

APPLICATIONS OF CHIRAL ALUMINUM AND BORON CATALYSTS IN ASYMMETRIC SYNTHESIS

By

Li Zheng

A potent chiral aluminum catalyst has been developed for asymmetric MPV reduction of ketones with broad substrate scope and excellent yields and enantiomeric inductions. The catalyst consists an aluminum core, a VANOL-derived chiral ligand and an isopropoxy group. Different ligands have been screened and reaction parameters have been optimized. A variety of aromatic (both electron-poor and electron-rich) and aliphatic ketones were converted to chiral alcohols in good yields with high enantioselectivities (26 examples, 70-98% yield and 82-99% *ee*). This method operates under mild conditions (–10 ºC) and low catalyst loading (1–10 mol%). Furthermore, this process is catalyzed by the earth-abundant main group element aluminum and employs inexpensive and environmentally benign 2-propanol as hydride source. This catalyst has also been employed in resolution of racemic alcohols. The kinetic resolution of alcohols by Oppenauer oxidation has been achieved with moderate results. The formal dynamic kinetic resolution via Oppenauer oxidation/ MPV reduction sequence has also been examined and discussed, which avoided acylation and the use of enzymes.

A highly efficient asymmetric heteroatom Diels-Alder reaction between diene and aldehydes for the construction of 6-membered heterocycles catalyzed by chiral boron catalysts has been developed. A BINOL-derived propeller borate

is found to be effective catalyzing the reaction of aromatic aldehydes. A VANOL-derived *meso*-borate is found to be able to catalyze the reaction of both aromatic and aliphatic aldehydes with high asymmetric inductions. Excellent yields and enantioselectivities have been achieved after optimization. Furthermore, the skeleton of 6-carbon saccharides is synthesized in the reaction of 2-hydoxyacetaldehyde with different protecting groups, which can be derivatized into many saccharide analogs. The mechanism of this reaction is proposed to be concerted based on experiments involving different methods for the reaction quench. A reversal of direction of the asymmetric induction by switching boron to aluminum has been observed. Computational studies show that catalysts derived from boron and aluminum have different geometries at the Lewis acid center.

This thesis is dedicated to my parents, my wife, and my cats.

ACKNOWLEDGMENTS

First and foremost, I would like to thank my advisor Dr. Wulff. I am so grateful to have him as my mentor and words are never enough to tell how much I have learnt from him. Besides his extensive knowledge, his passion in chemistry inspired me the most. Once I asked him that why he did not take a vacation during Christmas, and he said that “I love and enjoy working on chemistry, so I do not need a vacation”. He is a great scientist and a patient teacher who devotes his whole life into chemistry. I thank him so much for explaining me different reaction mechanisms; for listening to me carefully when we have different opinions; for giving me advices whenever I meet problems; for letting me work on projects that I am interested in; for his wine, cheese and fun stories during the post-group meetings; and for his warm support and encouragement in lab and in life. I am so proud to be part of the Wulff group.

I would also like to thank Professor Borhan for being my second reader of my thesis. He is a good teacher and a very nice friend, but I was “scared” of him in the first one to two years of my PhD. I felt like he was so smart that just by looking into my eyes he could tell that “this kid does not know anything”. The pressure from him made me highly motivated and I thought that if I were not hard-working enough, horrible things would happen during my first committee meeting/ seminar/ second-year oral exam/ defense. He was the “demon” that made me a qualified PhD.

I would like to thank my committee member Professor Tepe and Professor Beck for their guidance in my research. Professor Tepe taught me to pay attention

to the replicability of reactions and Professor Beck encouraged me to learn computational chemistry. Their suggestions helped me a lot towards the completion of my PhD projects. I would also like to thank Professor Huang, Professor Maleczka, Professor Jackson and Professor Smith for their fantastic lectures. The knowledge they delivered and the problem-solving skills that I learnt from them are truly valuable. I would like to thank Dr. Azadnia for being my advisor in teaching for 5 years. I really enjoy being a teaching assistant for CEM 143, 252, 255, 355 and 356 under his supervision. And I will always remember the help from Dr. Holmes and Dr. Xie for their patient NMR training, as well as the help from Dr. Staples for solving the crystal structures of my samples. I also thank Professor Jones, Professor Sun and Dr. Chen for their assistance on Mass Spectrometry.

I am so proud to be the last PhD in the Wulff group and I will never forget those days I spent with all the senior lab members. I need to thank Dr. Xin Zhang first for his email before I came to US. In the email he described Dr. Wulff to be the world's nicest professor and encouraged me to join the Wulff group. I am so glad that I end up being one of Dr. Wulff's students and every day in the past five years proves that Xin did not lie to me. I thank Dr. Yubai Zhou, a crazy cat lover, for being a great friend. I miss the many poker games with you even though our "Boy Team" never won. I also thank Dr. Yijing Dai, a much better poker player, for beating me and Yubai every single time. I want to thank Dr. Xiaopeng Yin, my lab mentor, for teaching me how to conduct research and helping me patiently whenever I met a problem. He helped me a lot through my second-year seminar and oral exam. Without his mentorship and friendship, my PhD would be a lot harder. I would like

to thank Dr. Aliakbar Mohammadlou, a brilliant and hard-working chemist, for his company and support during the five years. He taught me a lot of chemistry as well as experimental technics and was always there to help. I thank several undergraduates in our group, Emily, Brendyn, Brian and Ryan for their help in the lab. I would also like to thank Dr. Yu Zhang, Dr. Hong Ren, Dr. Yong Guan and Dr. Wenjun Zhao, former members from the Wulff group, for their help and support in my research and life.

I would like to thank Hadi, Yi, Wei, Ding, Jun, Aritra, Debarshi, Saeedeh, Rahele and many other people from the Borhan group for their help and scientific advices during my PhD. I thank Dr. Tayeb Kakeshpour very much for teaching me how to run DFT calculations and explaining computational concepts to me. I also thank people in the “Chemistry Basketball Group”, Jun, Dan, Chenjia, Nate, Daoyang, Eli, Jia, Kunli, Zhen, Yuhan, Qianyi and Guangyao for those wonderful games we played together. I would like to thank Yiqing, Ke, Badru-Deen, Shuang, Zibin, Zhilin, Qianjie, Tian and other friends for all the wonderful moments we shared together.

Finally, I would like to give special thanks to my wife Xiaojing. It is so beautiful that we fell in love in college and got married in graduate school. Thank you so much for your endless support and encouragement over the years, and that is the most precious gift for me throughout my PhD journey.

TABLE OF CONTENTS

LIST OF TABLES xi

LIST OF FIGURES xii

LIST OF SCHEMES xiii

CHAPTER ONE ASYMMETRIC CATALYTIC MEERWEIN-PONNDORF-VERLEY REDUCTIONS IN THE LITERATURE 1
- 1.1 Introduction 1
- 1.2 Catalytic MPV reductions 2
- 1.3 Asymmetric catalytic MPV reductions 8
- 1.4 Aluminum-catalyzed asymmetric MPV reductions 12
- 1.5 Summary 15

REFERENCES 17

CHAPTER TWO ASYMMETRIC CATALYTIC MEERWEIN-PONNDORF-VERLEY REDUCTION OF KETONES WITH ALUMINUM(III)-VANOL CATALYSTS 24
- 2.1 Introduction 24
- 2.2 Initial study: Is switching BINOL to VANOL a way out? 25
- 2.3 Reaction optimizations 27
  - 2.3.1 Ligand screening 27
  - 2.3.2 Preliminary optimization of reaction parameters 31
  - 2.3.3 Further optimizations on the reduction of 2-bromoacetophenone 33
  - 2.3.4 Optimizations on the reduction of 4'-bromoacetophenone 40
- 2.4 Substrate scope for aromatic ketones 42
- 2.5 Substrate scope for aliphatic ketones 48
- 2.6 Scale up synthesis with 1 mol% catalyst loading 51
- 2.7 Reaction mechanism and computational study 52
  - 2.7.1 Mechanism of MPV reduction of ketones 52
  - 2.7.2 Computational study 53
- 2.8 Formal dynamic kinetic resolution of racemic alcohols via Oppenauer oxidation/MPV reduction 60
  - 2.8.1 Introduction 60
  - 2.8.2 Oxidative kinetic resolution of racemic alcohols with aluminum-VANOL catalysts 64
  - 2.8.3 Tentative formal dynamic kinetic resolution of racemic alcohols with aluminum-VANOL catalysts 66
- 2.9 Conclusion 69

REFERENCES 71

CHAPTER THREE ENANTIOSELECTIVE HETEROATOM DIELS-ALDER REACTION OF ALDEHYDES CATALYZED BY CHIRAL BORATE CATALYSTS 76
3.1 Introduction 76
3.1.1 Synthetic applications of heteroatom Diels-Alder reactions 76
3.1.2 Chiral borates in asymmetric reactions 99
3.2 Initial study 105
3.3 NMR study on catalysts 111
3.4 Optimization and substrate scope with catalysts **216** 114
3.5 Optimizations of asymmetric HDA reaction with catalyst **249** 117
3.6 Substrate scope of asymmetric HDA reaction with catalyst **249** 121
3.7 Study on asymmetric HDA reaction of α-alkoxyacetaldehyde 124
3.8 Reaction mechanism and computational study 130
3.8.1 Is the asymmetric HDA reaction catalyzed by VANOL borate complex concerted or stepwise? 130
3.8.2 Reversal of asymmetric induction 132
3.9 Conclusion 134
REFERENCES 136

CHAPTER FOUR EXPERIMENTAL SECTION 145
4.1 General information 145
4.2 Experimental information for chapter two 147
4.2.1 General procedure for catalytic asymmetric MPV reduction of aromatic ketones 147
4.2.2 General procedure for catalytic asymmetric MPV reduction of aliphatic ketones 170
4.2.3 Procedure for gram scale synthesis 174
4.2.4 Procedure for resolution of racemic alcohols 176
4.2.5 Computational study 178
4.3 Experimental information for chapter three 215
4.3.1 General procedure for preparing diene **93** 215
4.3.2 General procedure for preparing aldehyde **231w** 216
4.3.3 General procedure for preparing aldehyde **231y** 218
4.3.4 General procedure for preparation of catalysts 220
4.3.5 General procedure for asymmetric HDA reaction 226
4.3.6 Computational study 246
REFERENCES 251

LIST OF TABLES

Table 2.1 Screening of ligands for the MPV reduction of 2-bromoacetophenone 30

Table 2.2 Preliminary optimization of reaction conditions 32

Table 2.3 Solvent screening for the MPV reduction of 2-bromoacetophenone ... 33

Table 2.4 Study on different methods of preparing catalysts 34

Table 2.5 Concentration effect for the MPV reduction of 2-bromoacetophenone 36

Table 2.6 Test of replicability 37

Table 2.7 Alcohol Screening for the MPV reduction of 2-bromoacetophenone .. 38

Table 2.8 Further optimizations with **L21** as ligand 39

Table 2.9 Optimizations on the reduction of 4'-bromoacetophenone 40

Table 2.10 Reduction of 4'-bromoacetophenone with different ligands 42

Table 2.11 Optimization on the reduction of 3-phenyl-2-butanone 49

Table 2.12 Free energy differences at transition state with 30 ligands 55

Table 4.1 Free energy differences by HF/3-21G* in vacuum 180

Table 4.2 Free energy differences by B3LYP/6-31G(d) in vacuum 184

Table 4.3 Free energy differences by B3LYP/6-31G(d) in toluene 188

Table 4.4 Free energy differences by B3LYP/6-31G(d) in *n*-pentane 193

Table 4.5 Free energy differences by B3LYP/6-31G(d) in 2-propanol 197

Table 4.6 Calculated ΔΔG by HF/3-21G* in vacuum for 2-bromoacetophenone **55g** 201

LIST OF FIGURES

Figure 1.1 Aluminum complexes as catalysts for the MPV reduction 4

Figure 2.1 The use of BINOL derivatives as common solution 25

Figure 2.2 Ligands that were tested for MPV reaction 28

Figure 2.3 Computational study with 30 ligands 54

Figure 2.4 Transition states with (*S*)-**L21** in 2-propanol 57

Figure 2.5 Transition states with (*S*)-**L21** in the reduction of 2-bromoacetophenone 59

Figure 3.1 Six-membered heterocycles in natural products 77

Figure 3.2 Selected Lewis acid catalysts for asymmetric HDA reactions 90

Figure 3.3 Chiral organocatalysts in asymmetric HDA reactions 91

Figure 3.4 Selected chiral boron catalysts 100

Figure 3.5 Ligands screened 124

Figure 3.6 Boron and aluminum catalysts prepared from VANOL 133

LIST OF SCHEMES

Scheme 1.1 Classic MPV reduction of carbonyl compounds 2

Scheme 1.2 Addition of protic acid in MPV reduction/Oppenauer oxidation 3

Scheme 1.3 Alkali metal alkoxides in quinine oxidation and quininone reduction 6

Scheme 1.4 Inorganic bases in MPV reduction 7

Scheme 1.5 Asymmetric MPV reduction with chiral alcohols 9

Scheme 1.6 Asymmetric MPV reductions with chiral catalysts 10

Scheme 1.7 Asymmetric MPV reduction of glyoxylates 12

Scheme 1.8 Asymmetric catalytic MPV reductions with aluminum-BINOL catalysts 13

Scheme 1.9 Asymmetric MPV reductions with aluminum-calixarene catalysts .. 14

Scheme 2.1 Switching BINOL to VANOL 26

Scheme 2.2 Substrate scope for aromatic ketones I 43

Scheme 2.3 Substrate scope for aromatic ketones II 45

Scheme 2.4 Limitations on substrate scope 48

Scheme 2.5 Substrate scope for aliphatic ketones 51

Scheme 2.6 Scale up synthesis 52

Scheme 2.7 Mechanism of MPV reduction of ketones 53

Scheme 2.8 Explanation of stereo outcome 58

Scheme 2.9 Kinetic resolution and dynamic kinetic resolution 61

Scheme 2.10 Alcohol racemizations with ruthenium catalyst 62

Scheme 2.11 Chemo-enzymatic dynamic kinetic resolution of alcohols 62

Scheme 2.12 Non-enzymatic dynamic kinetic resolution of alcohols 63

Scheme 2.13 Oxidative kinetic resolution of racemic alcohols 66

Scheme 2.14 Formal dynamic kinetic resolution of racemic alcohols..... 68

Scheme 3.1 Normal HDA reaction and inverse electron-demand HDA reaction 78

Scheme 3.2 Aldehyde as dienophile of HDA reactions in total syntheses..... 79

Scheme 3.3 HDA reactions with Danishefsky's diene in total syntheses 80

Scheme 3.4 Constructing aromatic heterocycles by HDA reactions..... 82

Scheme 3.5 Inverse electron-demand HDA reactions in total syntheses 85

Scheme 3.6 HDA reactions in the construction of spiro compounds 86

Scheme 3.7 HDA reactions with uncommon dienophiles in total syntheses 88

Scheme 3.8 Chromium catalyst **147** with alkynals in total syntheses..... 92

Scheme 3.9 Chromium catalyst **147** with aldehyde **170** in total syntheses 94

Scheme 3.10 Asymmetric HDA reactions with chiral aldehydes or dienes..... 96

Scheme 3.11 Rhodium-catalyzed asymmetric HDA reactions in total syntheses 97

Scheme 3.12 Copper-catalyzed asymmetric HDA reactions in total syntheses . 98

Scheme 3.13 Chiral borate catalysts in asymmetric Diels-Alder reaction..... 101

Scheme 3.14 Chiral spiro-borate catalysts..... 102

Scheme 3.15 Chiral boroxinate in asymmetric catalysis 104

Scheme 3.16 Oxa-Diels-Alder reaction with BOROX catalysts 106

Scheme 3.17 Oxa-Diels-Alder reaction with BLA catalyst **222** 107

Scheme 3.18 Optimization of the ligand and the temperature..... 108

Scheme 3.19 Control experiments and screening of the boron source 109

Scheme 3.20 Can the same syringe be used for two injections of BH_3•Me_2S? 112

Scheme 3.21 Catalyst prepared from BINOL 114

Scheme 3.22 Optimizations with catalyst **216** 116

Scheme 3.23 Substrate scope of asymmetric HDA reaction with catalyst **216** 117

Scheme 3.24 Optimization of the HDA reaction of benzaldehyde with catalyst **249** 119

Scheme 3.25 The optimization of aliphatic aldehyde with catalyst **249** 120

Scheme 3.26 Substrate scope with catalyst **249** 121

Scheme 3.27 Failed substrates with catalyst **249** 123

Scheme 3.28 Attempts at optimizations of aldehyde **231f** 125

Scheme 3.29 Optimization of aldehyde **231w** in the reaction with diene **93** 127

Scheme 3.30 Optimizations on aldehyde **231x** 128

Scheme 3.31 Optimizations of aldehyde **231y** 129

Scheme 3.32 Two possible pathways 130

Scheme 3.33 Different quenching methods 131

Scheme 3.34 Asymmetric HDA reaction with boron and aluminum catalysts .. 132

CHAPTER ONE

ASYMMETRIC CATALYTIC MEERWEIN-PONNDORF-VERLEY REDUCTIONS IN THE LITERATURE

1.1 Introduction

The reduction of carbonyl compounds is one of the most important functional group manipulations in organic chemistry.[1] Amont various methods developed during the past century, the Meerwein-Ponndorf-Verley (MPV) reaction holds a prominent and historical position. In 1925, the reduction of carbonyl compounds with aluminum ethoxide ($Al(OEt)_3$) and ethanol was discovered independently by Meerwein and Schmidt[2], and by Verley[3]. Aldehydes and a few ketones were reduced to their corresponding alcohols at the expense of one equivalent of ethanol that is oxidized to acetaldehyde. The reaction is reversible, but the equilibrium can be shifted to the completion of reduction by removal of acetaldehyde with a dry hydrogen or nitrogen stream.[4] In 1926, Ponndorf established an efficient method with the use of aluminum isopropoxide ($Al(O\textit{i}Pr)_3$) and isopropanol. Aldehydes as well as ketones were reduced satisfactorily, with the acetone formed being removed by distillation.[5] Futhermore, the reversible nature of the Meerwein-Ponndorf-Verley reaction was employed to achieve oxidation of alcohols with aluminum *t*-butoxide ($Al(O\textit{t}Bu)_3$) in the presence of a large excess of acetone, known as the Oppenauer oxidation.[6,7]

The Meerwein-Ponndorf-Verley reaction utilizes inexpensive 2-propanol as reducing agent to generate primary or secondary alcohols from aldehydes or ketones that are activated though coordination to a Lewis acidic aluminum center.[8]

The mechanism involves the hydride transfer from 2-propanol to carbonyl compounds via a six-membered ring transition state (Scheme 1.1).[9] The classic MPV reduction of ketones is relatively slow, so it usually requires more than stoichiometric amounts of aluminum isopropoxide ($Al(OiPr)_3$) to achieve a satisfactory yield.[10] Therefore, it was largely replaced by methods using boron and aluminum hydrides after 1950.[11] However, efforts to improve the MPV reduction never diminished since the use of 2-propanol as hydride source is very attractive.

Scheme 1.1 Classic MPV reduction of carbonyl compounds

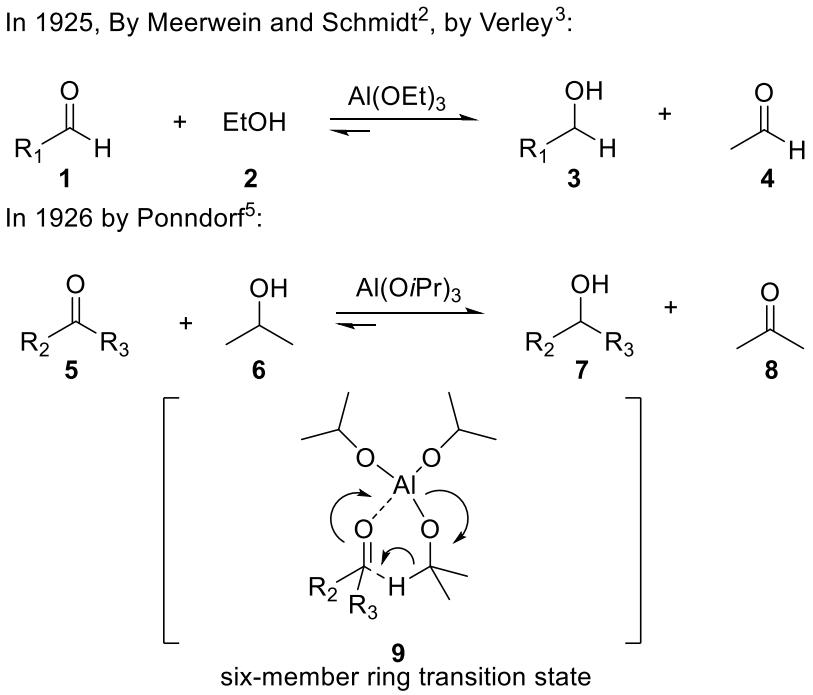

1.2 Catalytic MPV reductions

To make aluminum based MPV reductions “truly catalytic”, many methods have been established. Rathke and co-workers[12] initially discovered rate enhancement with addition of protic acid in 1977. They found that the oxidation of cyclohexanol by benzaldehyde could be dramatically improved with the addition of

trifluoroacetic acid (TFA) or hydrochloric acid (HCl) in presence of a catalytic amount (5 mol%) of Al(O*t*Bu)$_3$ (Scheme 1.2). In 1995, Akamanchi et al.[13] employed 8.2 mol% Al(O*i*Pr)$_3$ with 0.32 mol% TFA as co-catalyst to achieve catalytic reduction of carbonyl compounds with 1 equivalent of isopropanol at room temperature. The reduction of aldehydes was carried out in 15 min to 4 hours with 61 to 100% conversion, while lower conversion and longer reaction times were observed for ketones (44% conversion in 22 hours for acetophenone).

Scheme 1.2 Addition of protic acid in MPV reduction/Oppenauer oxidation

In 1977 by Rathke et al.[12]:

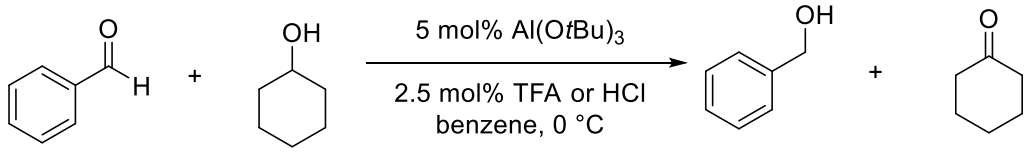

10 (2 equiv.) + **11** (1 equiv.) → **12** + **13**

In 1995 by Akamanchi et al.[13]:

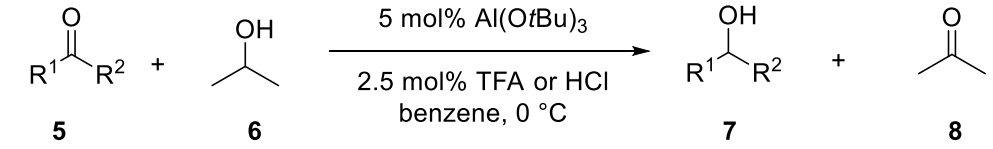

5 (1 equiv.) + **6** (1 equiv.) → **7** + **8**

Proposed Lewis acidity enhancement:

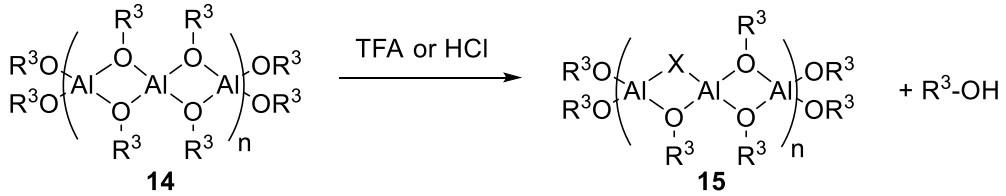

14 → **15**

R^3 = *i*Pr or *t*Bu; X = CF_3COO^- or Cl^-

As solid Al(O*i*Pr)$_3$ is known to be in a high aggregation state as indicated in **14** with isopropoxy as bridging units[14], it was proposed that the protic acid additive

could replace some of the alkoxy groups and generate a new aluminum species **15** that is more electronegtive. Therefore, the catalyst becomes more Lewis acidic and the coordination between a carbonyl substrate and aluminum was enhanced, which increased the overall reactivity of the catalyst.[15] The aluminum alkoxide/protic acid combination is the first example of a catalytic MPV reduction/Oppenauer oxidation catalyzed by aluminum. However, this combination is also found to be a potent catalyst for the undesired aldol condensation as a side reaction. According to Rathke's results, heptanal was self condensed with 90% yield in 5 minutes in the presence of 5 mol% Al(O*t*Bu)$_3$ and 2.5 mol% TFA.[12] Therefore, the applications of this method in organic synthesis are limited.

Figure 1.1 Aluminum complexes as catalysts for the MPV reduction

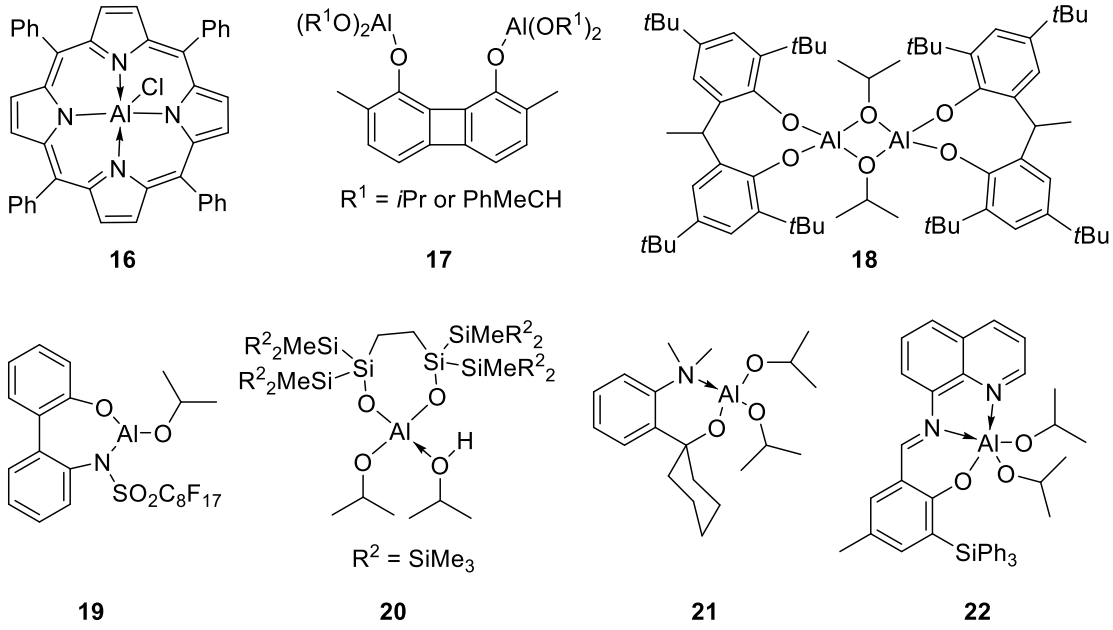

Replacement of aluminum isopropoxide with other aluminum complexes that are coordinated to multidentate ligands can make the catalytic reduction highly efficient (Figure 1.1). In 1988, Inoue and co-workers[16] found that aluminum

porphyrin **16** showed novel catalytic prowess with 20 mol% catalyst loading in the reduction of aldehydes or ketones with alcohols as reductant. High stereoselectivities were observed with the reduction of 2-methylcyclohexanone, which gave up to a 93:7 *trans* to *cis* ratio in the corresponding product. Bidentate aluminum alkoxides **17** have been found as efficient catalysts for the MPV reduction of aldehydes and ketones with 5 mol% catalyst loading and one equivalent of isopropanol.[17] The catalyst **17** bearing two aluminums in one molecule were able to capture both of the oxygen lone pairs simultaneously, which enables double activation of the carbonyl group.[10] Dimeric biphenoxyalkoxide **18** could catalyze the reduction of aldehydes with 2 equivalents of isopropanol at ambient conditions.[18] Aluminum sulfonamide **19** could readily reduce various ketones under mild conditions owing to its high Lewis acidity.[19] A sterically overloaded siloxide-supported aluminum species **20** was found to be capable of reducing a wide range of aldehydes and ketones with very low catalyst loading (0.05 mol% to 0.7 mol%).[20] Bidentate *N,O*-aluminum complex **21** and tridentate imino-phenolate aluminum complex **22** also showed catalytic activity in MPV reductions.[21,22]

It has been shown that reducing the aggregation state of aluminum alkoxides leads to enhancement of catalytic properties. The use of $Al(O\textit{t}Bu)_3$ instead of $Al(O\textit{i}Pr)_3$ was found to accelerate ketone reductions[23] because its favorable dimeric structure in benzene has more exchangeable ligands compared with the tetrameric structure of $Al(O\textit{i}Pr)_3$.[24] Nguyen and co-workers demonstrated that low-aggregated $Al(O\textit{i}Pr)_3$ freshly prepared from $AlMe_3$ and 2-propanol was

essential to achieve high catalytic activity in the MPV reduction of aldehydes and ketones.[25]

Scheme 1.3 Alkali metal alkoxides in quinine oxidation and quininone reductions

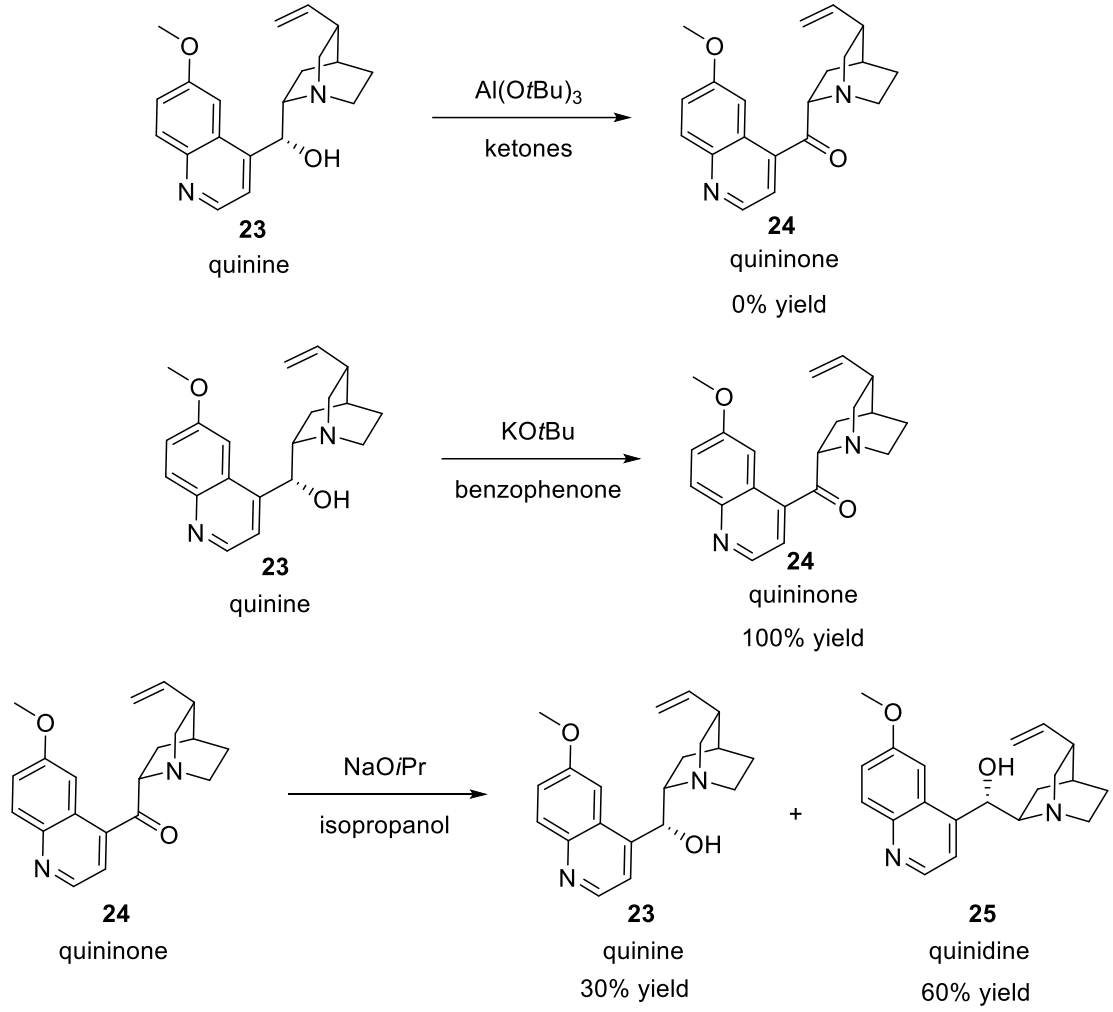

MPV reductions with isopropanol could also be catalyzed by other metals. In 1945, Woodward and co-workers[26] first discovered the use of alkali metal alkoxides in the so-called “modified Oppenauer oxidation”.[9] Quinine was not oxidized by Oppenauer method using aluminum *t*-butoxide and phenoxide as catalysts and a variety of ketones as oxidants (Scheme 1.3), probably due to the basicity of nitrogen that binds to aluminum and kill the catalysts. The use of 2.5

equivalent of freshly prepared potassium *t*-butoxide and 5 equivalent of benzophenone successfully oxidized quinine to quininone in quantitative yield. Furthermore, quininone was reduced to quinine and quinidine with sodium isopropoxide and isopropanol. Although these methods required far more than stoichiometric amounts of metal alkoxides, it indicates that alkali metal alkoxides can be possible catalysts in MPV reductions.

Scheme 1.4 Inorganic bases in MPV reduction

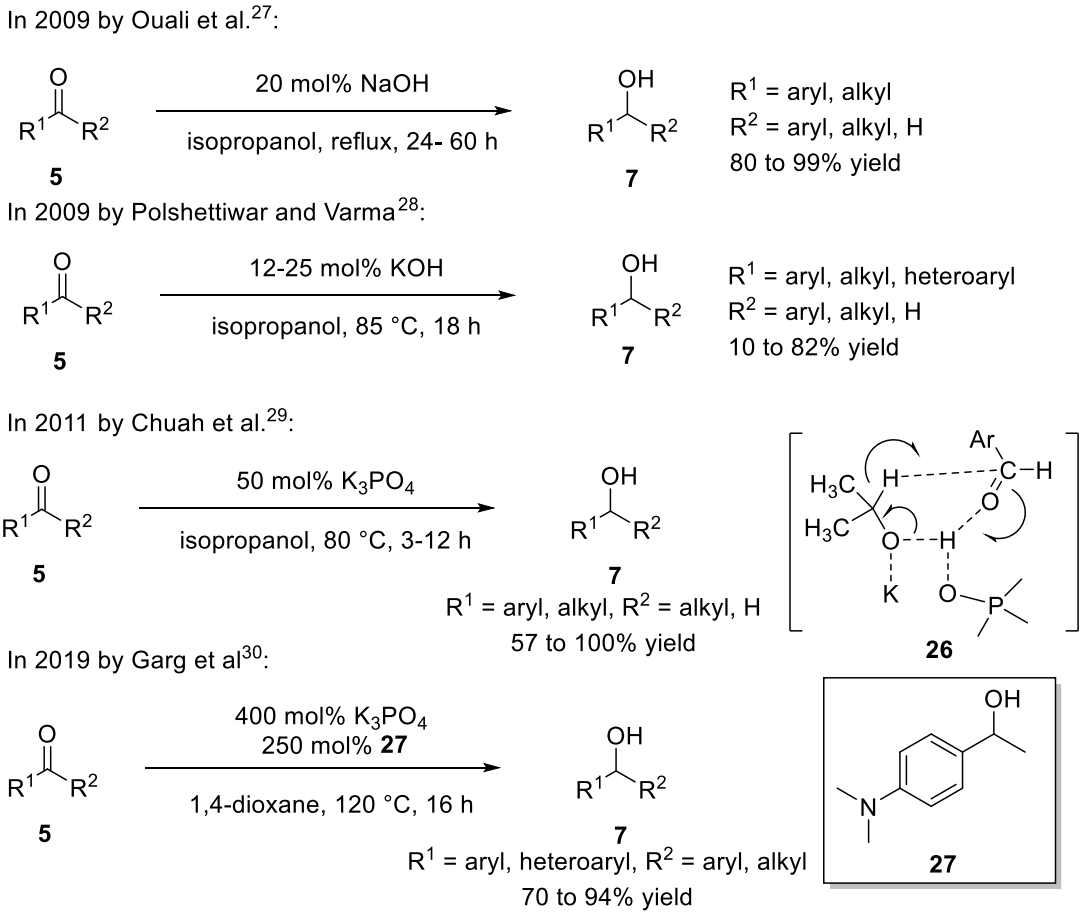

Recently, the use of inorganic bases such as sodium hydroxide (NaOH)[27], potassium hydroxide (KOH)[28], and potassium phosphate (K_3PO_4)[29] have been found to be effective in aldehyde and ketone reductions (Scheme 1.4). Catalytic

amounts of NaOH, KOH and the weaker base K_3PO_4 can reduce aldehydes and ketones with isopropanol as solvent. The active catalytic species was proposed to be an in-situ generated sodium or potassium isopropoxide and a novel six-membered ring transition state **26** was proposed by Chuah[29]. Garg and co-workers[30] employed K_3PO_4 and alcohol **27** instead of isopropanol to achieve ketone reductions for many heterocycles.

The reduction of ketones with isopropanol catalyzed by transition metal systems have also been reported and include samarium[31], ruthenium[32,33], rhodium[34], tin[35], zirconium[36-40], indium[22,41], ytterbium[42] and yttrium[43]. However, some of these ketone reductions catalyzed by transition metals via the transfer hydrogenation from alcohols are not considered as MPV reductions by some[44]. With metal-hydride species as the real catalyst in these reactions, the most common hydride source is formic acid instead of isopropanol.[45,46]

1.3 Asymmetric catalytic MPV reductions

The asymmetric MPV reduction of ketones can be achieved by two strategies. One is the use of chiral alcohols as sacrificial hydride source instead of 2-propanol, which requires far more than stoichiometric amounts of enantiopure reagent.[47] The first asymmetric MPV reduction induced by chiral alcohols was reported by Doering and Young in 1950 with the use of aluminum alkoxides as catalysts.[48] Maruoka and co-workers[17] employed 5 mol% catalyst **17** and 1 equivalent of enantiopure alcohol (*R*)-**30** as sacrificial hydride source to achieve enantioenriched alcohol **29** from ketone **28** in 51% yield and 82% *ee*. Other chiral alcohols such as (*R*)-*sec*-phenethyl alcohol (*R*)-**31** gave lower asymmetric

inductions. Nguyen et al. also found that the same reaction could be achieved without the use of a ligand on aluminum.[25] With 10 mol% trimethylaluminum as pre-catalyst and 1 equivalent of (*R*)-**31**, ketone **28** was reduced in 70% *ee* but no reported yield. For using 1 equivalent of (*R*)-**30**, a range of 86 to 81% ee was observed. The enantioselectivity of product **29** decreased slowly over time, because of the reversible nature of this reaction.

Scheme 1.5 Asymmetric MPV reduction with chiral alcohols

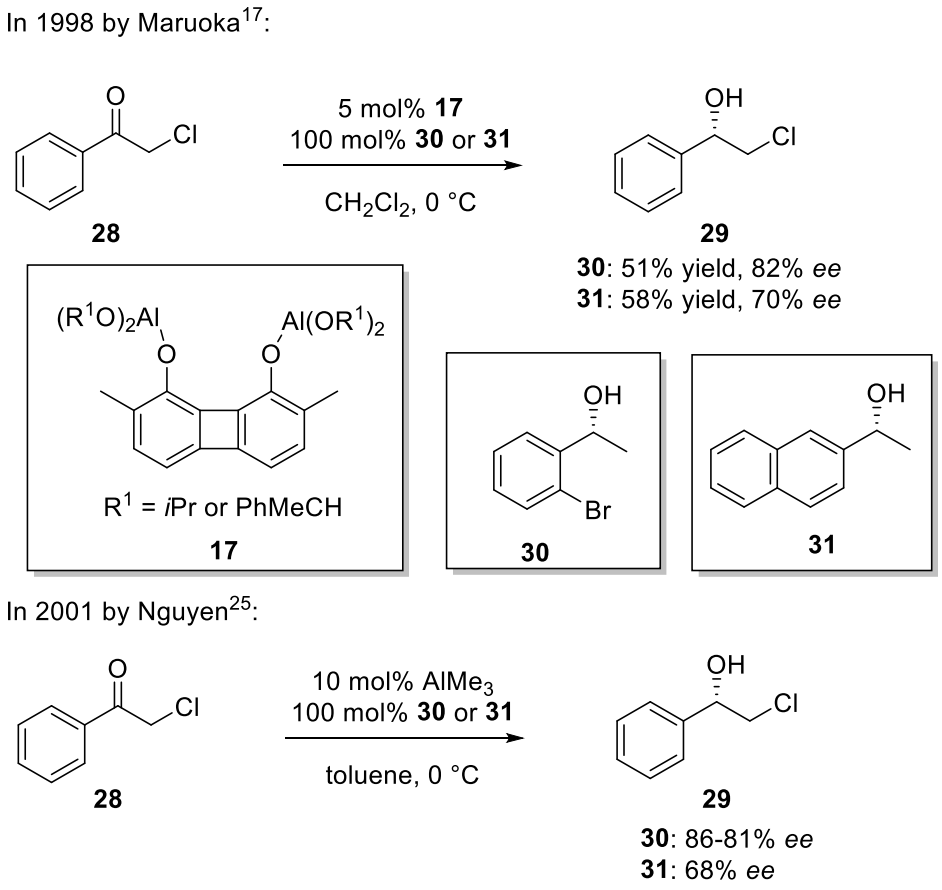

Scheme 1.6 Asymmetric MPV reductions with chiral catalysts

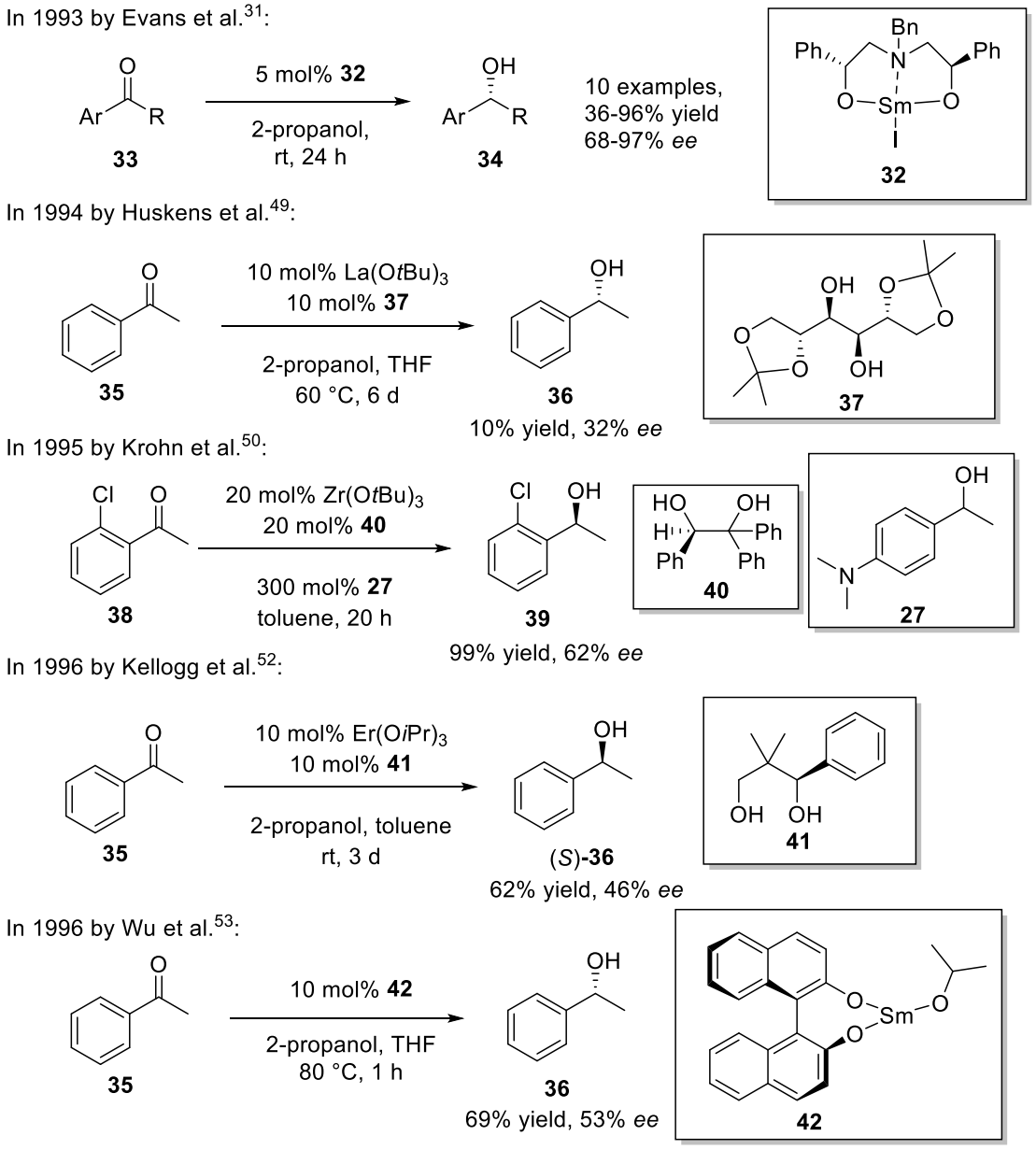

The other strategy for asymmetric MPV reactions employs a chiral Lewis acid complex as catalyst and achiral 2-propanol as reductant to achieve the prochiral ketone reduction. Evans and co-workers[31] in 1993 reported an asymmetric ketone reduction with a Samarium-based chiral catalyst. The *C*$_2$-symmetric samarium catalyst **32** could catalyze the reduction of aromatic ketones

in 36-96% yield and 68-97% *ee*. The hydrogen atoms at the two tertiary carbons next to oxygen in the chiral ligand did not participate in the MPV reduction as hydride source (Scheme 1.6). The samarium-iodide bond was found to be essential in the system. Furthermore, a non-linear effect was observed, giving the alcohol product in 95% *ee* while using a ligand that was 80% *ee*.

Huskens et al. in 1994 studied lanthanide alkoxide catalyzed asymmetric MPV reduction of acetophenone **35** with the chiral ligand **37**, however, only 10% yield was obtained after six days.[49] Krohn et al. employed zirconium *t*-butoxide and chiral diol **40** to asymmetrically reduce ketone **38** in 99% yield and 62% *ee* with 3 equivalents of alcohol **27** as hydride source.[50,51] Kellogg et al. reported the reduction of acetophenone **35** catalyzed by erbium isopropoxide and chiral diol **41** in moderate yield and *ee*.[52] Wu and co-workers[53] used samarium catalyst **42** that is derived from 1,1'-bi-2-naphthol (BINOL)[54] to achieve asymmetric reduction of acetophenone **35**. However, the enantioselectivity was not as good as samarium catalyst developed by Evans. Notably, BINOL has been used in asymmetric reduction of ketones with stoichiometric amount of lithium aluminum hydride.[55-61]

Other than simple ketones, glyoxylates could also be reduced with isopropanol as hydride source. In 2017, Feng, Lin and co-workers[43] developed an asymmetric MPV reduction of glyoxylates **44** to get access to a variety of optically active α-hydroxyesters **45** in high yield and *ee*. The co-catalyst system with 50 mol% $Al(O\mathit{t}Bu)_3$, 10 mol% $Y(OTf)_3$ and 10 mol% chiral *N,N*'-dioxide ligand[62] **43** were found to be essential for good results, giving 20 α-hydroxyesters **45** in 98-99% yield and 84-92% *ee*. Other transition metals like scandium and zirconium instead

of yttrium did not work, while in the absence of Al(O*t*Bu)$_3$ or molecular sieves a drop in yield and *ee* were observed. The good enantioselectivity observed resulted from the multidentate nature of glyoxylates, which was proposed in the paper. Under the same conditions, simple ketones gave low enantioselectivity or no reactivity. Only 2-bromoacetophenone, which can bind to metals in two points, gave a 95% yield and 81% *ee*.

Scheme 1.7 Asymmetric MPV reduction of glyoxylates

In 2017 by Feng, Lin and co-workers[43]:

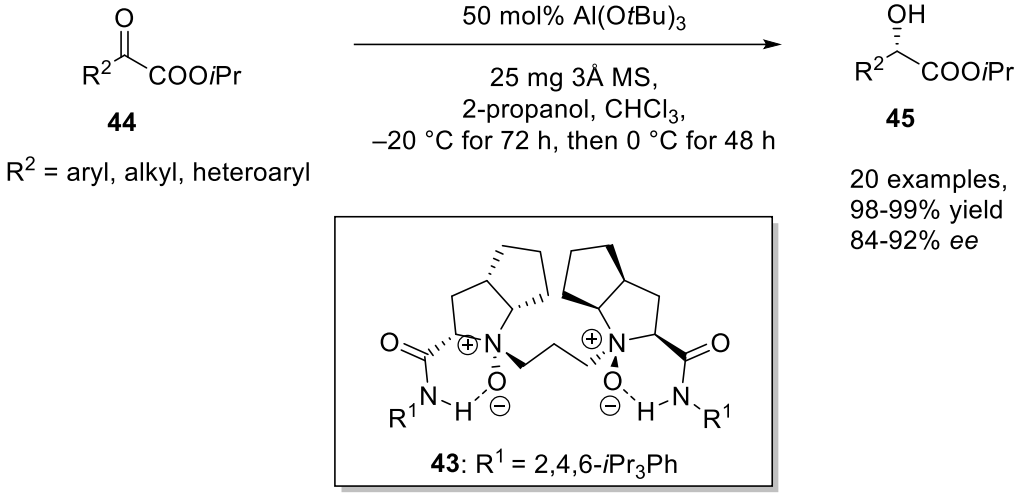

1.4 Aluminum-catalyzed asymmetric MPV reductions

In 2002, Nguyen and co-workers established the first catalytic enantioselective MPV reduction with an aluminum catalyst.[63] Catalyst **48** was generated in-situ from trimethylaluminum (AlMe$_3$), BINOL and 2-propanol as shown in Scheme 1.8. After 16 h at room temperature chiral 1-phenylethanol was obtained in 58% yield and 28% *ee*. Only ketones capable of 2-point binding to aluminum, such as 2-haloacetophenones, were reduced to alcohols with excellent

yield (99% yield) and good enantioselectivity (80-83% *ee*). Except for 2-haloacetophenone, other substrates all gave moderate yield and *ee* (20-95% yield, 8-61% *ee*). Increasing the loading of 2-propanol from 4 equivalents to 15 equivalents led to higher yield but lower *ee*. They proposed that 2-propanol kicked out some of BINOL ligands and formed Al(O*i*Pr)$_3$ as an achiral catalyst for the MPV reduction. It has been studied by the same group that MPV reduction of ketones could be achieved with aluminum alkoxide catalyst freshly prepared from trimethylaluminum and 2-propanol.[25]

Scheme 1.8 Asymmetric catalytic MPV reductions with aluminum-BINOL catalysts

In 2002 by Nguyen et al.[63]:

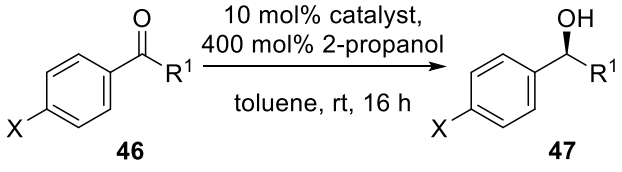

46 **47**

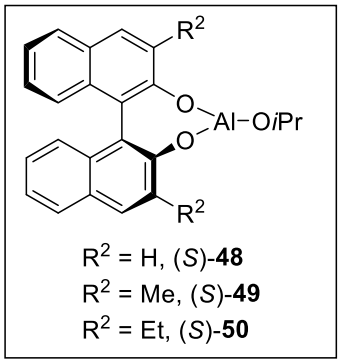

R^2 = H, (*S*)-**48**
R^2 = Me, (*S*)-**49**
R^2 = Et, (*S*)-**50**

With X = H, R^1 = CH_2Br as substrate:[a]

catalyst (*S*)-**48**: 99% yield, 83% ee
catalyst (*S*)-**49**: 98% yield, 50% ee
catalyst (*S*)-**50**: 97% yield, 26% ee

With (*S*)-**48** as catalyst:[a]

X	R^1	yield (%)	*ee* (%)
H	CH_3	58	28
H	CH_2Cl	99	80
H	CH_2Br	99	83
H	CH_2CH_3	30	50
H	$CH(CH_3)_2$	20	61
H	$CH_2CH(CH_3)_2$	32	53
H	CH_2OCH_3	95	8
CH_3	CH_3	44	30
F	CH_3	55	30
Cl	CH_3	70	30
Br	CH_3	70	30

[a]Reaction conditions: (*S*)-catalyst (0.02 mmol), ketone (0.20 mmol), and toluene (0.5 ml); room temperature, N_2 for 16 h; yield and *ee* were determined by chiral GC.

Density functional theory (DFT) was employed to study the mechanism computationally.[64] The direct hydrogen transfer from 2-propanol to ketone substrate via a six-member ring transition state was supported by calculations. In

the reduction of acetophenone with 2-propanol catalyzed by catalyst **48**, the activation energy difference (ΔΔG) between the two transition states towards (*R*)-1-phenylethanol and (*S*)-1-phenylethanol have been calculated as 0.5 kcal/mol, which is not large enough to give good enantioselectivity and is consistent with the experimental result (28% *ee*). They believe that the small energy difference between two transition states is due to the similar structures in both transition states, which means that the asymmetrical discrimination brought by the chiral ligand BINOL is not enough. In their subsequent mechanistic studies,[65] it was demonstrated that the use of 3,3'-disubstituted BINOL derived catalysts **49** and **50** gave lower asymmetric induction under the same conditions. Catalyst **48** has also been used in the MPV reduction of imines.[66] However, the catalyst did not turn over and 1.2 equivalent of **48** was required to achieve completion of the imine reduction.

Scheme 1.9 Asymmetric MPV reductions with aluminum-calixarene catalysts

In 2014 by Nandi, Katz and co-workers[67]:

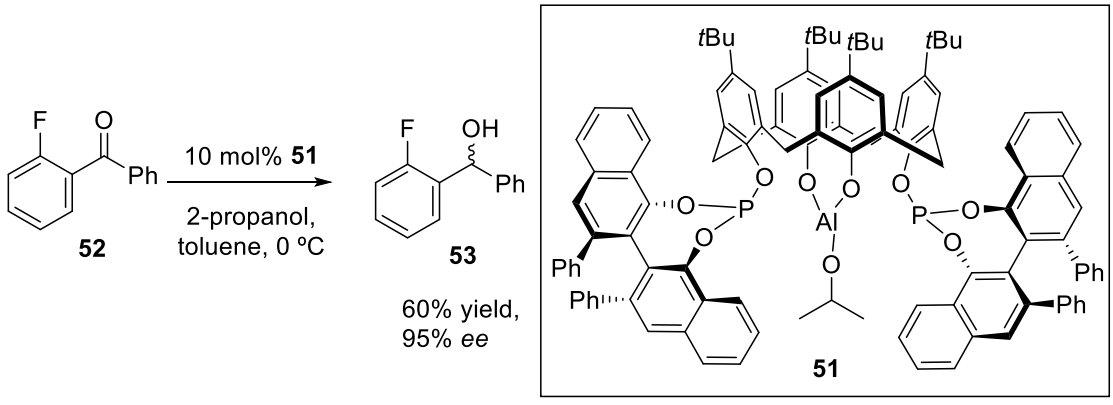

The only other example to date in aluminum-catalyzed asymmetric MPV reduction was developed by Nandi, Katz and coworkers.[67] They have developed a calix[4]arene phosphite ligand[68] for an aluminum-catalyzed MPV reduction with

excellent enantioselectivity (Scheme 1.9). Unfortunately, the scope of this method was limited to ketones with two binding sites such as 2-fluorobenzophenone **52**.

1.5 Summary

In this chapter, the development of catalytic asymmetric Meerwein-Ponndorf-Verley reductions of carbonyl compounds has been discussed. While this reaction first developed in the mid 1920s employs stoichiometric amounts of an aluminum alkoxide, a lot of effort has been taken to make the MPV reduction catalytic. Efficient solutions include the addition of protic acid to increase the Lewis acidity of aluminum, and the use of ligands to prevent the aggregation of the aluminum alkoxide. Some alkali metals and transition metals have been found to be capable of catalyzing ketone reductions with 2-propanol as hydride source, either via a classic MPV reduction or a transfer hydrogenation mechanism. Previous asymmetric MPV reductions employ a chiral alcohol as sacrificial reductant, while modern asymmetric MPV reductions could be carried out catalytically with chiral metal complexes. Many chiral transition metal complexes have been studied and the best asymmetric inductions are given by a chiral samarium complex developed by Evans, and a chiral yttrium-aluminum complex developed by Feng and Lin. However, the former is limited to aromatic ketones and the latter is limited to glyoxylates. Two examples of asymmetric MPV reduction of ketones catalyzed by aluminum catalysts have been reported. However, high enantioselectivities are only observed for ketones with two binding sites.

To date, there is no aluminum catalyst that can catalyze the asymmetric MPV reduction of simple aromatic and aliphatic ketones with high asymmetric

inductions. Considering the advantages that include the use of the non-transition metal aluminum as catalyst, and the use of inexpensive and environmentally benign 2-propanol as hydride source, it is very attractive to develop a highly applicable aluminum-catalyzed MPV reduction for the synthesis of enantioenriched chiral alcohols. In chapter two we will discuss the development of enantioselective MPV reduction of ketones catalyzed by aluminum-VANOL catalysts.

REFERENCES

REFERENCES

1. Nishide, K.; Node, M. Recent development of asymmetric syntheses based on the Meerwein-Ponndorf-Verley reduction. *Chirality* **2002**, *14*, 759-767.

2. Meerwein, H.; Schmidt, R. Ein neues Verfahren zur Reduktion von Aldehyden und Ketonen. *Justus Liebigs Ann. Chem.* **1925**, *39*, 221-238.

3. Verley, M. Sur l'échange de groupements fonctionnels entre deux molécules. Passage des cétones aux alcohols et inversement. *Bull. Soc. Chim. Fr.* **1925**, *37*, 871-874.

4. Wilds, A. L. Reduction with Aluminum Alkoxides (The Meerwein-Ponndorf-Verley Reduction). *Org. React.* **1944**, 178-223.

5. Ponndorf, W. Der reversible Austausch der Oxydations-stufen zwischen Aldehyden oder Ketonen einerseits und primären oder sekundären Alkoholen anderseits. *Angew. Chem.* **1926**, *39*, 138-143.

6. Oppenauer, R. V. Eine Methode der Dehydrierung von sekundären Alkoholen zu Ketonen. I. Zur Herstellung von Sterinketonen und Sexualhormonen. *Recl. Trav. Chim. Pays-Bas* **1937**, *56*, 137–144.

7. Djerassi, C. The Oppenauer Oxidation. *Org. React.* **1951**, 207-272.

8. Cha, J. S. Recent Developments In Meerwein−Ponndorf−Verley and Related Reactions for the Reduction of Organic Functional Groups Using Aluminum, Boron, and Other Metal Reagents: A Review. *Org. Proc. Res. & Devel.* **2006**, *10*, 1032-1053.

9. de Graauw, C. F.; Peters, J. A.; van Bekkum, H.; Huskens, J. Meerwein-Ponndorf-Verley Reductions and Oppenauer Oxidation: An Integrated Approach. *Synthesis* **1994**, 1007-1017.

10. Ooi, T.; Miura, T.; Itagaki, Y.; Ichikawa, H.; Maruoka, K. Catalytic Meerwein-Ponndorf-Verley (MPV) and Oppenauer (OPP) Reactions: Remarkable Acceleration of the Hydride Transfer by Powerful Bidentate Aluminum Alkoxides. *Synthesis*, **2002**, 279-291.

11. Nikonov, G. I. New Tricks for an Old Dog: Aluminum Compounds as Catalysts in Reduction Chemistry. *ACS Catalysis*, **2017**, *7*, 7257-7266.

12. Kow, R.; Nygren, R.; Rathke, M. W. Rate enhancement of the Meerwein-Ponndorf-Verley-Oppenauer reaction in the presence of proton acids. *J. Org. Chem.* **1977**, *42*, 826-827.

13. Akamanchi, K. G.; Noorani, V. R. Truly catalytic Meerwein-Ponndorf-Verley (MPV) reduction. *Tetrahedron Lett.* **1995**, *36*, 5085-5088.

14. Fieggen, W.; Gerding, H. Structure and physical properties of aluminium alkoxides. Part II: Changes in physical properties of liquid aluminium isopropoxide during storage. *Trav. Chim. Pays-Bas* **1970**, *89*, 175-185.

15. Graves, C. R.; Campbell E. J.; Nguyen, S. T. Aluminum-based catalysts for the asymmetric Meerwein-Schmidt-Ponndorf-Verley-Oppenauer (MSPVO) reaction manifold. *Tetrahedron: Asymmetry*, **2005**, *16*, 3460-3468.

16. Konishi, K.; Kazuyuki, M.; Aida, T.; Inoue, S. Highly stereoselective hydrogen transfer from alcohols to carbonyl compounds catalysed by aluminium porphyrins. *J. Chem. Soc., Chem. Commun.* **1988**, 643-645.

17. Ooi, T.; Miura, T.; Maruoka, K. Highly Efficient, Catalytic Meerwein-Ponndorf-Verley Reduction with a Novel Bidentate Aluminum Catalyst. *Angew. Chem., Int. Ed.* **1998**, *37*, 2347-2349.

18. Ko, B.-T.; Wu, C.-C.; Lin, C.-C. Preparation, Characterization, and Reactions of $[(EDBP)Al(\mu\text{-}O^iPr)]_2$, a Novel Catalyst for MPV Hydrogen Transfer Reactions. *Organometallics* **2000**, *19*, 1864-1869.

19. Ooi, T.; Ichikawa, H.; Maruoka, K. Practical Approach to the Meerwein-Ponndorf-Verley Reduction of Carbonyl Substrates with New Aluminum Catalysts. *Angew. Chem., Int. Ed.* **2001**, *40*, 3610-3612.

20. McNerney, B.; Whittlesey, B.; Cordes, D. B.; Krempner, C. A Well-Defined Monomeric Aluminum Complex as an Efficient and General Catalyst in the Meerwein–Ponndorf–Verley Reduction. *Chem. Eur. J.* **2014**, *20*, 14959-14964.

21. Hua, Y.; Guo, Z.; Suo, H.; Wei, X. Bidentate N, O-aluminum complexes: Synthesis, characterization and catalytic study for MPV reduction reactions. *J. Organomet. Chem.* **2015**, *794*, 59-64.

22. Normand, M.; Kirillov, E.; Roisnel, T.; Carpentier, J.-F. Meerwein–Ponndorf–Verley-Type Reduction Processes in Aluminum and Indium Isopropoxide Complexes of Imino-Phenolate Ligands. *Organometallics*, **2012**, *31*, 5511-5519.

23. Flack, K.; Kitagawa, K.; Pollet, P.; Eckert, C. A.; Richman, K.; Stringer, J.; Dubay, W.; Liotta, C. L. $Al(OtBu)_3$ as an Effective Catalyst for the Enhancement of Meerwein–Ponndorf–Verley (MPV) Reductions. *Org. Process Res. Dev*. **2012**, *16*, 1301-1306.

24. Shiner, V. J.; Whittaker, D.; Fernandez, V. P. The Structures of Some Aluminum Alkoxides. *J. Am. Chem. Soc.* **1963**, *85*, 2318–2322.

25. Campbell, E. J.; Zhou, H.; Nguyen, S. T. Catalytic Meerwein−Pondorf−Verley Reduction by Simple Aluminum Complexes. *Org. Lett.* **2001**, *3*, 2391-2393.

26. Woodward, R. B.; Wendler, N. L.; Brutschy, F. J. Quininone. *J. Am. Chem. Soc.* **1945**, *67*, 1425-1429.

27. Ouali, A.; Majoral, J.-P.; Caminade, A.-M.; Taillefer, M. NaOH-Promoted Hydrogen Transfer: Does NaOH or Traces of Transition Metals Catalyze the Reaction? *ChemCatChem* **2009**, *1*, 504− 509.

28. Polshettiwar, V.; Varma, R. S.; Revisiting the Meerwein–Ponndorf–Verley reduction: a sustainable protocol for transfer hydrogenation of aldehydes and ketones. *Green Chem.* **2009**, *11*, 1313−1316.

29. Radhakrishan, R.; Do, D. M.; Jaenicke, S.; Sasson, Y.; Chuah, G.-K. Potassium Phosphate as a Solid Base Catalyst for the Catalytic Transfer Hydrogenation of Aldehydes and Ketones. *ACS Catal.* **2011**, *1*, 1631−1636.

30. Boit, T. B.; Mehta, M. M.; Garg, N. K. Base-Mediated Meerwein–Ponndorf–Verley Reduction of Aromatic and Heterocyclic Ketones. *Org. Lett.* **2019**, *21*, 6447-6451.

31. Evans, D. A.; Nelson, S. G.; Gagne, M. R.; Muci, A. R. A chiral samarium-based catalyst for the asymmetric Meerwein-Ponndorf-Verley reduction. *J. Am. Chem. Soc.* **1993**, *115*, 9800-9801.

32. Hasiguchi, S.; Fujii, A.; Takehara, J.; Ikariya, T.; Noyori, R., Asymmetric Transfer Hydrogenation of Aromatic Ketones Catalyzed by Chiral Ruthenium(II) Complexes. *J. Am. Chem. Soc.* **1995**, *117*, 7562-7563.

33. Noyori, R.; Hashiguchi, S. Asymmetric Transfer Hydrogenation Catalyzed by Chiral Ruthenium Complexes. *Acc. Chem. Res.* **1997**, *30*, 97-102.

34. Gladiali, S.; Pinna, L.; Delogu, G.; De Martin, S.; Zassinovich, G.; Mestroni, G. Optically active phenanthrolines in asymmetric catalysis. III. Highly efficient enantioselective transfer hydrogenation of acetophenone by chiral rhodium/3-alkyl phenanthroline catalysts.*Tetrahedron: Asymmetry*, **1990**, *9*, 635-648.

35. Corma, A.; Domine, M. E.; Nemeth, L.; Valencia, S. Al-Free Sn-Beta Zeolite as a Catalyst for the Selective Reduction of Carbonyl Compounds (Meerwein-Ponndorf-Verley Reaction). *J. Am. Chem. Soc.* **2002**, *124*, 3194-3195.

36. Zhu, Y.; Chuah, G. K.; Jaenicke, S. Al-free Zr-zeolite beta as a regioselective catalyst in the Meerwein–Ponndorf–Verley reaction. *Chem. Commun.* **2003**, 2734-2735.

37. Battilocchio, C.; Hawkins, J. M.; Ley, S. V. A Mild and Efficient Flow Procedure for the Transfer Hydrogenation of Ketones and Aldehydes using Hydrous Zirconia. *Org. Lett.* **2013**, *15*, 2278-2281.

38. Song, J.; Zhou, B.; Zhou, H.; Wu, L.; Meng, Q.; Liu, Z.; Han, B. Porous Zirconium-Phytic Acid Hybrid: a Highly Efficient Catalyst for Meerwein-Ponndorf-Verley Reductions. *Angew. Chem. Int. Ed.* **2015**, 54, 9399-9403.

39. Plessers, E.; Fu, G.; Tan, C.; De Vos, D.; Roeffaers, M. Zr-Based MOF-808 as Meerwein–Ponndorf–Verley Reduction Catalyst for Challenging Carbonyl Compounds. *Catalysts* **2016**, *6*, 104-114.

40. Leng, Y.; Shi, L.; Du, S.; Jiang, J.; Jiang, P. A tannin-derived zirconium-containing porous hybrid for efficient Meerwein–Ponndorf–Verley reduction under mild conditions. *Green Chem.* **2020**, *22*, 180-186.

41. Lee, J.; Ryu, T.; Park, S.; Lee, P. H. Indium Tri(isopropoxide)-Catalyzed Selective Meerwein–Ponndorf–Verley Reduction of Aliphatic and Aromatic Aldehydes. *J. Org. Chem.* **2012**, 77, 4821-4825.

42. Mollica, S.; Genovese, S.; Pinnen, S.; Stefanucci, A.; Curini, M.; Epifano, F. Ytterbium triflate catalysed Meerwein–Ponndorf–Verley (MPV) reduction. *Tetrahedron Lett.* **2012**, *53*, 890-892.

43. Wu, W.; Zou, S.; Lin, L.; Ji, J.; Zhang, Y.; Ma, B.; Liu, X.; Feng, X. Catalytic asymmetric Meerwein–Ponndorf–Verley reduction of glyoxylates induced by a chiral N,N′-dioxide/Y(OTf)3 complex. *Chem. Commun.* **2017**, *53*, 3232-3235.

44. Wang, D.; Astruc, D. The Golden Age of Transfer Hydrogenation. *Chem. Rev.* **2015**, *115*, 6621-6686.

45. Foubelo, F.; Najera, C.; Yus, M. Catalytic asymmetric transfer hydrogenation of ketones: recent advances. *Tetrahedron: Asymmetry*, **2015**, *26*, 769-790.

46. Gladiali, S.; Alberico, E. Asymmetric transfer hydrogenation: chiral ligands and applications. *Chem. Soc. Rev.* **2006**, *35*, 226-236.

47. Cram, D. J.; Elhafez, F. A. A. Studies in Stereochemistry. X. The Rule of “Steric Control of Asymmetric Induction” in the Syntheses of Acyclic Systems. *J. Am. Chem. Soc.* **1952**, *74*, 5828–5835.

48. Doering, W. E.; Young, R. W. Partially Asymmetric Meerwein-Ponndorf-Verley Reductions. *J. Am. Chem. Soc.* **1950**, *72*, 631.

49. Huskens, J.; de Graauw, C. F.; Peters, J. A.; van Bekkum, H. Chiral induction in lanthanide(III)-alkoxide-catalyzed Meerwein-Ponndorf-Verley reductions. *Recl. Trav. Chim. Pays-Bas* **1994**, *113*, 488-491.

50. Krohn, K.; Knauer, B. The diastereoselectivity of zirconium alkoxide catalyzed Meerwein-Ponndorf-Verley reductions. *Liebigs Ann.* **1995**, 1347–1351.

51. Krohn, K.; Knauer, B. Asymmetric induction in kinetically controlled zirconium-catalyzed catalyzed Meerwein-Ponndorf-Verley reductions. *Recl. Trav. Chim. Pays-Bas* **1996**, *115*, 140–144.

52. Hu, X.; Kellogg, R. M. Asymmetric reduction and Meerwein-Ponndorf-Verley reaction of prochiral aromatic ketones in the presence of optically pure 1-aryl-2,2-dimethylpropane-1,3-diols. *Recl. Trav. Chim. Pays-Bas* **1996**, *115*, 410-417.

53. Ding, Z.-B.; Cheng, K.-J.; Wu, S.-H. Asymmetric Meerwein-Ponndorf-Verley reaction catalyzed by a new type of chiral binaphthol-samarium complex. *Chin. J. Chem.* **1996**, *14*, 561–564.

54. Brunel, J. M. BINOL: A Versatile Chiral Reagent. *Chem. Rev.* **2005**, *105*, 857−897.

55. Noyori, R.; Tomino, I.; Tanimoto, Y. Virtually complete enantioface differentiation in carbonyl group reduction by a complex aluminum hydride reagent. *J. Am. Chem. Soc.* **1979**, *101*, 3129-3131.

56. Noyori, R.; Tomino, I.; Tanimoto, Y.; Nishizawa, M. Asymmetric synthesis via axially dissymmetric molecules. 6. Rational designing of efficient chiral reducing agents. Highly enantioselective reduction of aromatic ketones by binaphthol-modified lithium aluminum hydride reagents. *J. Am. Chem. Soc.* **1984**, *106*, 6709-6716.

57. Noyori, R.; Tomino, I.; Yamada, M.; Nishizawa, M. Asymmetric synthesis via axially dissymmetric molecules. 7. Synthetic applications of the enantioselective reduction by binaphthol-modified lithium aluminum hydride reagents. *J. Am. Chem. Soc.* **1984**, *106*, 6717-6725.

58. Nishizawa, M.; Yamada, M.; Noyori, R. Highly enantioselective reduction of alkynyl ketones by a binaphthol-modified aluminum hydride reagent. Asymmetric synthesis of some insect pheromones. *Tetrahedron Lett.* **1981**, *22*, 247-250.

59. Noth, H.; Schlegel, A.; Suter, M. A study of Noyori's reagent. *J. Organomet. Chem.* **2001**, *621*, 231-241.

60. Matsuki, K.; Inoue, H.; Ishida, A.; Takeda, M.; Nakagawa, M.; Hino, T. Highly Enantioselective Reduction of *meso*-Cyclic-1,2-dicarboximides. Asymmetric Synthesis of Bicyclic 2-Pyrrolidinone and Its 5-Hydroxy Congener. *Heterocycles* **1993**, *36*, 937-940.

61. Matsuki, K.; Inoue, H.; Takeda, M. Highly enantioselective reduction of meso-1,2-dicarboxylic anhydrides. *Tetrahedron Lett.* **1993**, *34*, 1167-1170.

62. Liu, X. H.; Lin, L. L.; Feng, X. M. Chiral *N,N'*-Dioxides: New Ligands and Organocatalysts for Catalytic Asymmetric Reactions. *Acc. Chem. Res.* **2011**, *44*, 574-587.

63. Campbell, E. J.; Zhou, H.; Nguyen, S. T. The Asymmetric Meerwein–Schmidt–Ponndorf–Verley Reduction of Prochiral Ketones with iPrOH Catalyzed by Al Catalysts. *Angew. Chem. Int. Ed.* **2002**, *41*, 1020-1022.

64. Cohen, R.; Graves, C. R; Nguyen, S. T.; Martin, J. M. L.; Ratner, M. A. The Mechanism of Aluminum-Catalyzed Meerwein−Schmidt−Ponndorf−Verley Reduction of Carbonyls to Alcohols. *J. Am. Chem. Soc.* **2004**, *126*, 14796-14803.

65. Graves, C. R.; Zhou, H.; Stern, C. L.; Nguyen, S. T. A Mechanistic Investigation of the Asymmetric Meerwein−Schmidt−Ponndorf−Verley Reduction Catalyzed by BINOL/AlMe3. Structure, Kinetics, and Enantioselectivity. *J. Org. Chem.* **2007**, *72*, 9121-9133.

66. Graves, C. R.; Scheidt, K. A.; Nguyen, S. T. Enantioselective MSPV Reduction of Ketimines Using 2-Propanol and (BINOL)Al^{III}. *Org. Lett.* **2006**, *8*, 1229-1232.

67. Nandi, P.; Solovyov, A.; Okrut, A.; Katz, A. Al^{III}–Calix[4]arene Catalysts for Asymmetric Meerwein–Ponndorf–Verley Reduction. *ACS Catal.* **2014**, *4*, 2492-2495.

68. Nandi, P.; Matvieiev, Y. I.; Boyko, V. I.; Durkin, K. A.; Kalchenko, V. I.; Katz, A. MPV reduction using Al^{III}-calix[4]arene Lewis acid catalysts: Molecular-level insight into effect of ketone binding. *J. Catal.* **2011**, *284*, 42-49.

CHAPTER TWO

ASYMMETRIC CATALYTIC MEERWEIN-PONNDORF-VERLEY REDUCTION OF KETONES WITH ALUMINUM(III)-VANOL CATALYSTS

2.1 Introduction

The many advantages of the aluminum mediated MPV reduction of ketones include mild conditions, inexpensive reagents, ease of operation and the fact that aluminum is the most common metal in the earth's crust. Thus, it would be highly desirable to develop a catalytic asymmetric MPV reaction with a chiral aluminum catalyst that gave consistently high yields and asymmetric inductions. Considering that Dr. Nguyen's aluminum-BINOL catalyst[11] is easy to prepare but gives modest enantioselectivities for most of substrates, we want to see if we can enhance its chiral environment by using different chiral ligands.

We have developed a class of vaulted biaryl ligands that include VAPOL and VANOL for use in reactions where the BINOL ligand is not suitable.[1] The idea was that when VANOL and VAPOL are bound to a catalytic center via the phenol functions, the bulk of the space that is asymmetrically discriminated around the active site would be greater than it would be for BINOL catalysts. The vaulted biaryl ligands VANOL and VAPOL have been demonstrated to be useful in a variety of asymmetric reactions.[2-9] In this work, we describe the discovery of aluminum-VANOL catalysts that are the first aluminum MPV catalysts that can reduce a

variety of aromatic and aliphatic ketones to chiral alcohols with excellent yields and enantioselectivities.[10]

2.2 Initial study: Is switching BINOL to VANOL a way out?

In some reactions, BINOL as ligand provides modest asymmetric induction because its chiral pocket is far away from its active site (Figure 2.1). Adding substituents at 3,3‘-positions of BINOL is a common solution to increase the asymmetric induction, which brings the chiral pocket closer to the active site (Figure 2.1).

Figure 2.1 The use of BINOL derivatives as common solution

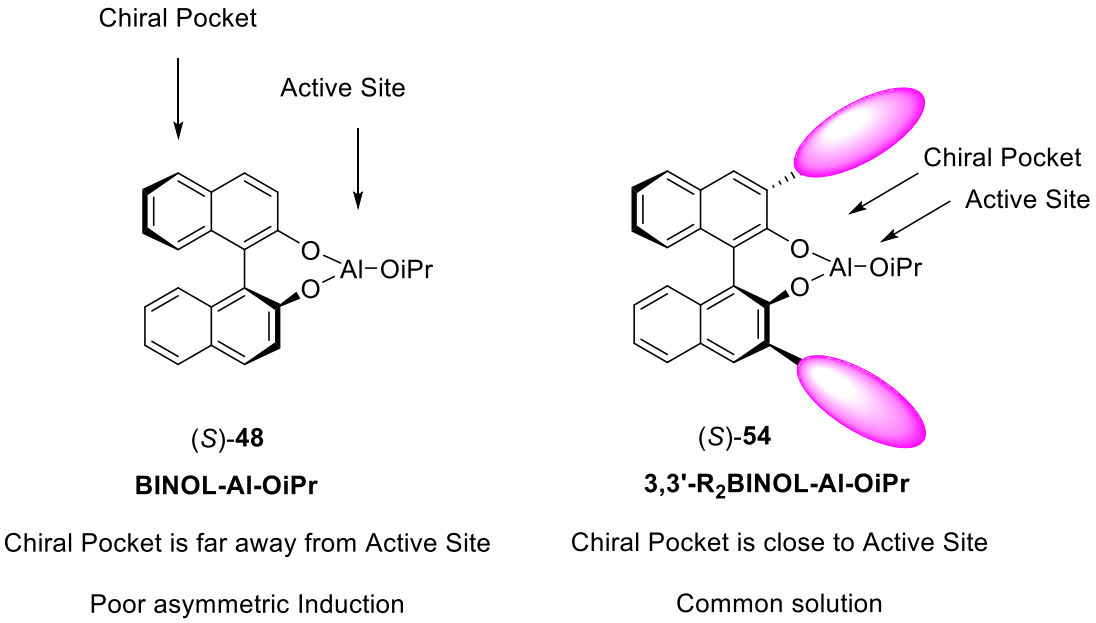

Thus, it is easy to assume that by replacing BINOL with other bulkier ligands such as 3,3’-disubstituted BINOL might dramatically improve the enantioselectivity of the MPV reduction. Dr. Nguyen’s group employed 3,3’-Me_2BINOL and 3,3’-Et_2BINOL to construct the chiral aluminum complex as catalyst and tried these two catalysts in the reduction of 2-bromoacetophenone **55g**.[11-13] Surprisingly, under

the same condition as using (*S*)-BINOL as ligand, using (*S*)-3,3'-Me_2BINOL and (*S*)-3,3'-Et_2BINOL as ligands gave only 50% *ee* and 26% *ee* respectively (Scheme 2.1). Compared with the result using BINOL without any substituent (83% *ee*), increasing the bulkiness at 3,3'-positions of BINOL actually decreased the asymmetric induction. Therefore, their attempt to obtain high enantioselectivity by using bulkier 3,3'-disubstituted BINOL was not successful.

Scheme 2.1 Switching BINOL to VANOL

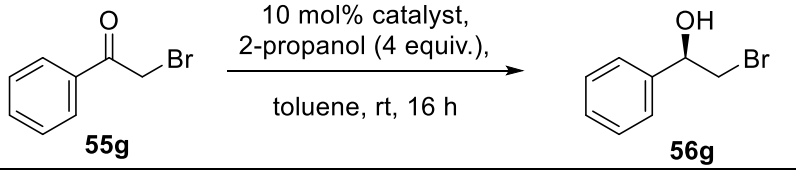

55g **56g**

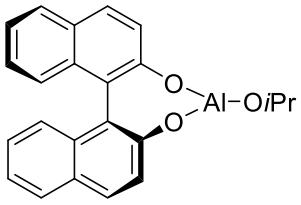

48

99% yield, 83% ee[a]
72% yield, 76% ee[b]

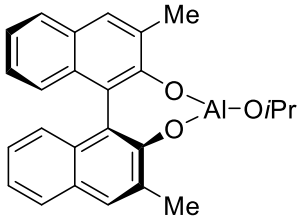

49

98% yield, 50% ee[a]

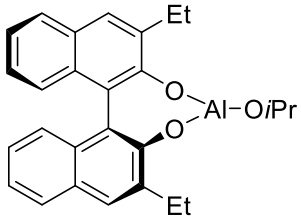

50

97% yield, 26% ee[a]

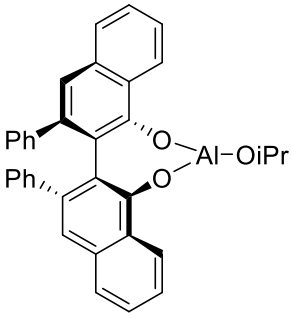

57

75% yield, 56% ee[b]

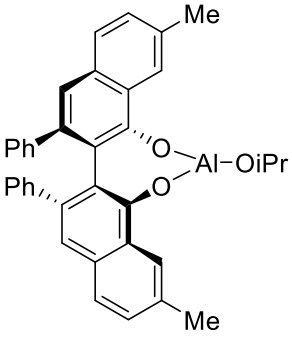

58

83% yield, 74% ee[b]

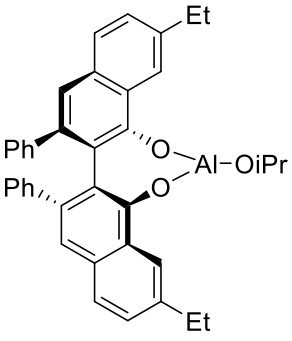

59

50% yield, 80% ee[b]

[a] Results from Nguyen's work.

[b] This work with modified conditions and 20 mol% catalyst used.

Our initial study started with switching BINOL to VANOL. As a control we first carried out the reaction with (*S*)-BINOL. With 4 equivalents of 2-propanol and 20 mol% catalyst generated from (*S*)-BINOL and trimethylaluminum, 2-bromoacetophenone **55g** was reduced to the corresponding alcohol (*R*)-**56g** in 72% yield and 76% *ee* (Scheme 2.1). It should be noted that these conditions were slightly different from those reported by Nguyen. By comparison, the catalyst **57** made from (*S*)-VANOL catalyzed the reduction of 2-bromoacetophenone **55g** with 75% yield and 56% *ee* (Scheme 2.1). These results (*ee* for BINOL is 20% higher than that for VANOL) were opposite to what we expected, as we thought that the asymmetric discrimination brought by VANOL should be greater than BINOL. We then tested VANOL derivatives with substituents at the 7,7'-positions, which were thought to provide a better chiral environment around the reactive site and were similar to that normally observed for 3,3'-substituted BINOL derivatives. To our delight, a different trend for enantioselectivities was found. Catalyst **58** made from 7,7'-Me_2VANOL gave 74% *ee* and catalyst **59** made from 7,7'-Et_2VANOL gave 80% *ee* (Scheme 2.1), which indicates that increasing the bulkiness of VANOL successfully increased the asymmetric induction. With this finding, we were glad to see that while making derivatizations on BINOL failed to enhance the enantioselectivity, switching BINOL to VANOL is a way out.

2.3 Reaction optimizations

2.3.1 Ligand screening

The initial study revealed that adding substituents on VANOL has positive effect on the asymmetric induction, which encouraged us to screen more

derivatives of vaulted biaryl ligands. We selected 2-bromoacetophenone **55g** as the model substrate for the screen of various ligands in the MPV reduction since it was the best substrate for the BINOL catalyst (Scheme 1.8).

Figure 2.2 Ligands that were tested for MPV reaction

a) BINOL and vaulted biaryl ligands

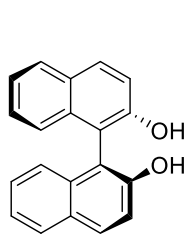

L1: BINOL

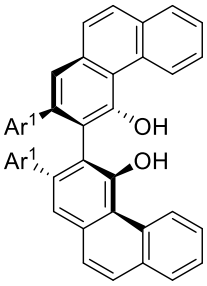

L2: Ar^1 = Ph, VAPOL
L3: Ar^1 = 4-OMe-3,5-Me_2-C_6H_5

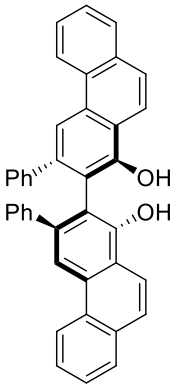

L4: *iso*VAPOL

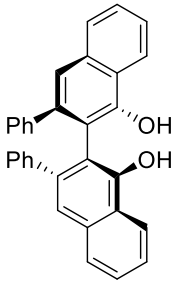

L5: VANOL

b) VANOL derivatives

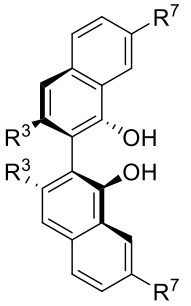

L6: R^3 = 4-OMe-C_6H_5, R^7 = H
L7: R^3 = 4-F-C_6H_5, R^7 = Br
L8: R^3 = 4-*n*Bu-C_6H_5, R^7 = Br
L9: R^3 = 4-OMe-3,5-Me_2-C_6H_5, R^7 = Br
L10: R^3 = Cy, R^7 = Br

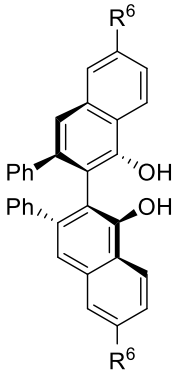

L13: R6 = 4-CF_3-C_6H_5

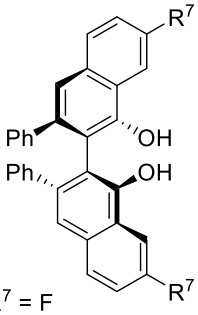

L15: R^7 = F
L16: R^7 = Cl
L17: R^7 = Me
L18: R^7 = Et
L19: R^7 = *n*Bu
L20: R^7 = *n*-hexyl
L21: R^7 = Cy
L22: R^7 = *t*Bu
L23: R^7 = adamantyl
L24: R^7 = 4-OMe-3,5-*t*Bu_2-C_6H_5
L25: R^7 = $SiPh_2$*t*Bu
L26: R^7 = 4-*t*Bu-C_6H_5
L27: R^7 = 3-thiopheneyl
L28: R^7 = 2-furyl
L29: R^7 = *i*Pr
L30: R^7 = *iso*pentyl
L31: R^7 = 3-phenylpropanyl

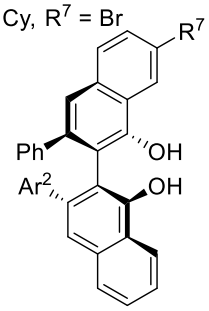

L11: Ar^2 = 4-OMe-3,5-Me_2-C_6H_5, R^7 = *t*Bu
L12: Ar^2 = 4-OMe-3,5-Me_2-C_6H_5, R^7 = I

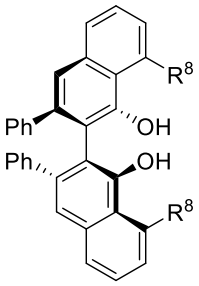

L14: R^8 = Ph

We first tried catalyst made from bulky vaulted biaryl ligand VAPOL (**L2**) as it was assumed that increasing the bulkiness of the ligand would enhance enantioselectivity. However, a 24% yield and 61% *ee* (Table 2.1, entry 2) was obtained for VAPOL (**L2**) and no conversion was observed for its derivative **L3** (Table 2.1, entry 3). **L4** as an isomer of **L2** gave 70% yield and 62% *ee* while VANOL (**L5**) gave 75% yield and 56% *ee* (Table 2.1, entries 4-5). Considering that VAPOL catalysts gave much slower reactions than that of VANOL and derivitization of *iso*VAPOL is not as easy as it is with VANOL, we decided to screen a large number of VANOL ligands that we have previously prepared (Figure 2.2).[14] We started with catalysts generated from the ligands **L6** to **L10** (Table 2.1) that are derivatives of VANOL at the 3,3'-positions in the VANOL backbone. The idea of screening these types of ligands is that a change in the dihedral angle between the naphthalenes in these ligands might enhance the asymmetric inductions, but to no avail. Moderate to good yields with 43-55% *ee* were obtained (entry 6-9) for those with derivatization on the phenyl groups in the 3.3'-positions, while none of them gave higher *ee* than VANOL. **L10** with a cyclohexyl group instead of phenyl group at the 3,3'-positions did not work (entry 10), probably because of the destruction of the π-system in the VANOL skeleton. The results obtained from the C_1-symmetrical ligands **L11** and **L12** did not lead to any significantly enhanced results (entry 11-12). The catalyst generated from the 6,6'-substituted VANOL **L13** increased the *ee* to 78% with good yield, indicating that changes made on naphthalene rings were more efficient than those on the backbone of the ligands (entry 13 vs entries 6-10). Low conversion was observed when the 8,8'-diphenyl

VANOL **L14** was used, presumably due to the steric bulk near the active site which might have either slowed down the reaction or hindered the formation of catalyst.

Table 2.1 Screening of ligands for the MPV reduction of 2-bromoacetophenone

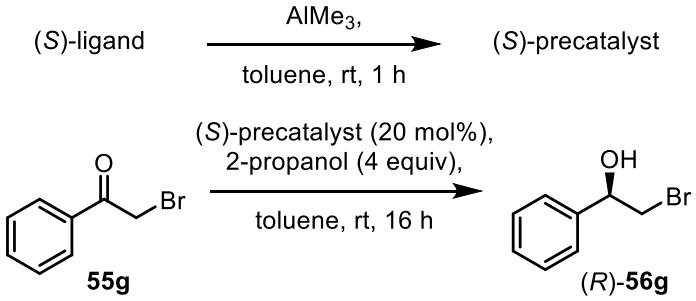

55g (*R*)-**56g**

Entry[a]	Ligand	% Yield[b]	% *ee*[c]	Entry[a]	Ligand	% Yield[b]	% *ee*[c]
1	(*S*)-**L1**	72	76	15	(*S*)-**L15**	68	60
2	(*S*)-**L2**	24	61	16	(*S*)-**L16**	74	58
3	(*S*)-**L3**	(<1)	—	17	(*S*)-**L17**	83	74
4	(*R*)-**L4**	70	-62	18	(*S*)-**L18**	50	80
5	(*S*)-**L5**	75	56	19	(*R*)-**L19**	72	-85
6	(*S*)-**L6**	41	53	20	(*S*)-**L20**	77	79
7	(*S*)-**L7**	71	43	21	(*S*)-**L21**	86	92
8	(*S*)-**L8**	70	45	22	(*S*)-**L22**	77	62
9	(*S*)-**L9**	79	55	23	(*S*)-**L23**	31	10
10	(*S*)-**L10**	(<1)	—	24	(*S*)-**L24**	(<5)	—
11	(*S*)-**L11**	(<5)	—	25	(*S*)-**L25**	(<1)	—
12	(*S*)-**L12**	66	65	26	(*S*)-**L26**	48	58
13	(*S*)-**L13**	53	78	27	(*R*)-**L27**	25	-43
14	(*S*)-**L14**	(<3)	—	28	(*R*)-**L28**	46	-33

[a] Reactions were performed on 0.25 mmol scale at 0.1 M. [b] Isolated yields are reported; Yields in parentheses are determined by crude ^{1}H NMR using triphenylmethane as an internal standard.[c] Determined by chiral HPLC; Minus *ee* means that the product is the enantiomer of (*R*)-**56g**.

Gratifyingly, modification of the 7,7'-positions of VANOL gave promising results especially for those with aliphatic substituents (entry 15-28). **L15** and **L16** bearing fluorine and chlorine and thus electron-deficient ligands showed neither acceleration of reactions nor notable enhancement of asymmetric inductions (entry

15-16). When aliphatic substituents were attached at 7,7'-positions of VANOL, significant improvements in the enantioselectivity was observed from methyl groups (74% *ee*, entry 17), ethyl groups (80% *ee*, entry 18) to *n*-butyl groups (85% *ee*, entry 19). The longer substituent (*n*-hexyl) led to a drop in *ee* (79% *ee*, entry 20), which stopped us from making any longer groups, but rather turned to bulkier groups. However, *t*-butyl groups decreased the *ee* to 62% (entry 22) and adamantyl groups resulted in both low conversion and low *ee* (entry 23), which indicated that tertiary groups might be too bulky. Unsurprisingly, **L21** with secondary cyclohexyl groups were found to have the best size and won the championship with 86% yield and 92% *ee* (entry 21). Further investigation found that various aryl and heteroaryl groups as well as silyl groups were not nearly as effective, giving either low conversion or modest enantioselectivities (entry 24-28).

2.3.2 Preliminary optimization of reaction parameters

After ligand screening, **L22** (7,7'-*t*Bu$_2$VANOL) was chosen as the ligand to do further optimization on various reaction parameters because of its ready availability and because it only had a moderate asymmetric induction. The precatalyst was prepared by addition of trimethylaluminum into **L22** toluene solution at room temperature. Stirring for 5 min gave lower yield and *ee* than stirring for 1 h (Table 2.2, entries 1-2). Then the reaction solution was charged with 2-propanol and 2-bromoacetophenone **55g** to initiate the asymmetric MPV reduction. Changing the ligand/ trimethylaluminum ratio led to a drop in yield and no improvement in *ee*, no matter whether excess trimethylaluminum or excess ligand was used (entries 3-6). Changing the loading of 2-propanol to 2 equivalents

decreased the yield while the use of 3 or 5 equivalents of 2-propanol had no significant differences from 4 equivalents (entry 7-9). The temperature effect was studied and the finding was that lower temperatures helped obtain higher asymmetric induction (entries 10-14). However, the reaction slowed down dramatically at –40 ˚C, and gave only a 23% isolated yield after 48 hours.

Table 2.2 Preliminary optimization of reaction conditions

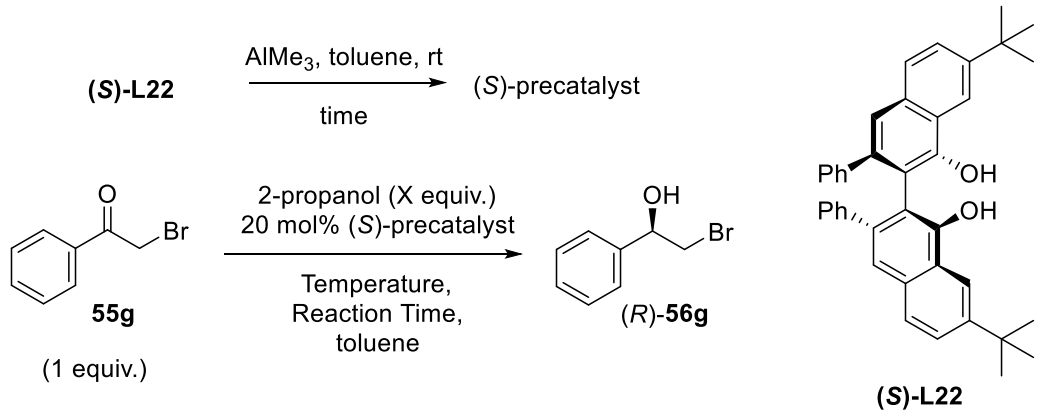

entry[a]	ligand : $AlMe_3$ ratio	time	X equiv.	Temperature (°C)	Reaction Time (h)	% yield[b]	% *ee*[c]
1	1 : 1	5 min	4	r.t.	16	44	52
2	1 : 1	1 h	4	r.t.	16	67	57
3	1 : 1.2	1 h	4	r.t.	16	47	55
4	1 : 1.5	1 h	4	r.t.	16	37	11
5	1.2 : 1	1 h	4	r.t.	16	37	57
6	2.0 : 1	1 h	4	r.t.	16	36	58
7	1 : 1	1 h	2	r.t.	16	31	56
8	1 : 1	1 h	3	r.t.	16	64	58
9	1 : 1	1 h	5	r.t.	16	57	57
10	1 : 1	1 h	4	100	16	62	5
11	1 : 1	1 h	4	60	16	71	13
12	1 : 1	1 h	4	40	16	73	51
13	1 : 1	1 h	4	-20	16	28	68
14	1 : 1	1 h	4	-40	48	23	69

[a] Reactions were performed on 0.25 mmol scale at 0.2 M. [b] Isolated yields are reported.
[c] Determined by chiral HPLC.

2.3.3 Further optimizations on the reduction of 2-bromoacetophenone

Table 2.3 Solvent screening for the MPV reduction of 2-bromoacetophenone

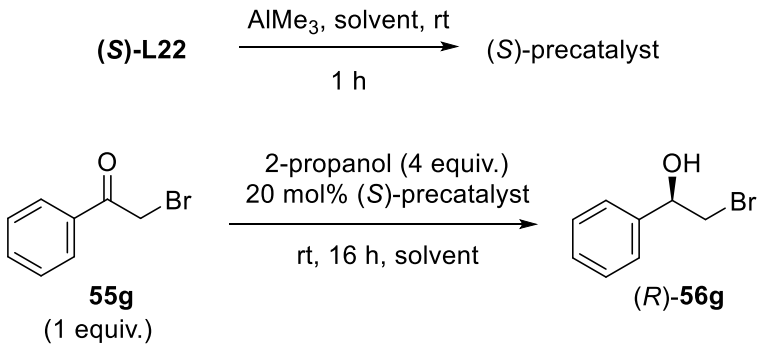

entry[a]	solvent	yield[b] (%)	*ee*[c] (%)	dielectric constant
1	THF	1	27	7.52
2	Et_2O	31	43	4.27
3	anisole	56	19	4.33
4	DCE	70	44	10.42
5	DCM	60	48	9.08
6	toluene	73	54	2.38
7	m-xylene	73	56	2.37
8	benzene	80	56	2.28
9	mesitylene	78	58	2.40
10	cyclohexane	73	61	2.02
11	*n*-hexanes	82	59	1.89
12	*n*-pentane	79	62	1.84

[a] Reactions were performed on 0.25 mmol scale at 0.3 M. [b] Isolated yields are reported. [c] Determined by chiral HPLC. THF = tetrahydrofuran, Et_2O = diethyl ether, DCE = 1,2-dichloroethane, DCM = dichloromethane.

When the reduction of 2-bromoacetophenone **55g** was screened in different solvents with a constant amount of 2-propanol (4 equiv.), it was found that strongly coordinating solvents such as THF and diethyl ether resulted in a dramatic drop in yield (Table 2.3, entries 1-2). This is presumably due to the coordination of solvent

to the aluminum preventing the coordination of the ketone and the formation of the proper 4 or 5 coordinate aluminum transition state.[13] The weakly coordinating solvent anisole and the polar solvents dichloromethane and 1,2-dichloroethane gave both lower yield and *ee* compared non-polar solvents such as toluene, benzene and cyclohexane (entries 3-12). The highest asymmetric induction was achieved with *n*-pentane, which has the lowest dielectric constant among common organic solvents (entry 12).

Table 2.4 Study on different methods of preparing catalysts

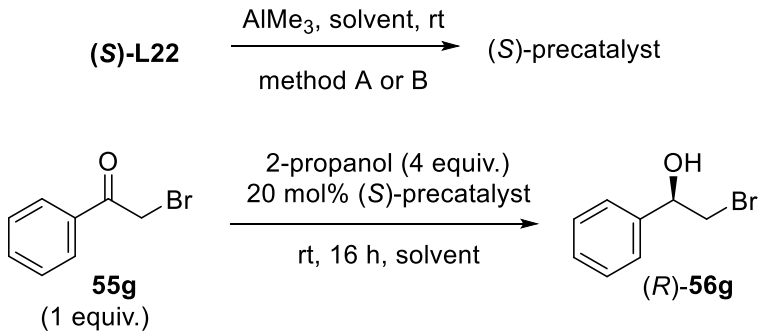

entry[a]	solvent	method	yield[b] (%)	*ee*[c] (%)
1	toluene	A	73	54
2	toluene	B	81	54
3	*n*-pentane	A	79	62
4	*n*-pentane	B	70	62
5	mesitylene	A	78	58
6	mesitylene	B	79	57

[a] Reactions were performed on 0.25 mmol scale at 0.3 M. Method A: Ligand and trimethylaluminum were stirred in toluene for 1 h before the addition of 2-propanol and 2-bromoacetophenone. Method B: Ligand and trimethylaluminum were stirred in toluene for 0.5 h before the addition of 0.2 equivalent of 2-propanol. The rest of 2-propanol (3.8 equiv.) and 2-bromoacetophenone were added after another 0.5 h. [b] Isolated yields are reported. [c] Determined by chiral HPLC.

In previous experiments, 2-propanol and 2-bromoacetophenone **55g** were added to the reaction solution containing the precatalyst at the same time (Table 2.4, method A). So once the active catalyst was in-situ generated, it would start catalyzing the reduction of ketones. It was important to see if forming the active catalyst before adding ketones would make any difference. Therefore, the active catalyst was prepared according to method B (Table 2.4). A solution of the ligand (0.2 equiv.) and trimethylaluminum (0.2 equiv.) was stirred for 0.5 h before the addition of 2-propanol (0.2 equiv.). After another 0.5 h, ketone (1 equiv.) and the rest of 2-propanol (3.8 equiv.) were charged into the reaction solution. Toluene, *n*-pentane and mesitylene were used as solvent to study the difference between method A and B, but no significant change in yield and *ee* was observed (entry 1-6). Therefore, method A was still employed for following studies.

Then the concentration effect was studied by changing the amount of solvent used in the reaction. Notably, lowering the concentration of the reaction had significant impact on the enantioselectivities. When toluene was used as solvent, a 15% increase in *ee* was achieved by diluting the reaction from 0.6 M to 0.1 M (Table 2.5, entries 1-4). Further dilution failed to give better results (entries 5-6). Same trends were observed while using mesitylene (7% *ee* increase upon diluting from 0.3 M to 0.1 M, entries 8-10) and *n*-pentane (10% *ee* increase upon diluting from 0.3 M to 0.1 M, entries 11-12) as solvent. This “dilution effect” is probably due to the aggregation of the aluminum complex at higher concentration. It has been shown that aluminum alkoxides can dimerize ($Al(O\textit{t}Bu)_3$) or tetramerize ($Al(O\textit{i}Pr)_3$) in solution.[15]

Table 2.5 Concentration effect for the MPV reduction of 2-bromoacetophenone

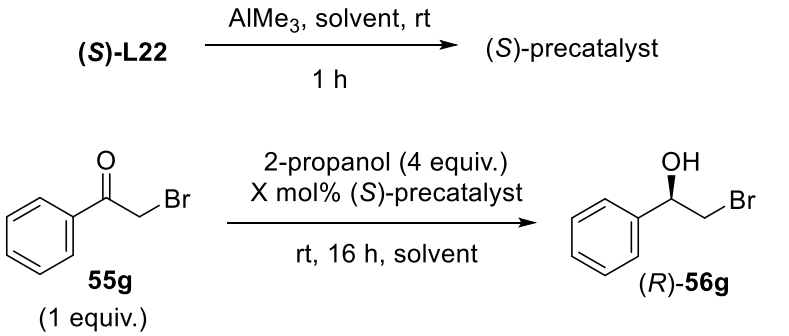

entry[a]	solvent	concentration (M)	X mol%	yield[b] (%)	*ee*[c] (%)
1	toluene	0.6	20	70	47
2	toluene	0.3	20	74	52
3	toluene	0.2	20	64	54
4[d]	toluene	0.1	20	77	62
5[e]	toluene	0.05	20	71	60
6[e]	toluene	0.025	20	56	59
7	toluene	0.1	10	68	60
8	mesitylene	0.3	20	65	55
9	mesitylene	0.2	20	70	59
10	mesitylene	0.1	20	69	62
11	*n*-pentane	0.3	20	79	62
12	*n*-pentane	0.1	20	71	72

[a] Reactions were performed on 0.25 mmol scale. [b] Isolated yields are reported. [c] Determined by chiral HPLC. [d] Result is the average of 4 runs. [e] Result is the average of 2 runs.

To make sure that the results obtained during the optimization process were reliable, the replicability of this MPV reduction was tested. Under the same conditions, 2-bromoacetophenone **55g** was reduced to the corresponding alcohol on different dates with different batches of trimethylaluminum, toluene and 2-propanol (Table 2.6). Consistent results were obtained as 72-83% yield and 61-63% *ee* with an average of 77% yield and 62% *ee* from 4 runs. The ± 6% yield and

± 1% *ee* were in reasonable ranges to be considered as systematic errors, which revealed satisfactory reproducibility on this asymmetric MPV reaction.

Table 2.6 Test of replicability

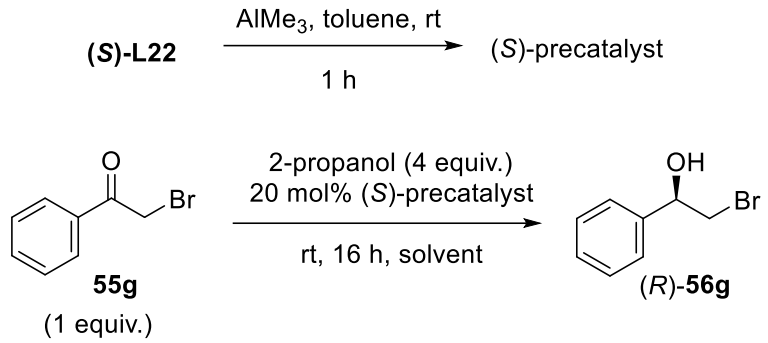

entry[a]	Date[b]	solvent	yield[c] (%)	*ee*[d] (%)
1	2017/2/17	toluene	72	63
2	2017/3/19	toluene	83	61
3	2017/4/23	toluene	77	61
4	2017/4/23	toluene	76	62

[a] Reactions were performed on 0.25 mmol scale at 0.1 M. [b] Date when these reactions were run on. [c] Isolated yields are reported. [d] Determined by chiral HPLC.

Some other alcohols as hydride source instead of 2-propanol were screened. Since the MPV reduction first employed ethanol as hydride source[16,17], we started with the screening of primary alcohols. However, none of these primary alcohols worked (Table 2.7, entries 1-9). Secondary alcohols like cyclohexanol, 2-butanol, 2-hexanol and 3,3-dimethyl-2-butanol all worked but were not as good as 2-propanol (entries 11, 14-17), the 2˚ alcohols 3-pentanol and 2,4-dimethyl-3-pentanol gave low induction and opposite stereochemical outcome compared with 2-propanol (entries 12-13). Two diols with bidentate properties were also tested but both failed (entries 18-19).

Table 2.7 Alcohol Screening for the MPV reduction of 2-bromoacetophenone

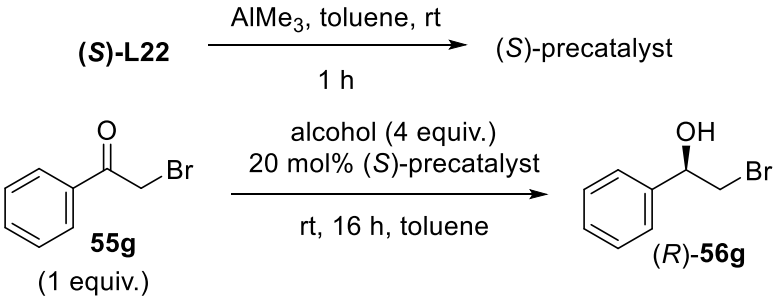

entry[a]	alcohol	type	yield[b] (%)	*ee*[c] (%)
1	methanol	primary	(<1%)	—
2	ethanol	primary	(<1%)	—
3	1-butanol	primary	(<1%)	—
4	1-octanol	primary	(<1%)	—
5	2-ethyl-1-butanol	primary	(<1%)	—
6	cyclopropanemethanol	primary	(<1%)	—
7	cyclohexanemethanol	primary	(<1%)	—
8	prop-2-en-1-ol	primary	(<1%)	—
9	4-pentyn-1-ol	primary	(<1%)	—
10[d]	2-propanol	achiral	77	62
11	cyclohexanol	achiral	64	54
12	3-pentanol	achiral	83	-5
13	2,4-dimethyl-3-pentanol	achiral	40	-22
14	2-butanol	racemic	81	47
15	2-hexanol	racemic	76	53
16	2-octanol	racemic	(<1%)	—
17	3,3-dimethyl-2-butanol	racemic	44	36
18	2,3-butanediol	diol	(<1%)	—
19	2,5-hexanediol	diol	(<1%)	—

[a] Reactions were performed on 0.25 mmol scale at 0.1 M. [b] Isolated yields are reported; Yields in parentheses are determined by crude ^{1}H NMR using triphenylmethane as an internal standard.[c] Determined by chiral HPLC; Minus *ee* means that the product is the enantiomer of (*R*)-**56g**.[d] Result is the average of 4 runs.

After the study of the reaction parameters with **L22**, we have a better understanding about how those conditions influence the yield and enantioselectivity of this asymmetric MPV reduction. And then **L21**, which was harder to synthesize but gave the best result during ligand screening, was employed in further optimizations (Table 2.8). It was possible to reduce the catalyst loading to 5 mol% without erosion of asymmetric induction while using *n*-pentane as solvent (entries1-3). Shortening the reaction time to 6 hours had no significant impact on yield while lowering the temperature to 0 ˚C increased the *ee* to 94% (entry 4-5).

Table 2.8 Further optimizations with **L21** as ligand

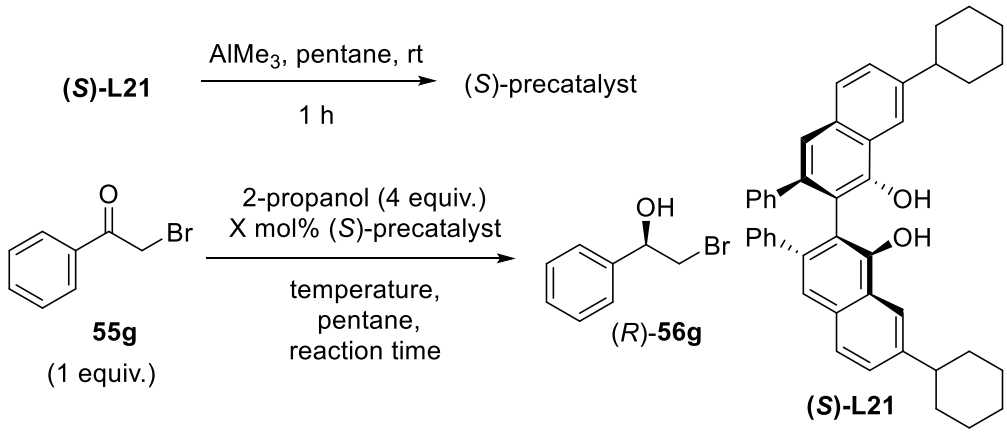

entry[a]	catalyst loading X mol%	temperature	reaction time (h)	% yield[b]	% *ee*[c]
1	20	rt	16	86	91
2	10	rt	16	85	91
3	5	rt	16	90	92
4	5	rt	6	85	92
5	5	0 °C	6	77	94

[a] Reactions were performed on 0.25 mmol scale at 0.1 M. [b] Isolated yields are reported. [c] Determined by chiral HPLC.

2.3.4 Optimizations on the reduction of 4'-bromoacetophenone

Considering that 2-bromoacetophenone **55g** is the best substrate in Nguyen's aluminum-BINOL system owing to its bidentate nature, it was important to study how the current catalyst works on other ketones without the 2-halo functional group. Therefore, further study was performed on 4'-bromoacetophenone **55u**, which gave the alcohol **56u** in 70% yield with 30% ee with the BINOL catalyst **48** in toluene under the conditions in Scheme 1.8.

Table 2.9 Optimizations on the reduction of 4'-bromoacetophenone

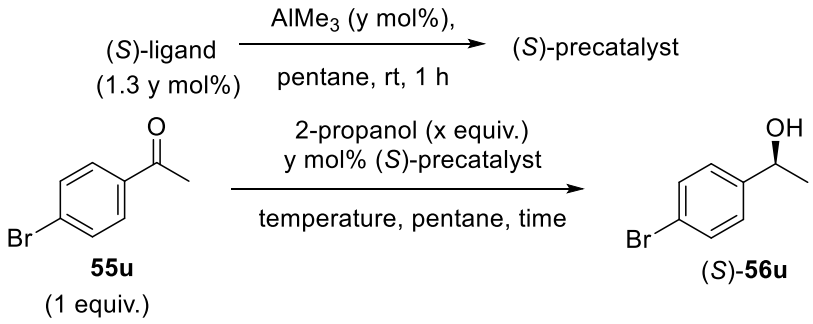

entry[a]	ligand	time (h)	temperature (°C)	x equiv.	y mol%	% yield[b]	% *ee*[c]
1	(*S*)-**L21**	6	rt	4	5	76	85
2	(*R*)-**L21**	6	0	4	5	48	-92
3	(*R*)-**L21**	6	0	10	5	53	-90
4	(*R*)-**L21**	6	0	20	5	67	-90
5	(*S*)-**L21**	6	0	40	5	79	94
6	(*S*)-**L21**	6	0	80	5	91	94
7	(*S*)-**L21**	6	0	40	2	67	95
8	(*S*)-**L21**	24	0	80	2	81	93
9	(*S*)-**L21**	12	0	40	1	(<5)	—
10	(*S*)-**L21**	6	-10	80	5	84	96
11[d]	(*R*)-**L21**	6	-10	80	5	94	-96

[a] Reactions were performed on 0.25 mmol scale at 0.1 M. [b] Isolated yields are reported; Yields in parentheses are determined by crude ^{1}H NMR using triphenylmethane as an internal standard.[c] Determined by chiral HPLC; Minus *ee* means that the product is the enantiomer of (*S*)-**56u**. [d] With 4 Å MS (100 mg/mmol).

With 5 mol% catalyst prepared from (*S*)-**L21** (7,7'-Cy_2VANOL), the corresponding alcohol (*S*)-**56u** was obtained in 76% yield and 85% *ee* at room temperature in *n*-pentane (Table 2.9, entry 1). Lowering the temperature to 0 ºC increased the induction to 92% *ee* but the yield dropped to 48% (entry 2). However, if the amount of 2-propanol was increased from 4 equivalents to 80 equivalents, the yield was greatly improved from 48% to 91% at the same reaction time without erosion of enantioselectivity (entries 2-6). It was not surprising that the yield was improved since increasing the loading of 2-propanol helps drive the reaction forward. Nguyen and co-workers have demonstrated that higher loading of 2-propanol resulted in a drop of enantioselectivities,[11] which was not observed in our VANOL catalysts. Notably, the catalyst loading could be reduced to 2 mol%, providing **56u** with 81% yield and 93% *ee* after 24 hours (entry 8). The best result (94% yield and 96% ee) was obtained while running the reaction at –10 ºC with the addition of 4 Å molecular sieves (entry 11).

Under the optimal conditions in Table 2.9 (entry 11), other ligands were examined to compare with the results from **L21**. The use of **L29** (7,7'-*i*Pr_2VANOL, Table 2.10, entry 2) and **L30** (7,7'-isopentyl$_2$VANOL, entry 3) gave no better yield or *ee* than that of **L21**, while **L31** (7,7'-(3-penylpropyl)$_2$VANOL, entry 4) showed low conversion. It was observed that reactions with VANOL (**L5**) and BINOL (**L1**) catalysts under the same conditions gave less than 1-2% of the reduced product **56u** (entries 5-6), indicating the importance of attaching proper substituents at the 7,7'-positions of the VANOL ligand. It is possible that one role of the cyclohexyl groups helps to prevent aggregation or oligomerization of the catalyst.

Table 2.10 Reduction of 4'-bromoacetophenone with different ligands

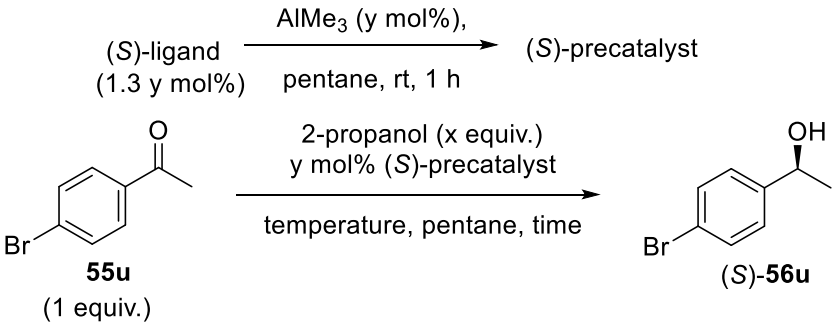

entry[a]	ligand	time (h)	temperature (°C)	x equiv.	y mol%	% yield[b]	% *ee*[c]
1	(*R*)-**L21**	6	-10	80	5	94	-96
2	(*S*)-**L29**	6	-10	80	5	82	94
3	(*S*)-**L30**	6	-10	80	5	89	95
4	(*S*)-**L31**	6	-10	80	5	(<5)	—
5	(*S*)-**L5**	6	-10	80	5	(<2)	—
6	(*S*)-**L1**	6	-10	80	5	(<1)	—

[a] Reactions were performed on 0.25 mmol scale at 0.1 M with 4 Å MS (100 mg/mmol). [b] Isolated yields are reported; Yields in parentheses are determined by crude ^{1}H NMR using triphenylmethane as an internal standard.[c] Determined by chiral HPLC; Minus *ee* means that the product is the enantiomer of (*S*)-**56u**.

2.4 Substrate scope for aromatic ketones

Under the optimal conditions established above, a variety of aromatic ketones were examined. Acetophenone **55a** was reduced in 88% yield and 94% *ee* (Scheme 2.2) to the alcohol **56a** by the catalyst prepared from **L21**, whereas the reduction with BINOL catalyst **48** from Nguyen's work[11] gave 58% yield and 28% *ee* (Scheme 1.8). Likewise, 2-acetonaphthanone **55b** and 1-acetonaphthanone **55c** were reduced to the corresponding alcohols **56b** and **56c** in 78% yield, 91% *ee* and 95% yield, 98% *ee* respectively. Ketones with 2-halo methyl groups were the only type of ketones that gave high asymmetric inductions with Nguyen's BINOL catalyst (Scheme 1.8), possibly because the coordination

between 2-halo substituent and the carbonyl oxygen with the aluminum center gave a penta-coordinated aluminum species in the transition state.

Scheme 2.2 Substrate scope for aromatic ketones I

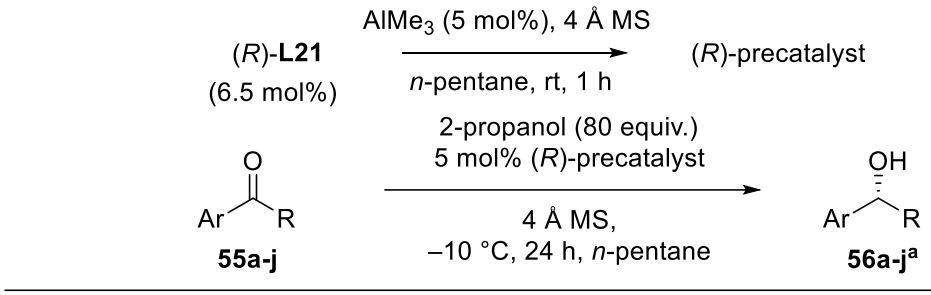

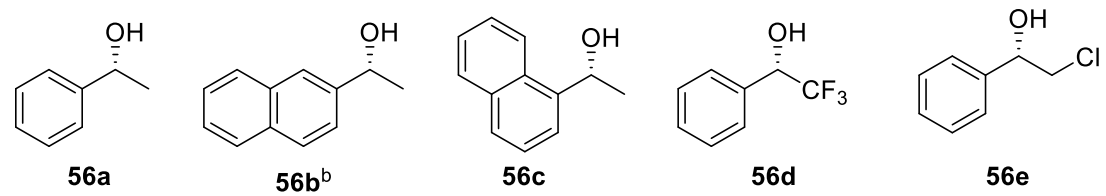

56a	56b[b]	56c	56d	56e
88% yield 94% ee	78% yield 91% ee	95% yield 98% ee	71% yield 96% ee	98% yield 99% ee

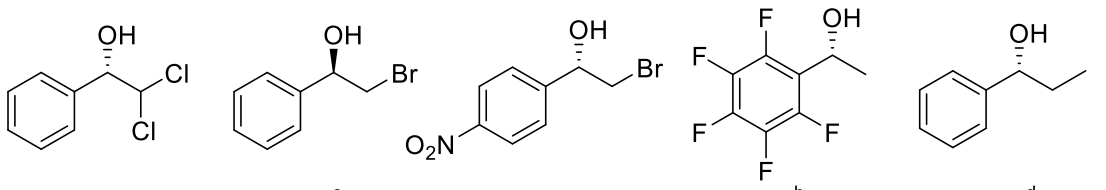

56f	56g[c]	56h	56i[b]	56j[d]
94% yield >99% ee	87% yield 97% ee	95% yield 98% ee	80% yield 99% ee	57% yield 74% ee

[a] Reactions were performed on 0.25 mmol scale at 0.1 M with 4 Å MS (100 mg/mmol); isolated yields are reported; *ee* is Determined by chiral HPLC. [b] With 10 mol% precatalyst used instead of 5 mol%. [c] (S)-**L21** was used as ligand and reaction was carried at 0 °C for 6 h. [d] Reaction was carried at rt and gave 65% conversion.

A number of acetophenone derivatives with halogens at the 2-positon were tested with the catalyst prepared from **L21**. High yields with excellent enantioselectivities were obtained under optimal conditions for 2,2,2-trifluoro, 2-chloro, 2,2-dichloro, 2-bromo and 2-bromo-4'-nitroacetophenones. Electron-deficient penta-fluoroacetophenone **55i** was reduced in 80% yield and 99% *ee*.

However, low conversion was observed when propiophenone **55j** was reduced under the same conditions, however a 57% yield and 74% *ee* was obtained by running the reaction at room temperature. The absolute configurations of the products were confirmed by comparing their optical rotations with literature values, and in addition, the absolute configuration of **56h** was confirmed by its crystal structure.

It is obvious that the electron density of the substrate will have significant impact on the reactivity of these ketone reductions. Thus, a wide range of acetophenone derivatives were examined with both electron-rich and electron-poor substituents at the *ortho*, *meta* and *para* positions of phenyl group (Scheme 2.3). *Ortho*-substituted acetophenones with electron-withdrawing groups such as chloro, bromo and iodo as well as electron-donating groups such as methoxy were all reduced in excellent yields and excellent enantioselectivities. The reduction of 2'-methylacetophenone **55n** gave lower conversion at standard conditions, but 94% yield and 96% *ee* was achieved by increasing the catalyst loading to 10 mol%. It was a little surprising to find that 2'-methoxyacetophenone **55o** was reduced faster than 2'-methylacetophenone **55n** with 5 mol% catalyst loading, considering that the former is more electron-rich, which should be disfavored in reduction of ketones. An explanation might be that the oxygen at *ortho*-position could coordinate to the aluminum center, serving a similar role as the 2-halo functional groups. In the *meta* positions, the electron-withdrawing group bromine gave 91% yield and 97% *ee*. Electron-releasing groups as methyl and methoxy gave slower reduction under the standard conditions. Increasing catalyst loading to 10 mol%

for 3'-methylacetophenone **55q** resulted in 82% yield and 90% *ee*, while increasing both the catalyst loading and reaction temperature gave 84% yield and 88% *ee* on the reduction of 3'-methoxyacetophenone **55r**.

Scheme 2.3 Substrate scope for aromatic ketones II

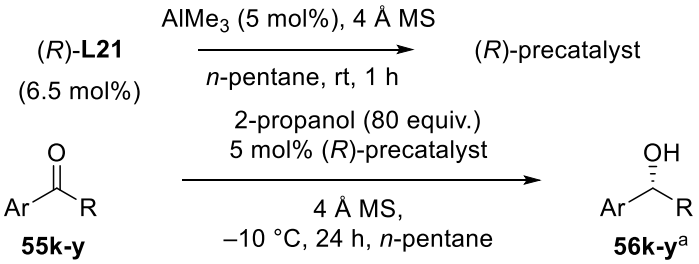

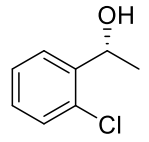

56k[b]

96% yield
99% ee

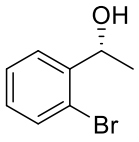

56l

90% yield
99% ee

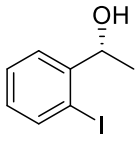

56m

96% yield
93% ee

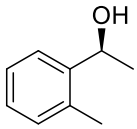

56n[c,d]

94% yield
96% ee

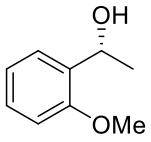

56o

93% yield
94% ee

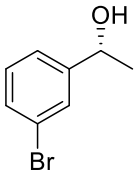

56p

91% yield
97% ee

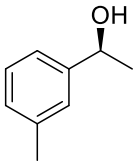

56q[c,d]

82% yield
90% ee

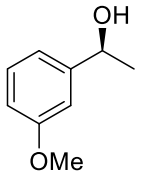

56r[c,d,e]

84% yield
88% ee

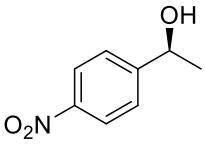

56s[c]

92% yield
97% ee

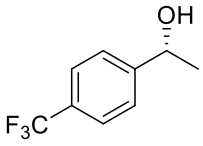

56t

91% yield
97% ee

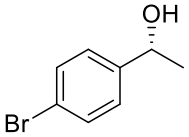

56u[b]

94% yield
96% ee

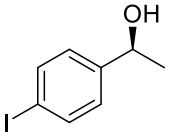

56v[c,d]

89% yield
93% ee

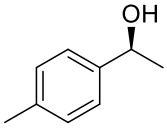

56w[c,d]

70% yield
92% ee

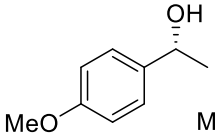

56x

<1% yield

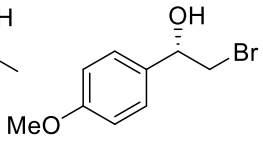

56y[d]

71% yield
83% ee

[a] Reactions were performed on 0.25 mmol scale at 0.1 M with 4 Å MS (100 mg/mmol); isolated yields are reported; *ee* is Determined by chiral HPLC. [b] Reaction time is 6 h. [c] (S)-**L21** was used as ligand. [d] With 10 mol% precatalyst used instead of 5 mol%. [e] Reaction was carried at 0 °C.

As for the *para* positions, a number of electron-withdrawing groups did not seem to affect the asymmetric induction, such as 4'-nitroacetophenone **55s**, 4'-trifluoromethylacetophenone **55t**, 4'-bromoacetophenone **55u** and 4'-iodoacetophenone **55v**, where 89-94% yield and 93-97% *ee* were observed. Although the 4'-methylacetophenone **55w** can be reduced effectively with 10 mol% catalyst loading, the 4'-methoxyacetophenone **55x** is not reduced at all. It is possible that the oxygen at the *ortho*-position coordinates to the aluminum while the oxygen at the *para*-position is too far away to form a penta-coordinated aluminum species. Another possibility is that *ortho*-substitution resulted in poor delocalization due to the steric hindrance that the carbonyl group and phenyl group are not on the same plane. The electron density of **55o** is lower than that of **55x** and thus **55o** showed higher reactivity. It is interesting to observe that the presence of a bromo group alpha to the ketone can largely offset the effect of the 4-methoxy group, with 71% yield and 83% *ee* achieved on the reduction of 2-bromo-4'-methoxyacetophenone **55y**.

There are also limitations on the substrate scope of this asymmetric MPV reduction (Scheme 2.4). Penta-methylacetophenone **5a** was not reduced under the standard conditions, which might result from its steric bulkiness that prevents the coordination with aluminum and also its electron density that makes the carbonyl less reactive. It was previously shown that propiophenone **55j** gave lower yield and asymmetric induction (Scheme 2.2). Increasing the bulkiness of the ketone substituent to *n*-propyl and phenyl shuts down the reaction as observed for **5b** and **5c**. Therefore, this catalytic system is limited to the reduction of methyl

ketones. Enone **5d** and ynone **5e** were also tested but failed. A free hydroxy group and amino group on the acetophenone in the *ortho*-position were not tolerated, probably because they could kill the catalyst by binding to the aluminum and replace the VANOL ligand or an isopropoxide (**5f-g**). An acetoxy group is not tolerated either, possibly due to competition between the acetoxy and acetyl carbonyls in coordinating to the catalyst (**5h**). Unfortunately, ketones bearing a heterocycle were not reduced. The basicity of pyridyl group might kill the catalyst and the high electron density of pyrrolyl, thiophenyl and furyl groups might be responsible for their low reactivities (**5i-l)**.

Despite these limitations in the substrate scope, the present aluminum-VANOL catalyst is far superior to previously reported aluminum catalysts for MPV reduction.[11,18] Their systems only gave high asymmetric inductions on ketones with two binding sites, such as 2-haloacetophenone, while our aluminum-VANOL catalysts gave high yield and enantioselectivities on many simple aromatic ketones with different electron densities that have only one binding site. With many excellent results gained from aryl alkyl ketones, we learned that the catalyst has great ability in distinguishing sp^3 carbons from sp^2 carbons. Our attention was turned to the more challenging task of distinguishing sp^3 carbons from other sp^3 carbons.

Scheme 2.4 Limitations on substrate scope

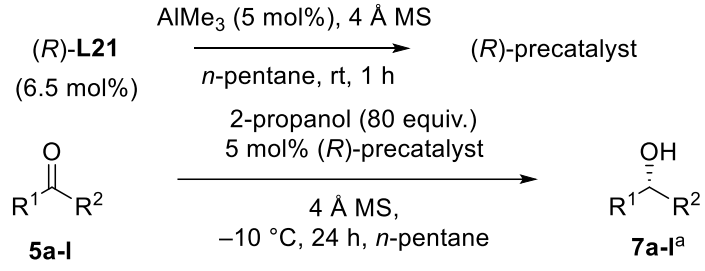

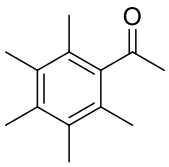 **5a** <1 conv.	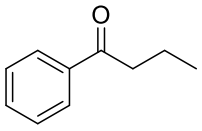 **5b** <1% conv.	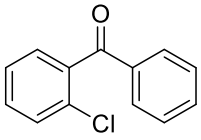 **5c** <1% conv.	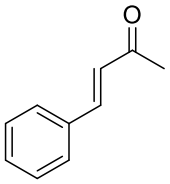 **5d** <1% conv.
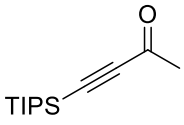 **5e** <1% conv.	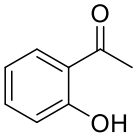 **5f** <1% conv.	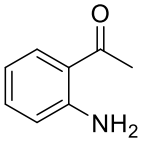 **5g** <1% conv.	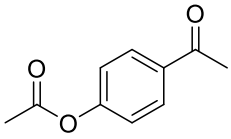 **5h** <1% conv.
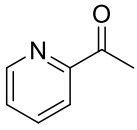 **5i** <1% conv.	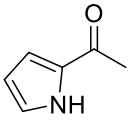 **5j** <1% conv.	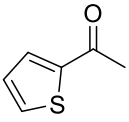 **5k** <1% conv.	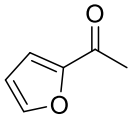 **5l** <5% conv.

[a] Reactions were performed on 0.25 mmol scale at 0.1 M with 4 Å MS (100 mg/mmol); conversion is determined by crude ^{1}H NMR with triphenylmethane as internal standard.

2.5 Substrate scope for aliphatic ketones

The asymmetric reduction of simple dialkyl ketones with a chiral aluminum catalyst has never been reported. Thus, it is important to examine the ability of our catalyst in the reduction of aliphatic ketones. The substrate we chose for further optimization was 3-phenyl-2-butanone **57a**, which bears a phenyl group that is not in conjugation with the carbonyl group. The reason **57a** was chosen is that it has

good UV absorption at 210 nm, so the corresponding alcohol **58a** can be detected on chiral HPLC to measure its enantioselectivity without derivatization. Under the optimal conditions for aromatic ketones, the ketone **57a** was reduced in 84% yield and 74% *ee* (Table 2.11, entry 7). Screening catalysts prepared from other ligands (entries 8-10) revealed that 7,7'-*i*pentyl$_2$VANOL **L30** gave the best asymmetric induction (entries 1-6). Changing the temperature to –20 ˚C gave the reduction product **58a** in 91% yield and 82% *ee*, while increasing or decreasing the temperature resulted in a drop in both yield and *ee* (entry 4).

Table 2.11 Optimization on the reduction of 3-phenyl-2-butanone

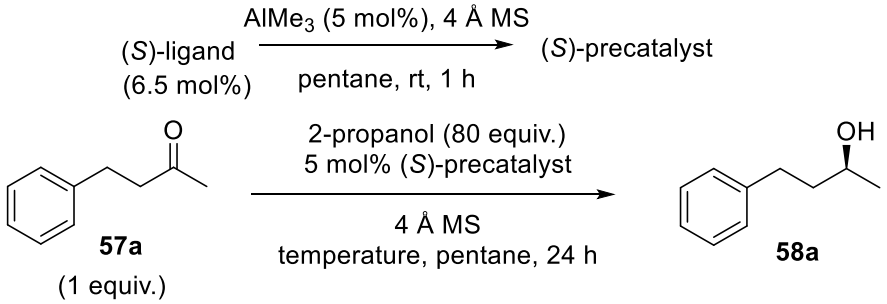

entry[a]	ligand	temperature (°C)	% yield[b]	% *ee*[c]
1	7,7'-*i*Pentyl$_2$VANOL (*S*)-**L30**	rt	73	70
2	7,7'-*i*Pentyl$_2$VANOL (*S*)-**L30**	0	74	80
3	7,7'-*i*Pentyl$_2$VANOL (*S*)-**L30**	-10	87	80
4	7,7'-*i*Pentyl$_2$VANOL (*S*)-**L30**	-20	91	82
5	7,7'-*i*Pentyl$_2$VANOL (*S*)-**L30**	-30	75	81
6	7,7'-*i*Pentyl$_2$VANOL (*S*)-**L30**	-40	63	77
7	7,7'-Cy$_2$VANOL (*S*)-**L21**	-10	84	74
8	7,7'-*t*Bu$_2$VANOL (*S*)-**L22**	-20	40	68
9	7,7'-*i*Pr$_2$VANOL (*S*)-**L29**	-20	71	69
10	7,7'-(3-phenylpropyl)$_2$VANOL (*S*)-**L31**	-20	12	54

[a] Reactions were performed on 0.25 mmol scale at 0.1 M with 4 Å MS (100 mg/mmol).
[b] Isolated yields are reported.[c] Determined by chiral HPLC.

Anticipating that the degree of asymmetric induction would correlate with the steric differential of the two alkyl groups on the ketone, two other ketones bearing a 2˚ cyclohexyl group **57b** and a 3˚ adamantyl group **57c** were examined (Scheme 2.5). Due to the lack of chromophore for these two substrates, the yield and *ee* were determined after making the corresponding 4-fluorobenzoic ester of the alcohol products. The most difficult substrate in terms of steric differential between the two alkyl groups was 3-phenyl-2-butanone **57a** with 91% yield and 82% *ee*, which has a methyl group and an unbranched alkyl group to be distinguished by the catalyst. Better results were obtained on substrate **57b** at –10 ˚C, which has a methyl group and a cyclohexyl group on the ketone. After derivatizing to the corresponding 4-fluorobenzoic ester, 81% yield and 88% *ee* were observed. Unsurprisingly, the ketone **57c** with the bulkiest substituent gave the highest stereochemical outcome of 94% *ee* in 84% yield. This study illustrates the first examples of aluminum-catalyzed asymmetric reduction of aliphatic ketones.

Scheme 2.5 Substrate scope for aliphatic ketones

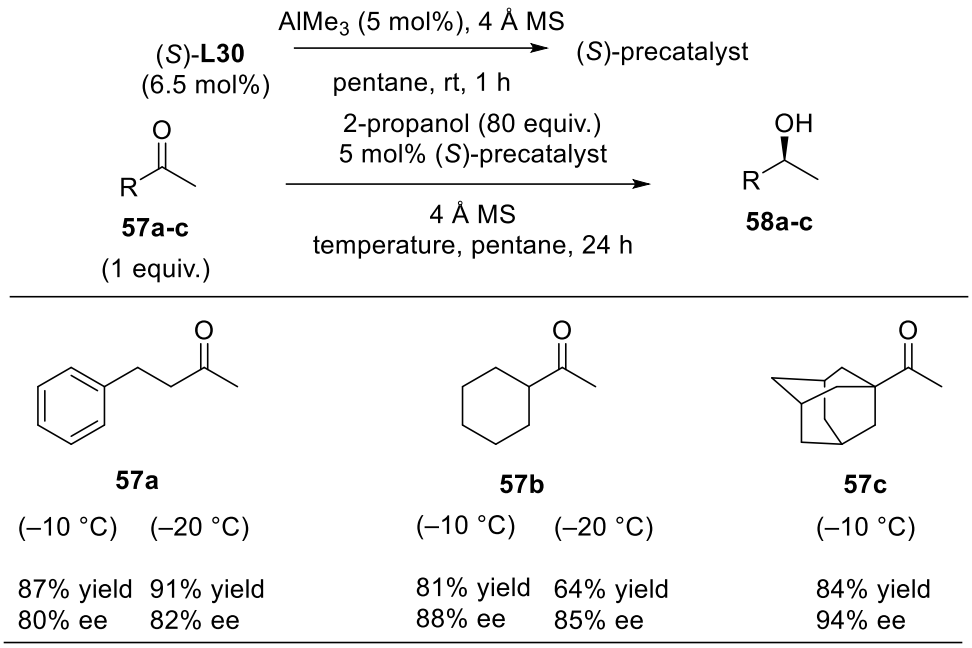

[a] Reactions were performed on 0.25 mmol scale at 0.1 M with 4 Å MS (100 mg/mmol); isolated yields are reported; *ee* is determined by chiral HPLC. [b] Yield and ee are determined after making the corrsponding 4-fluorobenzoic ester.

2.6 Scale up synthesis with 1 mol% catalyst loading

The scalability of this MPV reduction was examined on a 32-fold increase in scale of the reduction of 2-bromoacetopheone **55g** (Scheme 2.6). On an 8 mmol scale the reduction proceeded smoothly with the catalyst loading reduced to 1 mol% catalyst to give the alcohol **56g** in 90% yield and 97% *ee*. This result is essentially unchanged from the 0.25 mmol scale reaction at 5 mol% catalyst (Scheme 2.2). The corresponding alcohol (*(S)*-**56g**) was then treated with potassium carbonate to give chiral epoxide **59** with retention of enantiomeric purity (Scheme 2.6).

Scheme 2.6 Scale up synthesis

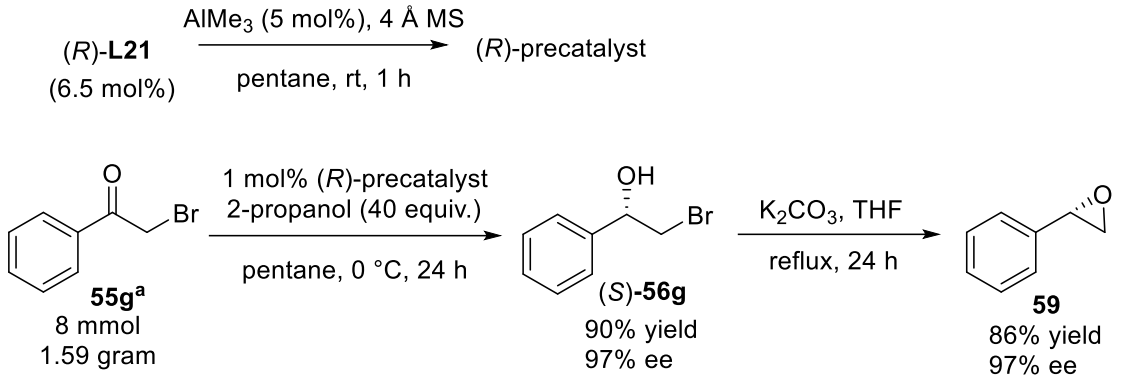

[a] Reduction was performed at 0.2 M with 800 mg 4 Å MS in 16 ml pentane and 24 ml 2-propanol. Epoxidation was performed at 0.2 M in THF with 1.5 equiv. anhydrous potassium carbonate.

2.7 Reaction mechanism and computational study

2.7.1 Mechanism of MPV reduction of ketones

The mechanism of the MPV has long been thought to involve a four-coordinate aluminum transition state with an intramolecular transfer of hydride from an isopropoxy substituent on aluminum to a molecule of ketone coordinated to the aluminum as indicated in Scheme 2.7a.[12] In the particular case of the BINOL aluminum catalyst **48** developed by Nguyen, the mechanism of reduction was explored by DFT analysis and this direct transfer was found to be more energetically favorable that either a radical mechanism or a hydride mechanism involving an aluminum hydride (Scheme 2.7b).[12] In the case of the substrate **55g**, a transition state for direct transfer with a five-coordinate aluminum was proposed (Scheme 2.7c).[13]

Scheme 2.7 Mechanism of MPV reduction of ketones

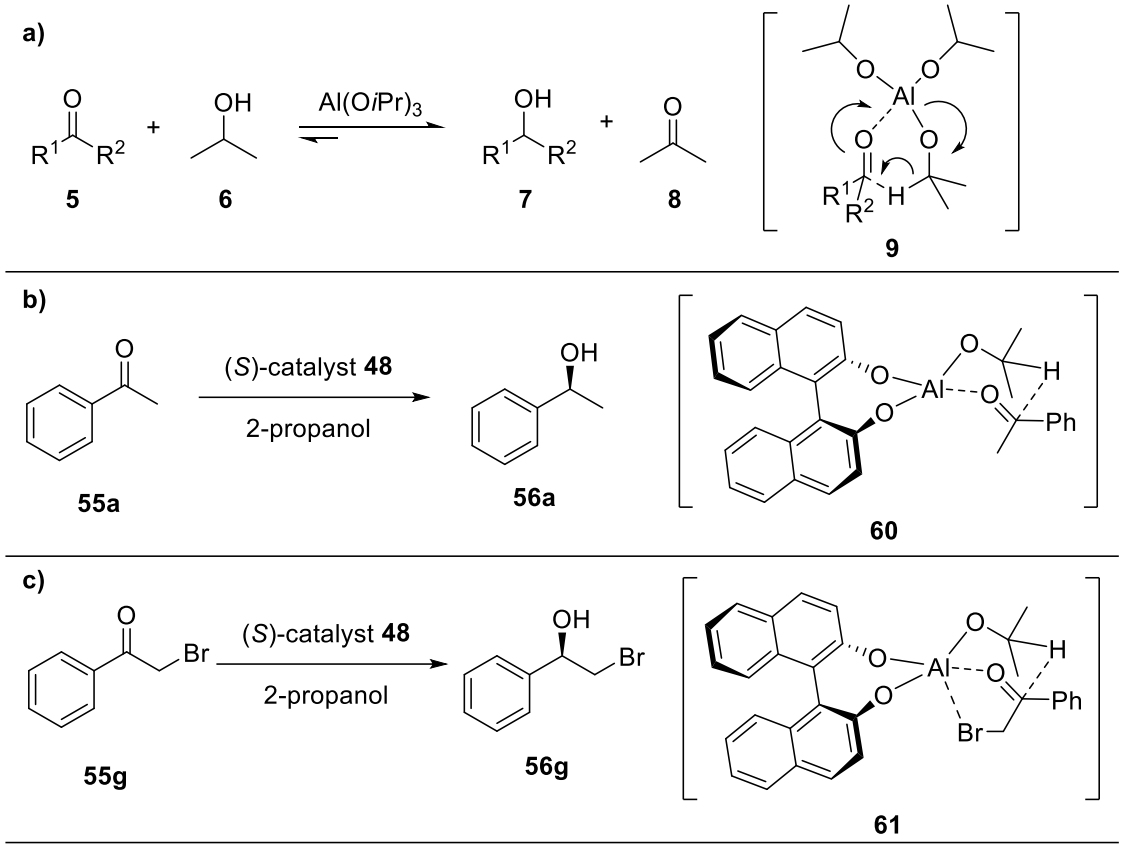

a) Widely-accepted mechanism of MPV reduction of ketones with a six-member ring hydride transfer transition state. **b)** The asymmetric reduction of acetophenone with Nguyen's BINOL catalyst and the proposed tetra-coordinated aluminum in the transition state. **c)** The asymmetric reduction of 2-bromoacetophenone with Nguyen's BINOL catalyst and the proposed penta-coordinated aluminum in the transition state.

2.7.2 Computational study

During the discovery of this MPV reduction methodology, a lot of effort was expended to predict the best ligand for this reaction employing computational study. Over 2000 transition state energies with 30 different ligands have been calculated and analyzed. Twelve of these ligands (**L5-L31**) have been synthesized and screened in this asymmetric MPV reaction, while the other eighteen ligands (**L32-L49**) were designed and studied by computational modelling only (Figure 2.3). The transition state with a six-member ring hydride transfer on the reduction of

acetophenone **55a** was modeled as shown in Figure 2.3. With all ligands being *S*, **TS-S** is the transition state towards the formation of *S* product (*S*)-1-phenyl-ethanol and **TS-R** is the transition state towards the formation of *R* product (*R*)-1-phenyl-ethanol. Transition state energies (electronic energies, enthalpies and free energies) for both **TS-S** and **TS-R** have been calculated to elucidate and predict the enantioselectivity of the asymmetric reduction.

Figure 2.3 Computational study with 30 ligands

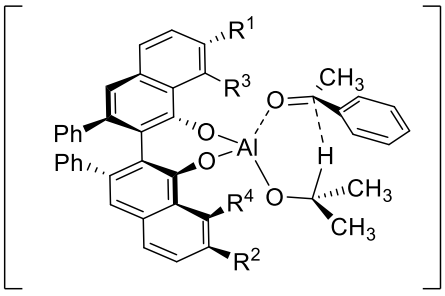

TS-S

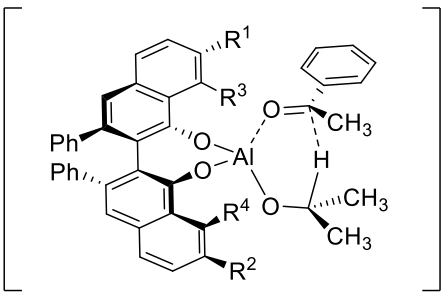

TS-R

L5: $R^1 = R^2 = R^3 = R^4 = H$
L14: $R^1 = R^2 = H$, $R^3 = R^4 = Ph$
L17: $R^1 = R^2 = Me$, $R^3 = R^4 = H$
L18: $R^1 = R^2 = Et$, $R^3 = R^4 = H$
L19: $R^1 = R^2 = n$Bu, $R^3 = R^4 = H$
L20: $R^1 = R^2 = n$-hexyl, $R^3 = R^4 = H$
L21: $R^1 = R^2 =$ Cy, $R^3 = R^4 = H$
L22: $R^1 = R^2 = t$Bu, $R^3 = R^4 = H$
L23: $R^1 = R^2 =$ adamantyl, $R^3 = R^4 = H$
L29: $R^1 = R^2 = i$Pr, $R^3 = R^4 = H$
L30: $R^1 = R^2 =$ isopentyl, $R^3 = R^4 = H$
L31: $R^1 = R^2 =$ 3-phenylpropyl, $R^3 = R^4 = H$
L32: $R^1 = R^2 =$ Bn, $R^3 = R^4 = H$
L33: $R^1 = R^2 =$ Ph, $R^3 = R^4 = H$
L34: $R^1 =$ Me, $R^2 = R^3 = R^4 = H$
L35: $R^1 = t$Bu, $R^2 = R^3 = R^4 = H$
L36: $R^1 =$ Ph, $R^2 = R^3 = R^4 = H$
L37: $R^1 =$ adamantyl, $R^2 = R^3 = R^4 = H$
L38: $R^1 =$ methoxybutyl, $R^2 = R^3 = R^4 = H$
L39: $R^1 =$ methoxypropyl, $R^2 = R^3 = R^4 = H$
L40: $R^1 =$ trifluoromethylpropyl, $R^2 = R^3 = R^4 = H$
L41: $R^1 = R^2 = H$, $R^3 = R^4 = Me$
L42: $R^1 = R^2 =$ 1-naphthyl, $R^3 = R^4 = H$
L43: $R^1 = R^2 =$ 2-naphthyl, $R^3 = R^4 = H$
L44: $R^1 = R^2 = n$Pr, $R^3 = R^4 = H$
L45: $R^1 = R^2 = n$-pentyl, $R^3 = R^4 = H$
L46: $R^1 = R^2 = n$-heptyl, $R^3 = R^4 = H$
L47: $R^1 = R^2 = n$-octyl, $R^3 = R^4 = H$
L48: $R^1 = R^2 =$ 2-phenylethyl, $R^3 = R^4 = H$
L49: $R^1 = R^2 =$ 3-(*para*-*t*butylphenyl)propyl, $R^3 = R^4 = H$

Computations have been achieved with both Hartree-Fock and density functional theory in Gaussian 16[19]. Geometry optimizations were carried out at

HF/3-21G* or B3LYP/6-31G(d) level of theory in vacuum. Transition states of this asymmetric MPV reduction of acetophenone were simulated at HF/3-21G* or B3LYP/6-31G(d) level in vacuum and in three solvent: toluene, *n*-pentane and 2-propanol with CPCM as solvation method. The free energy differences (ΔΔG) between **TS-S** and **TS-R** have been calculated (ΔΔG = ΔG(**TS-R**) – ΔG(**TS-S**)) and analyzed in Table 2.12 for 30 different ligands.

Table 2.12 Free energy differences at transition state with 30 ligands

Entry	Ligand	ΔΔG (kcal/mol)				
		HF/3-21G*	DFT/B3LYP/6-31G(d)			
		vacuum	vacuum	toluene	*n*-pentane	2-propanol
1	(*S*)-**L17**	0.380	0.155	-0.491	0.708	0.036
2	(*S*)-**L22**	0.524	0.869	0.857	0.828	0.289
3	(*S*)-**L23**	0.526	—	-0.126	0.152	0.045
4	(*S*)-**L18**	0.446	0.281	0.092	0.747	0.350
5	(*S*)-**L32**	0.100	-0.091	0.726	1.013	-0.126
6	(*S*)-**L33**	-0.363	-0.078	0.270	-0.115	-0.981
7	(*S*)-**L30**	0.286	0.149	0.385	0.370	-0.102
8	(*S*)-**L29**	0.565	1.156	0.189	0.268	0.088
9	(*S*)-**L21**	0.663	0.413	0.383	0.599	0.823
10	(*S*)-**L34**	0.306	0.048	-0.134	0.025	-0.105
11	(*S*)-**L35**	0.225	-0.321	0.309	0.291	0.114
12	(*S*)-**L36**	-0.105	-0.075	0.055	0.050	-0.146
13	(*S*)-**L37**	1.055	0.457	2.181	1.070	0.626
14	(*S*)-**L38**	2.843	0.390	-0.424	—	0.109
15	(*S*)-**L39**	0.166	-0.014	0.242	0.264	0.662
16	(*S*)-**L40**	-0.203	—	—	—	—
17	(*S*)-**L5**	0.247	-0.029	—	—	0.146
18	(*S*)-**L41**	-0.125	-0.104	0.107	0.124	-0.100
19	(*S*)-**L14**	-1.284	-0.379	-0.363	-0.335	0.003
20	(*S*)-**L42**	-0.093	-0.349	-0.419	-0.351	0.193
21	(*S*)-**L43**	-0.264	-0.196	0.213	-0.040	0.373
22	(*S*)-**L44**	0.451	-0.043	0.026	0.259	0.849
23	(*S*)-**L19**	0.391	-0.072	0.323	-0.009	0.476

Table 2.12 (cont'd)

24	(*S*)-**L45**	3.427	2.861	3.457	3.503	2.929
25	(*S*)-**L20**	0.374	0.129	0.226	0.490	0.693
26	(*S*)-**L46**	0.372	0.056	0.780	0.068	0.812
27	(*S*)-**L47**	0.370	—	0.593	0.476	0.119
28	(*S*)-**L48**	-0.213	-0.106	0.353	0.453	-0.666
29	(*S*)-**L31**	0.427	0.392	0.697	—	0.604
30	(*S*)-**L49**	0.424	0.601	—	—	0.166

Experimentally, the best ligand was found to be **L21** in the reduction of aromatic ketones. Although the free energy differences (ΔΔG) in 5 calculations were not large enough (0.383 to 0.823 kcal/mol) to match the induction observed (94% *ee* at –10˚C), they all favored **TS-S** leading to the correct enantiomer produced (Table 2.12, entry 9). The transition state geometries with (*S*)-**L21** in the reduction of acetophenone **55a** are shown as an example in Figure 2.4, with DFT/B3LYP/6-31G(d) level of calculation and CPCM as solvation method in 2-propanol. A tetra-coordinated aluminum center with a six-member ring hydride transfer was shown, supporting the previously proposed mechanism.[11] The π–π interaction between two phenyl groups at 3,3'-positions of naphthalene was observed, which is in correlation with the experimental results showing that replacing phenyl with cyclohexyl groups shuts down the reaction (Table 2.1, entry 10). Substituents at the 7,7'-positions of the ligand provide a better chiral environment around the active site of the catalyst compared with other positions, and thus was supported by observations during ligand screening process (Table 2.1). Steric effects seem to be responsible for the asymmetric discrimination between **TS-S** and **TS-R**.

Figure 2.4 Transition states with (*S*)-**L21** in 2-propanol

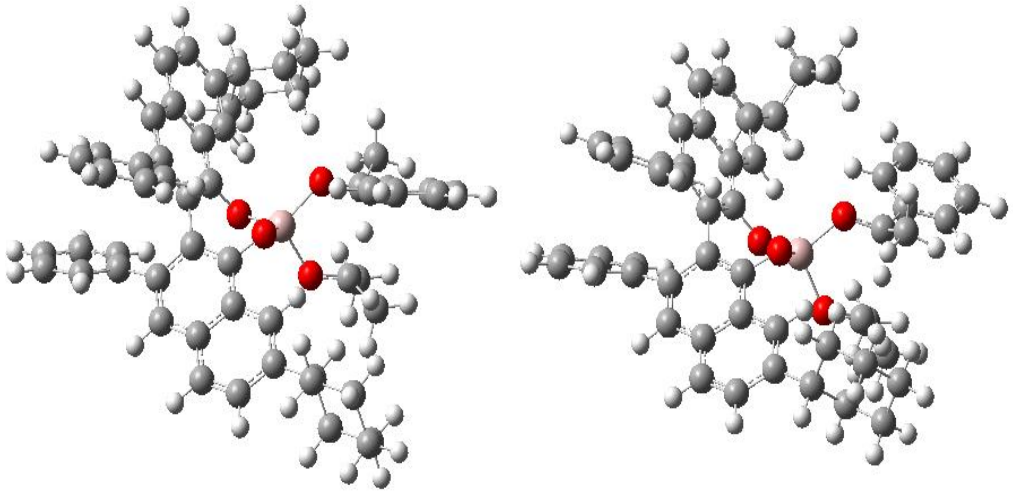

TS-S-L21-p **TS-R-L21-p**

According to the computational models, an explanation of the stereochemical outcome is indicated in Scheme 2.8. With (*S*)-**L21** as ligand and acetophenone as substrate, **TS-R** is disfavored due to the steric interaction between the cyclohexyl group on catalyst complex and the phenyl group on the ketone. Therefore, distinguishing the small group (methyl) and large group (phenyl) on the ketone is the key to achieve high asymmetric inductions. Unsurprisingly, replacement of the methyl group by an ethyl group on the ketone resulted in a drop in *ee* in the reduction of propiophenone **55j** (94% to 74% *ee*, Scheme 2.2). Meanwhile, the steric hindrance between ligand and 2-propanol is observed on both **TS-S** and **TS-R**, which is consistent with the finding that any alcohol bigger than 2-propanol led to worse results (Table 2.7).

Scheme 2.8 Explanation of stereo outcome

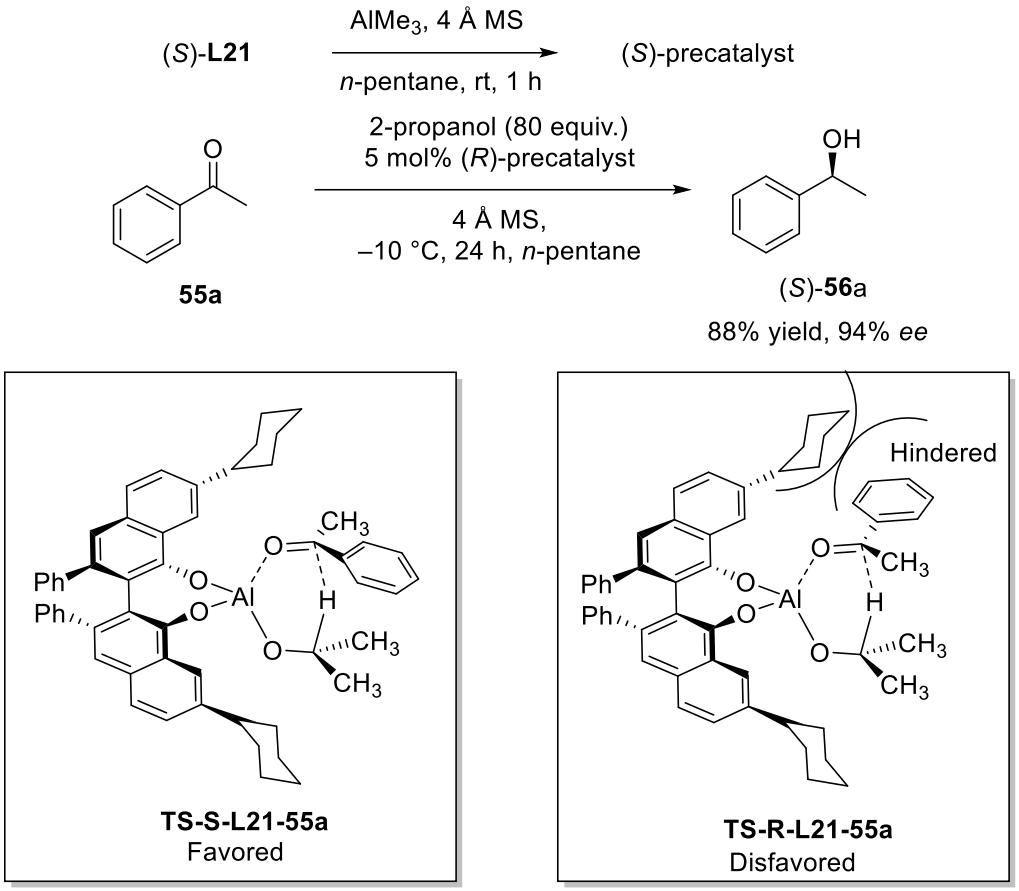

As for the reduction of 2-haloacetophenones, a penta-coordinated aluminum in the transition state has been proposed for BINOL catalyst (Scheme 2.7). To understand the behavior of VANOL catalyst in the reduction of 2-bromoacetophenone **55g**, calculations have been completed under HF/3-21G* level of theory in vacuum. The transition states with ligand (*S*)-**L21** are shown in Figure 2.5 as examples. The geometries are very similar to those when acetophenone is used as substrate, with a tetra-coordinated aluminum and six-member ring hydride transfer. Steric interaction between cyclohexyl group on the ligand and the phenyl group on the ketone is still the key to the stereochemical

outcome, and the bromine at the 2-position of the ketone barely changes the geometry of the transition states. A higher ΔΔG (1.16 kcal/mol) between **TS-S** and **TS-R** with the reduction of 2-bromoacetophenone has been observed in the current model, compared with the ΔΔG (0.383 to 0.823 kcal/mol) for acetophenone reduction.

Figure 2.5 Transition states with (*S*)-**L21** in the reduction of 2-bromoacetophenone

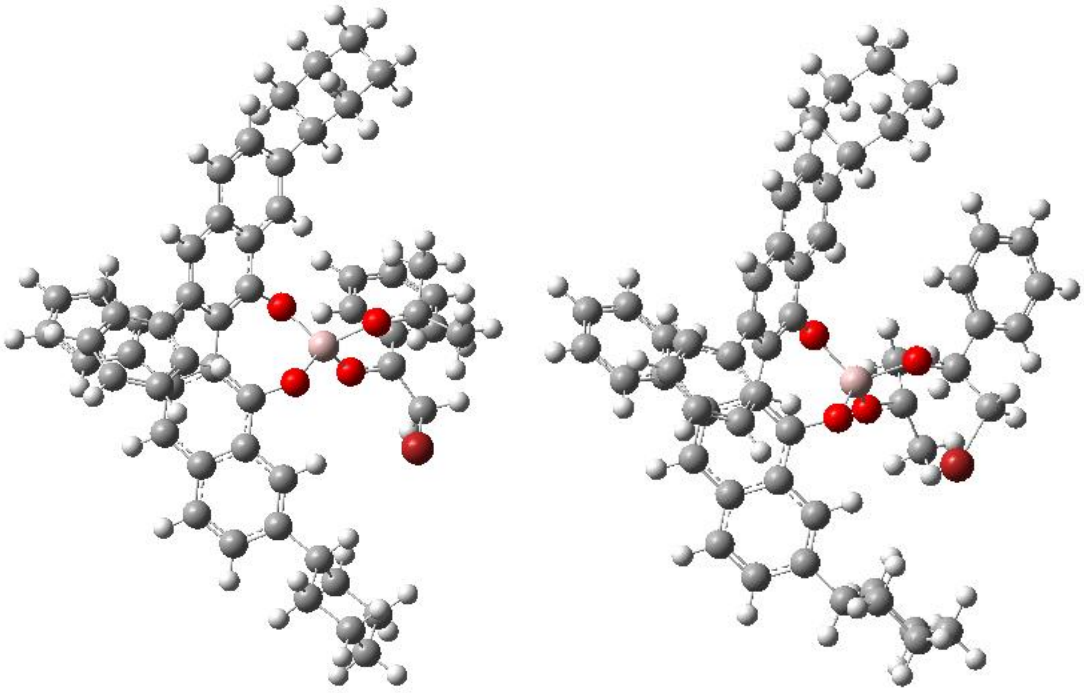

TS-S-L21-55g **TS-R-L21-55g**

The proposed coordination between aluminum and bromine is not found, with the distance between aluminum and bromine being 3.97 Å (**TS-S**) and 3.66 Å (**TS-R**). It is too early to exclude the existence of a penta-coordinated aluminum before running more calculations at a higher level of theory. However, it is not surprising that a similar transition state was found, given that a bidentate ketone is

not required in our aluminum-VANOL system since simple monodentate ketones also give excellent results.

2.8 Formal dynamic kinetic resolution of racemic alcohols via Oppenauer oxidation/MPV reduction

2.8.1 Introduction

Chiral catalysts can be used in the kinetic resolution of racemic compounds, due to the fact that enantiomers undergo reactions with different rates in a chiral environment. When exposed to chiral reagents or catalysts, one enantiomer of the substrate can react faster than the other. In Scheme 2.9a this is illustrated for situation where the (*S*)-substrate reacts faster than (*R*)-substrate ($K_S > K_R$). Usually, this process would lead to the formation of enantioenriched (*S*)-product and recovery of unreacted (*R*)-Substrate. The enantiopurity of the (*S*)-product and (*R*)-Substrate is highly dependent on the rate difference (K_S/K_R), which results from the asymmetric discrimination of the chiral environment. With reliance on a significant technology with enzymes as well as the development of many chiral reagents/catalysts, kinetic resolution of racemic compounds has been one of the most important approaches to obtain enantiopure species, especially in industry.[20] However, an inherent drawback of kinetic resolution is that the theoretical maximum yield for kinetic resolution is 50%. This situation changes when the (*S*)-Substrate and (*R*)-Substrate can undergo fast interconversion with each other (Scheme 2.9b). The simplest example is that of a substrate bears a labile stereogenic center that is capable of undergoing epimerization during the reaction.[21,22] When the rate of epimerization is higher than the rate of reaction for

the slow enantiomer ($K_{inv}>K_R$), in principle, enantioenriched (*S*)-Product can be produced in 100% yield instead of 50%.[22] This process couples the epimerization of substrate and the subsequential kinetic resolution to convert both (*R*)-and (*S*)-Substrate into a single product with a 100% theoretical yield, which is called dynamic kinetic resolution.[23] A variety of enzymatic and non-enzymatic methods for dynamic kinetic resolution have been developed for the preparation of chiral compounds.[24-26]

Scheme 2.9 Kinetic resolution and dynamic kinetic resolution

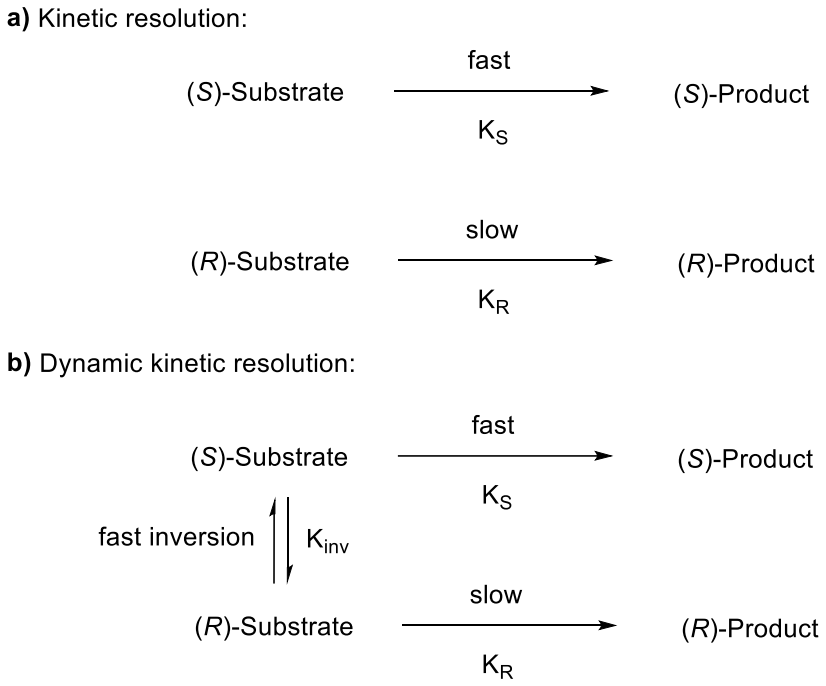

During the past decades, the dynamic kinetic resolution of racemic alcohols have been explored by several groups.[27] The general approach includes a metal-catalyzed racemization of alcohols and an enzymatic kinetic resolution. Some transition metals such as rhodium and ruthenium were found to be effective in catalyzing alcohol racemization. A simplified mechanism for alcohol racemization

with ruthenium catalysts is shown in Scheme 2.10[27]. The racemization occurs via ketone **67** as intermediate with a transfer hydrogenation mechanism.[28] Sometimes undesired ketone **67** was isolated, resulting in a drop in yield in the desired alcohol product.[27]

Scheme 2.10 Alcohol racemizations with ruthenium catalyst

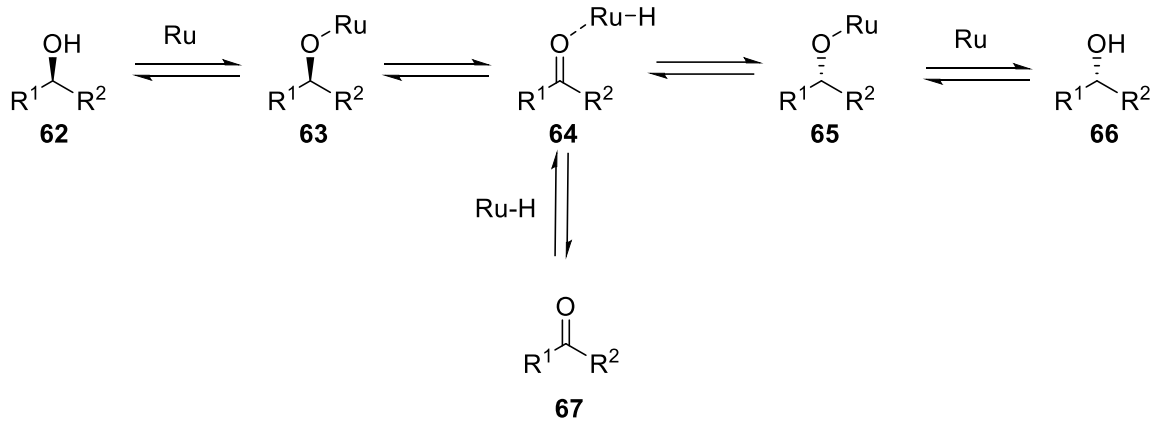

Scheme 2.11 Chemo-enzymatic dynamic kinetic resolution of alcohols

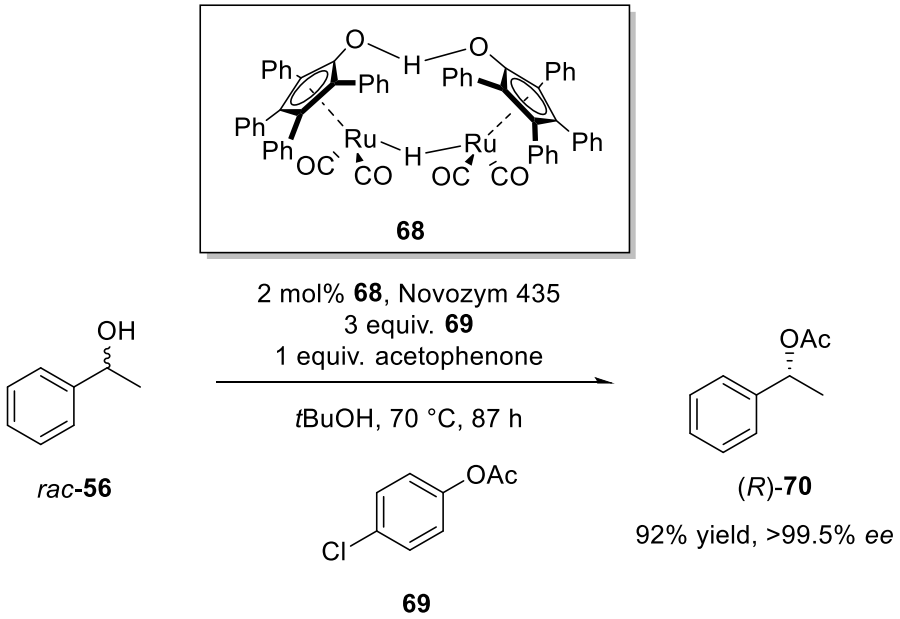

In 1997, Bäckvall and co-workers reported an efficient method for the dynamic kinetic resolution of alcohols via this chemo-enzymatic approach.[29] As shown in Scheme 2.11, racemization of alcohols was achieved with 2 mol% Shvo's catalyst **68** and 1 equivalent of acetophenone as hydride acceptor. The acylation was catalyzed by enzyme CALB (*Candida antarctica* lipase B, immobilized; Novozym 435) with the use of *para*-chlorophenyl acetate **69** as acyl donor. Optically pure (>99.5% *ee*) acylation product (*R*)-**70** was obtained in 92% yield after 87 hours. The substrate scope of this method has been extended to other aromatic and aliphatic alcohols.[30]

Scheme 2.12 Non-enzymatic dynamic kinetic resolution of alcohols

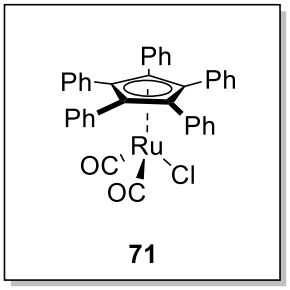

71

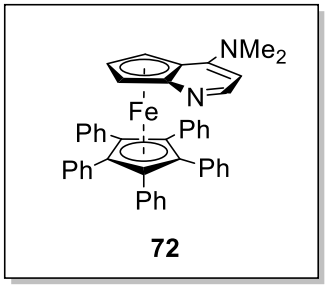

72

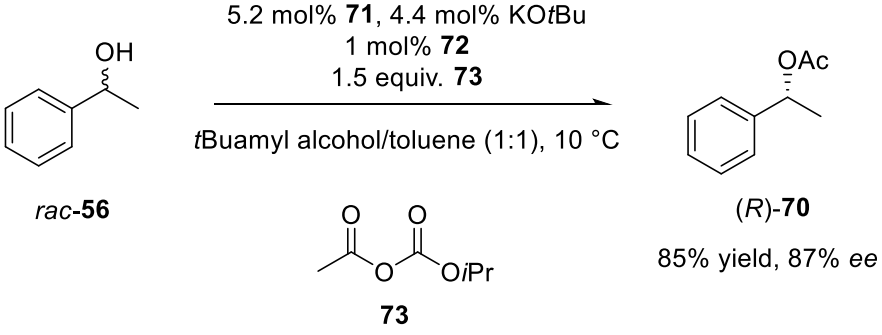

rac-**56**

73

(*R*)-**70**

85% yield, 87% *ee*

The first non-enzymatic dynamic kinetic resolution of secondary alcohols was illustrated by Fu and co-workers in 2012.[31] They employed ruthenium catalyst **71** to achieve racemization of the alcohol and the planar chiral ferrocene catalyst

72 to complete the acylation. While acetic anhydride as acyl source failed to give any product, the use of acetyl isopropyl carbonate **73** as acyl donor is the key as it avoids the deactivation of the ruthenium catalyst by acetate coordination.[32] A variety of aromatic carbinols with different electron densities as well as aromatic allylic alcohols were well tolerated in this protocol.

2.8.2 Oxidative kinetic resolution of racemic alcohols with aluminum-VANOL catalysts

Since the Oppenauer oxidation is the reverse reaction of the MPV reduction, the transition state in Oppenauer oxidation should be the same as it in MPV reduction. Given that excellent enantioselectivities have been observed in our asymmetric MPV reduction with aluminum-VANOL catalysts, we know that the activation energy difference (ΔΔG) between two transition states towards R and S products are high enough to give satisfactory asymmetric inductions. Therefore, we first tried an oxidative kinetic resolution of racemic alcohols using Oppenauer oxidation catalyzed by the same aluminum-VANOL catalyst. As shown in Scheme 2.13, racemic alcohol **56a** was treated with 10 mol% (*S*)-catalyst that was used in the MPV reductions. We first used cyclohexanone instead of acetone as oxidant because it is harder to make acetone anhydrous. With 2 equivalents of cyclohexanone at –10 ˚C, all of the alcohol **56a** was oxidized to ketone **55a** after 10 hours (entry 1). Reducing the reaction time to 4 hours gave 7% of recovered (*R*)-**56a** in 84% *ee* while reducing the loading of cyclohexanone to 1 equivalent gave (*R*)-**56a** 15% in 76% *ee* (entry 3). Yield of (*R*)-**56a** could be increased by cutting the reaction time, lowering the reaction temperature and the use of 0.5

equivalent of cyclohexanone. However, *ee* dropped dramatically with the increase of yield (entries 4-7).

Due to the unsatisfactory enantioselectivity, we turned to employ acetone instead of cyclohexanone as the oxidant, which is supposed to give better induction since 2-propanol is better than cyclohexanol in the MPV reduction with same catalyst. With 1 equivalent of acetone, a 40% yield of (*R*)-**56a** in 49% *ee* was obtained while the use of 0.5 equivalent of acetone gave 53% (*R*)-**56a** in 66% *ee* (entries 8-9). Switching the ligand from (*S*)-**L22** to (*S*)-**L21** with 0.6 equivalent of acetone improved the results to 46% recovery in 83% *ee* (entry 10). In this case, the selectivity factor of this oxidative kinetic resolution method is calculated to be s = 14.8 (using s = ln[(1-C)(1-*ee*)]/ln[(1-C)(1+*ee*)] where C is the conversion of ketone **55a**).[33]

Scheme 2.13 Oxidative kinetic resolution of racemic alcohols

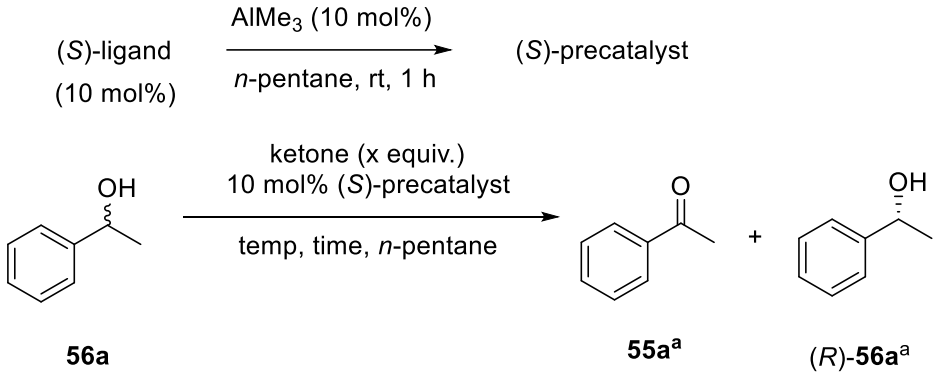

entry[a]	ligand	ketone	x equiv.	temp. (°C)	time (h)	% yield **55a**	% yield (*R*)-**56a**	% *ee* (*R*)-**56a**
1	(*S*)-**L22**	cyclohexanone	2	–10	10	>99	<1	-
2	(*S*)-**L22**	cyclohexanone	2	–10	4	93	7	84
3	(*S*)-**L22**	cyclohexanone	1	–10	4	85	15	76
4	(*S*)-**L22**	cyclohexanone	1	–10	1	75	25	83
5	(*S*)-**L22**	cyclohexanone	1	–40	8	70	30	49
6	(*S*)-**L22**	cyclohexanone	1	–78	8	46	54	31
7	(*S*)-**L22**	cyclohexanone	0.5	–10	24	46	54	23
8	(*S*)-**L22**	acetone	1	–10	24	60	40	49
9	(*S*)-**L22**	acetone	0.5	–20	24	47	53	66
10	(*S*)-**L21**	acetone	0.6	–40	24	54	46	83

[a] Reactions were performed on 0.25 mmol scale at 0.1 M; yields are determined by crude ^{1}H-NMR with triphenylmethane as internal standard; *ee* is Determined by chiral HPLC.

2.8.3 Tentative formal dynamic kinetic resolution of racemic alcohols with aluminum-VANOL catalysts

To take advantage of the reversible nature of MPV reductions, a formal dynamic kinetic resolution of racemic alcohols via Oppenauer oxidation/ MPV reduction sequence is proposed. A single aluminum-VANOL catalyst is responsible for both oxidation and reduction. This method starts with an aluminum-catalyzed Oppenauer oxidation of racemic alcohols with a ketone oxidant, followed

by the addition of 2-propanol as reductant to accomplish the in-situ MPV reduction with the same aluminum catalyst, giving enantioenriched alcohol product in theoretical 100% yield. It is not a real dynamic kinetic resolution, since there is no racemization of substrates. However, this method has the potential to give optically active chiral alcohols from racemic alcohols in a stepwise/one-pot process, and most importantly, with a single catalyst.

According to the kinetic resolution attempts that we have done so far, 2 equivalents of cyclohexanone is capable of oxidizing both enantiomers of racemic alcohols in 10 hours at –10 ˚C (Scheme 2.13, entry 1). Further experiments revealed that the use of 2 equivalents of acetone or cyclohexanone could fully oxidize alcohol **56a** to ketone **55a** in one hour at room temperature. We first tried to add 2 equivalents of acetone and 80 equivalents of 2-propanol at the same time to avoid the stepwise process (Scheme 2.14, entry 1). However, the kinetic resolution product (*R*)-**56a** instead of the dynamic resolution product (*S*)-**56a** was formed even with a large excess of 2-propanol as reductant. A stepwise procedure gave desired isomer (*S*)-**56a** in 10% yield and 10% *ee* (entry 2), while switching from acetone to cyclohexanone increased yield to 44% (entry 3). Using 1 instead of 2 equivalents of ketone improved *ee* to 39% (entry 4). After changing the loading of 2-propanol to 4 equivalents, a 61% yield and 32% ee was obtained (entries 4-8). Best result was obtained with the use of (*S*)-**L21** with 1.2 equivalent of cyclohexanone at –10 ˚C, where 79% yield and 73% *ee* was observed (entry 11).

Scheme 2.14 Formal dynamic kinetic resolution of racemic alcohols

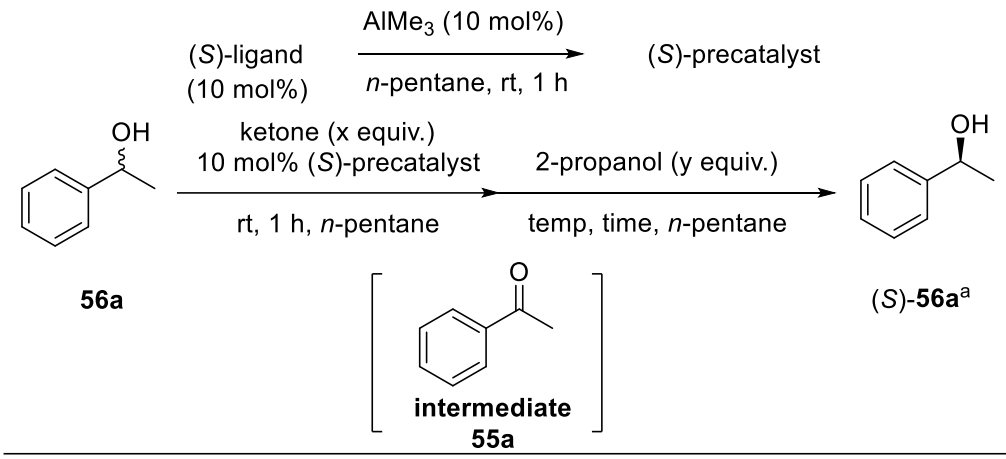

entry[a]	ligand	ketone	x equiv.	y equiv.	temp. (°C)	time (h)	% yield (*S*)-**56a**	% *ee* (*R*)-**56a**
1[b]	(*S*)-**L22**	acetone	2	80	rt	24	38	–25[c]
2	(*S*)-**L22**	acetone	2	80	rt	12	10	10
3	(*S*)-**L22**	cyclohexanone	2	80	rt	12	44	7
4	(*S*)-**L22**	cyclohexanone	1	80	rt	12	30	39
5	(*S*)-**L22**	cyclohexanone	1	20	rt	12	54	35
6	(*S*)-**L22**	cyclohexanone	1	10	rt	12	35	20
7	(*S*)-**L22**	cyclohexanone	1	4	rt	12	61	32
8	(*S*)-**L22**	cyclohexanone	1	1	rt	12	20	19
9	(*S*)-**L22**	cyclohexanone	1	4	–10	12	53	53
10	(*S*)-**L22**	cyclohexanone	1.2	4	–10	24	75	59
11	(*S*)-**L21**	cyclohexanone	1.2	4	–10	24	79	73

[a] Reactions were performed on 0.25 mmol scale at 0.1 M; yields are determined by crude ^{1}H-NMR with triphenylmethane as internal standard; *ee* is Determined by chiral HPLC.[b] 2-propanol and acetone were added at the same time.[c] Minus ee indicates that the kinetic resolution product (*R*)-**56a** instead of dynamic product is formed.

Further optimizations of the reaction temperature, solvent and concentration failed to improve the selectivity of this process. However, this novel employment of the Oppenauer oxidation/ MPV reduction sequence in resolution of racemic alcohols provides a new strategy for accessing chiral alcohols, which avoids the use of enzymes and the acylation of substrates.

2.9 Conclusion

Motivated by the unsatisfactory enantioselectivities observed in the asymmetric MPV reduction of ketones with Nguyen's BINOL catalyst, we focused on the development of VANOL catalysts. While adding substituents on the BINOL ligand failed to give higher induction, the use of 7,7'-disubstituted VANOL ligands dramatically improved the results. After screening different ligands and optimizing reaction parameters, the substrate scope has been extensively studied. Computational studies on the transition state has been carried out with Gaussian 16 and reaction mechanism has been discussed. A tentative formal dynamic kinetic resolution of racemic alcohols has been proposed and preliminarily examined.

In conclusion, it is reported here the development of the first highly enantioselective aluminum catalyzed MPV reduction of ketones to access chiral alcohols. Aromatic ketones with different electron densities and substituents are well-tolerated and most of them can be reduced with >90% yield and >90% *ee*. Notably, aliphatic ketones were also addressed with good to excellent enantioselectivity for the first time. The aluminum catalyst generated from trimethylaluminum and the 7,7'-dicyclohexyl substituted VANOL ligand **L21** is very efficient giving high yields and enantioselectivities of the reduced products under the same conditions where the VANOL ligand without the cyclohexyl groups gives no product at all (<2%). It is possible that the presence of the cyclohexyl groups helps to prevent aggregation or oligomerization of the catalyst. Computational study suggests that the steric interactions between the cyclohexyl group on the

ligand and ketone is the key to achieve high asymmetric inductions. The present chiral aluminum catalyst is far superior to previously reported aluminum catalysts for the MPV reduction.[10,18] Given that this catalyst gives high asymmetric induction at 1-10 mol% catalyst loading, it is on par with the previously reported best systems with samarium[34] and ruthenium[35] catalysts and in addition gives good to excellent inductions for dialkyl ketones.

REFERENCES

REFERENCES

1. Bao, J.; Wulff, W. D.; Dominy J. B.; Fumo, M. J.; Grant, E. B.; Rob, A. C.; Whitcomb, M. C.; Yeung, S.-M.; Ostrander, R. L.; Rheingold, A. L. Synthesis, Resolution, and Determination of Absolute Configuration of a Vaulted 2,2‘-Binaphthol and a Vaulted 3,3‘-Biphenanthrol (VAPOL). *J. Am. Chem. Soc.* **1996**, *118*, 3392-3405.

2. Bao, J.; Wulff, W. D.; Rheingold, A. L. Vaulted biaryls as chiral ligands for asymmetric catalytic Diels-Alder reactions. *J. Am. Chem. Soc.* **1993**, *115*, 3814-3815.

3. Antilla, J. C.; Wulff, W. D. Catalytic Asymmetric Aziridination with a Chiral VAPOL−Boron Lewis Acid. *J. Am. Chem. Soc.* **1999**, *121*, 5099-5100.

4. Desai, A. A.; Wulff, W. D. Controlled Diastereo- and Enantioselection in a Catalytic Asymmetric Aziridination. *J. Am. Chem. Soc.* **2010**, *132*, 13100-13103.

5. Newman, C. A.; Antilla, J. C.; Chen, P.; Predeus, A. V.; Fielding, L.; Wulff, W. D. Regulation of Orthogonal Functions in a Dual Catalyst System. Subservient Role of a Nonchiral Lewis Acid in an Asymmetric Catalytic Heteroatom Diels−Alder Reaction. *J. Am. Chem. Soc.* **2007**, *129*, 7216-7217.

6. Ren, H.; Wulff, W. D. Direct Catalytic Asymmetric Aminoallylation of Aldehydes: Synergism of Chiral and Nonchiral Brønsted Acids. *J. Am. Chem. Soc.* **2011**, *133*, 5656-5659.

7. Zhao, W.; Huang, L.; Guan, Y.; Wulff, W. D. Three-component asymmetric catalytic Ugi reaction--concinnity from diversity by substrate-mediated catalyst assembly. *Angew. Chem. Int. Ed.* **2014**, *53*, 3436-3441.

8. Zhang, X.; Staples, R. J.; Rheingold, A. L.; Wulff, W. D. Catalytic Asymmetric α-Iminol Rearrangement: New Chiral Platforms. *J. Am. Chem. Soc.* **2014**, *136*, 13971-13974.

9. Gupta, A. K.; Yin, X.; Mukherjee, M.; Desai, A. A.; Mohammadlou, A.; Jurewicz, K.; Wulff, W. D. Catalytic Asymmetric Epoxidation of Aldehydes with Two VANOL-Derived Chiral Borate Catalysts. *Angew. Chem. Int. Ed.* **2019**, *58*, 3361-3367.

10. Zheng, L.; Yin, X.; Mohammadlou, A.; Sullivan, R. P.; Guan, Y.; Staples, R. J.; Wulff, W. D. Asymmetric Catalytic Meerwein-Ponndorf-Verley Reduction of Ketones with Aluminum(III)-VANOL Catalysts. *ACS Catal.* **2020**, *10*, 7188-7194.

11. Campbell, E. J.; Zhou, H.; Nguyen, S. T. The Asymmetric Meerwein–Schmidt–Ponndorf–Verley Reduction of Prochiral Ketones with iPrOH Catalyzed by Al Catalysts. *Angew. Chem. Int. Ed.* **2002**, *41*, 1020-1022.

12. Cohen, R.; Graves, C. R; Nguyen, S. T.; Martin, J. M. L.; Ratner, M. A. The Mechanism of Aluminum-Catalyzed Meerwein−Schmidt−Ponndorf−Verley Reduction of Carbonyls to Alcohols. *J. Am. Chem. Soc.* **2004**, *126*, 14796-14803.

13. Graves, C. R.; Zhou, H.; Stern, C. L.; Nguyen, S. T. A Mechanistic Investigation of the Asymmetric Meerwein−Schmidt−Ponndorf−Verley Reduction Catalyzed by BINOL/AlMe3. Structure, Kinetics, and Enantioselectivity. *J. Org. Chem.* **2007**, *72*, 9121-9133.

14. Guan, Y.; Ding, Z.; Wulff, W. D. Vaulted Biaryls in Catalysis: A Structure–Activity Relationship Guided Tour of the Immanent Domain of the VANOL Ligand. *Chem. Eur. J.* **2013**, *19*, 15565-15571.

15. Shiner, V. J.; Whittaker, D.; Fernandez, V. P. The Structures of Some Aluminum Alkoxides. *J. Am. Chem. Soc.* **1963**, *85*, 2318–2322.

16. Meerwein, H.; Schmidt, R. Ein neues Verfahren zur Reduktion von Aldehyden und Ketonen. *Justus Liebigs Ann. Chem.* **1925**, *39*, 221-238.

17. Verley, M. Sur l'échange de groupements fonctionnels entre deux molécules. Passage des cétones aux alcohols et inversement. *Bull. Soc. Chim. Fr.* **1925**, *37*, 871-874.

18. Nandi, P.; Solovyov, A.; Okrut, A.; Katz, A. Al^{III}–Calix[4]arene Catalysts for Asymmetric Meerwein–Ponndorf–Verley Reduction. *ACS Catal.* **2014**, *4*, 2492-2495.

19. Gaussian 16, Revision A.03, Frisch, M. J.; Trucks, G. W.; Schlegel, H. B.; Scuseria, G. E.; Robb, M. A.; Cheeseman, J. R.; Scalmani, G.; Barone, V.; Petersson, G. A.; Nakatsuji, H.; Li, X.; Caricato, M.; Marenich, A. V.; Bloino, J.; Janesko, B. G.; Gomperts, R.; Mennucci, B.; Hratchian, H. P.; Ortiz, J. V.; Izmaylov, A. F.; Sonnenberg, J. L.; Williams-Young, D.; Ding, F.; Lipparini, F.; Egidi, F.; Goings, J.; Peng, B.; Petrone, A.; Henderson, T.; Ranasinghe, D.; Zakrzewski, V. G.; Gao, J.; Rega, N.; Zheng, G.; Liang, W.; Hada, M.; Ehara, M.; Toyota, K.; Fukuda, R.; Hasegawa, J.; Ishida, M.; Nakajima, T.; Honda, Y.; Kitao, O.; Nakai, H.; Vreven, T.; Throssell, K.; Montgomery, J. A., Jr.; Peralta, J. E.; Ogliaro, F.; Bearpark, M. J.; Heyd, J. J.; Brothers, E. N.; Kudin, K. N.; Staroverov, V. N.; Keith, T. A.; Kobayashi, R.; Normand, J.; Raghavachari, K.; Rendell, A. P.; Burant, J. C.; Iyengar, S. S.; Tomasi, J.; Cossi, M.; Millam, J. M.; Klene, M.; Adamo, C.; Cammi, R.; Ochterski, J. W.; Martin, R. L.; Morokuma, K.; Farkas, O.; Foresman, J. B.; Fox, D. J. Gaussian, Inc., Wallingford CT, 2016.

20. Keith, J. M.; Larrow, J. F.; Jacobsen, E. N. Practical Considerations in Kinetic Resolution Reactions. *Adv. Synth. Catal.* **2001**, *343*, 5-26.

21. Armstrong, III, J. D.; Eng, K. K.; Keller, J. L.; Purick, R. M.; Hartner, Jr., F. W.; Choi, W.-B.; Askin, D.; Volante, R. P. An efficient asymmetric synthesis of (R)-3-amino-

2,3,4,5-tetrahydro-1H-[1]benzazepin-2-one. *Tetrahedron Lett.* **1994**, *35*, 3239-3242.

22. Noyori, R.; Tokunaga, M.; Kitamura, M. Stereoselective Organic Synthesis via Dynamic Kinetic Resolution. *Bull. Chem. Soc. Jpn.*, **1995**, *68*, 36-56.

23. Echeverria, P.-G.; Ayad, T.; Phansavath, P.; Ratovelomanana-Vidal, V. Recent Developments in Asymmetric Hydrogenation and Transfer Hydrogenation of Ketones and Imines through Dynamic Kinetic Resolution. *Synthesis* **2016**, *48*, 2523-2539.

24. Pellissier, H. Dynamic kinetic resolution. *Tetrahedron* **2003**, *59*, 8291-8327.

25. Pellissier, H. Recent developments in dynamic kinetic resolution. *Tetrahedron* **2008**, *64*, 1563-1601.

26. Pellissier, H. Recent developments in dynamic kinetic resolution. *Tetrahedron* **2011**, *67*, 3769-3802.

27. Lee, J.; Choi, Y. K.; Park, J.; Kim, M.-J. Dynamic Kinetic Resolution of Alcohols, Amines, and Amino Acids. *Green Biocatalysis* Chapter 5.

28. Ahn, Y.; Ko, S.-B.; Kim, M.-J.; Park J. Racemization catalysts for the dynamic kinetic resolution of alcohols and amines. *Coord. Chem. Rev.* **2008**, *252*, 647−658.

29. Larsson, A. L. E.; Persson, B. A.; Bäckvall, J. E. Enzymatic Resolution of Alcohols Coupled with Ruthenium-Catalyzed Racemization of the Substrate Alcohol. *Angew. Chem. Int. Ed.* **1997**, *36*, 1211-1212.

30. Persson, B. A.; Larsson, A. L. E.; Ray, M. L.; Bäckvall, J. E. Ruthenium- and Enzyme-Catalyzed Dynamic Kinetic Resolution of Secondary Alcohols. *J. Am. Chem. Soc.* **1999**, *121*, 1645-1650.

31. Lee, S. Y.; Murphy, J. M.; Ukai, A.; Fu, G. C. Nonenzymatic Dynamic Kinetic Resolution of Secondary Alcohols via Enantioselective Acylation: Synthetic and Mechanistic Studies. *J. Am. Chem. Soc.* **2012**, *134*, 15149-15153.

32. Díaz-Álvarez, A. E.; Mesas-Sánchez, L.; Dinér, P. Non-Enzymatic Dynamic Kinetic Resolution of Secondary Aryl Alcohols: Planar Chiral Ferrocene and Ruthenium Catalysts in Cooperation. *Angew. Chem. Int. Ed.* **2013**, *52*, 502-504.

33. Ferreira, E. M.; Stoltz, B. M. The Palladium-Catalyzed Oxidative Kinetic Resolution of Secondary Alcohols with Molecular Oxygen. *J. Am. Chem. Soc.* **2001**, *123*, 7725-7726.

34. Evans, D. A.; Nelson, S. G.; Gagne, M. R.; Muci, A. R. A chiral samarium-based catalyst for the asymmetric Meerwein-Ponndorf-Verley reduction. *J. Am. Chem. Soc.* **1993**, *115*, 9800-9801.

35. Hasiguchi, S.; Fujii, A.; Takehara, J.; Ikariya, T.; Noyori, R., Asymmetric Transfer Hydrogenation of Aromatic Ketones Catalyzed by Chiral Ruthenium(II) Complexes. *J. Am. Chem. Soc.* **1995**, *117*, 7562-7563.

CHAPTER THREE

ENANTIOSELECTIVE HETEROATOM DIELS-ALDER REACTION OF ALDEHYDES CATALYZED BY CHIRAL BORATE CATALYSTS

3.1 Introduction

3.1.1 Synthetic applications of heteroatom Diels-Alder reactions

The Diels-Alder reaction has been one of the most fundamental transformations in chemistry since its discovery in 1928 by Otto Diels and Karl Alder.[1] The construction of six-membered rings with 100% atom economy makes it extremely popular in organic synthesis.[2] The heteroatom Diels-Alder (HDA) reaction is one of the most important variants of the Diels-Alder reaction, as it constructs six-membered heterocycles that widely exist in natural products or bioactive compounds.[3] Some examples of natural products containing six-membered heterocycle skeletons are shown in Figure 3.1, such as bistramide A, polycavernoside A, phyllanthine, luotonin A and pederin.[4] To construct these six-membered heterocycles using HDA reactions, a carbon on either the dienophile or the diene is replaced by a heteroatom such as oxygen or nitrogen. Similar to the classic Diels-Alder reaction, the normal HDA reaction employs an electron-poor dienophile (aldehyde, imine…) and electron-rich diene (Scheme 3.1a), which is favored because of the better overlap between the lower LUMO of dienophile and the higher HOMO of diene.[5] The inverse electron-demand HDA reaction usually employs an electron-poor α,β-unsaturated species as the diene and an electron-rich alkene as the dienophile, in which the interaction between the LUMO of the

diene and the HOMO of the dienophile is favored (Scheme 3.1b).[5] Except for the popular use of carbonyl compounds,[6] many other heteroatomic substrates have been used as dienophiles such as nitroso compounds,[7] nitriles,[8] imines,[9] azodicarboxylates,[10] singlet oxygen,[11] and sulfur dioxide.[12]

Figure 3.1 Six-membered heterocycles in natural products

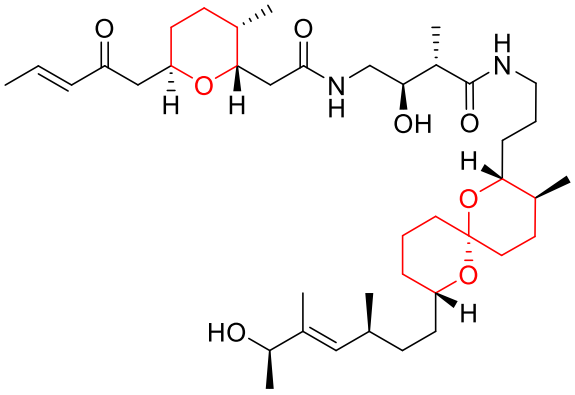

74 bistramide A

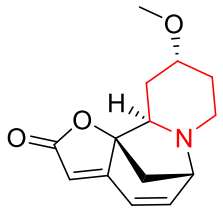

75 phyllanthine

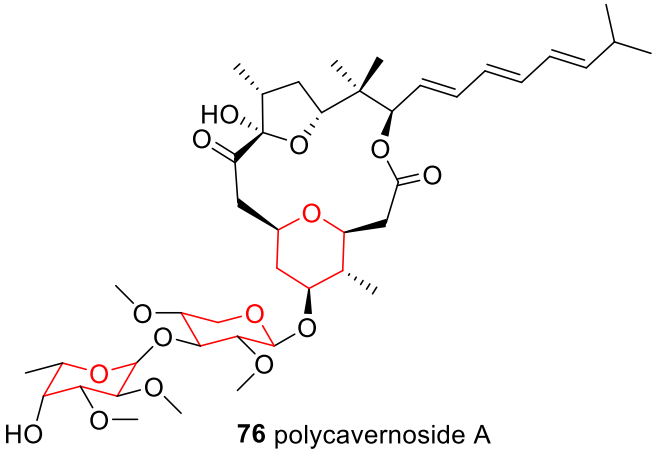

76 polycavernoside A

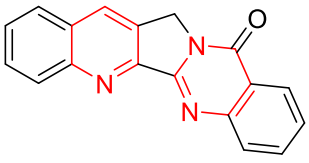

77 luotonin A

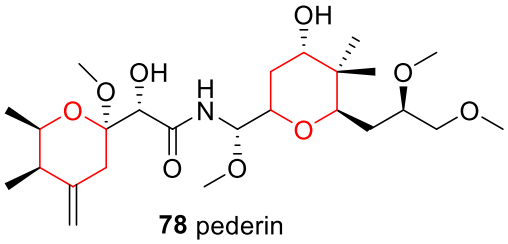

78 pederin

Scheme 3.1 Normal HDA reaction and inverse electron-demand HDA reaction[5]

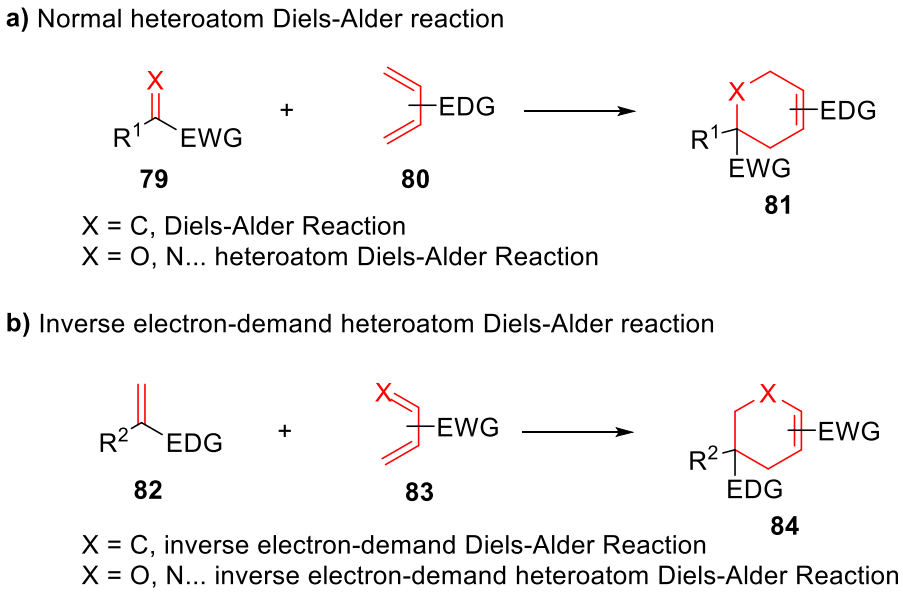

During the past several decades, heteroatom Diels-Alder reactions have been widely used in the total synthesis of natural products. For example, the first total synthesis of (+)-keto-deoxyoctulosonate **89** was achieved by Danishefsky and coworkers, with the HDA reaction as the key cyclization to construct the saccharide skeleton.[13] The reaction between α-selenoaldehyde **85** and highly functionalized diene **86** was activated by Lewis acid BF_3•Et_2O and followed by acidic cleavage of the silyl group, to give the cyclized products **87** and **88** in a 5:1 ratio. The favored *endo* product **87** was then derivatized into (+)-keto-deoxyoctulosonate (Scheme 3.2a). Rawal et al. has employed the HDA reaction in the total synthesis of pederin, a vesicant natural product isolated from beetles.[14] Aldehyde **90** and diene **91** were transformed into pyrone **92** catalyzed by various Lewis acids. Using 2 equivalents of BF_3•Et_2O as the Lewis acid gave the undesired isomer as the major product. The use of $TiCl_4$ (2 equivalents) gave the desired isomer **92** (*syn*) but with only

60:40 diastereomeric ratio. The best diastereoselectivity (dr = 92:8) was produced by the addition of an aluminum catalyst (20 mol%) and TMSOTf (200 mol%), in where the activation of the aluminum alkoxide with TMSOTf was essential for success. These reactions both employed very electron-rich dienes bearing a siloxy group and a methoxy group, which synergistically enhanced the reactivity and stereoselectivity.

Scheme 3.2 Aldehyde as dienophile of HDA reactions in total syntheses

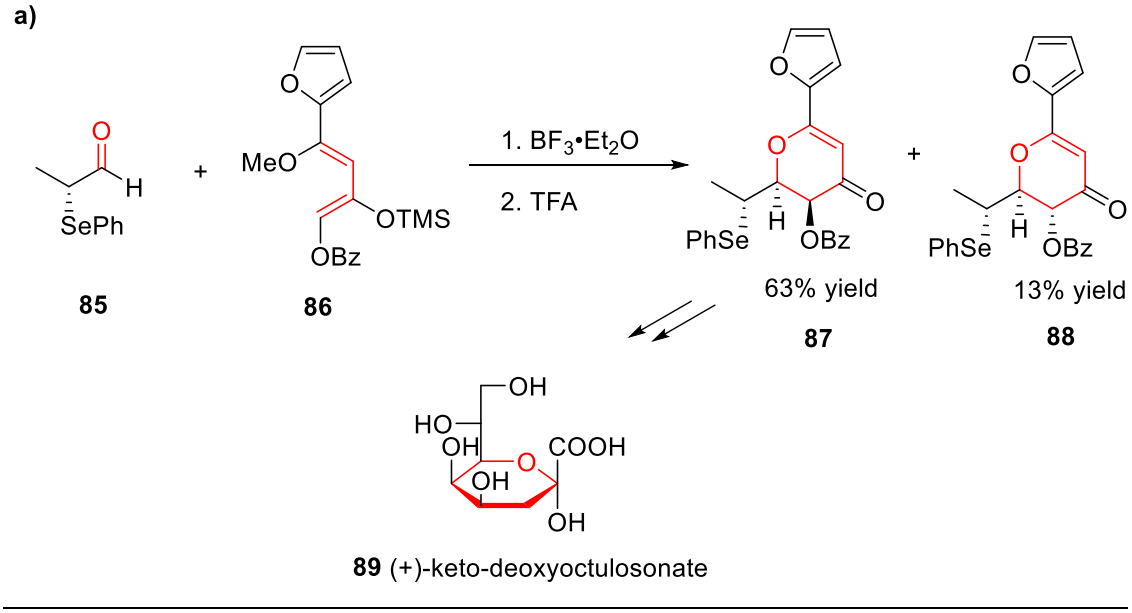

Scheme 3.3 HDA reactions with Danishefsky's diene in total syntheses

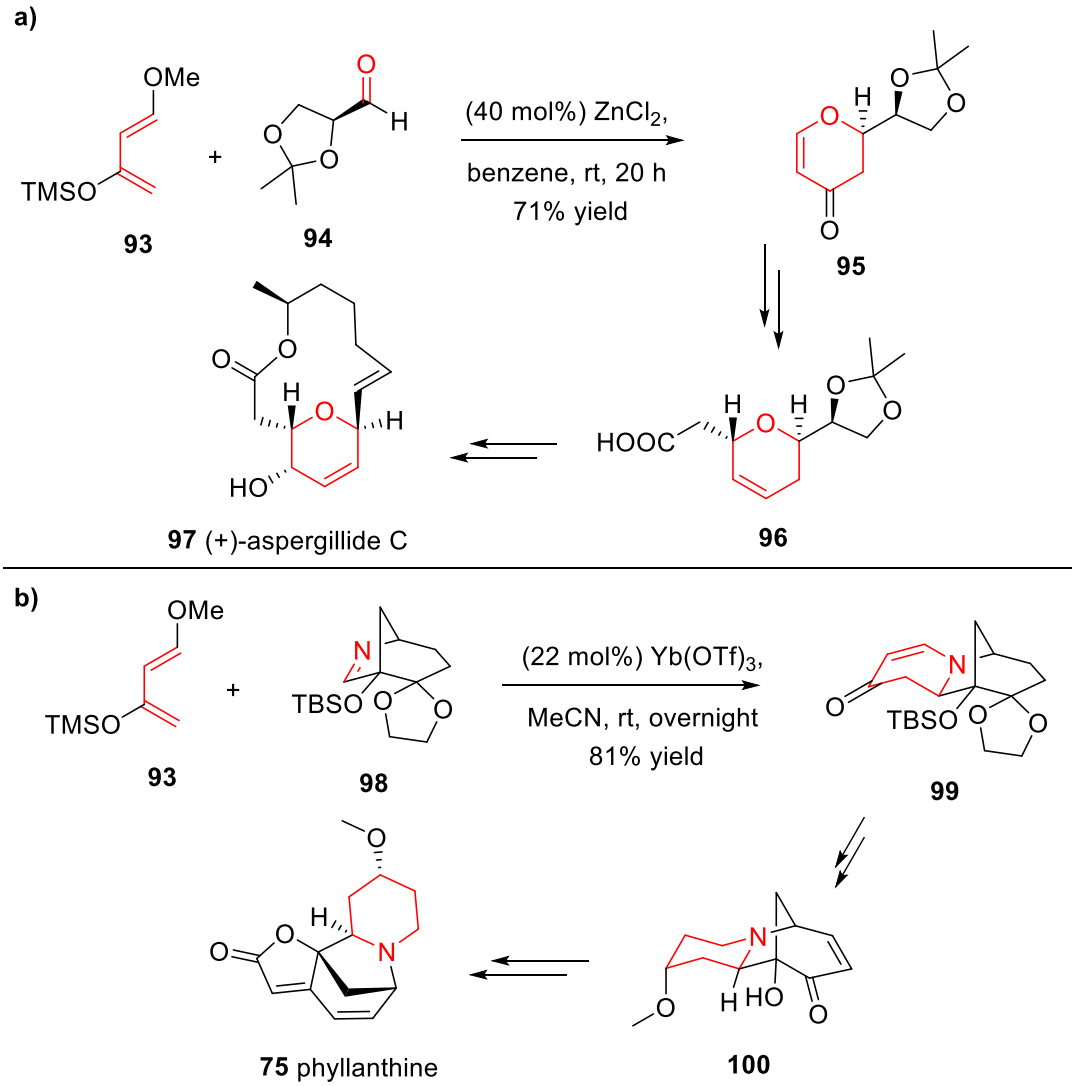

The simplest diene **93** with oxygen substituents in the 1,3-positions was developed for the Diels-Alder reaction of activated alkenes by Danishefsky in 1974.[15] After acidic hydrolysis of silyl enol ether and then elimination of the methoxy group, cyclic α,β-unsaturated ketone was obtained. Diene **93** has subsequently widely used in HDA reactions with aldehydes and imines owing to its high reactivity. In the total synthesis of (+)-aspergillide C **97**, Waters and co-workers employed diene **93** and (*S*)-glyceraldehyde acetonide **94**, prepared from

(+)-arabinose, to construct the dihydropyran skeleton in (+)-aspergillide C.[16] The reaction was catalyzed by zinc chloride and a single diastereomer **95** was obtained in 71% yield. The carbonyl group was then reduced, acylated, and then displaced in a S_N2' reaction with the installment of a side chain next to the oxygen (Scheme 3.3a). Diene **93** has also been used to react with an imine in the total synthesis of phyllanthine **75** by Weinreb and co-workers.[17] Imine **98**, prepared from the corresponding tosyl amine, was employed as dienophile in the HDA reaction to construct the piperidine skeleton in phyllanthine **75**. While a variety of common Lewis acid catalysts ($SnCl_4$, $TiCl_4$ et al.) resulted in low yield due to the destruction of the sensitive ketal and silyl either groups, dihydropyridone **99** was obtained in 81% yield with 22 mol% $Yb(OTf)_3$ as catalyst. It was also found that this HDA reaction could be completed at high pressure without any catalyst (71% yield, 12 kbar). The structure of **99** was confirmed by X-ray crystallography, indicating that the desired *exo* product was formed in the reaction. This is not surprising because imine **98** has bulky groups next to carbon nitrogen double bond, which favors the attack of diene from less hindered *exo* side, and also it lacks a π-system to provide orbital overlap, making the *endo* attack less favored. After reduction, deprotection, Julia olefination and further derivatizations, the first total synthesis of natural product **75** phyllanthine was achieved (Scheme 3.3b).

Scheme 3.4 Constructing aromatic heterocycles by HDA reactions

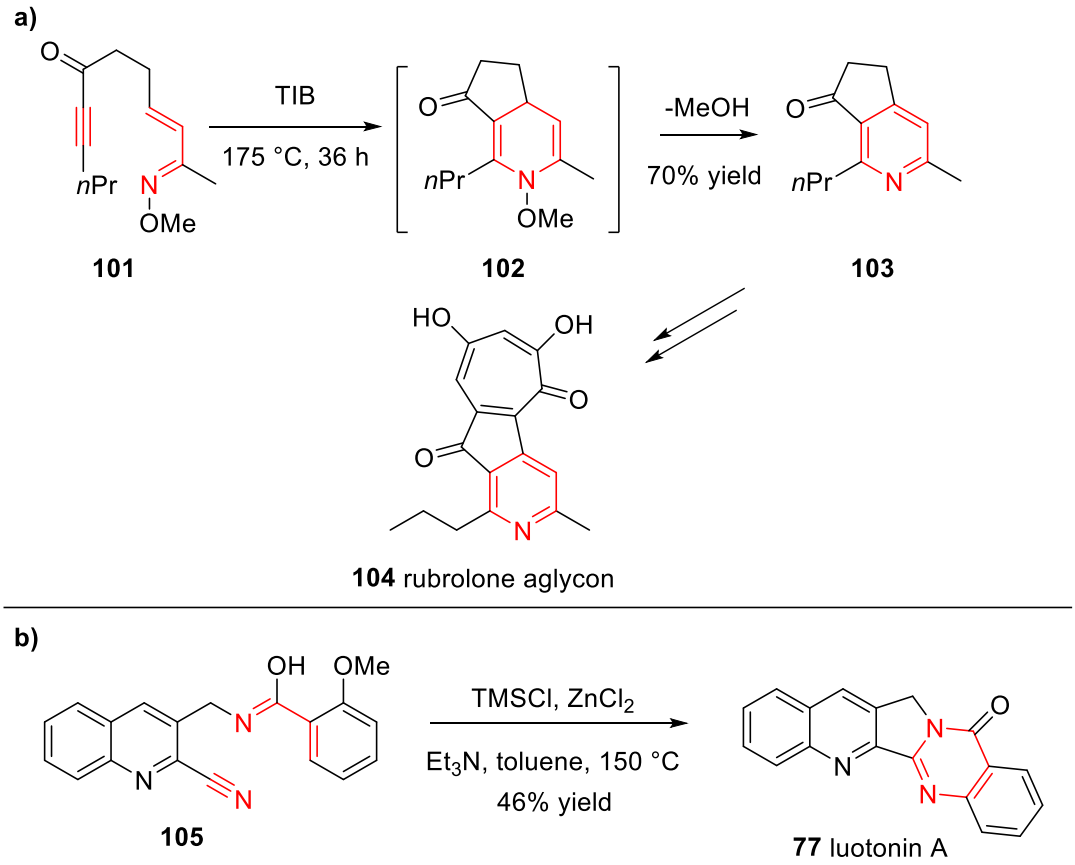

HDA reactions have also been used to synthesize aromatic rings. Due to the lack of proper degree of unsaturation in the product when using dienophile with double bonds, triple bonded species such as alkynes and nitriles have been used as dienophiles in the HDA reaction for the purpose of accessing aromatic heterocycles. Boger et al. employed an intramolecular HDA reaction between an oxime ether moiety as the diene and an alkyne moiety as dienophile to build up the pyridine skeleton in the total synthesis of rubrolone aglycone.[18] Heating oxime ester **101** in 1,3,5-triisopropylbenzene (TIB) at 175 ˚C for 36 hours afforded the in-situ aromatized product **103** via intermediate adduct **102** by the loss of methanol (Scheme 3.4a). The attachment of the methyl ether on the nitrogen was proposed

to be the key in achieving this HDA reaction, as it injected sufficient electron density into the diene moiety.[3] In the total synthesis of luotonin A by Nomura and co-workers, an intramolecular HDA reaction between a cyanide and a tautomerized amide led to the formation of luotonin A after aromatization (Scheme 3.4b).[19] These examples further established the significance for intramolecular HDA reactions in the synthesis of polycyclic compounds.

The inverse electron-demand strategy has often been employed using an α,β-unsaturated ketone or imine as diene, taking advantage of the electron deficient nature of these compounds. A tandem Knoevenagel condensation-intramolecular inverse electron-demand HDA reaction was used in the total synthesis of leporin A by Snider and Lu.[20] Pyridone **106** and dienal **107** underwent Knoevenagel condensation in the presence of triethylamine, giving intermediate **108**. The enone moiety was then attacked by the double bond to achieve an intramolecular inverse electron-demand HDA reaction. This one pot process afforded tricyclic adduct **109** in 35% yield. Further hydroxylation and methylation completed the total synthesis of leporin A **110** (Scheme3.5a). A biomimic total synthesis of variecolortide A using a late-stage HDA reaction was developed by Zipse and Trauner et al.[21]. The HDA reaction between enone **111** and dienophile **112** under thermal conditions followed by aromatization-induced 1,5-hydrogen shift and oxidation afforded variecolortide A **113** in 48% yield in one step (Scheme 3.5b). DFT calculations supported that the cyclization step was concerted instead of stepwise. Rizzacasa et al. applied the HDA reaction to build up the key spiroketal fragment in the total synthesis of (–)-reveromycin A **117**.[22] Enone **114** and

methylene pyran **115** underwent HDA cyclization thermally to produce spiroketal **116** as single diastereomer in 26% yield in the absence of a catalyst. The stereochemistry of the spiro core was set by an axial approach of the carbonyl group in the transition state. They later improved this step by using a Lewis acid to promote the inverse electron-demand HDA reaction.[23] Siproketal **116** was obtained in 86% yield in the presence of $Eu(fod)_3$ (Scheme 3.5c).

Another example of using the HDA reaction to construct spiroketals was presented by Tietze et al. in the total synthesis of mycotoxin (–)-talaromycin B.[24] Enone **118** reacted with methylene pyran **119** to generate siprokital **120** via an inverse electron-demand HDA reaction. Reduction of acid and deprotection of the alcohol led to the synthesis of (–)-talaromycin B **121** (Scheme 3.6a).[25] Other spiro-fused rings could also be built up by the HDA reaction, as illustrated in the total synthesis of antiviral spirooliganone A and B by Tong and co-workers.[26] Spiro-adduct **124** was formed in 79% with a 1:1 diastereomeric ratio. The two isomers of **124** were separately derivatized into spirooliganone A **125** and B **126** (Scheme 3.6b).

Scheme 3.5 Inverse electron-demand HDA reactions in total syntheses

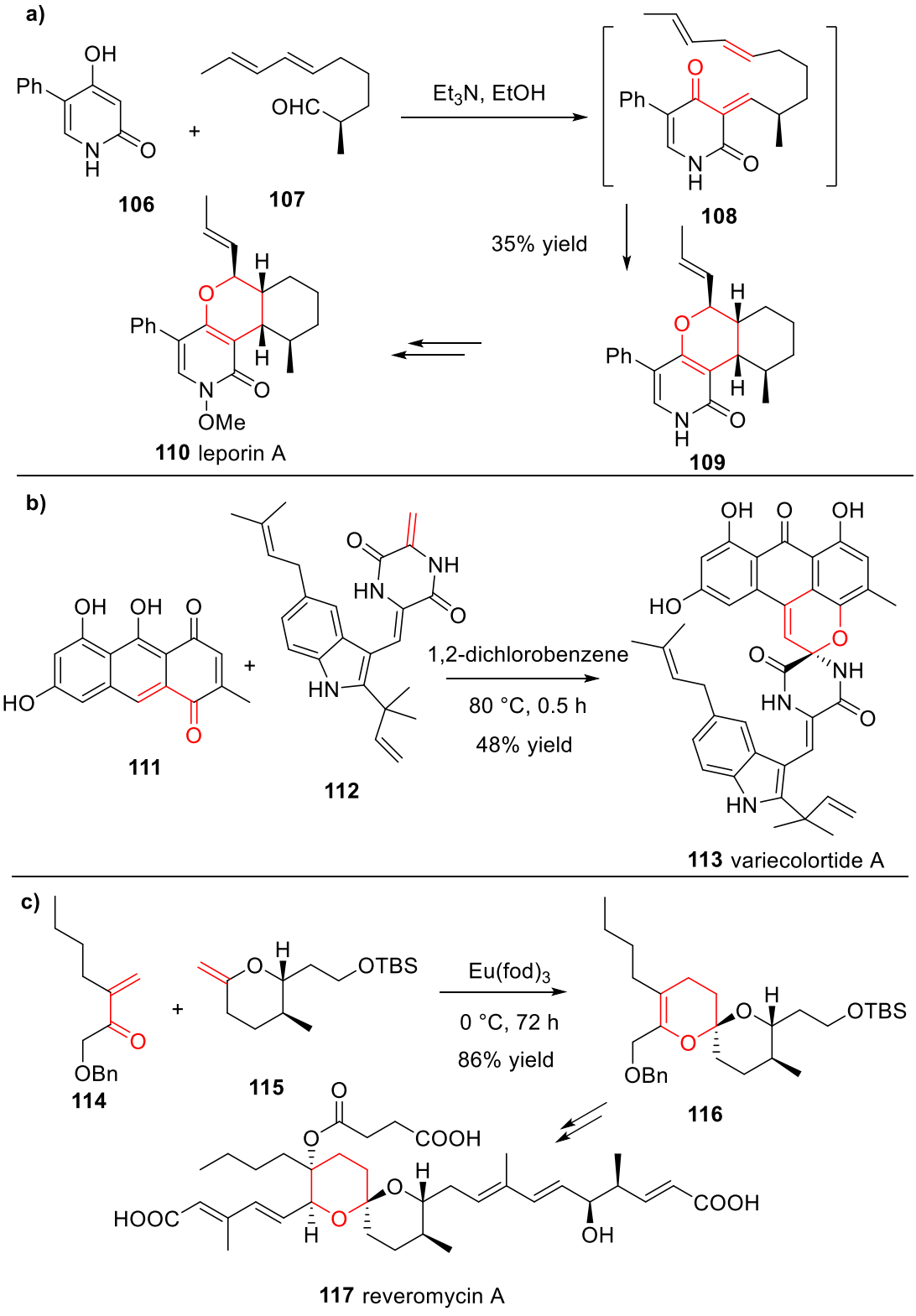

Scheme 3.6 HDA reactions in the construction of spiro compounds

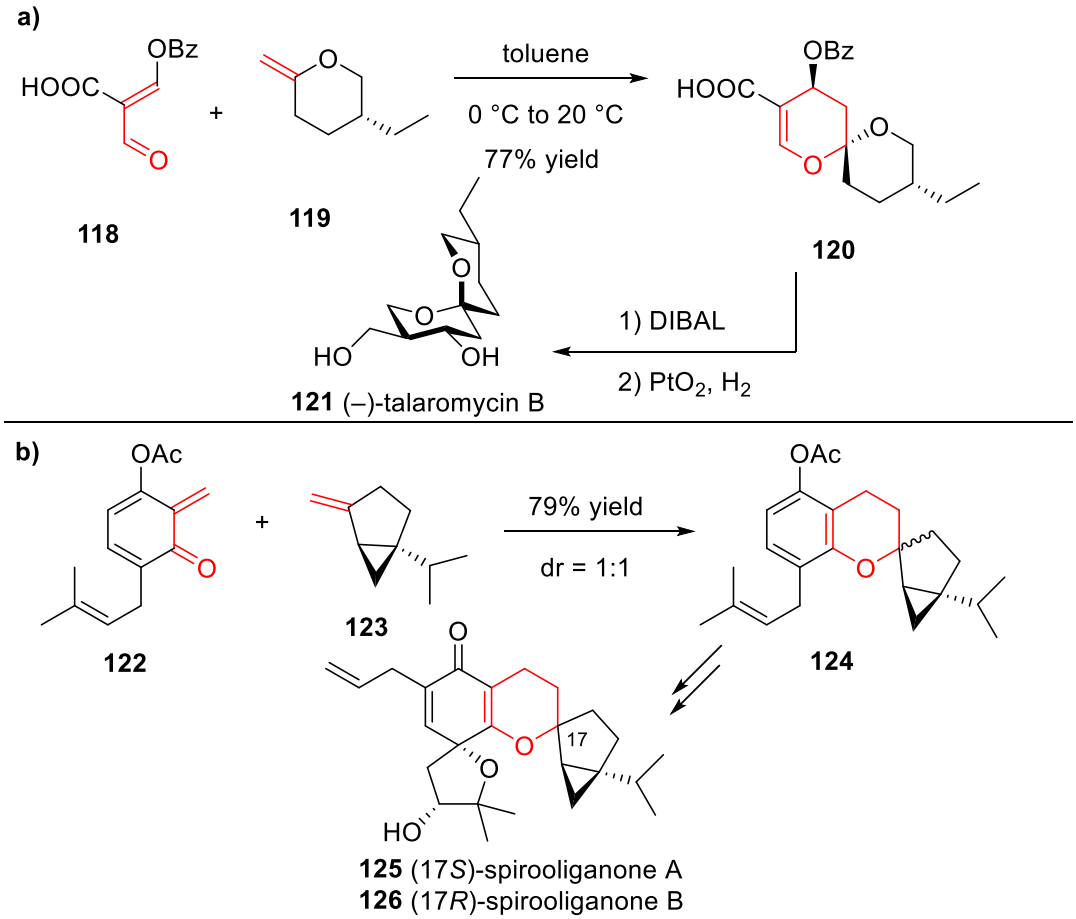

HDA reactions with other uncommon dienophiles have been used in total synthesis, either to construct important skeletons or to generate important synthetic intermediates. In the total synthesis of agelastatin A by Weinreb and co-workers, *N*-sulfinylmethylcarbamate **127** was employed as dienophile to produce adduct **129** with cyclopentadiene **128** via a HDA reaction.[27] Subsequent Grignard addition, [2,3]-sigmatropic rearrangement and carbamate formation led to bicyclic **132**, which is the precursor to agelastatin A (Scheme 3.7a).[3] In the total synthesis of fasicularin and lepadiformine, Kibayashi and co-workers employed an intramolecular HDA reaction with an *N*-acylnitroso moiety as dienophile.[28]

Oxidation of previously prepared chiral substrate **134** using $NaIO_4$ in aqueous media in situ generated *N*-acylnitroso compound **135**, which in-situ proceeded to undergo the intramolecular HDA reaction with the diene moiety giving bicyclic *trans*-adduct **136** as major product, which was taken on to lepadiformine **138**. With modification of substrate **134** that led to the formation of the *cis*-adduct, access was also proceeded to fasicularin **137** (Scheme 3.7b). The use of an allene as dienophile in the HDA reaction was explored in the total synthesis of zincophorin by Hsung and co-workers.[29,30] Chiral enone **139** was prepared from commercially available chiral hydroxy ester and chiral allene **140** was synthesized from ephedrine and urea followed by propargylation and isomerization. The HDA reaction of **139** and **140** under thermal conditions gave methylene pyran adduct **141** in 85% yield and 95:5 diastereomeric ratio. Subsequent hydrogenation of the *exo*-cyclic olefin with palladium on carbon established the desired stereochemistry, which was then derivatized into zincophorin **142** (Scheme 3.7c).

Scheme 3.7 HDA reactions with uncommon dienophiles in total syntheses

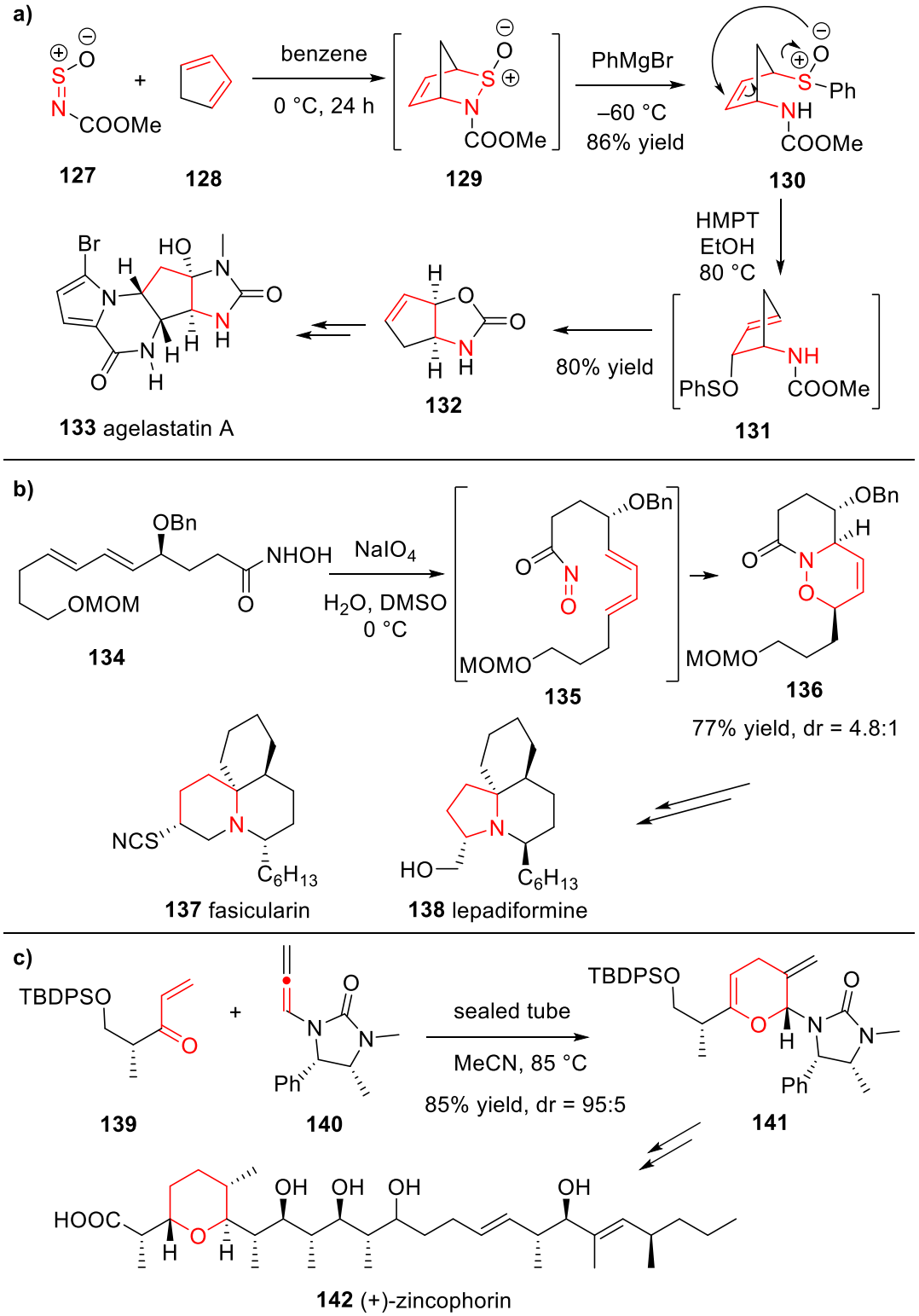

Because of the usefulness of HDA reactions in the total synthesis of natural products and bioactive molecules as discussed above, there is a high demand for the development of asymmetric HDA reactions that allow access to optically pure six-membered heterocycles.[31] Some of examples illustrated above employed chiral dienes or dienophiles, in which the stereochemistry was determined by previously installed chiral moieties. A more efficient way to control the stereochemical outcome of reactions is to develop enantioselective reactions with chiral catalysts, which allows the direct formation of chiral heterocycles from achiral substrates with sub-stoichiometric amount of chiral materials.[32]

Since Lewis acids can promote both normal HDA reactions and inverse electron-demand HDA reactions by lowering the corresponding LUMO orbitals, many chiral Lewis acid catalysts have been developed during the past several decades as shown in Figure 3.2. Danishefsky et al. in 1983 employed $Eu(hfc)_3$ **143** as a chiral catalyst in the HDA reaction with diene bearing chiral auxiliaries.[33] Yamamoto and co-workers in 1988 established the first efficient asymmetric HDA reaction catalyzed by a chiral organoaluminum catalyst **144**.[34] The catalyst **144** was found to be effective in reaction between various aldehydes and Danishefsky's diene. Another aluminum catalyst **145** with a hyper-coordinating nature was developed by Jørgensen and gave up to 97% yield and >99% *ee* in enantioselective HDA reactions.[35] Chromium catalysts such as **146** (Cr-salen) and **147** (Cr-Schiff base) were developed by Jacobson et al. and have been applied to many total syntheses of natural products.[36,37] These chromium-catalyzed HDA reactions were found to proceed through a concerted mechanism, while chiral

oxazaborolidine **148** catalyzed the HDA reaction via the Mukaiyama aldol pathway.[38] Many other Lewis acid catalysts derived from chiral ligands and transition metals such as zirconium[39], rhodium[40], titanium[41,42] and copper[43] have been found to be effective in the asymmetric HDA reactions.

Figure 3.2 Selected Lewis acid catalysts for asymmetric HDA reactions

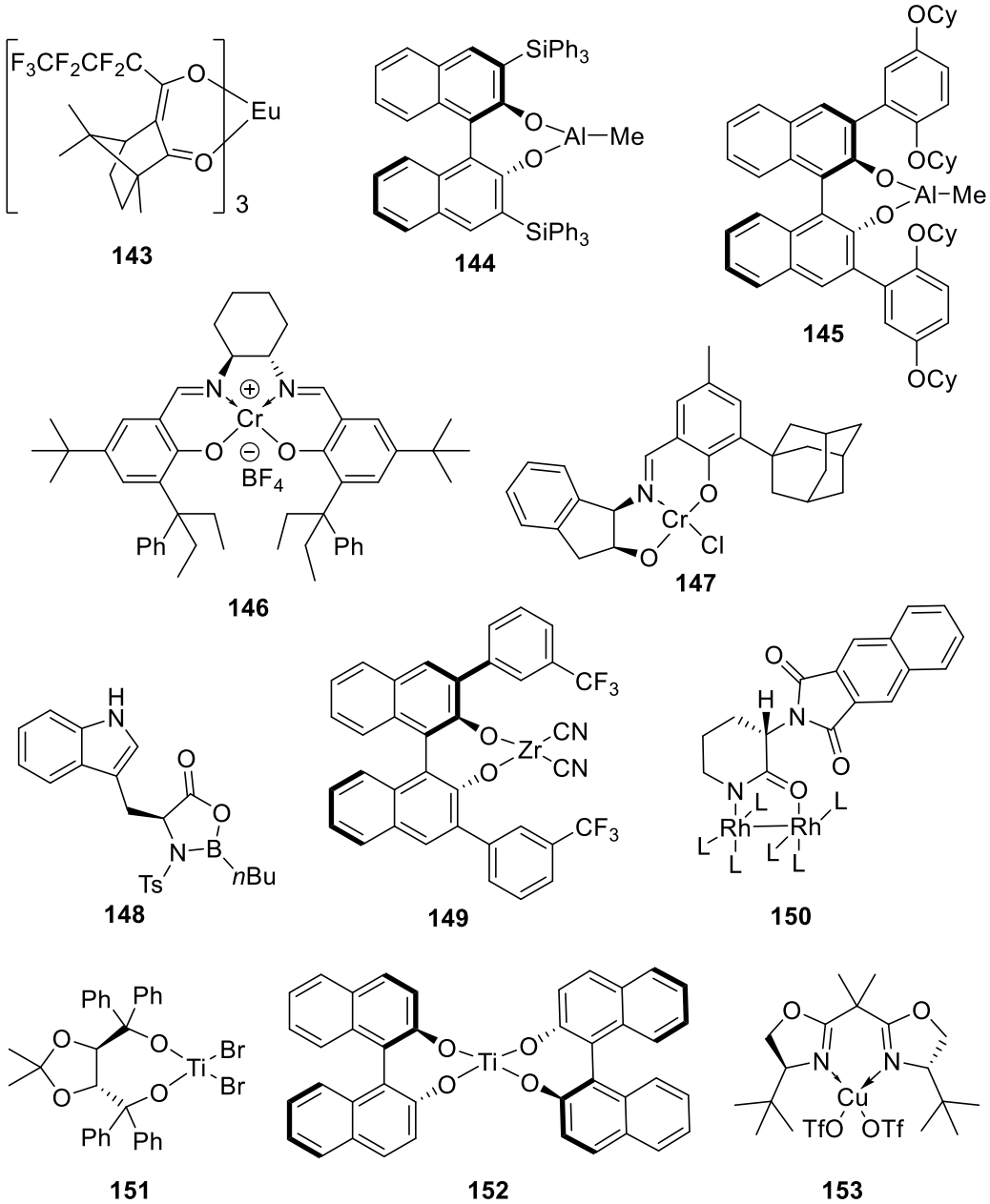

Chiral organocatalysts (Figure 3.3) have also been used in the asymmetric HDA reactions, in which the substrates are activated via hydrogen-bonding to catalysts. Rawal et al. in 2003 employed TADDOL derivative **154** as hydrogen-bond donor to catalyze the reaction between dienes and aldehydes with excellent enantioselectivities.[44] Ding and co-workers in 2004 found that BINOL-derived hydrogenphosphate **155** could activate carbonyl groups and catalyze the asymmetric HDA reaction between dienes and glyoxylates.[45] Chiral disulfonimide **156** was used as catalyst in the HDA reaction between Danishefsky's diene **93** and aldehydes with high asymmetric inductions developed by List et al. in 2012.[46]

Figure 3.3 Chiral organocatalysts in asymmetric HDA reactions

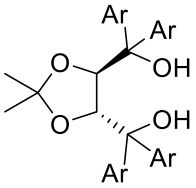

Ar = 1-naphthyl

154

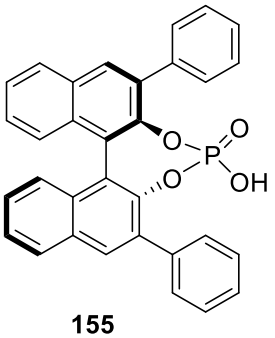

155

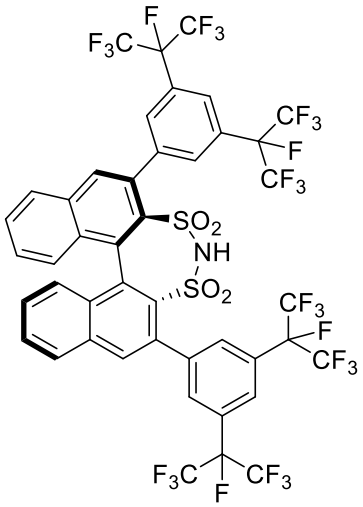

156

Among these chiral Lewis acid catalysts and organocatalysts, chromium catalyst **147** plays a predominant role in the total synthesis of natural products. The asymmetric HDA reactions between dienes and alkynals catalyzed by **147** produced enantioenriched alkynyl dihydropyran species, which were used in the

enantioselective total synthesis of aphadilactone A-D[47], GEX1Q1[48], anguinomycin C and D[49] (Scheme 3.8). Excellent asymmetric inductions were observed.

Scheme 3.8 Chromium catalyst **147** with alkynals in total syntheses

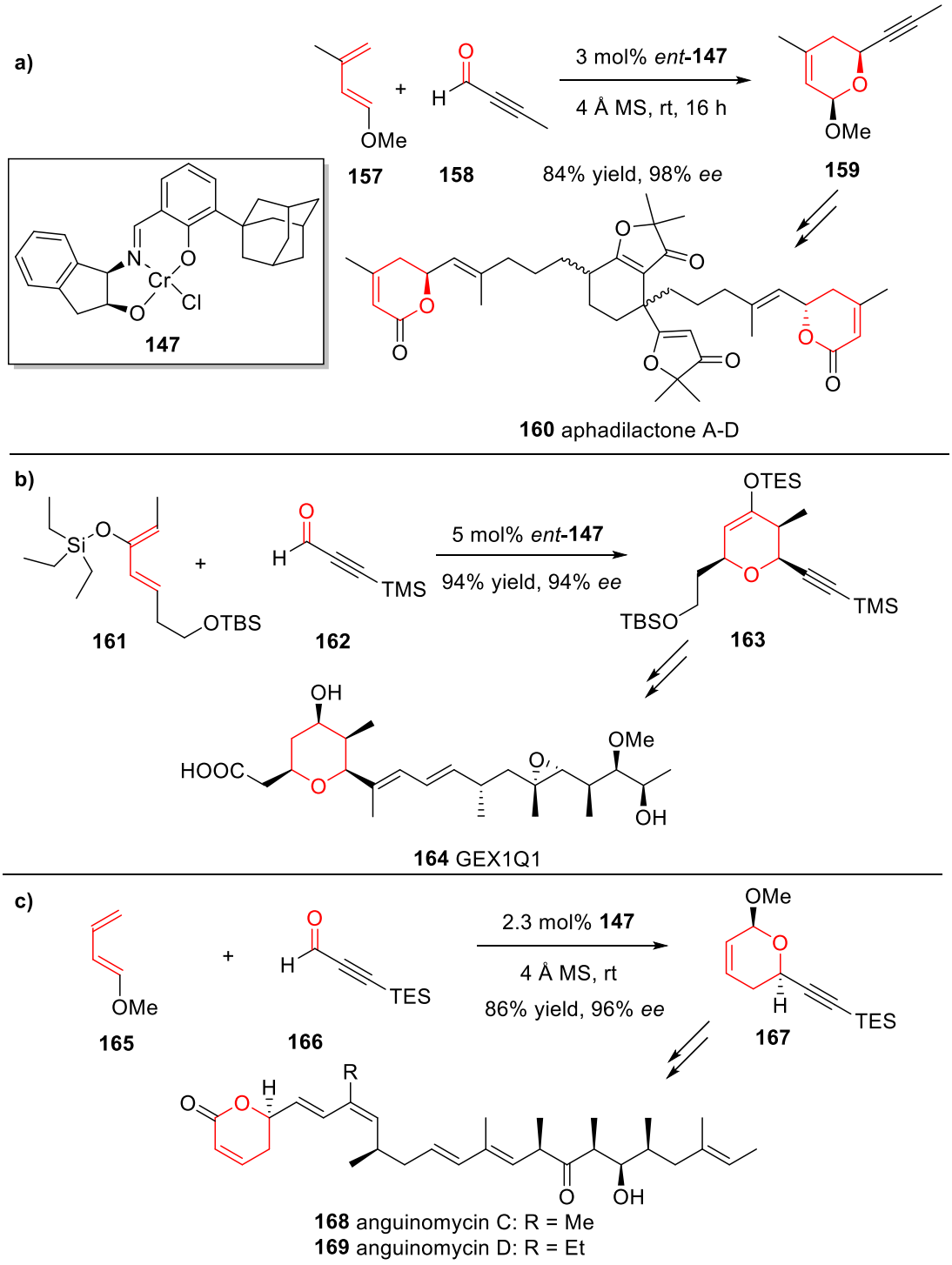

The asymmetric HDA reaction between a diene and an acetaldehyde that bears oxygen substituents at α-position has drawn a lot of attention from chemists, as it allows for the construction of hexose skeleton with designed stereochemistry. The enantioselective HDA reactions of (*tert*-butyldimethylsilyloxy)acetaldehyde **170** and various dienes catalyzed by chromium catalyst **147** have been studied and applied in the total syntheses of many natural products (Scheme 3.9). In 2012, Sasaki and co-workers employed the catalytic asymmetric HDA reaction of aldehyde **170** and diene **171** to build up the key tetrahydropyran structure in the total synthesis of (–)-polycavernoside A.[50] With 3 mol% of catalyst **147**, two chiral centers in the target were realized and *endo*-adduct **172** was produced as single diastereomer in 60% yield and 96% *ee*. Following derivatizations such as hydrogenation of the tetrahydropyran ring set up additional stereo centers based on the existing chiral environment. Thus, the enantioselective total synthesis of polycavernoside A could be accomplished by taking advantage of the catalytic asymmetric HDA reactions in an early stage of the synthesis. Asymmetric HDA reactions between aldehyde **170** and different dienes catalyzed by the chromium complex **147** led to the construction of various enantioenriched cycloadducts as key building blocks, which have been used in total synthesis of neosidomycin,[51] dactylolide,[52] leucascandrolide A,[53] and lasonolide A.[54] *Endo*-cyclization products were generally favored and high diastereomeric ratio were observed with excellent enantioselectivities (94-99% *ee*). The regiochemistry could be programmed by changing the position of the electron-donating groups on the diene. With silyloxy group at the 2-position, diene **171** gave adduct **172** with the aldehyde oxygen being

connected with the carbon at 4-position of diene, while with methoxy group at 1-position, opposite regiochemistry was observed.

Scheme 3.9 Chromium catalyst **147** with aldehyde **170** in total syntheses

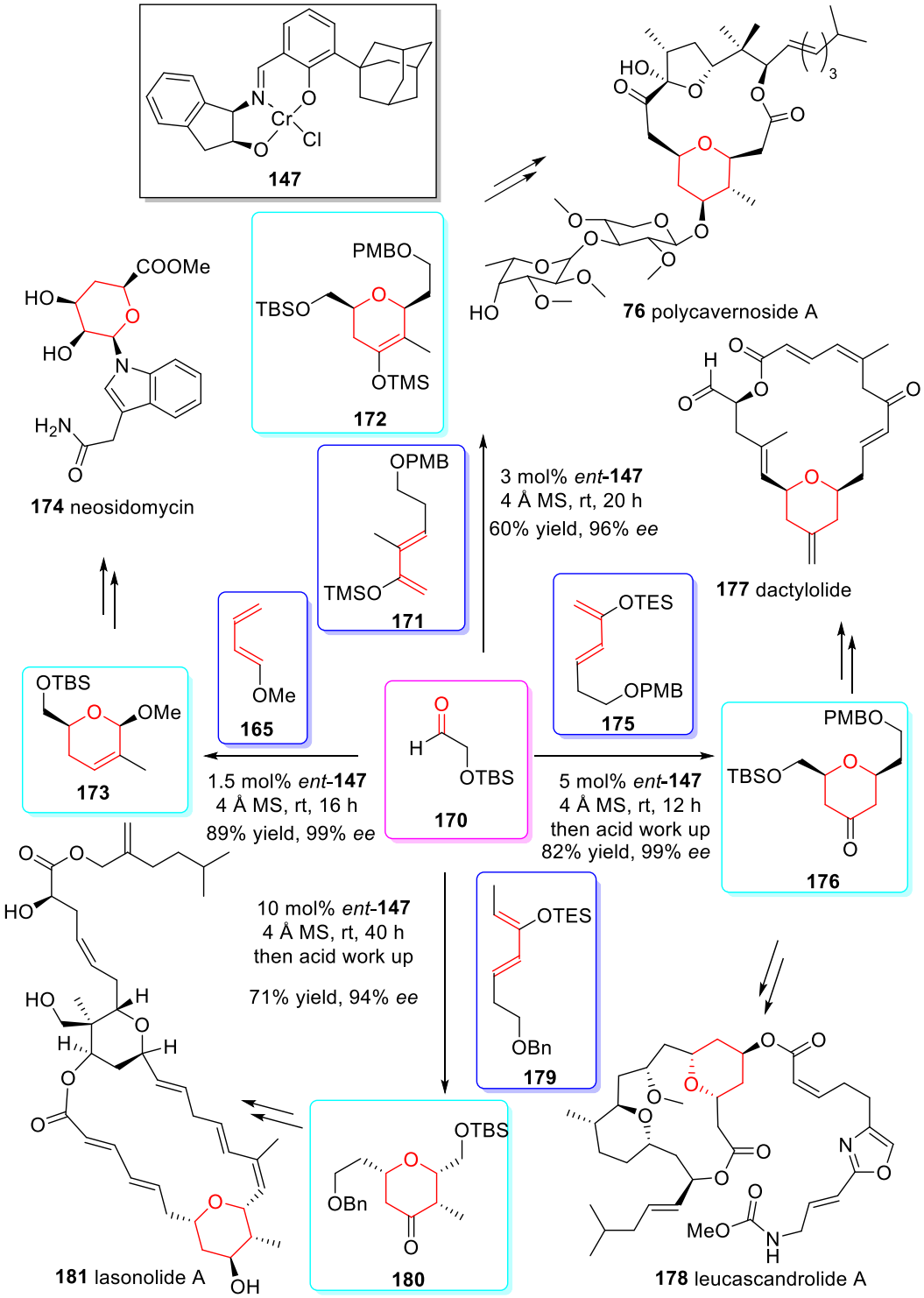

Some total syntheses have employed asymmetric HDA reactions between chiral aldehydes or chiral dienes. The potent catalyst **147** was able to control the stereochemical outcome of cycloadduct in high diastereomeric ratio, regardless of the chirality previously installed in the aldehyde or the diene (Scheme 3.10). In the enantioselective total synthesis of neopeltolide **185** by Ghosh et al., diene **183** with three chiral centers was reacted with aldehyde **182** in the presence of 10 mol% catalyst **147**.[55] After acidic work up, the silyl protecting groups were removed and adduct **184** was formed in 83% yield with diastereomeric ratio of 97:3. The tosylate moiety on **184** was then replaced by a cyano group followed by hydrolysis and macrolactonization. The carbonyl group was reduced and a subsequent Mitsunobu esterification installed the side chain and completed the total synthesis of neopeltolide **185**. Another total synthesis of neopeltolide was developed by Paterson et al., who utilized aldehyde **186** instead of diene **183** with the proper chiral centers in the asymmetric HDA reaction catalyzed by **147**.[56] It was not surprising to find that the HDA reaction between the two bulky substrates **186** and **187** required a prolonged reaction time (8 days), compared with the reaction of the less sterically hindered aldehyde **182**. In the total synthesis of bistramide A by Floreancig, both aldehyde **189** and diene **190** have chiral centers.[57] It was confirmed that the use of achiral aldehyde and diene analogs produced adducts with same stereochemistry. Oxidation of the silyl enol ether adduct by DDQ gave dihydropyrone, which was attacked by the oxygen on the side chain after acidic work up. Spiroketal **191** was achieved in 58% yield in a one-pot process, which is the precursor of bistramide A **74**.

Scheme 3.10 Asymmetric HDA reactions with chiral aldehydes or dienes

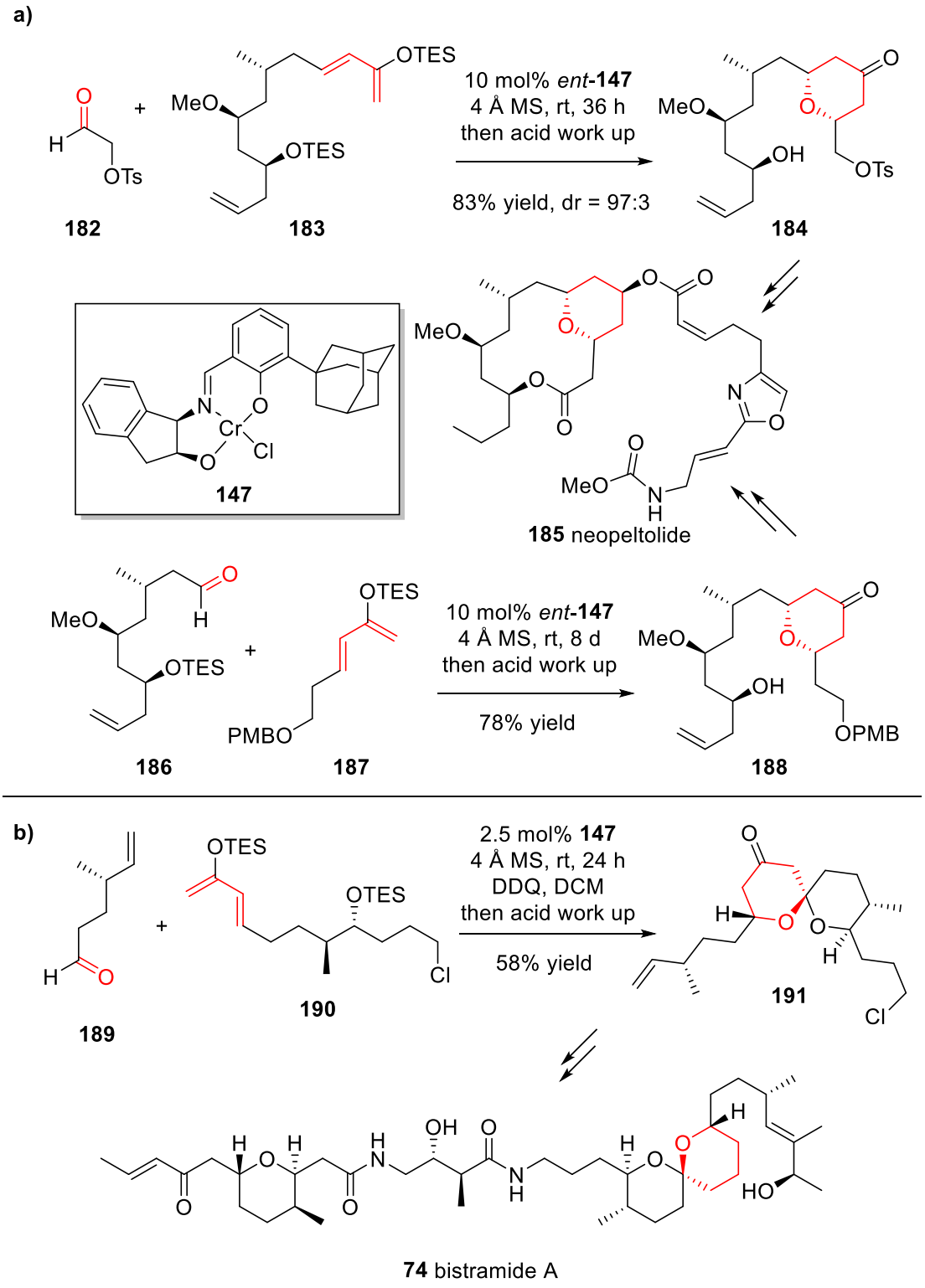

Scheme 3.11 Rhodium-catalyzed asymmetric HDA reactions in total syntheses

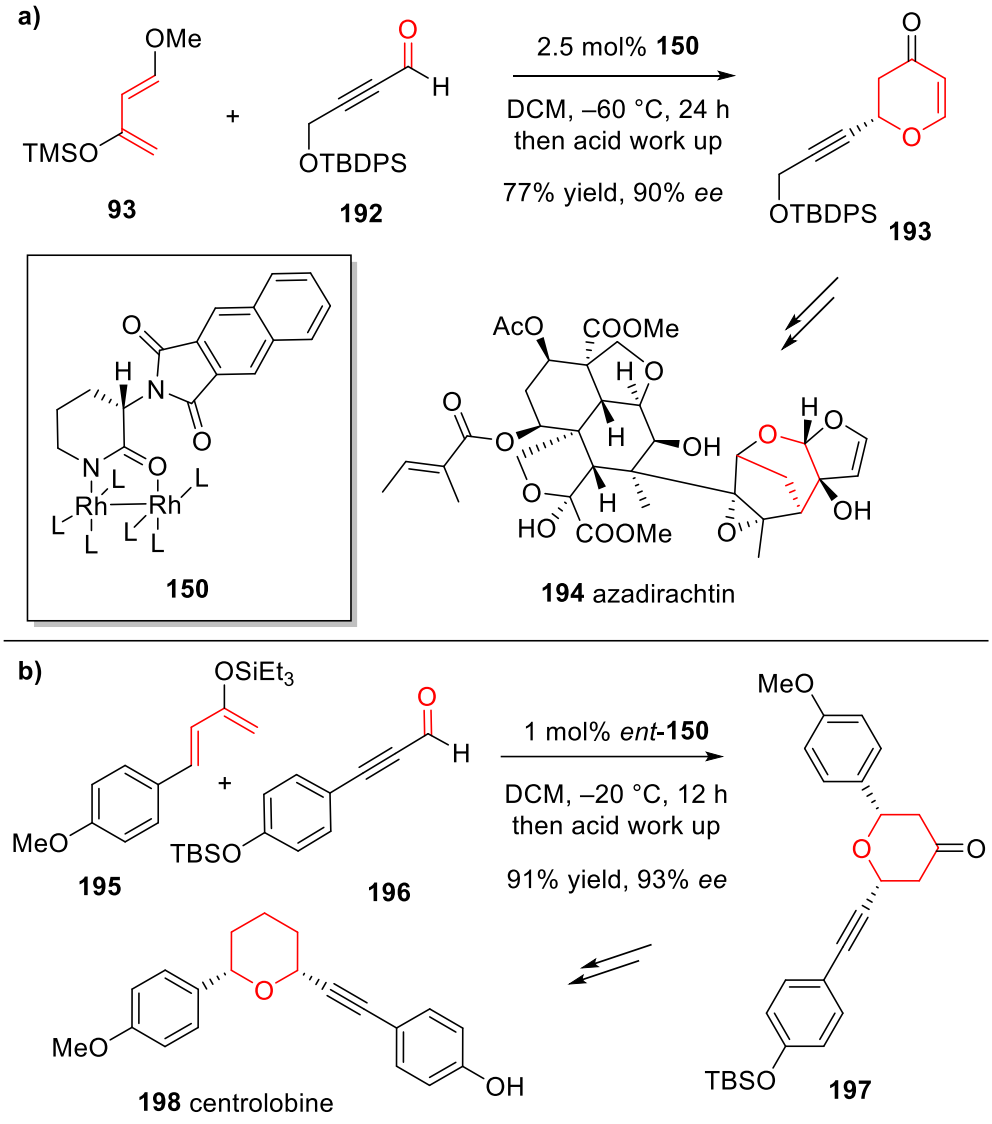

Second to the most popular chromium catalyst **147**, are rhodium (Scheme 3.11) catalyzed asymmetric HDA reactions, which have also been employed in total syntheses. In the total synthesis of azadirachtin **194** by Ley and co-workers,[58] the asymmetric HDA reaction between Danishefsky's diene and alkynal **192** was utilized to build up the tetrahydropyran moiety with a tethered alkynyl group.[59] Many catalysts were inappropriate for this transformation while the rhodium

catalyst **150** was found to be effective, giving adduct **193** in 77% yield and 90% *ee*. The same catalyst was also useful in the reaction between diene **195** and alkynal **196**, which tied into the total synthesis of centrolobine **198**.[60,61]

Scheme 3.12 Copper-catalyzed asymmetric HDA reactions in total syntheses

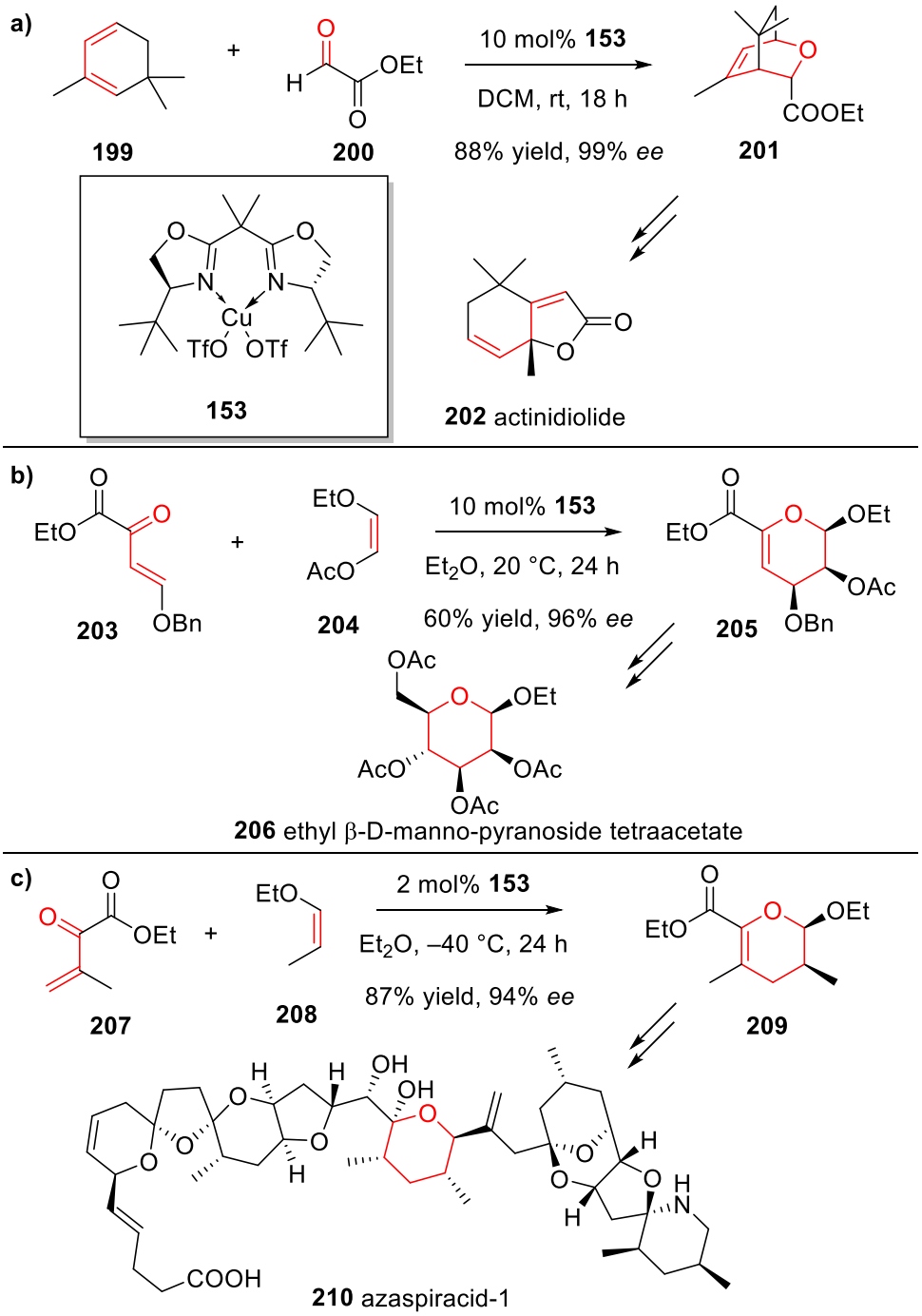

Examples of copper-catalyzed asymmetric HDA reactions in total syntheses are shown in Scheme 3.12. Cu-BOX catalyst **153** was used in the reaction between cyclic diene **199** and glyoxylate **200**, giving the bicyclic adduct **201** in 88% yield and 99% *ee*. After hydrolysis, rearrangement and elimination, actinidiolide **202** was synthesized from **201**.[62] An inverse electron-demand HDA reaction catalyzed by **153** was used to construct the hexose skeleton in the total synthesis of ethyl β-D-manno-pyranoside tetraacetate **206**.[63] The use of electron-deficient diene **203** and electron-rich dienophile **204** created adduct **205** with high asymmetric induction. A similar reaction was employed in the total synthesis of azaspiracid-1 **210** to construct the middle tetrahydropyran ring, as illustrated by Evans and co-workers in 2008.[64]

3.1.2 Chiral borates in asymmetric reactions

Boron species are one of the most important Lewis acids among all main group elements owing to its electron-deficient nature. Many chiral boron catalysts (Figure 3.4) have been developed since Mamedov first employed BF_3•mentholOEt in the asymmetric Diels-Alder reaction in 1976.[65] Some chiral oxazaborolidine catalysts were found to be effective in a number of asymmetric reactions with carbonyl compounds, such as CBS reduction,[66] Diels-Alder reaction,[67] cyclopropanation[68] and Roskamp reaction.[69] In 1988, Yamamoto and co-workers reported an asymmetric Diels-Alder reaction with excellent enantioselectivity catalyzed by a chiral acyloxyborane (CAB) catalyst **213** that is derived from tartaric acid.[70] They later employed this type of catalyst in asymmetric aldol reactions,[71] aldehyde allylations[72] and aza-Diels-Alder reactions.[73] The CAB catalysts were

proposed to be a Brønsted acid assisted Lewis acid, known as BLA catalyst.[74] The hydrogen bonding between carboxylic acid and the oxygen on the oxazoborolidine enhanced the Lewis acidity of the boron by reducing electron density on the oxygen next to boron.

Figure 3.4 Selected chiral boron catalysts

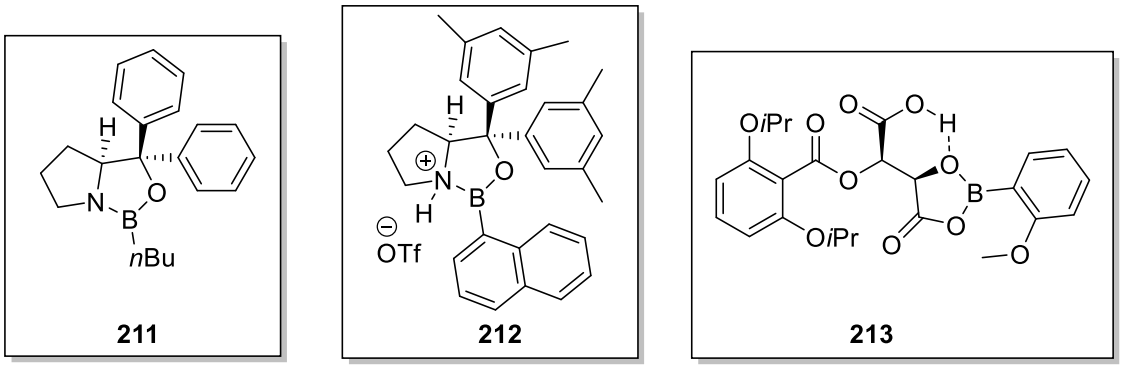

Kaufmann et al. in 1990 reported the first chiral borate-catalyzed asymmetric Diels-Alder reaction.[75] By reacting 3 equivalent of BINOL with 2 equivalent of $H_2BrB{\bullet}SMe_2$, a propeller-like borate species **216** was generated and utilized as a catalyst in reaction between methacrolein **214** and cyclopentadiene **128**. *Exo*-adduct **215** was formed in 85% yield and 99% *ee* after 2 days at –78˚. BLA catalyst **217** developed by Yamamoto was found to be effective in the same asymmetric Diels-Alder reaction, which reduced reaction time to 4 hours.[76] To investigate the importance of the hydrogen bonding in **217** to activate the Lewis acidic boron center in the BLA catalyst, the free phenolic group was protected with benzyl giving catalyst **218**. Unsurprisingly, the use of **218** as catalyst, which lacks hydrogen bonding donor to enhance the Lewis acidity, resulted in lower enantioselectivity.[76] BLA catalysts **219** and **220** were derived from boronic acids with a chiral triol.[77,78] While both catalysts were efficient in the asymmetric Diels-

Alder reaction, catalyst **219** with boron connected to two oxygens on the chiral ligand gave higher yield, regioselectivity and enantioselectivity (Scheme 3.13).

Scheme 3.13 Chiral borate catalysts in asymmetric Diels-Alder reaction

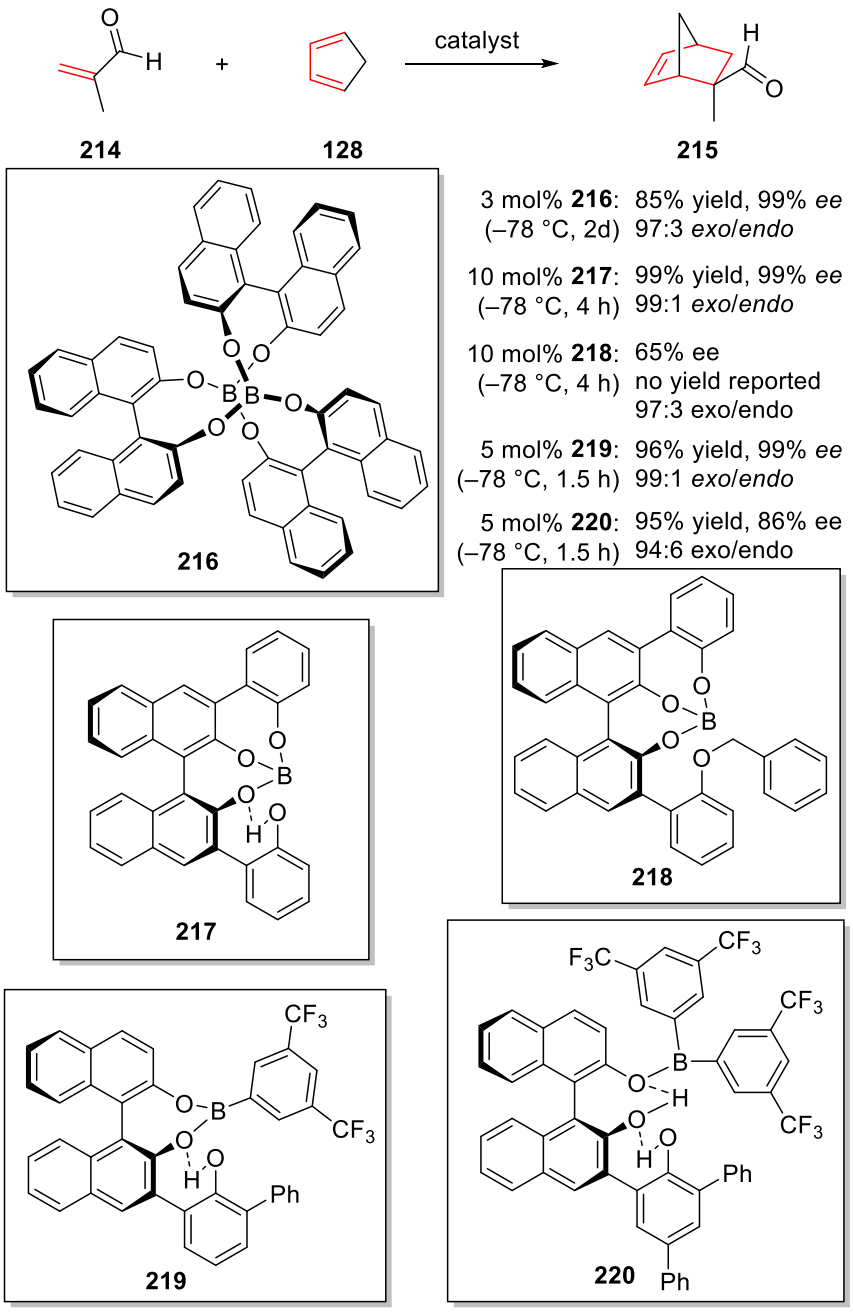

A spiro-borate catalyst **221** has been developed by Yamamoto and co-workers in the asymmetric HDA reaction between an imine and Danishefsky's

diene (Scheme 3.14).[79] It was deprotonated by imine substrates and the structure was confirmed by X-ray crystallography, which could be classified as one of the earliest examples of asymmetric counterion directed catalysis.[80] However, due to the higher basicity of adduct **224**, no catalyst turnover was observed and a stoichiometric amount of **221** was required. One equivalent of catalyst **221** has also been used in the Mannich reaction to give the β-amino ester **227**.[81] It has been shown that a catalytic amount of **221** was able to catalyze an asymmetric aziridination reaction with moderate yield and low *ee*.[82]

Scheme 3.14 Chiral spiro-borate catalysts

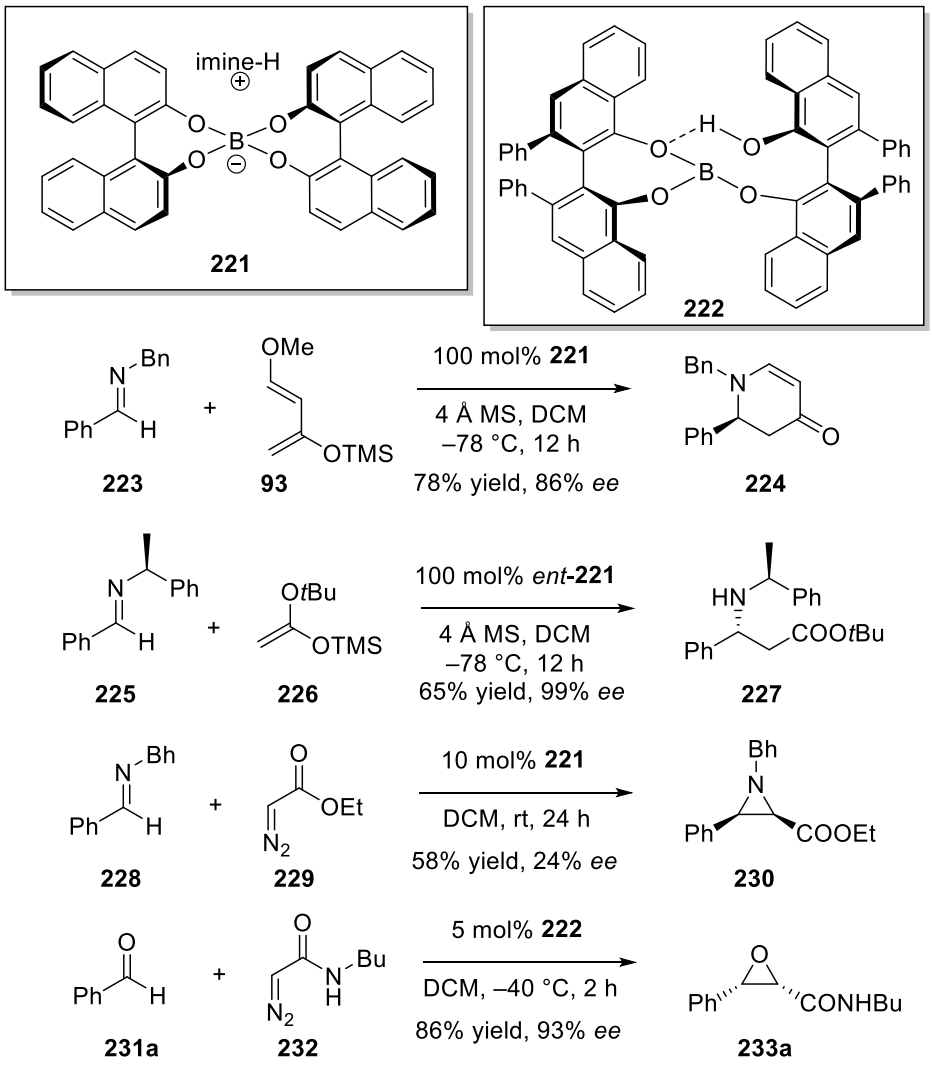

A VANOL-derived borate **222** has been shown to be involved in an asymmetric epoxidation reaction between an aldehyde and diazo compound (Scheme 3.14).[83] The substrates were not basic enough to deprotonate the catalyst, thus a Lewis acid behavior was proposed. In ^{11}B NMR, catalyst **222** showed a broad peak at ~20 ppm, supporting the existence of a tri-covalent borate species. After adding 1 equivalent of imine to **222**, a sharp peak at 9 ppm was observed, indicating the deprotonated spiro-borate species. Hydrogen bonding between free hydroxy group and an oxygen on the other ligand was found in DFT calculation, suggesting that **222** is a BLA catalyst.[84]

The Wulff group has developed a novel boroxinate catalyst **234** (BOROX) derived from 1 equivalent of VANOL or VAPOL ligand and 3 equivalents of boron. The catalyst was first applied to asymmetric *cis*-aziridination in 1999,[85] but the structure of **234** was not confirmed until 2010, when the crystal structure **235** was obtained.[86] The BOROX species consists of one tetra-covalent borate and two tri-covalent borates. This unique feature provides multiple Lewis acidic boron centers and a chiral anion that directs iminium substrates and other hydrogen bond donors to the chiral pocket formed from VANOL/VAPOL ligand. A number of BOROX-catalyzed asymmetric reactions using imine as substrate have been developed by Wulff and co-workers in the past two decades, such as *trans*-aziridination,[87] aza-Diels-Alder reaction,[88] aza-Cope rearrangement,[89] and three-component Ugi reaction.[90] Notably, an orthogonal dual catalyst system with BOROX **234** and triphenylborate was established in the catalytic asymmetric aza-Diels-Alder

reaction to solve the turnover problem presented by the fact that adduct **240** is more basic than starting material **236**.[88]

Scheme 3.15 Chiral boroxinate in asymmetric catalysis

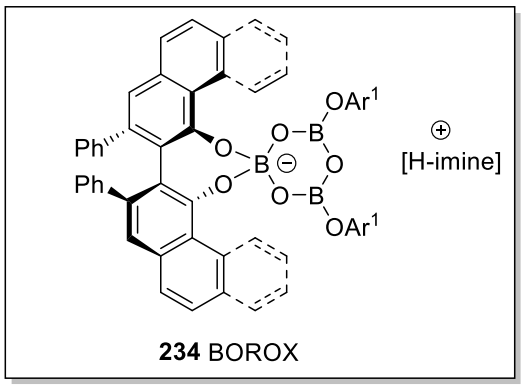

234 BOROX

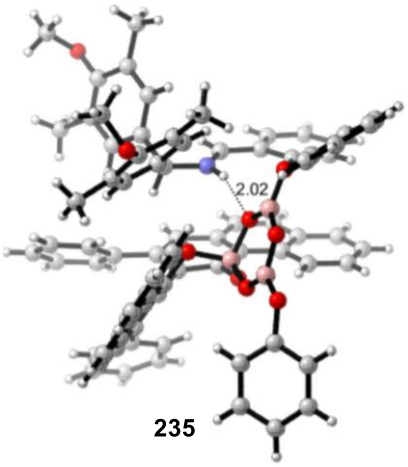

235

cis-aziridination[85]

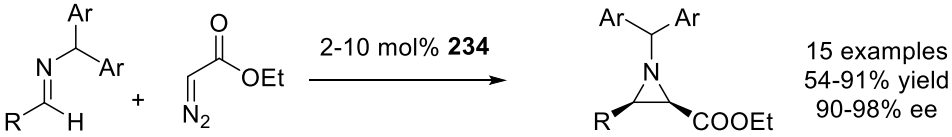

236 **229** **237**

15 examples
54-91% yield
90-98% ee

trans-aziridination[87]

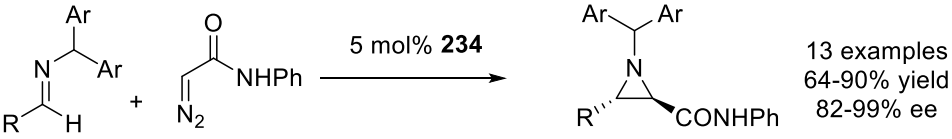

236 **238** **239**

13 examples
64-90% yield
82-99% ee

aza-Diels-Alder reaction[88]

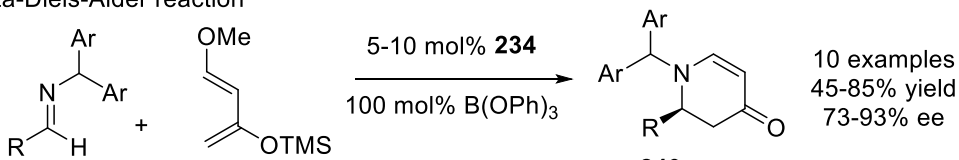

236 **93** **240**

10 examples
45-85% yield
73-93% ee

aza-Cope rearrangement[89]

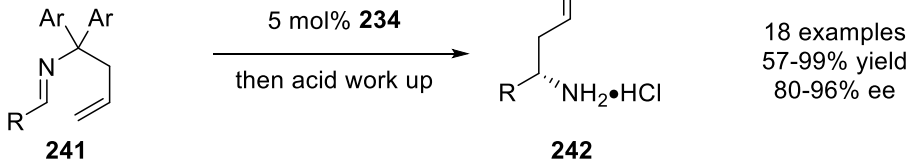

241 **242**

18 examples
57-99% yield
80-96% ee

three-component Ugi reaction[90]

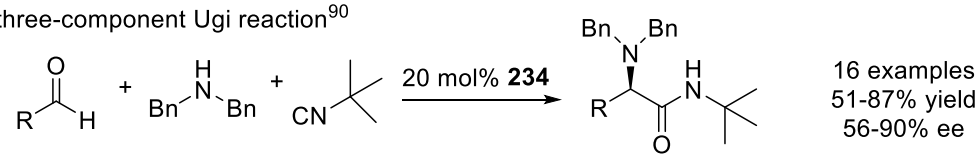

231 **243** **244** **245**

16 examples
51-87% yield
56-90% ee

3.2 Initial study

The BOROX catalyst **234** was prepared by mixing 1 equivalent of VAPOL and 3 equivalents of $B(OPh)_3$ during the development of aza-Diels-Alder reaction and the catalysts was proposed to be a Lewis acid species since the structure of catalyst has not determined at that time.[88] An oxa-Diels-Alder reaction between benzaldehyde and Danishefsky's diene **93** has been reported under the same condition as used in the aza-Diels-Alder reaction, and a 67% yield with 28% *ee* was obtained[84] (Scheme 3.16b). The research on oxa-Diels-Alder reaction was not further pursued until the structure of BOROX catalyst was determined, which revealed that a Lewis base such as an imine is required to form the boroxinate skeleton. It is not surprising that this catalyst system failed to promote the HDA reaction with aldehydes, because the carbonyl species is not basic enough to form the BOROX catalyst. To expand the use of BOROX in asymmetric reaction of aldehydes, a breakthrough was made in the development of an asymmetric epoxidation reaction between aldehydes and diazo compound by using basic additives, such as DMSO.[83] It was found that catalytic amount of DMSO successfully generated BOROX catalyst. The activation of aldehydes by the catalyst was probably the Lewis acid-Lewis base interaction between the sulfur on protonated DMSO and carbonyl on aldehydes. The same strategy was employed in the asymmetric HDA reaction with 10 mol% DMSO as additive, however, low conversion (<20% conv.) was observed (Scheme 3.16c).[84] The other catalyst used in the asymmetric epoxidation reaction is BLA catalyst **222**, and it has been found that the direct activation of aldehydes by Lewis acidic borate **222** was successful.

Therefore, 10 mol% catalyst **222** was employed in the oxa-Diels-Alder reaction. It was pleasing to find that the reaction in toluene at room temperature after 24 hours gave adduct **248b** in 79% yield and 62% ee (Scheme 3.17).[84]

Scheme 3.16 Oxa-Diels-Alder reaction with BOROX catalysts

a) Aza-Diels-Alder Reaction

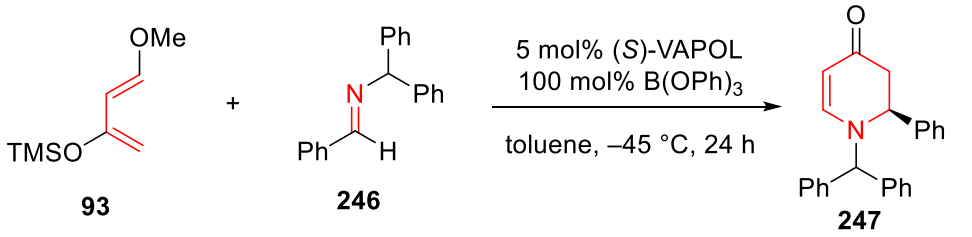

85% yield, 93% ee

b) Tentative Oxa-Diels-Alder Reaction (Unpublished Result)[84]

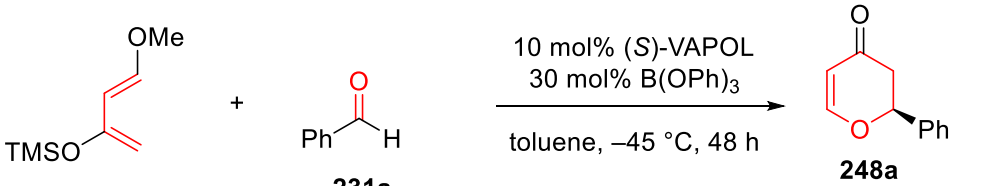

67% yield, 28% ee

c) Tentative Oxa-Diels-Alder Reaction with BOROX[84]

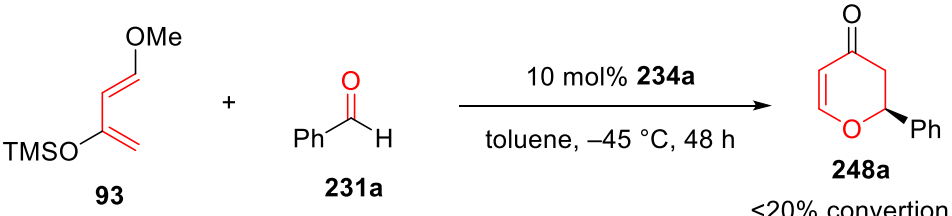

<20% convertion

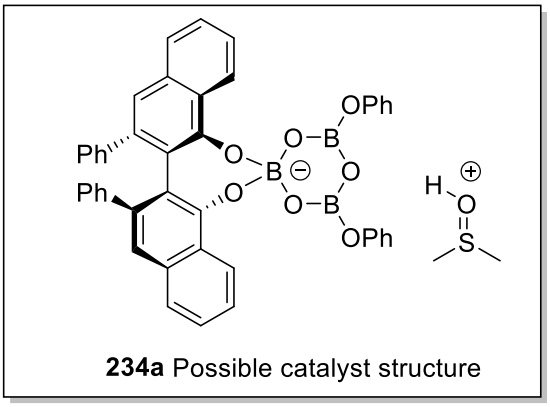

234a Possible catalyst structure

Scheme 3.17 Oxa-Diels-Alder reaction with BLA catalyst **222**

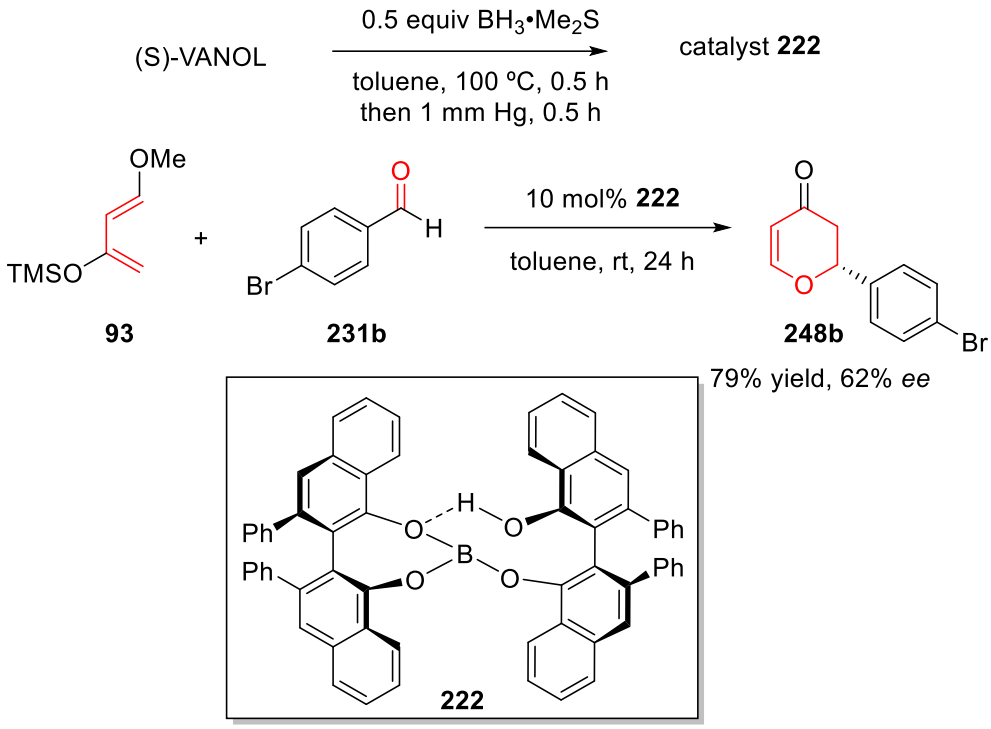

The catalyst **222** was prepared by heating 2 equivalents of (*S*)-VANOL (**L5**) and 1 equivalent of BH_3•Me_2S (borane dimethylsulfide) in toluene for 0.5 hour followed by pumping off solvent and volatiles. The reaction between Danishefsky's diene **93** and *para*-bromobenzaldehyde **231b** was achieved in 79% yield and 62% *ee* with 10 mol% catalyst loading. The use of (*S*)-BINOL (**L1**) as ligand improved results to 94% yield and 83% *ee* (Scheme 3.18, entry 2). Using VAPOL (**L2**) as ligand failed to give any product (entry 3), probably because the steric bulkiness of VAPOL hindered the formation of the 2:1 borate catalyst and a similar failure has been observed in the asymmetric epoxidation reaction.[83] Surprisingly, the use of another bulky ligand 7,7'-*t*Bu_2VANOL (**L22**) gave adduct **248b** in 90% yield and 64% *ee* (entry 4). Further study showed that the reaction is much faster than expected, with completion in 1 hour at room temperature.

Scheme 3.18 Optimization of the ligand and the temperature

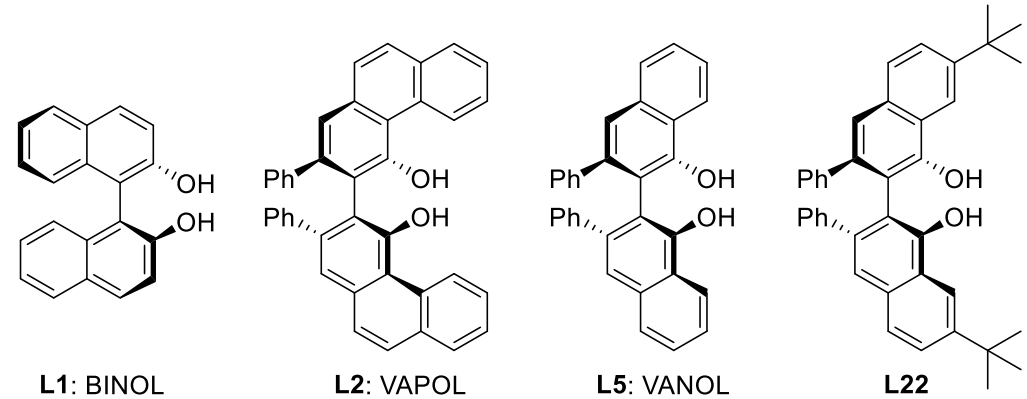

L1: BINOL **L2**: VAPOL **L5**: VANOL **L22**

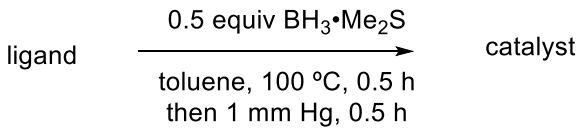

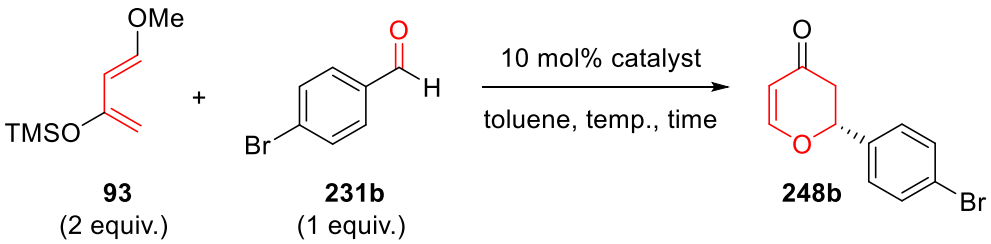

93 (2 equiv.) **231b** (1 equiv.) **248b**

entry[a]	ligand	temperature (°C)	time (h)	% yield[b]	% *ee*[c]
1[d]	(*S*)-**L5**	rt	24	79	62
2[d]	(*S*)-**L1**	rt	24	94	83
3[d]	(*S*)-**L2**	rt	24	0	N/A
4[d]	(*S*)-**L22**	rt	24	90	64
5	(*S*)-**L5**	–40	1	71	83
6	(*S*)-**L1**	–40	1	75	88
7	(*S*)-**L22**	–40	1	88	86
8	(*S*)-**L1**	–60	2	34	85
9	(*S*)-**L22**	–60	2	77	88

[a] Reactions were performed on 0.25 mmol scale at 0.1 M. [b] Isolated yields are reported. [c] Determined by chiral HPLC. [d] Results from Xiaopeng Yin.

It was interesting to find that decreasing the reaction temperature to –40 ˚C improved the *ee* by 21% and 22% for VANOL (**L5**) and 7,7'-*t*Bu$_2$VANOL (**L22**)

respectively, while only a 3% improvement was observed for BINOL (**L1**) (Scheme 3.18, entries 5-7). Further lowering temperature to –60 ˚C gave 77% yield and 88% ee for 7,7'-*t*Bu$_2$VANOL (**L22**) but a lower yield and *ee* for BINOL (**L1**) (entries 8-9).

Scheme 3.19 Control experiments and screening of the boron source

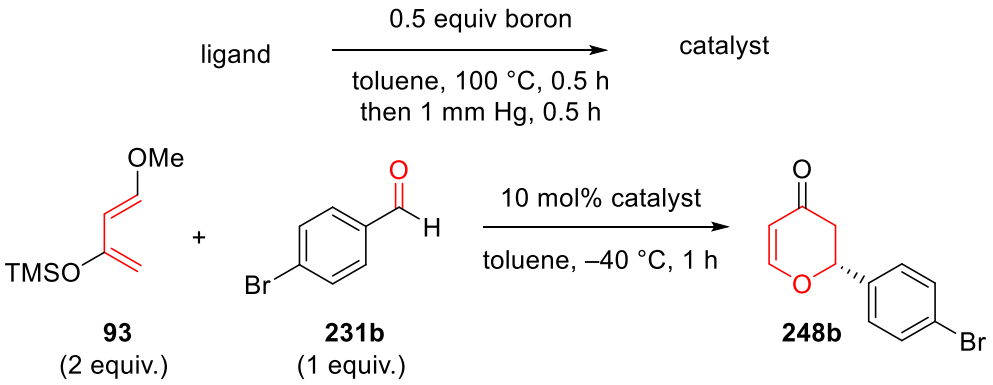

entry[a]	ligand	boron	% yield[b]	% *ee*[c]
1[d]	(*S*)-**L22**	none	0	N/A
2[d]	none	$B(OPh)_3$	0	N/A
3	(*S*)-**L22**	$B(OPh)_3$	95	38
4	(*S*)-**L1**	$B(OPh)_3$	27	57
5	(*S*)-**L22**	BH_3•Me_2S	88	86
6	(*S*)-**L1**	BH_3•Me_2S	75	88
7[e]	(*S*)-**L1**	BH_3•THF	74	81
8[f]	(*S*)-**L1**	BH_3•THF	79	76
9[g]	(*S*)-**L1**	BH_3•THF	83	87
10[h]	(*S*)-**L1**	BH_3•THF	32	68

[a] Reactions were performed on 0.25 mmol scale at 0.1 M. [b] Isolated yields are reported. [c] Determined by chiral HPLC. [d] No preparation of catalyst. [e] Preparation of catalyst is under rt. [f] Preparation of catalyst is under 40 °C. [g] Preparation of catalyst is under 60 °C. [h] Preparation of catalyst is under 80 °C.

Control experiments were carried out to determine the optimal boron source. The addition of only ligand or only triphenylborate ($B(OPh)_3$) resulted in no product being observed in both cases (Scheme 3.19, entries 1-2). When ligand **L22** and

$B(OPh)_3$ were used together, adduct **248b** was obtained in 95% yield and 38% *ee* (entry 3). The reason that $B(OPh)_3$ was chosen as catalyst in those control experiments is that it has three phenolic ligands at the boron center, which is similar to the structure of catalyst **222** (Scheme 3.17). Considering that the electronic nature of VANOL is close to that of phenol, the much higher reactivity observed for VANOL could be attributed to the intramolecular hydrogen bonding that makes it a BLA catalyst (Brønsted acid assisted Lewis acid). The hydrogen bonding reduces the Lewis basicity of the accepting oxygen, and as a result the Lewis acidity on boron center is enhanced. Therefore, the activation of aldehyde by BLA catalyst **222** is better than it by $B(OPh)_3$. While screening other boron sources, BH_3•Me_2S was found to be more efficient than $B(OPh)_3$, probably because of the water residue in commercial $B(OPh)_3$ that generates B-O-H bonds (entries 3-6).[86] Another possibility is that the free phenols in the system compete with VANOL ligand in binding to boron center, and $B(OPh)_3$ itself has been proven to be not able to catalyze the HDA reactions. BH_3•THF as boron source was also tested. Studies have been performed on preparing the catalyst at different temperature, but no better results were obtained compared with the use of BH_3•Me_2S (entries 7-10). Therefore, BH_3•Me_2S as optimal boron source was used in the following asymmetric HDA reactions.

3.3 NMR study on catalysts

The BH_3•Me_2S used in this reaction was purchased from Alfa Aesar as a 2 M solution in toluene. During catalyst preparation, BH_3•Me_2S was injected into the reaction solution containing the ligand via a 50 µl syringe that has been dried in

the oven for over 24 hours and flushed with nitrogen before use. Usually, two reactions were carried out at the same time and one syringe was responsible for two injections. After the first injection, the syringe was left on the bench (the needle had not been touched) for less than 10 seconds before the next measurement and injection. The preparation of the catalyst was studied using NMR. After pumping off the volatiles, Ph_3CH as internal standard was added to the catalyst, which was then dissolved in $CDCl_3$ for the NMR study. The protons at the 8,8'-positions of 7,7'-*t*Bu_2VANOL ligands in the catalyst **249** were integrated and the NMR yields of the catalyst were calculated and shown in Scheme 3.20. A total of 12 reactions were carried out in six pairs. For each pair, the same one syringe was used for the measurements and injections of BH_3•Me_2S. For example, entry 1 and 2 were carried out at the same time. The reaction in entry 1 was treated with BH_3•Me_2S via a syringe (taken out from oven and flushed with nitrogen). While for reaction in entry 2, BH_3•Me_2S was added using the same syringe used in entry 1. Interestingly, a statistical difference in results between odd entries and even entries was observed (75% average yield and 63% average yield).

Scheme 3.20 Can the same syringe be used for two injections of BH_3•Me_2S?

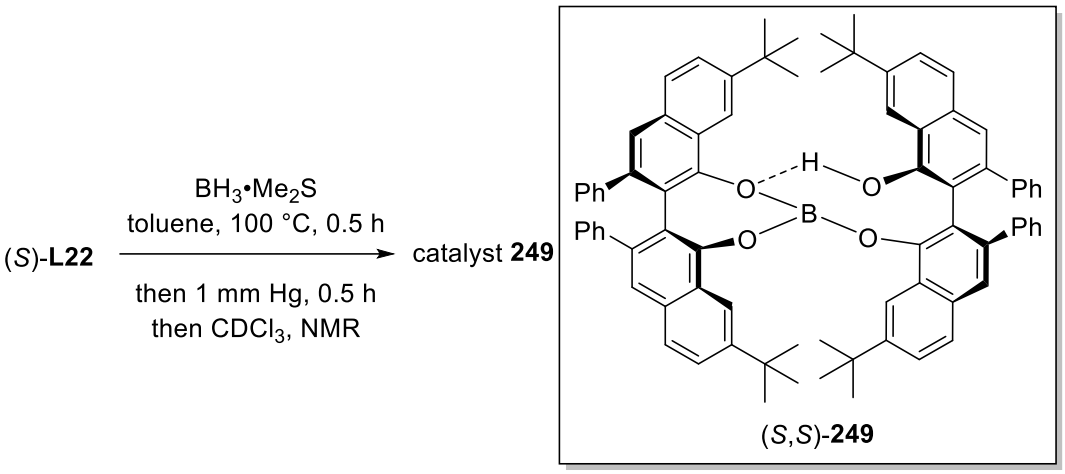

entry[a]	injection	% yield of **249**[c]	entry[b]	injection	% yield of **249**[c]
1	first	83	2	second	72
3	first	75	4	second	58
5	first	73	6	second	59
7	first	66	8	second	62
9	first	81	10	second	65
11	first	74	12	second	61
average yield of **249**: 75%			average yield of **249**: 63%		

[a] Reactions with an odd entry number were charged with BH_3•Me_2S in the first injection. [b] Reactions with an even entry number were charged with BH_3•Me_2S in the second injection. [c] Yield was determined by ^1H NMR with triphenylmethane as internal standard.

Since all other conditions are identical except for the addition of borane, it indicates that the order of adding borane matters. Obviously, the use of the same syringe for two injections of BH_3•Me_2S should be questioned. After the first injection, the BH_3•Me_2S residue in the needle is exposed to air because a dry box is not employed. Due to the moisture sensitivity of BH_3•Me_2S, it is possible that hydrolysis occurs on the residue in the needle and leads to the formation of boric acid that is injected into the second reaction as an impurity. In methodology development,

running multiple reactions at the same time and using the same syringe to measure the same compounds are typically considered expedient. It was found here that using the same syringe for multiple injections of air-sensitive compounds outside a dry box might be risky. The simplest solution to this finding is to use a new syringe for each injection. This strategy has been employed in all following reactions when air-sensitive compounds, such as borane, trimethylaluminum and TMSCl, were measured out via syringes.[i]

The structure of the catalyst prepared from BINOL (**L1**) under our conditions was first thought to be a 2:1 borate ester **250** (structure proposed by Yamamoto[79]), similar to catalyst **249** (Scheme 3.20) from 7,7'-*t*Bu$_2$VANOL (**L22**) and catalyst **222** (Scheme 3.17) from VANOL (**L5**). However, in this work the ^{1}H NMR study revealed that propeller borate **216**, a known species developed by Kaufmann[75], was obtained as the sole product under our standard conditions. The structure of **216** was confirmed by comparing the ^{1}H NMR spectrum with the previously reported data.[82] Only the free ligand (BINOL) and **216** were observed in the reaction mixture as indicated by ^{1}H NMR spectrum. Increasing the borane loading from 0.5 equivalent to 1 equivalent and 4 equivalents also gave **216** as single product in higher yield (Scheme 3.21). Notably, it is the first time that the propeller

[i] *Paying attention to details like this may not increase the yield of product dramatically, but it will definitely make results more reliable. During the long journey of optimizing reactions, I never felt upset by getting bad results because bad results would tell me where to go. I was disappointed only when a result could not be reproduced, as it indicated that at least one of the results was not reliable. Recalling the five years in my PhD career, I have spent months figuring out why inconsistent results were obtained. Sometimes it was because of an old bottle of reagent or a not fully dried solvent, and sometimes it was because of the use of one syringe in two injections. What I have learned is that paying 100% attention to every single detail and questioning myself in every single step while running a reaction will make results more reliable and avoid lots of detours in chasing the truth.*

borate **216** has been employed in the asymmetric HDA reaction. Even though **216** and **249** displayed a similar capacity in catalyzing reaction between Danishefsky's diene **93** and *para*-bromobenzaldehyde **231b** (Scheme 3.19, entries 5 and 6), they gave different responses to changes in the reaction parameters. Therefore, optimizations on catalyst **216** and **249** were performed separately.

Scheme 3.21 Catalyst prepared from BINOL

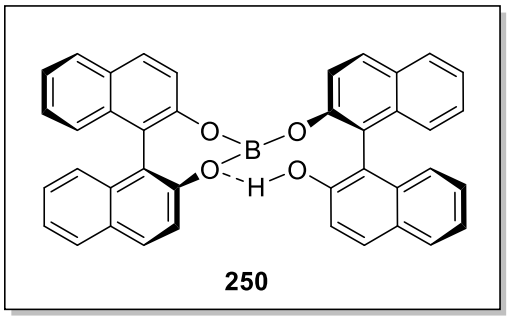

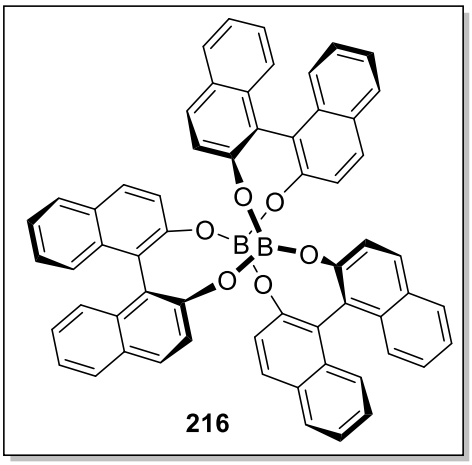

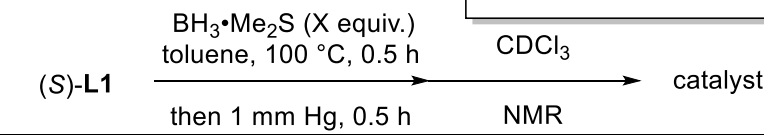

entry	X equiv.	ligand : boron	% yield of **250**[a]	% yield of **216**[a]
1	0.5	2:1	0	50
2	1	1:1	0	73
3	4	1:4	0	65

[a] Yield was determined by ^{1}H NMR with triphenylmethane as internal standard.

3.4 Optimization and substrate scope with catalysts 216

The reaction parameters of the asymmetric HDA reaction between diene **93** and aldehyde **231a** catalyzed by BINOL-derived propeller borate **216** have been studied. While moderate yield and *ee* were obtained with the reaction concentration at 0.25 M, diluting the reaction to 0.05 M gave adduct **248a** in an

improved 91% *ee* (Scheme 3.22, entries 1-4). Previous results by Dr. Xiaopeng Yin showed that the non-polar solvent toluene is superior to other polar solvents such as CH_2Cl_2 and THF.[84] Inspired by the success of using *n*-pentane as solvent in MPV reduction (Table 2.3), the asymmetric HDA reaction in *n*-pentane was carried out, but low conversion was observed (entry 7). This is possibly because of the low solubility of the catalyst in *n*-pentane. After the preparation of catalyst and pumping off volatiles, solvents and substrates were added to the flask containing the catalyst. It was observed that the catalyst stayed on the inner side of flask as a white powder and did not go into the reaction mixture when using *n*-pentane as solvent. Therefore, to decrease the polarity of the reaction, a mixture of toluene and *n*-pentane as co-solvent were employed. Toluene was added into the flask first to fully dissolve the catalyst, and then *n*-pentane was added. Using toluene/ *n*-pentane in 1:4 ratio improved the results to 90% yield and 94% *ee* (entry 5). Notably, even though the catalyst crashed out after the addition of *n*-pentane and the reaction turned cloudy (more precipitates were observed after cooling to –40 ˚C), high conversion and asymmetric induction were obtained. The reason that the heterogeneous mixture showed good results is not clear. It is possible that the concentration of active catalyst in solution remained constant owing to the low solubility of catalyst, which might contribute to a better reaction. Diluting the reaction to 0.025 M with toluene/ *n*-pentane in 1:9 ratio gave lower yield and slightly lower *ee* (entry 6). Lowering the reaction temperature to –60 ˚C resulted in a slower reaction (entry 8).

Scheme 3.22 Optimizations with catalyst **216**

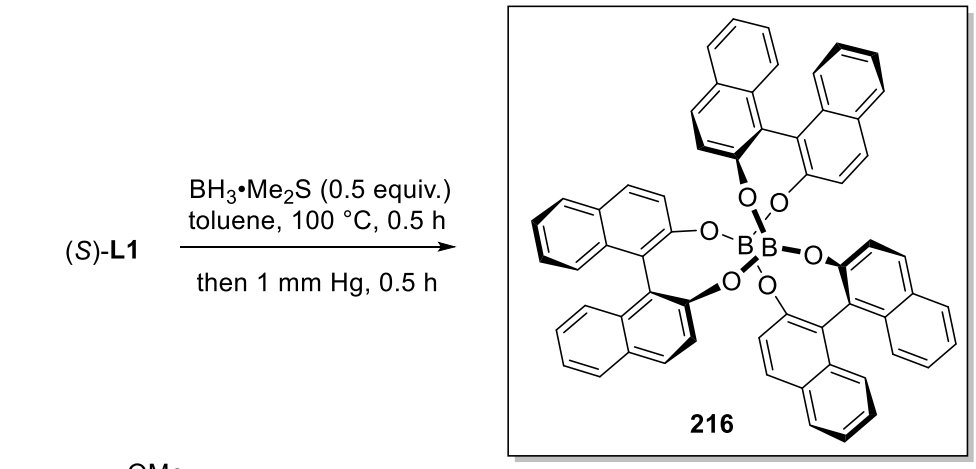

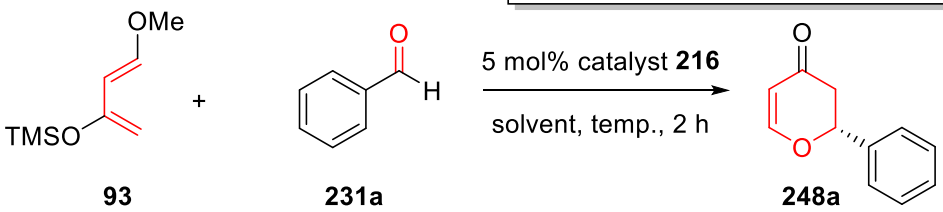

93 (2 equiv.) **231a** (1 equiv.) **248a**

entry[a]	temp. (°C)	solvent	concentration (M)	% yield[b]	% *ee*[c]
1	–40	toluene	0.25	70	74
2	–40	toluene	0.1	84	90
3	–40	toluene/*n*-pentane (1:1)	0.1	91	90
4	–40	toluene	0.05	87	91
5	–40	toluene/*n*-pentane (1:4)	0.05	90	94
6	–40	toluene/*n*-pentane (1:9)	0.025	61	92
7	–40	*n*-pentane	0.05	(19)	N/A
8	–60	toluene/*n*-pentane (1:4)	0.05	(30)	N/A

[a] Reactions were performed on 0.25 mmol scale. [b] Isolated yields are reported; numbers in parenthesis are NMR yield determined by internal standard triphenylmethane. [c] Determined by chiral HPLC.

With optimal conditions in hand, the substrate scope of the asymmetric HDA reaction catalyzed by propeller borate **216** was studied. Aromatic aldehydes were tolerated well, but aliphatic aldehydes were not (Scheme 3.23). No product was observed when aldehyde **231f** was used and only 25% yield and 59% *ee* was

obtained from the reaction of cyclohexanecarboxaldehyde **231e**. Despite the failure with aliphatic aldehydes, this is the first example of using the propeller catalyst **216** in asymmetric HDA reaction of aromatic aldehydes.

Scheme 3.23 Substrate scope of asymmetric HDA reaction with catalyst **216**

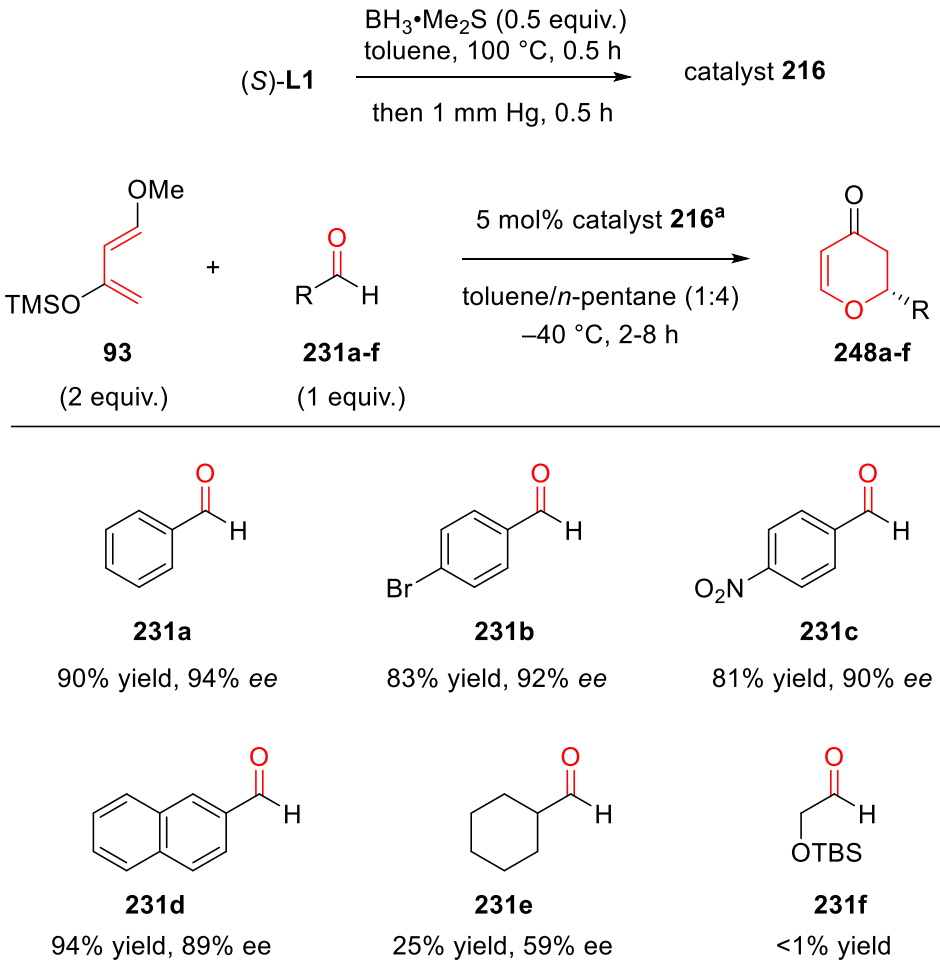

[a] Reactions were performed on 0.25 mmol scale at 0.05 M; isolated yields are reported; *ee* is determined by chiral HPLC.

3.5 Optimizations of asymmetric HDA reaction with catalyst 249

Due to the limitation in the scope with the asymmetric HDA reaction catalyzed by the propeller borate **216**, our attention was turned to the use of borate ester **249** as catalyst. The effect of concentration was first studied and 0.05 M was

found to be optimal, with higher concentrations causing lower *ee* and further dilution causing lower yields (Scheme 3.24, entries 1-4). The use of Et_2O as solvent gave adduct **248a** in only 37% yield, probably due to the coordination between the Lewis basic oxygen on ether and boron catalyst (entry 5). Polar solvent CH_2Cl_2 resulted in lower yield and *ee* compared with non-polar solvent toluene (entries 3 vs 6). The use of toluene/*n*-pentane as co-solvent decreased the polarity and increased enantioselectivity (entries 7-8). Unlike propeller borate **216**, the catalyst **249** could be dissolved by *n*-pentane at room temperature. The high solubility is presumably aided by the *tert*-butyl groups on 7,7'-*t*Bu_2VANOL ligand. Without those *tert*-butyl groups, the catalyst **222** prepared from VANOL displayed poor solubility in *n*-pentane. Unsurprisingly, using *n*-pentane as the sole solvent increased the results to 96% yield and 88% *ee* (entry 9). It is noteworthy that some of catalyst **249** still precipitated out when the reaction was run at –40 ˚C, but the heterogeneous mixture gave excellent results. Lowering the temperature to –60 ˚C gave adduct **248a** in 93% yield and 91% *ee* (entry 10). Running the reaction at –78 ˚C slowed down the reaction and did not improve the enantioselectivity (entry 11). The use of 20 mol% DMSO or benzoic acid as additive shut down the reaction, perhaps because of the destruction of catalyst (entries 12-13). Adding molecular sieves failed to enhance the results (entry 14). By cutting the catalyst loading to 5 mol%, a 90% yield and 93% *ee* was achieved (entry 15).

Scheme 3.24 Optimization of the HDA reaction of benzaldehyde with catalyst **249**

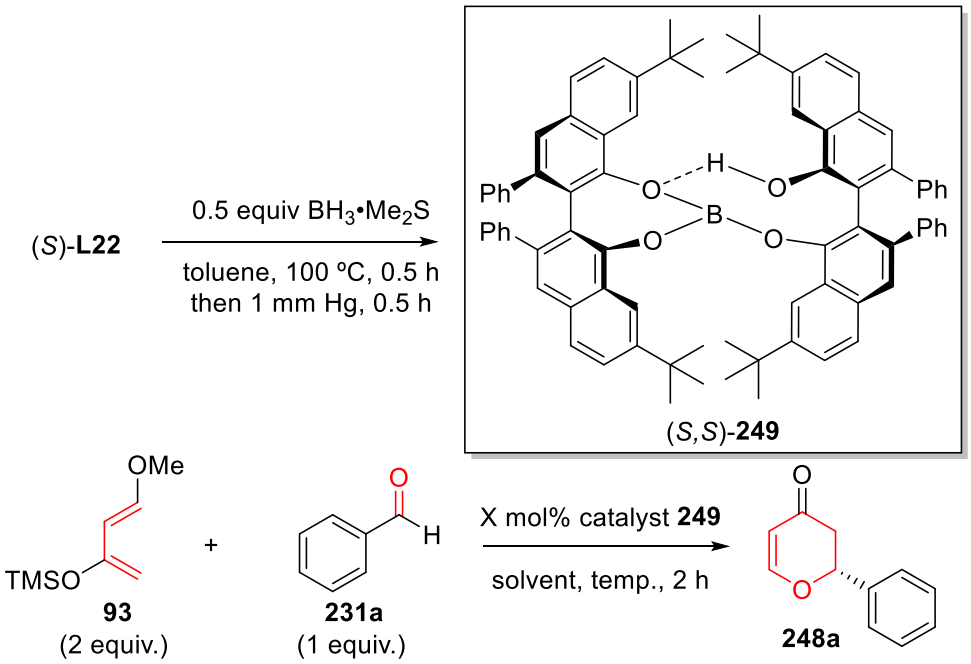

entry[a]	X mol (%)	temp. (°C)	solvent	concentration (M)	% yield[b]	% *ee*[c]
1	10	–40	toluene	0.25	92	81
2	10	–40	toluene	0.1	82	84
3	10	–40	toluene	0.05	89	86
4	10	–40	toluene	0.025	74	85
5	10	–40	Et_2O	0.05	37	60
6	10	–40	DCM	0.05	70	56
7	10	–40	toluene/*n*-pentane (1:1)	0.05	94	87
8	10	–40	toluene/*n*-pentane (1:4)	0.05	90	87
9	10	–40	*n*-pentane	0.05	96	88
10	10	–60	*n*-pentane	0.05	93	91
11	10	–78	*n*-pentane	0.05	55	91
12[d]	10	–60	*n*-pentane	0.05	(9)	N/A
13[e]	10	–60	*n*-pentane	0.05	(15)	N/A
14[f]	10	–60	*n*-pentane	0.05	81	90
15	5	–60	*n*-pentane	0.05	90	93

[a] Reactions were performed on 0.25 mmol scale. [b] Isolated yields are reported; numbers in parenthesis are NMR yields determined with Ph_3CH as internal standard. [c] Determined by chiral HPLC. [d] 20 mol% DMSO used as additive.[e] 20 mol% benzoic acid used as additive.[f] 25 mg 4 Å MS used as additive.

Catalyst **249** was also studied in the reaction between diene **93** and the aliphatic aldehyde **231e**. This reaction catalyzed by the propeller borate **216** gave **248w** in only 25% yield and 59% *ee*. To our delight, catalyst **249** was very effective with cyclohexanecarboxaldehyde **231e**. With toluene as solvent and with a concentration of 0.1 M, the adduct **248e** was obtained in 82% yield and 88% *ee* (Scheme 3.25, entry 1). Additional improvement was observed when a two-fold dilution and co-solvent was employed (entry 2). With 5 mol% catalyst loading and reaction running in *n*-pentane at –60 ˚C, a 97% yield and 98% *ee* of **248e** was accomplished (entry 3). This exciting finding indicated that the optimized conditions for benzaldehyde were also suitable for aliphatic aldehydes. Therefore, the substrate scope of the asymmetric HDA reaction catalyzed by borate **249** was studied under these optimal conditions.

Scheme 3.25 The optimization of aliphatic aldehyde with catalyst **249**

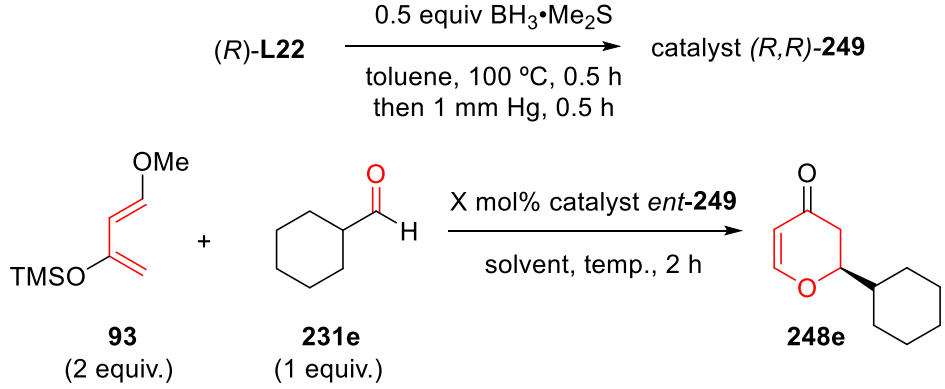

entry[a]	X mol (%)	temp. (°C)	solvent	concentration (M)	% yield[b]	% *ee*[c]
1	10	–40	toluene	0.1	82	88
2	10	–40	toluene/*n*-pentane (1:4)	0.05	94	96
3[d]	5	–60	*n*-pentane	0.05	97	98

[a] Reactions were performed on 0.25 mmol scale. [b] Isolated yields are reported.
[c] Determined by chiral HPLC. [d] Reaction run for 4 h.

3.6 Substrate scope of asymmetric HDA reaction with catalyst 249

Scheme 3.26 Substrate scope with catalyst **249**

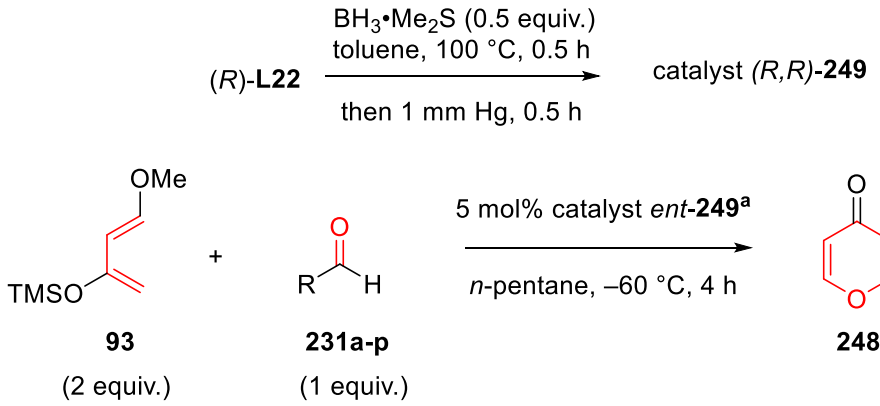

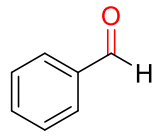

231a[b]

90% yield, 93% *ee*

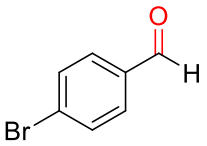

231b

94% yield, 91% *ee*

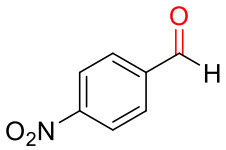

231c[b]

93% yield, 92% *ee*

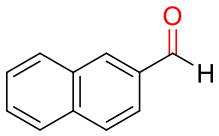

231d[b]

89% yield, 90% *ee*

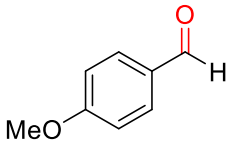

231g

78% yield, 92% *ee*

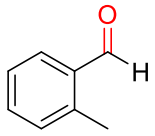

231h

91% yield, 93% *ee*

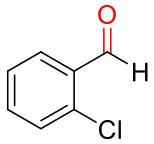

231i

94% yield, 90% *ee*

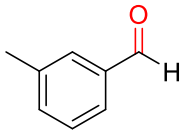

231j

96% yield, 95% *ee*

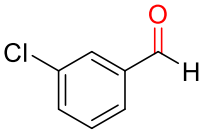

231k

88% yield, 90% *ee*

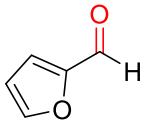

231l

86% yield, 94% *ee*

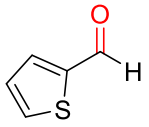

231m[c]

72% yield, 85% *ee*

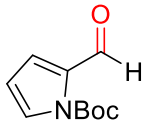

231n

92% yield, 93% *ee*

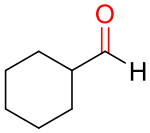

231e

97% yield, 98% *ee*

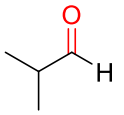

231o

81% yield, 89% *ee*

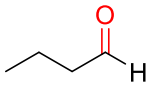

231p

95% yield, 90% *ee*

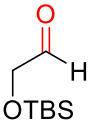

231f[d]

81% yield, 87% *ee*

[a] Reactions were performed on 0.25 mmol scale at 0.05 M; isolated yields are reported; *ee* is determined by chiral HPLC. [b] (*S*)-**L22** as ligand was used. [c] Toluene was used as solvent. [d] 10 mol% catalyst used.

The substrate scope of the asymmetric HDA reaction between aldehydes and diene **93** catalyzed by borate ester **249** has been studied under the optimal conditions shown in entry 3 of Scheme 3.25. Gratefully, a broad scope was found as shown in scheme 3.26. Aromatic aldehydes such as benzaldehyde **231a** and 2-naphthaldehyde **231d** gave the corresponding adducts with excellent asymmetric inductions. Changing the electron density on the aromatic rings showed little impact on enantioselectivities. Both electron-withdrawing substituents such as bromo (**231b**) and nitro (**231c**), and electron-donating group methoxy (**231g**) at *para*-position were tolerated well, giving 78-94% yield and 91-92% *ee*. A methyl group and a chloride as substituents at *ortho*- and *meta*-positions gave 88-96% yield and 90-95% *ee* (**231h-k**). Heterocycles such as furan (**231l**), thiophene (**231m**) and Boc-protected pyrrole (**231n**) were also well tolerated. The reaction of 2-thiophenecarboxaldehyde **231m** in *n*-pentane was unsuccessful due to the poor solubility of the aldehyd. Changing *n*-pentane to toluene gave adduct **248m** in 72% yield and 85% *ee*. Aliphatic aldehydes other than cyclohexanecarboxaldehyde **231e** were also tested. Branched aldehyde **231o** (isobutyraldehyde) and unbranched aldehyde **231p** (butyraldehyde) both gave high yield and *ee*. To our delight, an 81% yield and 87% *ee* was achieved for adduct **248f** when α-siloxyacetaldehyde **231f** was used. Aldehyde **231f** is one of the most important substrates, because it constructs the hexose skeleton in this asymmetric HDA reaction. Further derivatization of adduct **248f** could lead to a variety of saccharide analogs. Moreover, the chiral center installed on **248f** would help achieve stereoselective transformations such as α-alkylation, ketone reduction and

dihydroxylation to build up more chiral centers on the six-membered ring. The asymmetric HDA reactions of aldehyde **231f** have been used in total synthesis of neosidomycin,[51] dactylolide,[52] leucascandrolide A,[53] and lasonolide A[54] as shown in scheme 3.9.

Scheme 3.27 Failed substrates with catalyst **249**

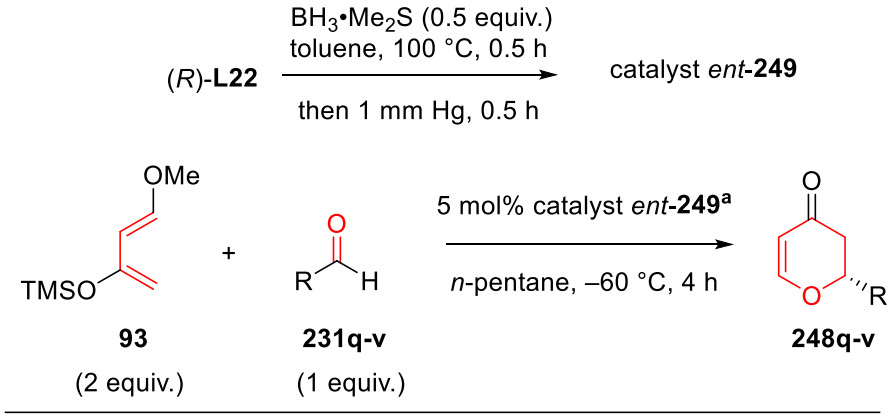

[a] Reactions were performed on 0.25 mmol scale at 0.05 M; yield is determined by crude ^{1}H NMR with triphenylmethane as internal standard.

There are also some aldehydes that are not tolerated in this asymmetric HDA reaction catalyzed by borate **249**, as shown in Scheme 3.27. Substrates with unprotected N-H bonds such as pyrrole (**231q**) and indole (**231r**) were not reactive under standard conditions. Aldehydes bearing strong base moieties such as

pyridinecarboxaldehyde **231s-t** and *para*-dimethylaminobenzaldehyde **231u** were not tolerated, possibly due to the deprotonation of catalyst **249** generating spiro-borate anion that is no longer has the Lewis acidity to activate the aldehyde. Aldehydes **231v** gave less than 1% yield, perhaps due to its steric bulkiness that hinders the Lewis acid-Lewis base interaction between the aldehyde and catalyst. In spite of these limitations, borate **249** has shown superior capability over borate **216** in catalyzing the asymmetric HDA reaction between aldehydes and Danishefsky's diene.

3.7 Study on asymmetric HDA reaction of α-alkoxyacetaldehyde

Figure 3.5 Ligands screened

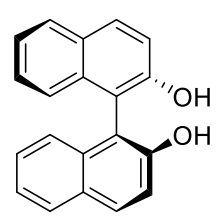

L1: BINOL

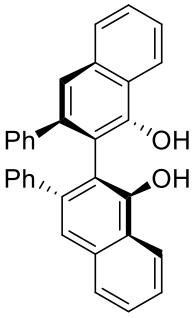

L5: VANOL

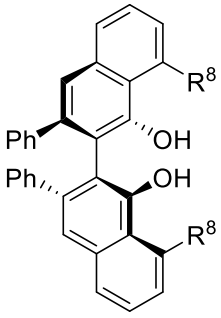

L14: R^8 = Ph

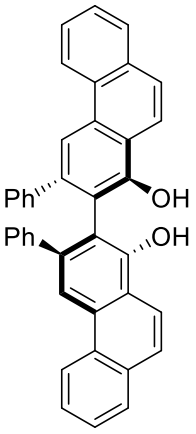

L4: *iso*VAPOL

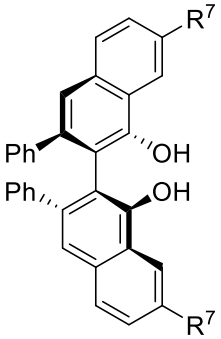

L21: R^7 = Cy
L22: R^7 = *t*Bu
L23: R^7 = adamantyl
L24: R^7 = 4-OMe-3,5-*t*Bu_2-C_6H_5
L25: R^7 = $SiPh_2$*t*Bu
L27: R^7 = 3-thiopheneyl
L29: R^7 = *i*Pr
L30: R^7 = *iso*pentyl
L43: R^7 = 2-naphthyl
L50: R^7 = Br

Most of aldehydes underwent asymmetric HDA reaction catalyzed by borate **249** in high yields and excellent asymmetric inductions. However, the reaction of

the α-siloxyacetaldehyde **231f** gave the important adduct **248f** in "only" 81% yield and 87% *ee* (Scheme 3.26). Driven by the significance and potential applications of this reaction, further studies on asymmetric HDA reaction of α-alkoxyacetaldehydes were performed. The optimization of asymmetric HDA reaction between diene **93** and aldehyde **231f** is shown in Scheme 3.28.

Scheme 3.28 Attempts at optimizations of aldehyde **231f**

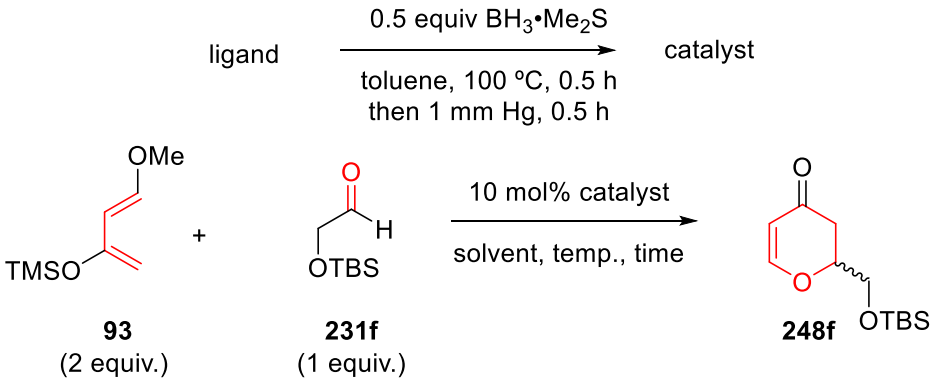

93 (2 equiv.) **231f** (1 equiv.) **248f**

entry[a]	ligand	solvent	temp. (°C)	time (h)	% yield[b]	% *ee*[c]
1	(*R*)-**L22**	*n*-pentane	–40	2	71	84
2	(*R*)-**L22**	*n*-pentane	–60	4	81	87
3	(*R*)-**L22**	*n*-pentane	–78	4	59	88
4	(*R*)-**L21**	*n*-pentane	–78	12	53	68
5	(*S*)-**L29**	*n*-pentane	–78	12	37	70
6	(*S*)-**L1**	*n*-pentane	–60	4	(<1)	N/A
7	(*S*)-**L5**	*n*-pentane	–60	4	69	71
8	(*R*)-**L14**	*n*-pentane	–60	4	(<1)	N/A
9	(*S*)-**L23**	*n*-pentane	–60	4	60	50
10	(*S*)-**L24**	*n*-pentane	–60	4	74	50
11	(*S*)-**L25**	*n*-pentane	–60	4	75	77
12	(*R*)-**L27**	*n*-pentane	–60	4	14	48
13	(*S*)-**L30**	*n*-pentane	–60	4	77	72

[a] Reactions were performed on 0.25 mmol scale at 0.05 M. [b] Isolated yields are reported; numbers in parenthesis are NMR yield determined by internal standerd triphenylmethane. [c] Determined by chiral HPLC.

The use of catalyst *(R,R)*-**249** generated from (*R*)-**L22** gave adduct **248f** in 71% yield and 84% *ee* at –40 ˚C (Scheme 3.28, entry 1). Lowering the temperature to –60 ˚C and –78 ˚C slowed down the reaction but increased enantioselectivity (entries 2-3). The less bulky ligand (*R*)-**L21** and (*S*)-**L29** resulted in lower conversion and a drop of *ee* (entry 4-5). BINOL (**L1**, entry 6) and 8,8'-diphenylVANOL (**L14**, entry 8) gave no product under the standard conditions. Other 7,7'-disubstituted VANOL as ligands were found to be not as good as (*R*)-**L22** and gave lower asymmetric inductions (entries 9-13). Thus, the best that was achieved in the formation of adduct **248f** was 88% *ee*, which is not satisfactory, especially considering its significant application in synthetic chemistry. During the ligand screening we found that bulkier ligands usually gave better yields and asymmetric inductions, which implied that aldehyde **231f** might not be bulky enough with the TBS group. Therefore, it was proposed that by switching the TBS group on the aldehyde to TBDPS, a bulkier protecting group, a better asymmetric discrimination in the transition states might be realized.

Aldehyde **231w** was synthesized by mono-protection of ethylene glycol followed by Swern oxidation. Screening of ligands for the asymmetric HDA reaction between aldehyde **231w** and diene **93** was performed and results are shown in Scheme 3.29. The catalyst prepared from BINOL (**L1**) gave no product as expected from the results in Scheme 3.23 (Scheme 3.29, entry 1), and the use of *iso*VAPOL (**L4**) and VANOL (**L5**) gave adduct **248w** in good to high yield and moderate *ee* (entries 2-3). It was surprising to find that different alkyl group at 7,7'-position of VANOL did not change the *ee* significantly with adduct **248w** formed in

70-90% yield and 75-82% *ee* (entries 4-8). The best enantioselectivity, but with lower yield, was obtained when 7,7'-TBDPS$_2$VANOL (**L25**) was used as ligand, giving adduct **248w** in 51% yield and 88% *ee* (entry 9). Due to the unsatisfactory results on α-siloxyacetaldehyde, other protecting groups were explored.

Scheme 3.29 Optimization of aldehyde **231w** in the reaction with diene **93**

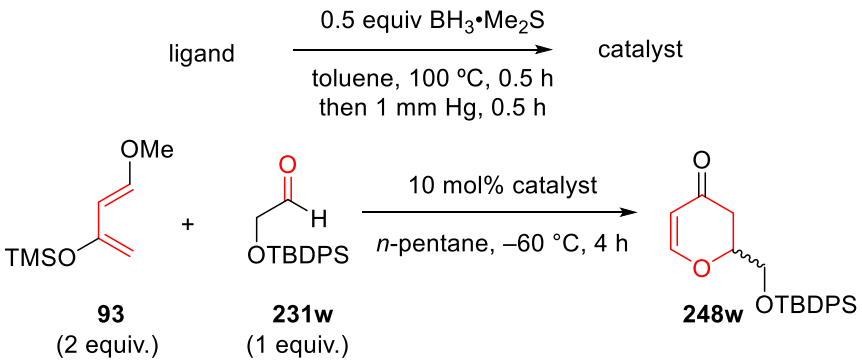

entry[a]	ligand	% yield[b]	% *ee*[c]
1	(*S*)-**L1**	(<1)	N/A
2	(*R*)-**L4**	46	70
3	(*S*)-**L5**	86	76
4	(*R*)-**L21**	78	80
5	(*R*)-**L22**	90	82
6	(*S*)-**L23**	79	75
7	(*R*)-**L29**	70	81
8	(*S*)-**L30**	84	79
9	(*S*)-**L25**	51	88

[a] Reactions were performed on 0.25 mmol scale at 0.05 M. [b] Isolated yields are reported; numbers in parenthesis are NMR yield determined by internal standerd triphenylmethane. [c] Determined by chiral HPLC.

the asymmetric HDA reaction between diene **93** and aldehyde **231x** that has benzyl as protecting group was studied and the results are shown in scheme 3.30. The reactions were first conducted in *n*-pentane but low conversions were observed (entries 1-3), and this is probably because of the poor miscibility between

aldehyde **231x** and solvent. When toluene was employed as solvent, reactions with different ligands proceeded well and gave adduct **248x** in high yields. However, only moderate enantioselectivities were observed for all of the ligands screened. We proposed that the lack of asymmetric induction resulted from less bulky benzyl substituent in aldehyde **231x**. Therefore, a much bigger protecting group triphenylmethyl (trityl) was installed on the aldehyde.

Scheme 3.30 Optimizations on aldehyde **231x**

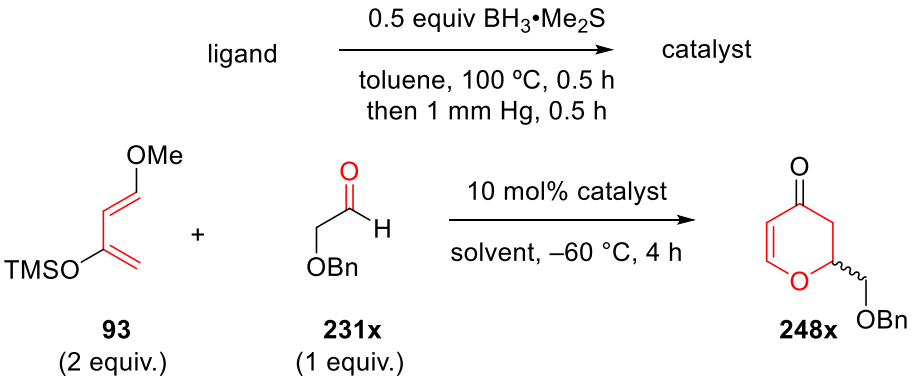

93 (2 equiv.) **231x** (1 equiv.) **248x**

entry[a]	ligand	solvent	% yield[b]	% *ee*[c]
1	(*S*)-**L1**	*n*-pentane	(<1)	N/A
2	(*R*)-**L22**	*n*-pentane	51	22
3	(*R*)-**L5**	*n*-pentane	20	48
4	(*S*)-**L23**	toluene	19	38
5	(*R*)-**L21**	toluene	88	21
6	(*S*)-**L25**	toluene	92	60
7	(*S*)-**L29**	toluene	93	10
8	(*S*)-**L30**	toluene	91	4
9	(*S*)-**L43**	toluene	30	30

[a] Reactions were performed on 0.25 mmol scale at 0.05 M. [b] Isolated yields are reported; numbers in parenthesis are NMR yield determined by internal standerd triphenylmethane. [c] Determined by chiral HPLC.

Scheme 3.31 Optimizations of aldehyde **231y**

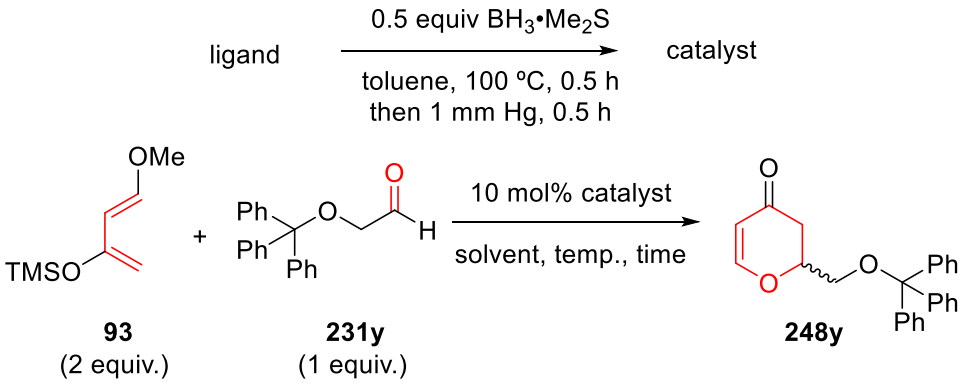

93 (2 equiv.) + **231y** (1 equiv.) → **248y**

entry[a]	ligand	solvent	temp. (°C)	time (h)	% yield[b]	% *ee*[c]
1	(*S*)-**L1**	toluene	–60	4	(<1)	N/A
2	(*S*)-**L5**	toluene	–60	4	85	72
3	(*R*)-**L21**	toluene	–60	4	62	75
4	(*R*)-**L22**	toluene	–60	4	80	79
5	(*S*)-**L23**	toluene	–60	4	69	59
6	(*R*)-**L29**	toluene	–60	4	91	82
7	(*S*)-**L30**	toluene	–60	4	72	65
8	(*S*)-**L50**	toluene	–60	4	49	50
9	(*R*)-**L22**	toluene/*n*-pentane (1:10)	–78	12	94	89
10[d]	(*R*)-**L29**	toluene/*n*-pentane (1:10)	–78	12	90	93
11[e]	(*S*)-**L29**	toluene/*n*-pentane (1:10)	–78	12	80	88

[a] Reactions were performed on 0.25 mmol scale at 0.05 M. [b] Isolated yields are reported; numbers in parenthesis are NMR yield determined by internal standerd triphenylmethane. [c] Determined by chiral HPLC. [d] Average of two runs. [e] 5 mol% catalyst was used.

The aldehyde **231y** was synthesized from triphenylmethylchloride and allylic alcohol followed by ozonolysis and was prepared as a stock solution in toluene before use. After ligand screening with toluene as solvent, the 7,7'-*i*Pr$_2$VANOL (**L29**) was found to be most effective in the asymmetric HDA reaction between diene **93** and aldehyde **231y**, giving adduct **248y** in 91% yield and 82% *ee* (Scheme 3.31, entry 6). The use of toluene/*n*-pentane in 1:10 ratio as co-solvent

and running reaction at –78 ˚C for 12 hours successfully gave adduct **248y** in 90% yield and 93% *ee* (entry 10, average of two runs). Finally, the achievement of excellent yield and excellent asymmetric induction for the HDA reaction on aldehyde **231y** provided an effective approach in the asymmetric synthesis of hexose skeleton, which potentially could lead to a variety of saccharide analogs.

3.8 Reaction mechanism and computational study

3.8.1 Is the asymmetric HDA reaction catalyzed by VANOL borate complex concerted or stepwise?

Scheme 3.32 Two possible pathways

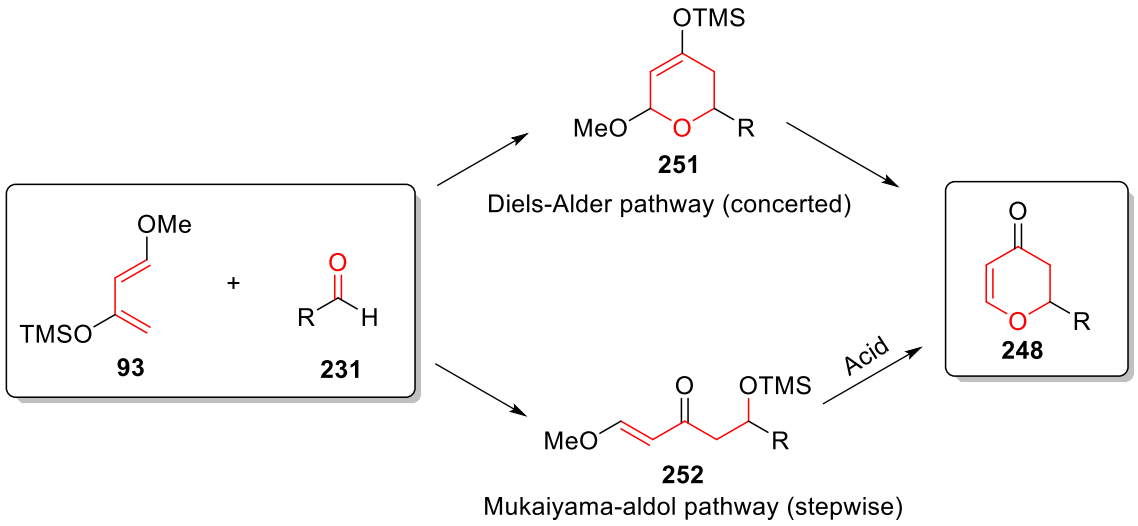

Two mechanistic pathways of the HDA reaction between aldehydes and Danishefsky's dienes have previously been proposed and studied (Scheme 3.32).[91,38,36] The first one is a concerted [4+2] cycloaddition pathway that is similar to the traditional Diels-Alder reaction. The second one is a stepwise pathway, undergoing Mukaiyama aldol reaction first followed by acid-promoted cyclization. It was determined by Danishefsky in 1985 that different catalysts can result in

different pathways in the same reaction.[91] Corey and co-workers have isolated the Mukaiyama aldol product **252** in a reaction catalyzed by a titanium-BINOL catalyst, with cyclization occuring after acidic treatment, which is evidenced that the reaction undergoes a stepwise pathway.[38] In the reaction catalyzed by Jacobson's chromium catalyst, no Mukaiyama aldol product **252** was detected. The intermediate **252** was synthesized independently and treated with the chromium catalyst under the same conditions, but no cyclization product was obtained.[36] Therefore, a concerted mechanism was suggested for this reaction.

Scheme 3.33 Different quenching methods

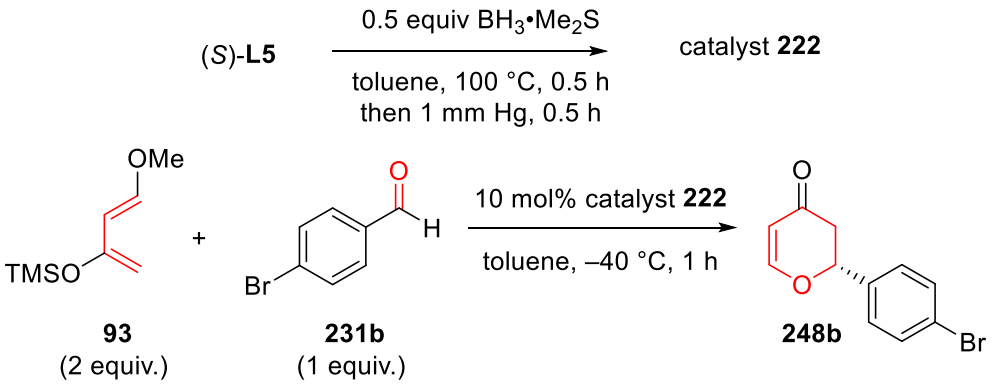

entry[a]	quenching method	yield[b] (%)	*ee*[c] (%)
1	Add TFA and stir for 1 h	92	84
2	Add 1M HCl in MeOH/H_2O (1:1) and stir for 1 h	89	83
3	Add EtOH/H_2O (1:1) and stir for 1 h	79	81

[a] Reactions were performed on 0.25 mmol scale at 0.1 M. [b] Isolated yields are reported. [c] Determined by chiral HPLC.

In our borate catalyzed asymmetric HDA reaction, a concerted mechanism was proposed and evidence was obtained for this by changing the quenching method. The addition of strong acids such as TFA or 1 M HCl in MeOH/H_2O (1:1) into the solution to quench the reaction was employed under standard conditions

(Scheme 3.33, entries 1-2). However, without acid, using ethanol/water mixture to quench the reaction also gave adduct **248b** in high yield and *ee* (entry 3). According to Corey's results, the Mukaiyama aldol product **252** would undergo cyclization only with acid promotion.[38] Therefore, the mechanism in our system is thought to be a concerted pathway, since no acid is required to achieve cyclization to the product **248**.

3.8.2 Reversal of asymmetric induction

Scheme 3.34 Asymmetric HDA reaction with boron and aluminum catalysts

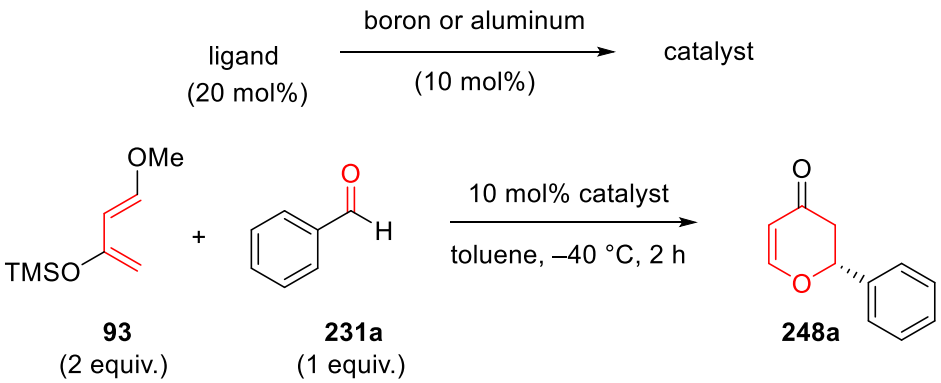

93 (2 equiv.) + **231a** (1 equiv.) → **248a**

entry[a]	ligand	boron/aluminum source	% yield[b]	% *ee*[c]
1	(*S*)-**L5**	BH_3•Me_2S	68	86
2	(*S*)-**L5**	$AlMe_3$	74	–40
3	(*S*)-**L22**	BH_3•Me_2S	89	86
4	(*S*)-**L22**	$AlMe_3$	70	–44

[a] Reactions were performed on 0.25 mmol scale at 0.05 M. [b] Isolated yields are reported; numbers in parenthesis are NMR yield determined by internal standard triphenylmethane. [c] Determined by chiral HPLC; minus ee means that *ent*-**248a** was formed as the major enantiomer.

The catalyst made from aluminum instead of boron has also been investigated in the asymmetric HDA reaction between aldehyde **231a** and diene **93**. A very interesting finding is that boron and aluminum catalysts made from the

same ligands gave the opposite chiral outcome, in other words, a reversal of direction of asymmetric induction was observed (Scheme 3.34). With the VANOL ligand (*S*)-**L5** and 7,7'-*t*Bu$_2$VANOL ligand (*S*)-**L22** were used to prepared boron catalyst, (*S*)-**248a** was generated as the major enantiomer. However, when reactions were catalyzed by aluminum catalysts prepared from (*S*)-**L5** and (*S*)-**L22** with trimethylaluminum, (*R*)-**248a** was formed as major enantiomer.

Figure 3.6 Boron and aluminum catalysts prepared from VANOL

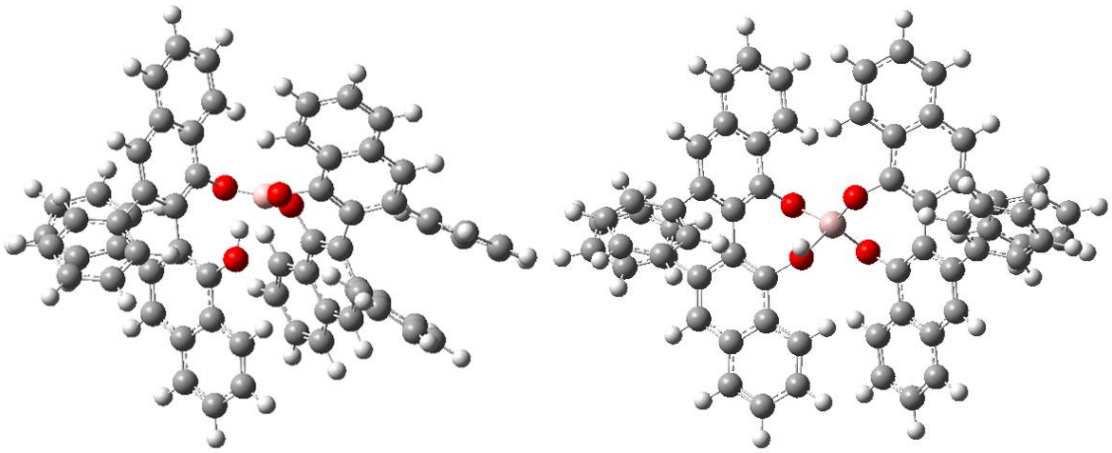

VANOL$_2$-Boron
222

VANOL$_2$-Aluminum
253

A similar reversal has been observed in asymmetric epoxidation reaction, where aluminum-VANOL catalyst and boron-VANOL catalyst led to different chiral outcomes in the epoxide.[92] However, the reason why the reversal occurs is not clear. In order to have some preliminary insights on understanding the behaviors of boron and aluminum catalysts, a computational study was performed and the structures of catalysts were optimized by DFT calculations as shown in Figure 3.6. Geometry optimizations were carried out in Gaussian 16 under DFT B3LYP 6-31g(d) level.[93] As for boron catalyst **222**, three oxygens of the ligands are bound

to a planar boron center with B-O distances of 1.36-1.38 Å. The fourth oxygen is not coordinating to the boron as indicated by its B-O distance at 3.48 Å. The hydrogen bonding between free OH group and an oxygen on the other ligand was observed, evidenced by the O-H distance at 2.08 Å. These features make the borate **222** a BLA catalyst, with enhancement of Lewis acidity on boron. As for aluminum catalyst **253**, the aluminum has bonds to all four oxygens in close to a tetrahedron geometry. Three of the oxygens are bound to aluminum at 1.74-1.75 Å and the fourth oxygen is coordinating to aluminum with an Al-O distance of 1.93 Å. A hydrogen bonding interaction between the OH and an oxygen on the other ligand is found at 2.59 Å, which is weaker than that observed in the boron catalyst **222**. In general, the aluminum catalyst **253** is symmetrical with the aluminum bound to four oxygens, while the boron catalyst **222** is twisted and only three oxygens are bound to boron. Certainly, the geometry of the ligand and catalyst will change after interacting with the substrates (aldehydes and dienes), but the very different geometries between the boron and aluminum catalysts might be responsible for the observed asymmetric induction reversal, especially when it is considered that aluminum can be five or six coordinate but boron can be four coordinate at maximum.

3.9 Conclusion

In this chapter, the significance of the heteroatom Diels-Alder reaction has been illustrated by its synthetic applications. Previously developed catalysts in asymmetric HDA reactions and their applications in total synthesis of natural

products have been discussed. The development of chiral borate catalysts in the asymmetric HDA reaction between dienes and aldehydes has been presented.

In conclusion, a highly efficient asymmetric heteroatom Diels-Alder reaction between dienes and aldehydes for the construction of 6-membered heterocycles catalyzed by chiral borate catalysts has been developed. A BINOL-derived propeller borate **216** was found to be effective in catalyzing the reaction of aromatic aldehydes. A VANOL-derived borate ester **249** was found to be able to catalyze the reaction of a variety of common aromatic and aliphatic aldehydes as well as some heterocyclic aldehydes. Excellent yields and enantioselectivities have been achieved after substantial optimization. Furthermore, the 6-carbon skeleton of saccharides has been synthesized in the reaction of α-oxyacetaldehyde with different protecting groups, which can be derivatized into many saccharide analogs. The mechanism of this reaction is proposed to be concerted based on experiments involving different methods for the reaction quench. A reversal of direction of the asymmetric induction by switching boron to aluminum has been observed. Computational studies show that catalysts derived from boron and aluminum have different geometries at the Lewis acid center.

REFERENCES

REFERENCES

1. Diels, O.; Alder, K. Synthesen in der hydroaromatischen Reihe. *Justus Liebigs Ann. Chem.* **1928**, *460*, 98-122.

2. Berson, J. A. Discoveries missed, discoveries made: creativity, influence, and fame in chemistry. *Tetrahedron* **1992**, *48*, 3-17.

3. Nicolaou, K. C.; Snyder, S. A.; Montagnon, T.; Vassilikogiannakis, G. The Diels–Alder Reaction in Total Synthesis. *Angew. Chem., Int. Ed.* **2002**, *41*,1668-1698.

4. Heravi, M. M.; Ahmadi, T.; Ghavidel, M.; Heidari, B.; Hamidi, H. Recent applications of the hetero Diels–Alder reaction in the total synthesis of natural products. *RSC Adv.* **2015**, *5*, 101999– 102075.

5. Ishihara, K.; Sakakura, A. In *Comprehensive Organic Synthesis II*, 2nd ed.; Knochel, P., Ed.; Elsevier, **2014**; pp 409– 465.

6. Gresham, T. L.; Steadman, T. R. A Diels-Alder Type Reaction with Formaldehyde. *J. Am. Chem. Soc.***1949**, *71*, 737−738.

7. Carosso, S.; Miller, M. J. Nitroso Diels–Alder (NDA) reaction as an efficient tool for the functionalization of diene-containing natural products. *Org Biomol Chem.* **2014**, *12*, 7445-7468.

8. Burger, K.; Goth, H.; Schontag, W.; Firl, J. The nitrile function of tetracyanoethylene as dienophile in diels-alder reactions. *Tetrahedron* **1982**, *38*, 287-289.

9. Hedberg, C.; Pinho, P.; Roth, P.; Andersson, P. G. Diels-Alder Reaction of Heterocyclic Imine Dienophiles. *J. Org. Chem.* **2000**, *65*, 2810-2812.

10. Okamoto, K.; Shiodera, K.; Kawamura, T.; Ogino, K. Synthesis and thermolysis of Diels–Alder adducts of 2,9-dialkylpentacenes with diethyl azodicarboxylate. *J. Phys. Org. Chem.* **2008**, *21*, 257-262.

11. Leach, A. G.; Houk, K. N. Diels–Alder and ene reactions of singlet oxygen, nitroso compounds and triazolinediones: transition states and mechanisms from contemporary theory. *Chem. Commun.* **2002**, 1243–1255

12. Roversi, E.; Scopelliti, R.; Solari, E.; Estoppey, R.; Vogel, P.; Braña, P.; Menendez, B.; Sordo, J. A. The Hetero-Diels–Alder Addition of Sulfur Dioxide to 1-Fluorobuta-1,3-dienes: The Sofa Conformations Preferred by 6-Fluorosultines (6-Fluoro-3,6-dihydro-1,2-oxathiin-2-oxides) Enjoy Enthalpic and Conformational Anomeric Effects. *Chem.-Eur. J.* **2002**, *8*, 1336-1355.

13. Danishefsky, S. J.; DeNinno, M. P.; Chen, S. H. Stereoselective total syntheses of the naturally occurring enantiomers of N-acetylneuraminic acid and 3-deoxy-D-manno-2-octulosonic acid. A new and stereospecific approach to sialo and 3-deoxy-D-manno-2-octulosonic acid conjugates. *J. Am. Chem. Soc.*, **1988**, *110*, 3929-3940.

14. Jewett, J. C.; Rawal, V. H. Total Synthesis of Pederin. *Angew. Chem., Int. Ed.*, **2007**, *46*, 6502-6504.

15. Danishefsky, S.; Kitahara, T. Useful diene for the Diels-Alder reaction. *J. Am. Chem. Soc.* **1974**, *96*, 7807–7808.

16. Panarese, J. D.; Waters, S. P. Enantioselective Formal Total Synthesis of (+)-Aspergillide C. *Org. Lett.* **2009**, *11*, 5086-5088.

17. Han, G.; LaPorte, M. G.; Folmer, J. J.; Werner, K. M.; Weinreb, S. M. Total Syntheses of the Securinega Alkaloids (+)-14,15-Dihydronorsecurinine, (−)-Norsecurinine, and Phyllanthine. *J. Org. Chem.* **2000**, *65*, 6293-6306.

18. Boger, D. L.; Ichikawa, S.; Jiang, H. Total Synthesis of the Rubrolone Aglycon. *J. Am. Chem. Soc.* **2000**, 122, 49, 12169-12173.

19. Ma, Z.-Z.; Hano, Y.; Nomura, T.; Chen, Y.-J. Two New Pyrroloquinazolinoquinoline Alkaloids from Peganum nigellastrum. *Heterocycles* **1997**, 541-546.

20. Snider, B. B.; Lu, Q. Total Synthesis of (±)-Leporin A. *J. Org. Chem.* **1996**, *61*, 2839-2844.

21. Kuttruff, C. A.; Zipse, H.; Trauner, D. Concise Total Syntheses of Variecolortides A and B through an Unusual Hetero-Diels-Alder Reaction. *Angew. Chem., Int. Ed.* **2011**, *50*, 1402-1405.

22. Rizzacasa, M. A.; El Sous, M. Hetero-Diels-Alder synthesis of the spiroketal fragment of reveromycin A. *Tetrahedron Lett.* **2000**, *41*, 8591-8594.

23. El Sous, M.; Ganame, D.; Tregloan, P. A.; Rizzacasa, M. A. Total Synthesis of (−)-Reveromycin A. *Org. Lett.* **2004**, *6*, 3001-3004.

24. Tietze, L. F.; Schneider, C. Enantioselective Total Synthesis of the Mycotoxin (–)-Talaromycin B by a Hetero Diels-Alder Reaction. *J. Org. Chem.* **1991**, *56*, 2476-2481.

25. Tietze, L. F.; Schneider, G.; Wolfling, J.; Fecher, A.; Nobel, T.; Petersen, S.; Schuberth, I.; Wulff, C. A Novel Approach in Drug Discovery: Synthesis of Estrone–Talaromycin Natural Product Hybrids. *Chem. Eur. J.* **2000**, 6, 3755-3760.

26. Song, L.; Yao, H.; Tong, R. Biomimetic Asymmetric Total Syntheses of Spirooliganones A and B. *Org. Lett.* **2014**, *16*, 3740-3743.

27. Stien, D.; Anderson, G. T.; Chase, C. E.; Koh, Y.-H.; Weinreb, S. M. Total Synthesis of the Antitumor Marine Sponge Alkaloid Agelastatin A. *J. Am. Chem. Soc.* **1999**, *121*, 9574-9579.

28. Abe, H.; Aoyagi, S.; Kibayashi, C. First Total Synthesis of the Marine Alkaloids (±)-Fasicularin and (±)-Lepadiformine Based on Stereocontrolled Intramolecular Acylnitroso-Diels−Alder Reaction. *J. Am. Chem. Soc.* **2000**, *122*, 4583-4592.

29. Wei, L.-L.; Hsung, R. P.; Xiong, H.; Mulder, J. A.; Nkansah, N. T. First Stereoselective Inverse Demand [4 + 2] Cycloaddition Reactions of Novel Chiral Allenamides with Heterodienes. Preparation of Highly Functionalized 2-Arylpyranyl Heterocycles. *Org*. *Lett*. **1999**, *1*, 2145-2148.

30. Song, Z.; Hsung, R. P.; Lu, T.; Lohse, A. G. Studies on a Urea-Directed Stork-Crabtree Hydrogenation. Synthesis of the C1-C9 Subunit of (+)-Zincophorin. *J. Org. Chem.* **2007**, *72*, 9722-9731.

31. Xie, M.; Lin, L.; Feng, X. Catalytic Asymmetric Inverse-Electron-Demand Hetero-Diels–Alder Reactions. *Chem. Rec.* **2017**, *17*, 1184-1202.

32. Jørgensen, K. A. Catalytic Asymmetric Hetero-Diels–Alder reactions of Carbonyl Compounds and Imines. *Angew. Chem., Int. Ed.* **2000**, *39*, 3558-3588.

33. Bednarski, M.; Danishefsky, S. On the Interactivity of Chiral Auxiliaries with Chiral Catalysts in the Hetero Diels-Alder Reaction: A New Route to L-Glycolipids. *J. Am. Chem. Soc.* **1983**, **105**, 6968-6969.

34. Maruoka, K.; Itoh, T.; Shirasaka, T.; Yamamoto, H. Asymmetric hetero-Diels-Alder reaction catalyzed by a chiral organoaluminum reagent. *J. Am. Chem. Soc.* **1988**, *110*, 310-312.

35. Simonsen, K. B.; Svenstrup, N.; Roberson, M.; Jørgensen, K. A. Development of an Unusually Highly Enantioselective Hetero-Diels-Alder Reaction of Benzaldehyde with Activated Dienes Catalyzed by Hypercoordinating Chiral Aluminum Complexes. *Chem. Eur. J.* **2000**, *6*, 123-128.

36. Schaus, S. E.; Brånalt, J.; Jacobsen, E. N. Asymmetric Hetero-Diels-Alder Reactions Catalyzed by Chiral (Salen)Chromium(III) Complexes. *J. Org. Chem.* **1998**, *63*, 403-405.

37. Dossetter, A. G.; Jamison, T. F.; Jacobsen, E. N. Highly Enantio- and Diastereoselective Hetero-Diels–Alder Reactions Catalyzed by New Chiral Tridentate Chromium(III) Catalysts. *Angew. Chem., Int. Ed.* **1999**, *38*, 2398-2400.

38. Corey, E. J.; Cywin, C. L.; Roper, T. D. Enantioselective Mukaiyama-aldol and aldol-dihydropyrone annulation reactions catalyzed by a tryptophan-derived oxazaborolidine. *Tetrahedron Lett.* **1992**, *33*, 6907-6910.

39. Kobayashi, S.; Kusakabe, K.-i.; Ishitani, H. Chiral Catalyst Optimization Using Both Solid-Phase and Liquid-Phase Methods in Asymmetric Aza Diels−Alder Reactions. *Org. Lett.* **2000**, *2*, 1225-1227.

40. Wang, Y. H.; Wolf, J.; Zavalij, P.; Doyle, M. P. Cationic Chiral Dirhodium Carboxamidates Are Activated for Lewis Acid Catalysis. *Angew. Chem., Int. Ed.* **2008**, *47*, 1439-1442.

41. Eiji, W.; Hiroshi, Y.; Shuji, K. Chiral Lewis Acid-Catalyzed Asymmetric Hetero Diels-Alder Reaction of (*E*)-2-Oxo-1-phenylsulfonyl-3-alkenes with Vinyl Ethers. *Chem. Lett.* **1994**, *23*, 1637-1640.

42. Keck, G. E.; Li, X.-Y.; Krishnamurthy, D. Catalytic Enantioselective Synthesis of Dihydropyrones via Formal Hetero Diels-Alder Reactions of "Danishefsky's Diene" with Aldehydes. *J. Org. Chem.* **1995**, 60, 5998-5999.

43. Zhuang, W.; Thorhauge, J.; Jørgensen, K. A. Synthesis of Optically Active Amino Sugar Derivatives Using Catalytic Enantioselective Hetero-Diels–Alder Reactions. *Chem. Commun.* **2000**, 459-460.

44. Huang, Y.; Unni, A. K.; Thadani, A. N.; Rawal, V. H. Single enantiomers from a chiral-alcohol catalyst. *Nature* **2003**, *424*, 146.

45. Du, H.; Zhao, D.; Ding, K. Enantioselective Catalysis of the Hetero-Diels–Alder Reaction between Brassard's Diene and Aldehydes by Hydrogen-Bonding Activation: A One-Step Synthesis of (*S*)-(+)-Dihydrokawain. *Chem. Eur. J.* **2004**, *10*, 5964-5970.

46. Guin, J.; Rabalakos, C.; List, B. Highly Enantioselective Hetero-Diels–Alder Reaction of 1,3-Bis(silyloxy)-1,3-dienes with Aldehydes Catalyzed by Chiral Disulfonimide. *Angew. Chem., Int. Ed.* **2012**, *51*, 8859-8863.

47. Yin, J.-P.; Gu, M.; Li, Y.; Nan, F.-J. Total Synthesis of Aphadilactones A–D. *J. Org. Chem.* **2014**, *79*, 6294-6301.

48. Ghosh, A. K.; Ma, N.; Effenberger, K. A.; Jurica, M. S. Total Synthesis of GEX1Q1, Assignment of C-5 Stereoconfiguration and Evaluation of Spliceosome Inhibitory Activity. *Org. Lett.* **2014**, *16*, 3154-3157.

49. Bonazzi, S.; Eidam, O.; Güttinger, S.; Wach, J.-Y.; Zemp, I.; Kutay, U.; Gademann, K. Anguinomycins and Derivatives: Total Syntheses, Modeling, and Biological Evaluation of the Inhibition of Nucleocytoplasmic Transport. *J. Am. Chem. Soc.* **2010**, *132*, 1432-1442.

50. Kasai, Y.; Ito, T.; Sasaki, M. Total Synthesis of (−)-Polycavernoside A: Suzuki–Miyaura Coupling Approach. *Org. Lett.* **2012**, *14*, 3186-3189.

51. Giguère, D.; Martel, J.; Shiao, T. C.; Roy, R. Enantioselective de Novo Synthesis of 4-Deoxy-D-hexopyranoses via Hetero-Diels−Alder Cycloadditions: Total Synthesis of Ezoaminuroic Acid and Neosidomycin. *J. Org. Chem.* **2011**, *76*, 9687-9698.

52. Louis, I.; Hungerford, N. L.; Humphries, E. J.; McLeod, M. D. Enantioselective Total Synthesis of (−)-Dactylolide. *Org. Lett.* **2006**, *8*, 1117-1120.

53. Paterson, I.; Tudge, M. Stereocontrolled Total Synthesis of (+)-Leucascandrolide A. *Angew. Chem., Int. Ed.* **2003**, *42*, 343-347.

54. Ghosh, A. K.; Gong, G. Total Synthesis of Potent Antitumor Agent (−) Lasonolide A: A Cycloaddition-Based Strategy. *Chem. Asian J.* **2008**, *3*, 1811-1823.

55. Ghosh A. K.; Shurrush, K. A.; Dawson, Z. L. Enantioselective total synthesis of macrolide (+)-neopeltolide. *Org. Biomol. Chem.* **2013**, *11*, 7768-7777.

56. Paterson, I.; Miller, N. A. Total synthesis of the marine macrolide (+)-neopeltolide. *Chem. Commun.* **2008**, 4708-4710.

57. Han, X.; Floreancig, P. E. Spiroacetal Formation through Telescoped Cycloaddition and Carbon–Hydrogen Bond Functionalization: Total Synthesis of Bistramide A. *Angew. Chem., Int. Ed.* **2014**, *53*, 11075-11078.

58. Ley, S. V.; Abad-Somovilla, A.; Anderson, J. C.; Ayats, C.; Bänteli, R.; Beckmann, E.; Boyer, A.; Brasca, M. G.; Brice, A.; Broughton, H. B.; Burke, B. J.; Cleator, E.; Craig, D.; Denholm, A. A.; Denton, R. M.; Durand-Reville, T.; Gobbi, L. B.; Gçbel, M.; Gray, B. L.; Grossmann, R. B.; Gutteridge, C. E.; Hahn, N.; Harding, S. L.; Jennens, D. C.; Jennens, L.; Lovell, P. J.; Lovell, H. J.; de la Puente, M. L.; Kolb, H. C.; Koot, W.-J.; Maslen, S. L.; McCusker, C. F.; Mattes, A.; Pape, A. R.; Pinto, A.; Santafianos, D.; Scott, J. S.; Smith, S. C.; Somers, A. Q.; Spilling, C. D.; Stelzer, F.; Toogood, P. L.; Turner, R. M.; Veitch, G. E.; Wood, A.; Zumbrunn, C. The Synthesis of Azadirachtin: A Potent Insect Antifeedant. *Chem. Eur. J.* **2008**, *14*, 10683-10704.

59. Boyer, A.; Veitch, G. E.; Beckmann, E.; Ley, S. V. Second-Generation Synthesis of Azadirachtin: A Concise Preparation of the Propargylic Mesylate Fragment. *Angew. Chem., Int. Ed.* **2009**, *48*, 1317-1320.

60. Anada, M.; Washio, T.; Shimada, N.; Kitagaki, S.; Nakajima, M.; Shiro, M.; Hashimoto, S. A New Dirhodium(II) Carboxamidate Complex as a Chiral Lewis Acid Catalyst for Enantioselective Hetero-Diels–Alder Reactions. *Angew. Chem., Int. Ed.* **2004**, *43*, 2665-2668.

61. Prasad, K. R.; Anbarasan, P. Stereoselective formal synthesis of (−)-centrolobine. *Tetrahedron* **2007**, *63*, 1089-1092.

62. Yao, S.; Johannsen, M.; Hazell, R. G.; Jørgensen, K. A. Total Synthesis of (*R*)-Dihydroactinidiolide and (*R*)-Actinidiolide Using Asymmetric Catalytic Hetero-Diels−Alder Methodology. *J. Org. Chem.* **1998**, *63*, 118-121.

63. Audrain, H.; Thorhauge, J.; Hazell, R. G.; Jørgensen, K. A. A Novel Catalytic and Highly Enantioselective Approach for the Synthesis of Optically Active Carbohydrate Derivatives. *J. Org. Chem.* **2000**, *65*, 4487-4497.

64. Evans, D. A.; Kværnø, L.; Dunn, T. B.; Beauchemin, A.; Raymer, B.; Mulder, J. A.; Olhava, E. J.; Juhl, M.; Kagechika, K.; Favor, D. A. Total Synthesis of (+)-Azaspiracid-1. An Exhibition of the Intricacies of Complex Molecule Synthesis. *J. Am. Chem. Soc.* **2008**, *130*, 16295-16309.

65. Guseinov, M. M., Akhmedov, I.M., and Mamedov, E.G. Asymmetric synthesis in the 1,4-addition of cyclopentadiene to (−)-menthyl methacrylate. *Azerb. Khim. Zh.* **1976**, 46-48.

66. Corey, E. J.; Bakshi, R. K.; Shibata, S. Highly enantioselective borane reduction of ketones catalyzed by chiral oxazaborolidines. Mechanism and synthetic implications. *J. Am. Chem. Soc.* **1987,** *109*, 5551-5553.

67. Corey, E. J.; Shibata, T.; Lee, T. W. Asymmetric Diels−Alder Reactions Catalyzed by a Triflic Acid Activated Chiral Oxazaborolidine. *J. Am. Chem. Soc.* **2002**, *124*, 3808-3809.

68. Gao, L.; Hwang, G.-S.; Ryu, D. H. Oxazaborolidinium Ion-Catalyzed Cyclopropanation of α-Substituted Acroleins: Enantioselective Synthesis of Cyclopropanes Bearing Two Chiral Quaternary Centers. *J. Am. Chem. Soc.* **2011,** *133*, 20708-20711.

69. S Gao, L.; Kang, B. C.; Hwang, G.-S.; Ryu, D. H. Enantioselective Synthesis of α-alkyl-β-ketoesters: Asymmetric Roskamp Reaction Catalyzed by an Oxazaborolidinium Ion. *Angew. Chem. Int. Ed.* **2012,** *51*, 8322-8325.

70. Furuta, K.; Miwa, Y.; Iwanaga, K.; Yamamoto, H. Acyloxyborane: an activating device for carboxylic acids. *J. Am. Chem. Soc.* **1988,** *110*, 6254-6255.

71. Furuta, K.; Maruyama, T.; Yamamoto, H. Chiral (Acyloxy)borane Catalyzed Asymmetric Aldol Type Reaction of Ketene Silyl Acetals with Aldehydes. *Synlett* **1991,** 439-440.

72. Furuta, K.; Mouri, M.; Yamamoto, H. Chiral (Acyloxy)borane Catalyzed Asymmetric Allylation of Aldehydes. *Synlett* **1991,** 561-562.

73. Gao, Q.; Maruyama, T.; Mouri, M.; Yamamoto, H. Asymmetric hetero Diels-Alder reaction catalyzed by stable and easily prepared chiral (acyloxy)borane (CAB) catalysts. *J. Org. Chem.* **1992,** *57,* 1951-1952.

74. Yamamoto, H.; Futatsugi, K. "Designer Acids": Combined Acid Catalysis for Asymmetric Synthesis. *Angew. Chem. Int. Ed.* **2005,** *44,* 1924-1942.

75. Kaufmann, D.; Boese, R. A Borate Propeller Compound as Chiral Catalyst for an Asymmetrically Induced Diels-Alder Reaction. *Angew. Chem. Int. Ed.* **1990,** *29*, 545-546.

76. Ishihara, K.; Yamamoto, H. Bronsted Acid Assisted Chiral Lewis Acid (BLA) Catalyst for Asymmetric Diels-Alder Reaction. *J. Am. Chem. Soc.* **1994,** *116,*1561-1562.

77. Ishihara, K.; Kurihara, H.; Yamamoto, H. A New Powerful and Practical BLA Catalyst for Highly Enantioselective Diels−Alder Reaction: An Extreme Acceleration of Reaction Rate by Brønsted Acid. *J. Am. Chem. Soc.* **1996**, *118,* 3049-3050.

78. Ishihara, K.; Kurihara, H.; Matsumoto, M.; Yamamoto, H. Design of Brønsted Acid-Assisted Chiral Lewis Acid (BLA) Catalysts for Highly Enantioselective Diels−Alder Reactions. *J. Am. Chem. Soc.* **1998,** *120*, 6920-6930.

79. Hattori, K.; Yamamoto, H. Asymmetric aza-Diels-Alder reaction mediated by chiral boron reagent. *J. Org. Chem.* **1992,** *57,* 3264-3265.

80. Mahlau, M.; List, B. Asymmetric Counteranion-Directed Catalysis: Concept, Definition, and Applications. *Angew. Chem. Int. Ed.* **2013,** *52*, 518-533.

81. Hattori, K.; Yamamoto, H. A Novel Stereocontrolled Synthesis of 3-(1′-Hydroxyethyl)-2-Azetidinone. *Synlett* 1993, 239-240.

82. Hu, G.; Gupta, A. K.; Huang, L.; Zhao, W.; Yin, X.; Osminski, W. E. G.; Huang, R. H.; Wulff, W. D.; Izzo, J. A.; Vetticatt, M. J. *Pyro*-Borates, *Spiro*-Borates, and Boroxinates of BINOL—Assembly, Structures, and Reactivity. *J. Am. Chem. Soc.* **2017**, *139*, 10267-10285.

83. Gupta, A. K.; Yin, X.; Mukherjee, M.; Desai, A. A.; Mohammadlou, A.; Jurewicz, K.; Wulff, W. D. Catalytic Asymmetric Epoxidation of Aldehydes with Two VANOL-Derived Chiral Borate Catalysts. *Angew. Chem., Int. Ed.* **2019**, *58*, 3361-3367.

84. Yin, X.; Wulff, W. D. Application of Chiral Borates in Asymmetric Catalysis and Chiral Resolution. Ph.D thesis. Michigan State University, **2018**.

85. Antilla, J. C.; Wulff, W. D. Catalytic Asymmetric Aziridination with a Chiral VAPOL-Boron Lewis Acid. *J. Am. Chem. Soc.* **1999,** *121*, 5099-5100.

86. Hu, G.; Gupta, A. K.; Huang, R. H.; Mukherjee, M.; Wulff, W. D. Substrate-Induced Covalent Assembly of a Chemzyme and Crystallographic Characterization of a Chemzyme-Substrate Complex. *J. Am. Chem. Soc.* **2010**, *132*, 14669-14675.

87. Desai, A. A.; Wulff, W. D. Controlled Diastereo- and Enantioselection in a Catalytic Asymmetric Aziridination. *J. Am. Chem. Soc.* **2010,** *132*, 13100-13103.

88. Newman, C. A.; Antilla, J. C.; Chen, P.; Predeus, A. V.; Fielding, L.; Wulff, W. D. Regulation of Orthogonal Functions in a Dual Catalyst System. Subservient Role of a Nonchiral Lewis Acid in an Asymmetric Catalytic Heteroatom Diels-Alder Reaction. *J. Am. Chem. Soc.* **2007,** *129*, 7216-7217.

89. Ren, H.; Wulff, W. D. Direct Catalytic Asymmetric Aminoallylation of Aldehydes: Synergism of Chiral and Nonchiral Brønsted Acids. *J. Am. Chem. Soc.* **2011,** *133*, 5656-5659.

90. Zhao, W.; Huang, L.; Guan, Y.; Wulff, W. D. Three-Component Asymmetric Catalytic Ugi Reaction—Concinnity from Diversity by Substrate-Mediated Catalyst Assembly. *Angew. Chem. Int. Ed.* **2014,** *53,* 3436-3441.

91. Danishefsky, S.; Larson, E.; Askin, D.; Kato N. On the scope, mechanism and stereochemistry of the Lewis acid catalyzed cyclocondensation of activated dienes with aldehydes: an application to the erythronolide problem. *J. Am. Chem. Soc.* **1985**, *107*, 1246-1255.

92. Mohammadlou, A.; Wulff, W. D. Application of Chameleon catalyst and VAPOL/VANOL imidodiphosphoramide catalysts in asymmetric catalysis. Ph.D thesis. Michigan State University, **2020**.

93. Gaussian 16, Revision A.03, Frisch, M. J.; Trucks, G. W.; Schlegel, H. B.; Scuseria, G. E.; Robb, M. A.; Cheeseman, J. R.; Scalmani, G.; Barone, V.; Petersson, G. A.; Nakatsuji, H.; Li, X.; Caricato, M.; Marenich, A. V.; Bloino, J.; Janesko, B. G.; Gomperts, R.; Mennucci, B.; Hratchian, H. P.; Ortiz, J. V.; Izmaylov, A. F.; Sonnenberg, J. L.; Williams-Young, D.; Ding, F.; Lipparini, F.; Egidi, F.; Goings, J.; Peng, B.; Petrone, A.; Henderson, T.; Ranasinghe, D.; Zakrzewski, V. G.; Gao, J.; Rega, N.; Zheng, G.; Liang, W.; Hada, M.; Ehara, M.; Toyota, K.; Fukuda, R.; Hasegawa, J.; Ishida, M.; Nakajima, T.; Honda, Y.; Kitao, O.; Nakai, H.; Vreven, T.; Throssell, K.; Montgomery, J. A., Jr.; Peralta, J. E.; Ogliaro, F.; Bearpark, M. J.; Heyd, J. J.; Brothers, E. N.; Kudin, K. N.; Staroverov, V. N.; Keith, T. A.; Kobayashi, R.; Normand, J.; Raghavachari, K.; Rendell, A. P.; Burant, J. C.; Iyengar, S. S.; Tomasi, J.; Cossi, M.; Millam, J. M.; Klene, M.; Adamo, C.; Cammi, R.; Ochterski, J. W.; Martin, R. L.; Morokuma, K.; Farkas, O.; Foresman, J. B.; Fox, D. J. Gaussian, Inc., Wallingford CT, 2016.

CHAPTER FOUR

EXPERIMENTAL SECTION

4.1 General information

All reactions were carried out in round bottom flasks with argon balloons unless otherwise indicated. Unless otherwise specified, all solvents used in reactions were strictly dried before use: dichloromethane and 1,2-dichloroethane were distilled over calcium hydride under nitrogen; tetrahydrofuran, ether, and toluene were distilled from sodium and benzophenone under nitrogen; *n*-pentane, hexanes, cyclohexane, benzene, *m*-xylene, mesitylene, and anisole were distilled from sodium under nitrogen; 2-propanol was distilled over calcium oxide under nitrogen. Hexanes and ethyl acetate for column chromatography were ACS grade and used as purchased. Commercially available ketones and aldehydes and other reagents were purchased from Sigma-Aldrich, Alfa-Aesar, Combi-Blocks or Oakwood and were purified by distillation or sublimation unless otherwise indicated. $AlMe_3$ was purchased from Sigma-Aldrich as a 2 M solution in toluene and was used as received. Borane dimethylsulfide (BH_3•Me_2S) was purchased from Alfa-Aesar as a 2 M solution in toluene and was used as received. VANOL, VAPOL and their derivatives were made according to known procedures.[1-4]

Melting points were recorded on a Thomas Hoover capillary melting point apparatus and are uncorrected. The ^{1}H NMR, ^{11}B NMR and ^{13}C NMR spectra were recorded on a Varian Unity Plus 500 MHz spectrometer using $CDCl_3$ as solvent (unless otherwise noted). The residual peak of $CDCl_3$ or TMS was used as the

internal standard for both ^{1}H NMR (δ = 7.26 ppm for $CDCl_3$ or δ = 0 ppm for TMS) and ^{13}C NMR (δ = 77.0 ppm). The 11B NMR spectra were done in a Norell® quartz NMR tube and referenced to external standard $BF_3 \bullet Et_2O$ (δ = 0 ppm). Chemical shifts were reported in parts per million (ppm). Analytical thin-layer chromatography (TLC) was performed on Silicycle silica gel plates with F-254 indicator. Visualization was by short wave (254 nm) and long wave (365 nm) ultraviolet light, or by staining with phosphomolybdic acid in ethanol. Column chromatography was performed with silica gel 60 (230 – 450 mesh). HPLC analyses were performed using Agilent 1100 or 1260 HPLC System with CHIRALCEL® OJ-H, OD and OD-H or CHIRALPAK® AD-H, AS-H and IA columns. HPLC grade hexanes (mixture of isomers) and 2-propanol were used for HPLC analyses. Optical rotations were obtained at a wavelength of 589 nm (sodium D line) using a 1.0 decimeter cell with a total volume of 1.0 mL. Specific rotations are reported in degrees per decimeter at 20 °C and the concentrations are given in gram per 100 mL in chloroform unless otherwise noted. IR spectra were recorded on NaCl disc (for liquids) on a Nicolet IR/42 spectrometer. High Resolution Mass Spectrometry was performed in the Department of Chemistry at Michigan State University Mass Facility.

4.2 Experimental information for chapter two

4.2.1 General procedure for catalytic asymmetric MPV reduction of aromatic ketones

Procedure A — illustrated for acetophenone **55a**

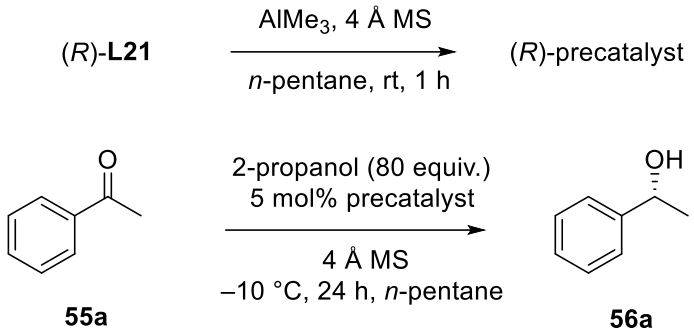

(R)-1-phenylethanol **56a**: To a 5 mL flame-dried round bottom flask equipped with a stir bar was charged (*R*)-**L21** ((*R*)-**7,7'-Cy$_2$VANOL**, 9.8 mg, 0.01625 mmol), 4 Å molecular sieves (25.0 mg, activated), and dry pentane (1 mL). Then a rubber septum stopper and argon balloon were attached. While stirring at room temperature, trimethylaluminum solution (6.2 µl, 0.0125 mmol, 2 M in toluene) was added to the reaction flask. After 1 hour, the flask containing the precatalyst was charged with dry 2-propanol (1.5 mL, 20 mmol) and chilled to –10 ˚C. To the mixture was added acetophenone **55a** (29.2 µl, 0.25 mmol) via micro-syringe and the resulting mixture was stirred for 24 hours at –10 ˚C. The reaction was quenched by the addition of 2 M HCl (1 mL) and then was warmed to room temperature. The mixture was transferred into a 60 mL separatory funnel and added 15 mL water before extracted with CH_2Cl_2 (15 mL × 3). Combined organic layer was concentrated under vacuum to afford the crude product. Purification of the crude product by silica gel chromatography (15 mm × 200 mm column, 5:1 hexanes/ EtOAc as eluent) afforded pure alcohol **56a** as a colorless oil in 88% isolated yield

(26.8 mg, 0.22 mmol); The optical purity of **56a** was determined to be 94% *ee* by HPLC (CHIRALCEL® OD-H column, 99:1 hexanes/2-propanol at 210 nm, flow-rate: 1 mL/min); retention times: R_t = 16.7 min (major enantiomer, **56a**) and R_t = 24.0 min (minor enantiomer, *ent*-**56a**). Each enantiomer was obtained and confirmed by reducing the ketone with sodium borohydride in methanol.

Spectral data for **56a**: R_f = 0.18 (CH_2Cl_2); $[\alpha]_D^{20}$ = +47.9 (*c*=1.0 in $CHCl_3$) 94% *ee* (*R*) (lit.[5] $[\alpha]_D^{22}$ = +49.0 (*c*=1.0 in $CHCl_3$) 98% *ee* (*R*)). ^{1}H NMR (500 MHz, $CDCl_3$) δ = 1.51 (d, *J* = 6.5, 3H), 2.04 (s, 1H), 4.90 (q, *J* = 6.5, 1H), 7.27 – 7.32 (m, 1H), 7.34 – 7.41 (m, 4H); ^{13}C NMR (126 MHz, $CDCl_3$) δ = 25.17, 70.41, 125.40, 127.47, 128.50, 145.80. These spectral data match those previously reported for this compound.[5]

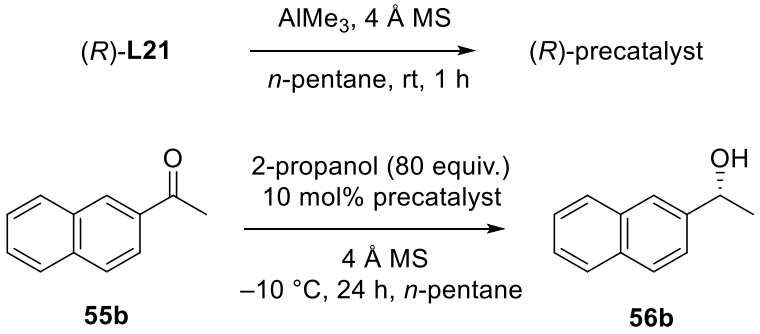

(R)-1-(2-naphthyl)ethanol **56b**: Ketone **55b** was reduced according to procedure A with 10 mol% precatalyst. Purification of the crude product by silica gel chromatography (15 mm × 200 mm column, 5:1 hexanes/ EtOAc as eluent) afforded pure alcohol **56b** as a white solid (m.p. 65-68 ˚C) in 78% isolated yield (33.8 mg, 0.20 mmol); The optical purity of **56b** was determined to be 91% *ee* by HPLC (CHIRALCEL® OJ-H column, 95:5 hexanes/2-propanol at 220 nm, flow-rate: 1 mL/min); retention times: R_t = 38.5 min (minor enantiomer, *ent*-**56b**) and R_t =

52.1 min (major enantiomer, **56b**). Each enantiomer was obtained and confirmed by reducing the ketone with sodium borohydride in methanol.

Spectral data for **56b**: R_f = 0.18 (CH_2Cl_2); $[\alpha]_D^{20}$ = +40.2 (*c*=1.0 in $CHCl_3$) 91% *ee* (*R*) (lit.[6] $[\alpha]_D^{23}$ = +43.1 (*c*=1.2 in $CHCl_3$) 93% *ee* (*R*)). ^{1}H NMR (500 MHz, $CDCl_3$) δ = 1.60 (d, *J* = 6.5, 3H), 1.96 (s, 1H), 5.09 (d, *J* = 6.5, 1H), 7.45 – 7.55 (m, 3H), 7.80 – 7.89 (m, 4H); ^{13}C NMR (126 MHz, $CDCl_3$) δ = 25.16, 70.56, 123.80, 123.81, 125.81, 126.16, 127.68, 127.93, 128.33, 132.91, 133.30, 143.16. These spectral data match those previously reported for this compound.[7]

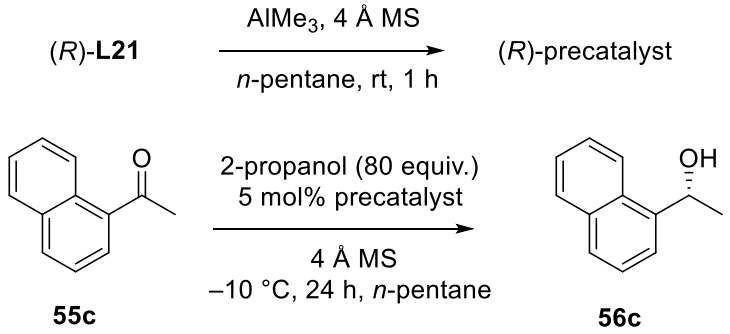

(R)-1-(1-naphthyl)ethanol **56c**: Ketone **55c** was reduced according to procedure A. Purification of the crude product by silica gel chromatography (15 mm × 200 mm column, 5:1 hexanes/ EtOAc as eluent) afforded pure alcohol **56c** as a white solid (m.p. 62-64 ˚C) in 95% isolated yield (41.1 mg, 0.24 mmol); The optical purity of **56c** was determined to be 98% *ee* by HPLC (CHIRALCEL® OD-H column, 90:10 hexanes/2-propanol at 210 nm, flow-rate: 0.8 mL/min); retention times: R_t = 7.0 min (minor enantiomer, *ent*-**56c**) and R_t = 11.1 min (major enantiomer, **56c**). Each enantiomer was obtained and confirmed by reducing the ketone with sodium borohydride in methanol.

Spectral data for **56c**: R_f = 0.18 (CH_2Cl_2); $[\alpha]_D^{20}$ = +74.5 (*c*=1.0 in $CHCl_3$) 98% *ee* (*R*) (lit.[6] $[\alpha]_D^{23}$ = +69.7 (*c*=1.1 in Et_2O) 90% *ee* (*R*)). ^{1}H NMR (500 MHz, $CDCl_3$) δ = 1.67 (d, *J* = 6.5, 3H), 2.22 (s, 1H), 5.66 (q, *J* = 6.5, 1H), 7.45 – 7.58 (m, 3H), 7.68 (dt, *J* = 7.1, 1.0, 1H), 7.80 (dt, *J* = 8.1, 1.0, 1H), 7.90 (dd, *J* = 8.0, 1.7, 1H), 8.07 – 8.13 (m, 1H); ^{13}C NMR (126 MHz, $CDCl_3$) δ = 24.37, 67.08, 122.00, 123.18, 125.55, 125.56, 126.04, 127.93, 128.90, 130.26, 133.79, 141.38. These spectral data match those previously reported for this compound.[7]

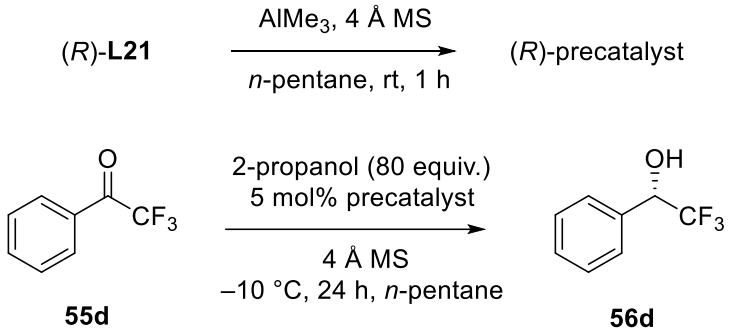

(S)-2,2,2-trifluoro-1-phenylethanol **56d**: Ketone **55d** was reduced according to procedure A. Purification of the crude product by silica gel chromatography (15 mm × 200 mm column, 5:1 hexanes/ EtOAc as eluent) afforded pure alcohol **56d** as a colorless oil in 71% isolated yield (31.2 mg, 0.18 mmol); The optical purity of **56d** was determined to be 96% *ee* by HPLC (CHIRALCEL® OD-H column, 99:1 hexanes/2-propanol at 210 nm, flow-rate: 1.0 mL/min); retention times: R_t = 33.2 min (major enantiomer, **56d**) and R_t = 43.3 min (minor enantiomer, *ent*-**56d**). Each enantiomer was obtained and confirmed by reducing the ketone with sodium borohydride in methanol.

Spectral data for **56d**: R_f = 0.16 (CH_2Cl_2); $[\alpha]_D^{20}$ = +23.4 (*c*=1.0 in $CHCl_3$) 96% *ee* (*S*) (lit.[8] $[\alpha]_D^{20}$ = +28.4 (*c*=1.3 in $CHCl_3$) 95% *ee* (*S*)). ^{1}H NMR (500 MHz,

$CDCl_3$) δ = 2.94 (s, 1H), 4.99 (d, *J* = 6.8, 1H), 7.44 (dd, *J* = 5.0, 2.0, 3H), 7.49 (dd, *J* = 6.9, 3.0, 2H); ^{13}C NMR (126 MHz, $CDCl_3$) δ = 72.84 (q, J = 32.0), 124.22 (q, J = 282.2), 127.46, 128.65, 129.60, 133.90. These spectral data match those previously reported for this compound.[8]

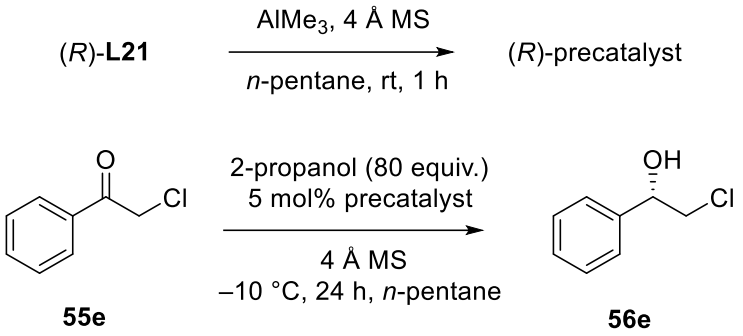

(S)-2-chloro-1-phenylethanol **56e**: Ketone **55e** was reduced according to procedure A. Purification of the crude product by silica gel chromatography (15 mm × 200 mm column, 5:1 hexanes/ EtOAc as eluent) afforded pure alcohol **56e** as a colorless oil in 98% isolated yield (38.5 mg, 0.24 mmol); The optical purity of **56e** was determined to be 99% *ee* by HPLC (CHIRALCEL® OD-H column, 99:1 hexanes/2-propanol at 210 nm, flow-rate: 1.0 mL/min); retention times: R_t = 18.6 min (major enantiomer, **56e**) and R_t = 23.5 min (minor enantiomer, *ent*-**56e**). Each enantiomer was obtained and confirmed by reducing the ketone with sodium borohydride in methanol.

Spectral data for **56e**: R_f = 0.17 (CH_2Cl_2); $[\alpha]_D^{20}$ = +53.8 (*c*=1.0 in $CHCl_3$) 99% *ee* (*S*) (lit.[5] $[\alpha]_D^{25}$ = +51.5 (*c*=1.1 in cyclohexane) 95% *ee* (*S*)). ^1H NMR (500 MHz, $CDCl_3$) δ = 2.78 (s, 1H), 3.66 (dd, *J* = 11.3, 8.8, 1H), 3.76 (dd, *J* = 11.3, 3.4, 1H), 4.92 (dd, *J* = 8.9, 3.4, 1H), 7.32 – 7.43 (m, 5H); ^{13}C NMR (126 MHz, $CDCl_3$)

δ = 50.93, 74.08, 126.06, 128.48, 128.68, 139.88. These spectral data match those previously reported for this compound.[9]

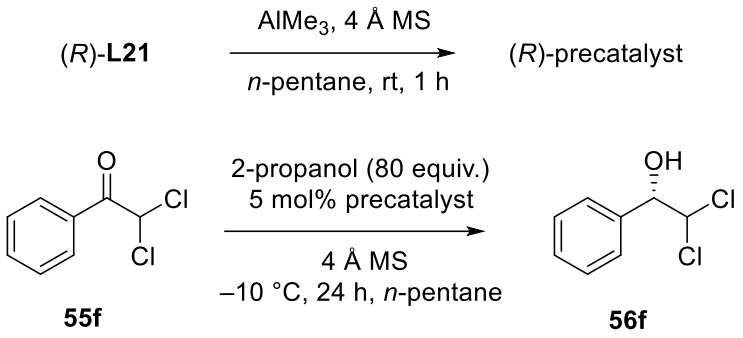

(S)-2,2-dichloro-1-phenylethanol **56f**: Ketone **55f** was reduced according to procedure A. Purification of the crude product by silica gel chromatography (15 mm × 200 mm column, 5:1 hexanes/ EtOAc as eluent) afforded pure alcohol **56f** as a colorless oil in 94% isolated yield (44.8 mg, 0.24 mmol); The optical purity of **56f** was determined to be >99% *ee* by HPLC (CHIRALCEL® OD-H column, 99:1 hexanes/2-propanol at 210 nm, flow-rate: 1.0 mL/min); retention times: R_t = 31.9 min (sole enantiomer, **56f**). Both **56f** and its enantiomer *ent*-**56f** were obtained and confirmed by reducing the ketone with sodium borohydride in methanol.

Spectral data for **56f**: R_f = 0.17 (CH_2Cl_2); $[\alpha]_D^{20}$ = +27.2 (*c*=1.0 in $CHCl_3$) >99% *ee* (*S*) (lit.[10] $[\alpha]_D^{20}$ = -21.7 (*c*=1.0 in $CHCl_3$) >99% *ee* (*R*)). ^{1}H NMR (500 MHz, $CDCl_3$) δ = 3.07 (s, 1H), 4.97 (d, *J* = 5.4, 1H), 5.83 (d, *J* = 5.4, 1H), 7.35 – 7.46 (m, 5H); ^{13}C NMR (126 MHz, $CDCl_3$) δ = 76.41, 78.81, 127.15, 128.54, 129.06, 137.36. These spectral data match those previously reported for this compound.[10]

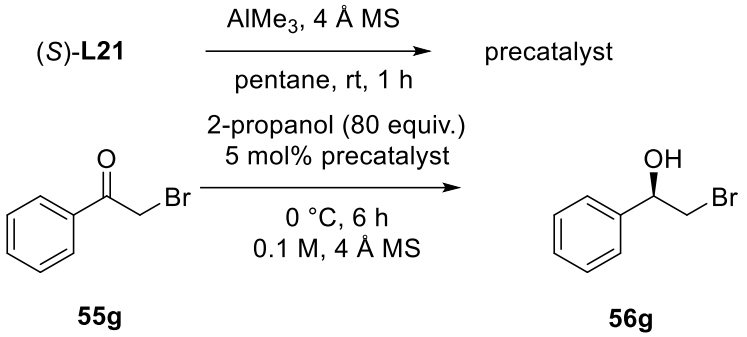

(R)-2-bromo-1-phenylethanol **56g**: Ketone **55g** was reduced according to procedure A with (*S*)-**L21** at 0 ˚C for 6 hours. Purification of the crude product by silica gel chromatography (15 mm × 200 mm column, 5:1 hexanes/ EtOAc as eluent) afforded pure alcohol **56g** as a yellow oil in 87% isolated yield (43.5 mg, 0.22 mmol); The optical purity of **56g** was determined to be 97% *ee* by HPLC (CHIRALCEL® OD-H column, 98:2 hexanes/2-propanol at 210 nm, flow-rate: 1.0 mL/min); retention times: 13.0 min (minor enantiomer, *ent*-**56g**) and R_t = 15.8 min (major enantiomer, **56g**). Each enantiomer was obtained and confirmed by reducing the ketone with sodium borohydride in methanol.

Spectral data for **56g**: R_f = 0.17 (CH_2Cl_2); $[\alpha]_D^{20}$ = -40.1 (*c*=1.0 in $CHCl_3$) 97% *ee* (*R*) (lit.[8] $[\alpha]_D^{20}$ = +42.3 (*c*=1.5 in CH_2Cl_2) 97% *ee* (*S*)). ^{1}H NMR (500 MHz, $CDCl_3$) δ = 2.64 (s, 1H), 3.53 (dd, *J* = 10.5, 9.0, 1H), 3.63 (dd, *J* = 10.5, 3.3, 1H), 4.91 (dd, *J* = 9.0, 2.6, 1H), 7.28 – 7.42 (m, 5H); ^{13}C NMR (126 MHz, $CDCl_3$) δ = 40.27, 73.81, 125.96, 128.48, 128.70, 140.24. These spectral data match those previously reported for this compound.[8]

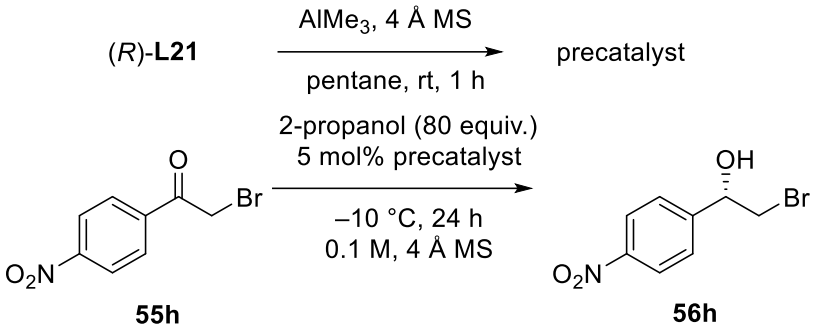

(S)-2-bromo-1-(4-nitrophenyl)ethanol **56h**: Ketone **55h** was reduced according to procedure A. Purification of the crude product by silica gel chromatography (15 mm × 200 mm column, 5:1 hexanes/ EtOAc as eluent) afforded pure alcohol **56h** as a white solid (m.p. 94-96 ˚C) in 95% isolated yield (58.1 mg, 0.24 mmol); The optical purity of **56h** was determined to be 98% *ee* by HPLC (CHIRALCEL® OJ-H column, 90:10 hexanes/2-propanol at 210 nm, flow-rate: 1.0 mL/min); retention times: R_t = 28.0 min (minor enantiomer, *ent*-**56h**) and R_t = 30.3 min (major enantiomer, **56h**). Each enantiomer was obtained and confirmed by reducing the ketone with sodium borohydride in methanol. The Crystal structure of **56h** was solved and absolute configuration was confirmed. **CCDC 1903110** contains details for it and could be found from The Cambridge Crystallographic Data Centre via **www.ccdc.cam.ac.uk/structures.**

Spectral data for **56h**: R_f = 0.16 (CH_2Cl_2); $[\alpha]_D^{20}$ = +31.4 (*c*=1.0 in $CHCl_3$) 98% *ee* (*S*) (lit.[6] $[\alpha]_D^{23}$ = +29.6 (*c*=1.1 in $CHCl_3$) 90% *ee* (*S*)). ^{1}H NMR (500 MHz, $CDCl_3$) δ = 2.79 (d, *J* = 3.6, 1H), 3.53 (dd, *J* = 10.6, 8.4, 1H), 3.68 (dd, *J* = 10.6, 3.4, 1H), 5.05 (s, 1H), 7.55 – 7.63 (m, 2H), 8.21 – 8.28 (m, 2H); ^{13}C NMR (126 MHz, $CDCl_3$) δ = 39.44, 72.66, 123.88, 126.92, 147.19, 147.83. These spectral data match those previously reported for this compound.[17]

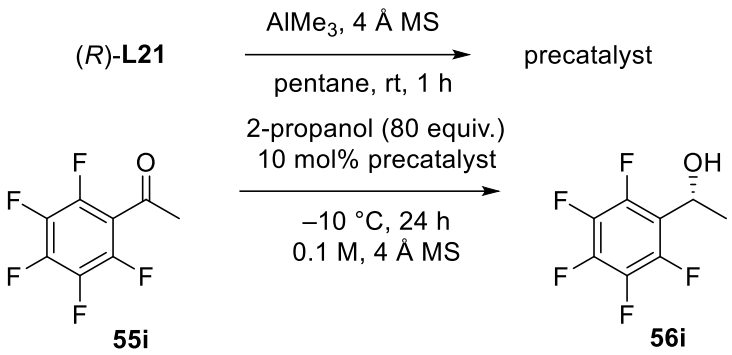

(R)-1-(pentafluorophenyl)ethanol **56i**: Ketone **55i** was reduced according to procedure A with 10 mol% precatalyst. Purification of the crude product by silica gel chromatography (15 mm × 200 mm column, 5:1 hexanes/ EtOAc as eluent) afforded pure alcohol **56i** as a colorless oil in 80% isolated yield (42.4 mg, 0.20 mmol); The optical purity of **56i** was determined to be 99% *ee* by HPLC (CHIRALPAK® AD-H column, 99:1 hexanes/2-propanol at 210 nm, flow-rate: 0.8 mL/min); retention times: R_t = 19.4 min (minor enantiomer, *ent*-**56i**) and R_t = 24.0 min (major enantiomer, **56i**). Each enantiomer was obtained and confirmed by reducing the ketone with sodium borohydride in methanol.

Spectral data for **56i**: R_f = 0.16 (CH_2Cl_2); $[\alpha]_D^{20}$ = +13.6 (*c*=1.0 in $CHCl_3$) 99% *ee* (*R*) (lit.[11] $[\alpha]_D^{22}$ = +13.0 (*c*=1.1 in $CHCl_3$) >99% *ee* (*R*)). ^{1}H NMR (500 MHz, $CDCl_3$) δ = 1.63 (dt, *J* = 6.8, 0.8, 3H), 2.68 (d, *J* = 6.8, 1H), 5.24 (t, *J* = 6.8, 1H); ^{13}C NMR (126 MHz, $CDCl_3$) δ = 22.95, 62.18, 117.84 (m), 137.53 (m), 140.44 (m), 144.57 (m). These spectral data match those previously reported for this compound.[11]

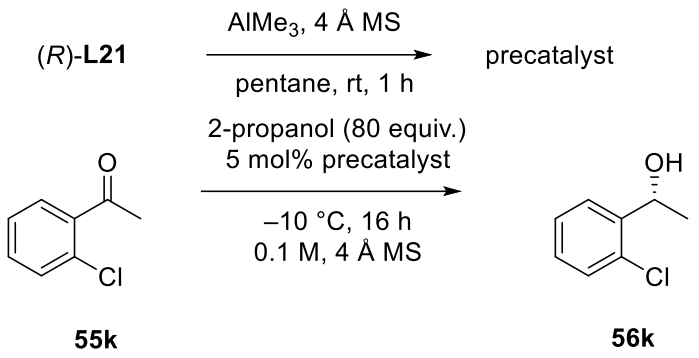

55k **56k**

(R)-1-(2-chlorophenyl)ethanol **56k**: Ketone **55k** was reduced according to procedure A after 16 hours. Purification of the crude product by silica gel chromatography (15 mm × 200 mm column, 5:1 hexanes/ EtOAc as eluent) afforded pure alcohol **56k** as a colorless oil in 96% isolated yield (37.7 mg, 0.24 mmol); The optical purity of **56k** was determined to be 99% *ee* by HPLC (CHIRALCEL® OD-H column, 99:1 hexanes/2-propanol at 210 nm, flow-rate: 1.0 mL/min); retention times: R_t = 12.0 min (major enantiomer, **56k**) and R_t = 13.2 min (minor enantiomer, *ent*-**56k**). Each enantiomer was obtained and confirmed by reducing the ketone with sodium borohydride in methanol.

Spectral data for **56k**: R_f = 0.17 (CH_2Cl_2); $[\alpha]_D^{20}$ = +60.7 (*c*=1.0 in $CHCl_3$) 99% *ee* (*R*) (lit.[9] $[\alpha]_D^{20}$ = +61.4 (*c*=1.0 in $CHCl_3$) 94% *ee* (*R*)). ^{1}H NMR (500 MHz, $CDCl_3$) δ = 1.47 – 1.52 (m, 3H), 2.17 (s, 1H), 5.30 (q, *J* = 6.4, 1H), 7.21 (td, *J* = 7.6, 1.7, 1H), 7.28 – 7.36 (m, 2H), 7.60 (dd, *J* = 7.8, 1.7, 1H); ^{13}C NMR (126 MHz, $CDCl_3$) δ = 23.51, 66.95, 126.39, 127.21, 128.40, 129.38, 131.61, 143.03. These spectral data match those previously reported for this compound.[9]

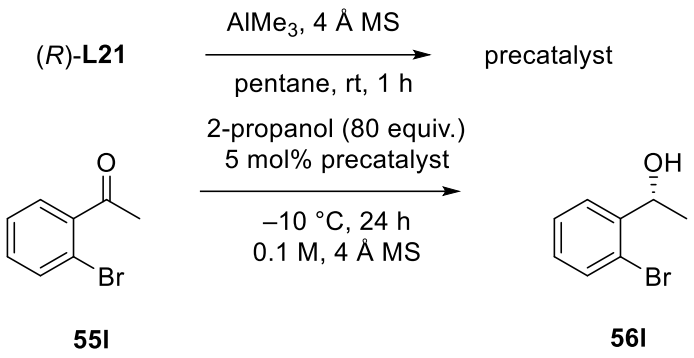

55l **56l**

(R)-1-(2-bromophenyl)ethanol **56l**: Ketone **55l** was reduced according to procedure A. Purification of the crude product by silica gel chromatography (15 mm × 200 mm column, 5:1 hexanes/ EtOAc as eluent) afforded pure alcohol **56l** as a colorless oil in 90% isolated yield (45.1 mg, 0.22 mmol); The optical purity of **56l** was determined to be 99% *ee* by HPLC (CHIRALCEL® OD-H column, 99:1 hexanes/2-propanol at 210 nm, flow-rate: 1.0 mL/min); retention times: R_t = 11.8 min (major enantiomer, **56l**) and R_t = 13.6 min (minor enantiomer, *ent*-**56l**). Each enantiomer was obtained and confirmed by reducing the ketone with sodium borohydride in methanol.

Spectral data for **56l**: R_f = 0.17 (CH_2Cl_2); $[\alpha]_D^{20}$ = +47.0 (*c*=1.0 in $CHCl_3$) 99% *ee* (*R*) (lit.[8] $[\alpha]_D^{20}$ = +50.8 (*c*=2.4 in CH_2Cl_2) 83% *ee* (*R*)). ^{1}H NMR (500 MHz, $CDCl_3$) δ = 1.48 (d, *J* = 6.4, 3H), 2.26 (s, 1H), 5.24 (q, *J* = 6.4, 1H), 7.13 (td, *J* = 7.6, 1.7, 1H), 7.35 (td, *J* = 7.7, 1.2, 1H), 7.52 (dd, *J* = 8.0, 1.2, 1H), 7.59 (dd, *J* = 7.8, 1.7, 1H); ^{13}C NMR (126 MHz, $CDCl_3$) δ = 23.58, 69.18, 121.69, 126.66, 127.85, 128.77, 132.64, 144.59. These spectral data match those previously reported for this compound.[8]

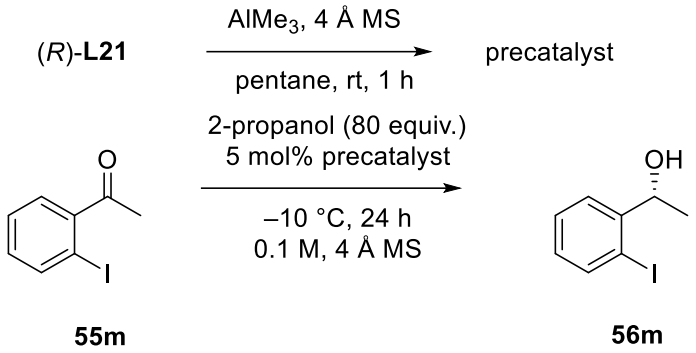

55m **56m**

(R)-1-(2-iodophenyl)ethanol **56m**: Ketone **55m** was reduced according to procedure A. Purification of the crude product by silica gel chromatography (15 mm × 200 mm column, 5:1 hexanes/ EtOAc as eluent) afforded pure alcohol **56m** as a white solid (m.p. 68-69 ˚C) in 96% isolated yield (59.5 mg, 0.24 mmol); The optical purity of **56m** was determined to be 99% *ee* by HPLC (CHIRALCEL® OD-H column, 99:1 hexanes/2-propanol at 210 nm, flow-rate: 1.0 mL/min); retention times: R_t = 12.8 min (major enantiomer, **56m**) and R_t = 14.6 min (minor enantiomer, *ent*-**56m**). Each enantiomer was obtained and confirmed by reducing the ketone with sodium borohydride in methanol.

Spectral data for **56m**: R_f = 0.17 (CH_2Cl_2); $[\alpha]_D^{20}$ = +67.0 (*c*=1.0 in $CHCl_3$) 99% *ee* (*R*) (lit.[12] $[\alpha]_D^{18}$ = +43.9 (*c*=0.5 in $CHCl_3$) 99% *ee* (*R*)). ^{1}H NMR (500 MHz, $CDCl_3$) δ = 1.46 (d, *J* = 6.4, 3H), 2.29 (s, 1H), 5.06 (q, *J* = 6.4, 1H), 6.93 – 7.01 (m, 1H), 7.38 (td, *J* = 7.5, 1.2, 1H), 7.56 (dd, *J* = 7.8, 1.7, 1H), 7.80 (dd, *J* = 7.9, 1.2, 1H); ^{13}C NMR (126 MHz, $CDCl_3$) δ = 23.77, 73.72, 97.23, 126.33, 128.74, 129.16, 139.30, 147.45. These spectral data match those previously reported for this compound.[13]

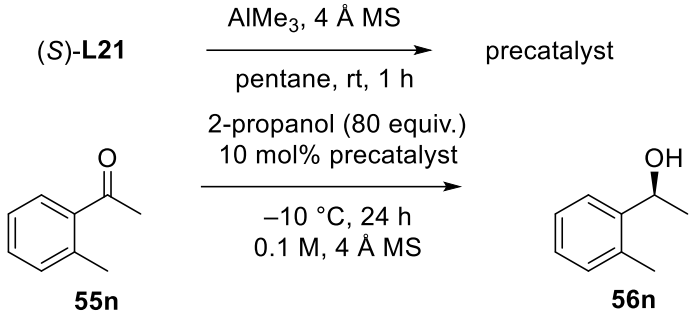

(S)-1-(2-methylphenyl)ethanol **56n**: Ketone **55n** was reduced according to procedure A with 10 mol% precatalyst made from (*S*)-**L21**. Purification of the crude product by silica gel chromatography (15 mm × 200 mm column, 5:1 hexanes/ EtOAc as eluent) afforded pure alcohol **56n** as a colorless oil in 94% isolated yield (32.1 mg, 0.24 mmol); The optical purity of **56n** was determined to be 96% *ee* by HPLC (CHIRALPAK® AD-H column, 98:2 hexanes/2-propanol at 210 nm, flow-rate: 0.8 mL/min); retention times: R_t = 15.7 min (minor enantiomer, *ent*-**56n**) and R_t = 17.8 min (major enantiomer, **56n**). Each enantiomer was obtained and confirmed by reducing the ketone with sodium borohydride in methanol.

Spectral data for **56n**: R_f = 0.18 (CH_2Cl_2); $[\alpha]_D^{20}$ = -54.1 (*c*=1.0 in $CHCl_3$) 96% *ee* (*S*) (lit.[13] $[\alpha]_D^{30}$ = +56.9 (*c*=0.41 in EtOH) 94% *ee* (*R*)). ^{1}H NMR (500 MHz, $CDCl_3$) δ = 1.48 (d, *J* = 6.4, 3H), 1.76 (s, 1H), 2.36 (s, 3H), 5.15 (q, *J* = 6.4, 1H), 7.13 – 7.21 (m, 2H), 7.23 – 7.28 (m, 1H), 7.50 – 7.56 (m, 1H); ^{13}C NMR (126 MHz, $CDCl_3$) δ = 18.94, 23.95, 66.83, 124.44, 126.38, 127.18, 130.37, 134.23, 143.82. These spectral data match those previously reported for this compound.[13]

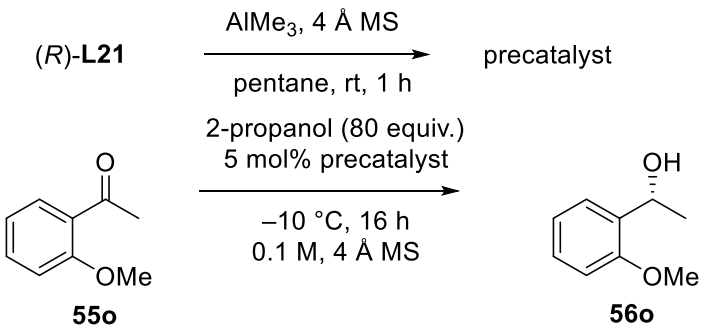

(R)-1-(2-methoxyphenyl)ethanol **56o**: Ketone **55o** was reduced according to procedure A after 16 hours. Purification of the crude product by silica gel chromatography (15 mm × 200 mm column, 5:1 hexanes/ EtOAc as eluent) afforded pure alcohol **56o** as a colorless oil in 93% isolated yield (35.5 mg, 0.23 mmol); The optical purity of **56o** was determined to be 94% *ee* by HPLC (CHIRALCEL® OD-H column, 99:1 hexanes/2-propanol at 210 nm, flow-rate: 1.0 mL/min); retention times: R_t = 17.8 min (minor enantiomer, *ent*-**56o**) and R_t = 19.2 min (major enantiomer, **56o**). Each enantiomer was obtained and confirmed by reducing the ketone with sodium borohydride in methanol.

Spectral data for **56o**: R_f = 0.18 (CH_2Cl_2); $[\alpha]_D^{20}$ = +28.1 (*c*=1.0 in $CHCl_3$) 94% *ee* (*R*) (lit.[13] $[\alpha]_D^{24}$ = +24.8 (*c*=2.0 in $CHCl_3$) 90% *ee* (*R*)). ^{1}H NMR (500 MHz, $CDCl_3$) δ = 1.52 (d, *J* = 6.5, 3H), 2.77 (s, 1H), 3.87 (s, 3H), 5.11 (d, *J* = 6.5, 1H), 6.90 (dd, *J* = 8.2, 1.0, 1H), 6.98 (td, *J* = 7.5, 1.0, 1H), 7.24 – 7.29 (m, 1H), 7.36 (dd, *J* = 7.5, 1.7, 1H); ^{13}C NMR (126 MHz, $CDCl_3$) δ = 22.86, 55.26, 66.51, 110.40, 120.79, 126.09, 128.29, 133.41, 156.52. These spectral data match those previously reported for this compound.[13]

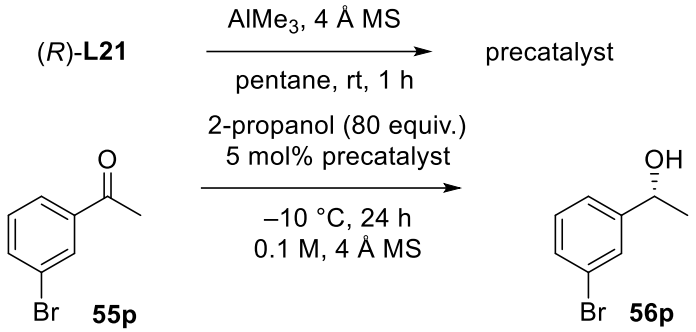

(R)-1-(3-bromophenyl)ethanol **56p**: Ketone **55p** was reduced according to procedure A. Purification of the crude product by silica gel chromatography (15 mm × 200 mm column, 5:1 hexanes/ EtOAc as eluent) afforded pure alcohol **56p** as a colorless oil in 91% isolated yield (45.5 mg, 0.23 mmol); The optical purity of **56p** was determined to be 97% *ee* by HPLC (CHIRALCEL® OD-H column, 99:1 hexanes/2-propanol at 210 nm, flow-rate: 1.0 mL/min); retention times: R_t = 17.6 min (minor enantiomer, *ent*-**56p**) and R_t = 19.5 min (major enantiomer, **56p**). Each enantiomer was obtained and confirmed by reducing the ketone with sodium borohydride in methanol.

Spectral data for **56p**: R_f = 0.17 (CH_2Cl_2); $[\alpha]_D^{20}$ = +46.5 (*c*=1.0 in $CHCl_3$) 97% *ee* (*R*) (lit.[14] $[\alpha]_D^{20}$ = +45.0 (*c*=1.0 in $CHCl_3$) 96% *ee* (*R*)). ^{1}H NMR (500 MHz, $CDCl_3$) δ = 1.47 (d, *J* = 6.5, 3H), 2.21 (s, 1H), 4.84 (q, *J* = 6.5, 1H), 7.21 (t, *J* = 7.7, 1H), 7.28 (dt, *J* = 7.7, 1.4, 1H), 7.40 (ddd, *J* = 7.8, 2.0, 1.2, 1H), 7.53 (t, *J* = 1.9, 1H); ^{13}C NMR (126 MHz, $CDCl_3$) δ = 25.25, 69.72, 122.58, 124.02, 128.55, 130.10, 130.45, 148.10. These spectral data match those previously reported for this compound.[14]

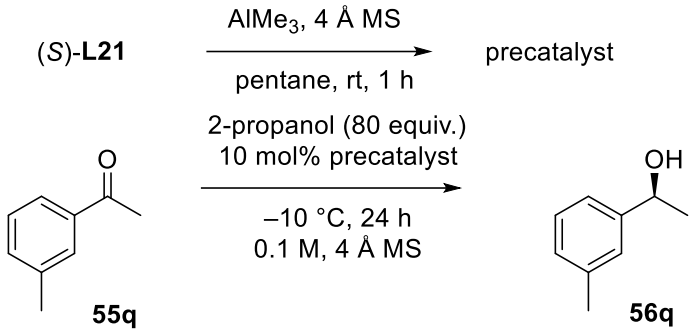

(S)-1-(3-methylphenyl)ethanol **56q**: Ketone **55q** was reduced according to procedure A with 10 mol% precatalyst made from (*S*)-**L21**. Purification of the crude product by silica gel chromatography (15 mm × 200 mm column, 5:1 hexanes/ EtOAc as eluent) afforded pure alcohol **56q** as a colorless oil in 82% isolated yield (27.8 mg, 0.20 mmol); The optical purity of **56q** was determined to be 90% *ee* by HPLC (CHIRALCEL® OD-H column, 98:2 hexanes/2-propanol at 210 nm, flow-rate: 1.0 mL/min); retention times: R_t = 9.0 min (minor enantiomer, *ent*-**56q**) and R_t = 12.4 min (major enantiomer, **56q**). Each enantiomer was obtained and confirmed by reducing the ketone with sodium borohydride in methanol.

Spectral data for **56q**: R_f = 0.17 (CH_2Cl_2); $[\alpha]_D^{20}$ = -35.9 (*c*=1.0 in $CHCl_3$) 90% *ee* (*S*) (lit.[15] $[\alpha]_D^{25}$ = -29.2 (*c*=0.5 in EtOH) 74% *ee* (*S*)). ^{1}H NMR (500 MHz, $CDCl_3$) δ = 1.50 (d, *J* = 6.5, 3H), 2.06 (s, 1H), 2.38 (d, *J* = 0.7, 3H), 4.87 (q, *J* = 6.5, 1H), 7.11 (ddt, *J* = 7.4, 1.8, 0.9, 1H), 7.15 – 7.22 (m, 2H), 7.26 (t, *J* = 7.5, 1H); ^{13}C NMR (126 MHz, $CDCl_3$) δ = 21.49, 25.13, 70.41, 122.44, 126.11, 128.21, 128.41, 138.15, 145.80. These spectral data match those previously reported for this compound.[15]

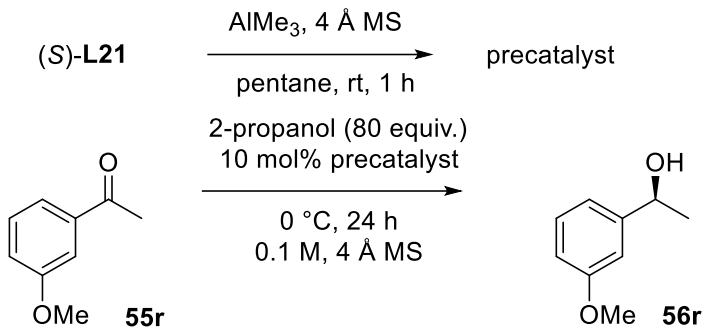

(S)-1-(3-methoxyphenyl)ethanol **56r**: Ketone **55r** was reduced according to procedure A at 0 ˚C with 10 mol% precatalyst made from (*S*)-**L21**. Purification of the crude product by silica gel chromatography (15 mm × 200 mm column, 5:1 hexanes/ EtOAc as eluent) afforded pure alcohol **56r** as a colorless oil in 84% isolated yield (32.0 mg, 0.21 mmol); The optical purity of **56r** was determined to be 88% *ee* by HPLC (CHIRALCEL® OD-H column, 98:2 hexanes/2-propanol at 210 nm, flow-rate: 1.0 mL/min); retention times: R_t = 18.6 min (minor enantiomer, *ent*-**56r**) and R_t = 24.1 min (major enantiomer, **56r**). Racemic product was prepared from reducing the ketone with sodium borohydride in methanol. Purification of the crude racemic product was the same as it for enantioenriched product. HPLC for racemic product was obtained. Each enantiomer was confirmed by comparing the retention time with racemic product under same HPLC conditions.

Spectral data for **56r**: R_f = 0.18 (CH_2Cl_2); $[\alpha]_D^{20}$ = -40.1 (*c*=1.0 in $CHCl_3$) 88% *ee* (*S*) (lit.[13] $[\alpha]_D^{22}$ = +38.1 (*c*=1.0 in $CHCl_3$) 96% *ee* (*R*)). ^{1}H NMR (500 MHz, $CDCl_3$) δ = 1.49 (d, *J* = 6.4, 3H), 2.06 (s, 1H), 3.82 (s, 3H), 4.87 (q, *J* = 6.5, 1H), 6.82 (ddd, *J* = 8.2, 2.5, 1.1, 1H), 6.93 – 6.97 (m, 2H), 7.27 (t, *J* = 8.1, 1H); ^{13}C NMR (126 MHz, $CDCl_3$) δ = 25.15, 55.22, 70.32, 110.88, 112.86, 117.68, 129.53, 147.60, 159.74. These spectral data match those previously reported for this compound.[13]

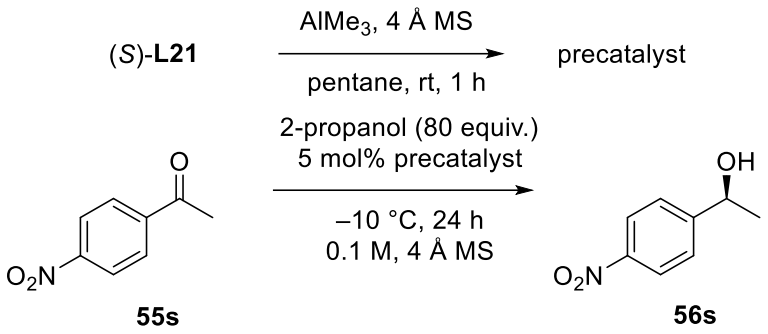

55s **56s**

(S)-1-(4-nitrophenyl)ethanol **56s**: Ketone **55s** was reduced according to procedure A with (*S*)-**L21**. Purification of the crude product by silica gel chromatography (15 mm × 200 mm column, 5:1 hexanes/ EtOAc as eluent) afforded pure alcohol **56s** as a colorless oil in 92% isolated yield (38.5 mg, 0.23 mmol); The optical purity of **56s** was determined to be 97% *ee* by HPLC (CHIRALPAK® AS-H column, 90:10 hexanes/2-propanol at 254 nm, flow-rate: 1.0 mL/min); retention times: R_t = 18.6 min (minor enantiomer, *ent*-**56s**) and R_t = 21.5 min (major enantiomer, **56s**). Racemic product was prepared from reducing the ketone with sodium borohydride in methanol. Purification of the crude racemic product was the same as it for enantioenriched product. HPLC for racemic product was obtained. Each enantiomer was confirmed by comparing the retention time with racemic product under same HPLC conditions.

Spectral data for **56s**: R_f = 0.15 (CH_2Cl_2); $[\alpha]_D^{20}$ = -31.8 (*c*=1.0 in $CHCl_3$) 97% *ee* (*S*) (lit.[8] $[\alpha]_D^{20}$ = +27.1 (*c*=2.2 in CH_2Cl_2) 98% *ee* (*R*)). ^{1}H NMR (500 MHz, $CDCl_3$) δ = 1.52 (d, *J* = 6.5, 3H), 2.04 – 2.25 (m, 1H), 5.02 (q, *J* = 6.5, 1H), 7.49 – 7.59 (m, 2H), 8.17 – 8.24 (m, 2H); ^{13}C NMR (126 MHz, $CDCl_3$) δ = 25.52, 69.50, 123.76, 126.12, 147.13, 153.09. These spectral data match those previously reported for this compound.[8]

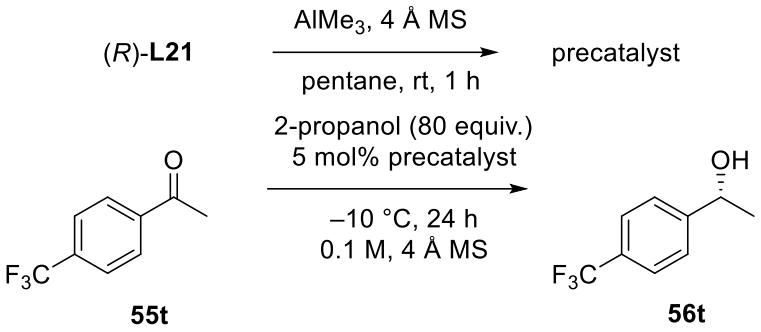

(R)-1-(4-trifluoromethylphenyl)ethanol **56t**: Ketone **55t** was reduced according to procedure A. Purification of the crude product by silica gel chromatography (15 mm × 200 mm column, 5:1 hexanes/ EtOAc as eluent) afforded pure alcohol **56t** as a colorless oil in 91% isolated yield (43.2 mg, 0.23 mmol); The optical purity of **56t** was determined to be 97% *ee* by HPLC (CHIRALCEL® OJ-H column, 99:1 hexanes/2-propanol at 210 nm, flow-rate: 1.0 mL/min); retention times: R_t = 20.3 min (minor enantiomer, *ent*-**56t**) and R_t = 22.7 min (major enantiomer, **56t**). Racemic product was prepared from reducing the ketone with sodium borohydride in methanol. Purification of the crude racemic product was the same as it for enantioenriched product. HPLC for racemic product was obtained. Each enantiomer was confirmed by comparing the retention time with racemic product under same HPLC conditions.

Spectral data for **56t**: R_f = 0.16 (CH_2Cl_2); $[\alpha]_D^{20}$ = +25.4 (*c*=1.0 in $CHCl_3$) 97% *ee* (*R*) (lit.[13] $[\alpha]_D^{26}$ = +17.9 (*c*=0.5 in $CHCl_3$) 94% *ee* (*R*)). ^{1}H NMR (500 MHz, $CDCl_3$) δ = 1.50 (d, *J* = 6.5, 3H), 2.23 (s, 1H), 4.95 (q, *J* = 6.5, 1H), 7.45 – 7.51 (m, 2H), 7.58 – 7.63 (m, 2H); ^{13}C NMR (126 MHz, $CDCl_3$) δ = 25.35, 69.80, 124.14 (q, *J* = 273), 125.42 (q, *J* = 3.8), 125.63, 129.58 (q, *J* = 32.4), 149.66. These spectral data match those previously reported for this compound.[13]

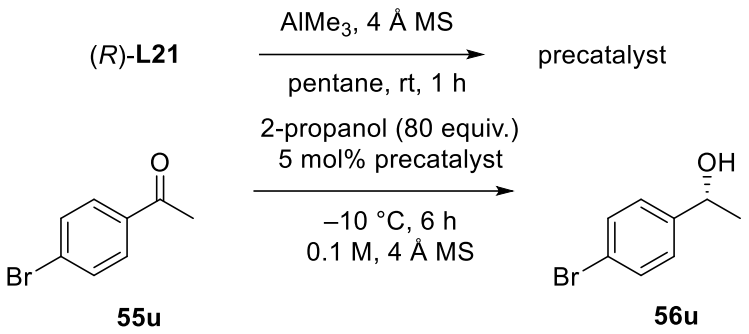

55u **56u**

(R)-1-(4-bromophenyl)ethanol **56u**: Ketone **55u** was reduced according to procedure A after 6 hours. Purification of the crude product by silica gel chromatography (15 mm × 200 mm column, 5:1 hexanes/ EtOAc as eluent) afforded pure alcohol **56u** as a colorless oil in 94% isolated yield (47.0 mg, 0.23 mmol); The optical purity of **56u** was determined to be 96% *ee* by HPLC (CHIRALCEL® OD-H column, 99:1 hexanes/2-propanol at 210 nm, flow-rate: 1.0 mL/min); retention times: R_t = 16.9 min (minor enantiomer, *ent*-**56u**) and R_t = 18.7 min (major enantiomer, **56u**). Racemic product was prepared from reducing the ketone with sodium borohydride in methanol. Purification of the crude racemic product was the same as it for enantioenriched product. HPLC for racemic product was obtained. Each enantiomer was confirmed by comparing the retention time with racemic product under same HPLC conditions.

Spectral data for **56u**: R_f = 0.17 (CH_2Cl_2); $[\alpha]_D^{20}$ = +35.1 (*c*=1.0 in $CHCl_3$) 96% *ee* (*R*) (lit.[8] $[\alpha]_D^{20}$ = +36.0 (*c*=1.7 in CH_2Cl_2) 95% *ee* (*R*)). ^{1}H NMR (500 MHz, $CDCl_3$) δ = 1.45 (dd, *J* = 6.5, 1.0, 3H), 2.20 (s, 1H), 4.84 (q, *J* = 6.4, 1H), 7.23 (d, *J* = 8.1, 2H), 7.46 (d, *J* = 7.4, 2H); ^{13}C NMR (126 MHz, $CDCl_3$) δ = 25.23, 69.73, 121.12, 127.15, 131.52, 144.76. These spectral data match those previously reported for this compound.[8]

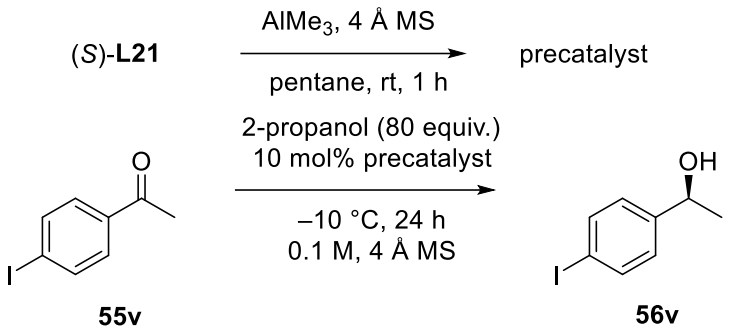

55v **56v**

(S)-1-(4-iodophenyl)ethanol **56v**: Ketone **55v** was reduced according to procedure A with 10 mol% precatalyst made from (*S*)-**L21**. Purification of the crude product by silica gel chromatography (15 mm × 200 mm column, 5:1 hexanes/ EtOAc as eluent) afforded pure alcohol **56v** as a yellow solid (m.p. 46-48 ˚C) in 89% isolated yield (54.9 mg, 0.22 mmol); The optical purity of **56v** was determined to be 93% *ee* by HPLC (CHIRALCEL® OD-H column, 98:2 hexanes/2-propanol at 220 nm, flow-rate: 0.8 mL/min); retention times: R_t = 14.7 min (major enantiomer, **56v**) and R_t = 15.6 min (minor enantiomer, *ent*-**56v**). Racemic product was prepared from reducing the ketone with sodium borohydride in methanol. Purification of the crude racemic product was the same as it for enantioenriched product. HPLC for racemic product was obtained. Each enantiomer was confirmed by comparing the retention time with racemic product obtained under same HPLC conditions.

Spectral data for **56v**: R_f = 0.17 (CH_2Cl_2); $[\alpha]_D^{20}$ = -37.0 (*c*=1.0 in $CHCl_3$) 93% *ee* (*S*) (lit.[12] $[\alpha]_D^{21}$ = +25.3 (*c*=0.6 in $CHCl_3$) 99% *ee* (*R*)). ^{1}H NMR (500 MHz, $CDCl_3$) δ = 1.47 (dd, *J* = 6.6, 1.4, 3H), 1.94 (s, 1H), 4.85 (d, *J* = 6.4, 1H), 7.13 (dd, *J* = 8.3, 1.6, 2H), 7.68 (dd, *J* = 8.3, 1.5, 2H); ^{13}C NMR (126 MHz, $CDCl_3$) δ = 25.25,

69.85, 92.73, 127.41, 137.52, 145.44. These spectral data match those previously reported for this compound.[16]

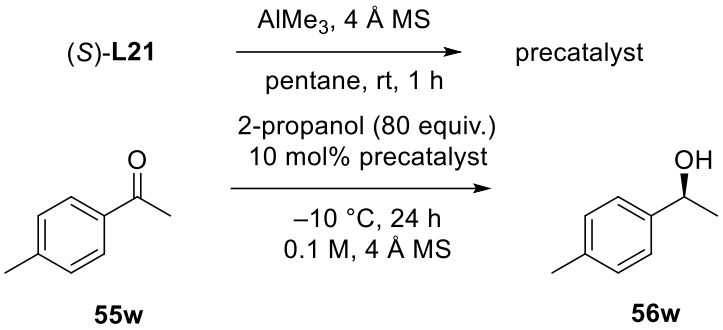

(S)-1-(4-methylphenyl)ethanol **56w**: Ketone **55w** was reduced according to procedure A with 10 mol% precatalyst made from (*S*)-**L21**. Purification of the crude product by silica gel chromatography (15 mm × 200 mm column, 5:1 hexanes/ EtOAc as eluent) afforded pure alcohol **56w** as a colorless oil in 70% isolated yield (23.7 mg, 0.17 mmol); The optical purity of **56w** was determined to be 92% *ee* by HPLC (CHIRALCEL® OJ-H column, 95:5 hexanes/2-propanol at 210 nm, flow-rate: 1.0 mL/min); retention times: R_t = 10.2 min (major enantiomer, **56w**) and R_t = 12.5 min (minor enantiomer, *ent*-**56w**). Racemic product was prepared from reducing the ketone with sodium borohydride in methanol. Purification of the crude racemic product was the same as it for enantioenriched product. HPLC for racemic product was obtained. Each enantiomer was confirmed by comparing the retention time with racemic product under same HPLC conditions.

Spectral data for **56w**: R_f = 0.17 (CH_2Cl_2); $[\alpha]_D^{20}$ = -42.3 (*c*=1.0 in $CHCl_3$) 92% *ee* (*S*) (lit.[16] $[\alpha]_D^{20}$ = -33.4 (*c*=1.0 in EtOH) 81% *ee* (*S*)). ^{1}H NMR (500 MHz, $CDCl_3$) δ = 1.49 (d, *J* = 6.6, 3H), 2.40 (s, 3H), 2.62 (s, 1H), 4.84 (d, *J* = 6.5, 1H), 7.19 (d, *J* = 7.9, 2H), 7.28 (d, *J* = 7.9, 2H); ^{13}C NMR (126 MHz, $CDCl_3$) δ = 21.15,

25.14, 70.11, 125.43, 129.13, 137.00, 143.02. These spectral data match those previously reported for this compound.[16]

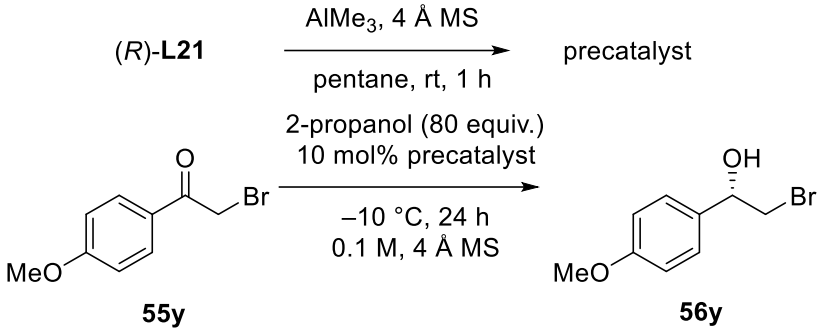

(S)-2-bromo-1-(4-methoxyphenyl)ethanol **56y**: Ketone **55y** was reduced according to procedure A with 10 mol% precatalyst. Purification of the crude product by silica gel chromatography (15 mm × 200 mm column, 5:1 hexanes/ EtOAc as eluent) afforded pure alcohol **56y** as a colorless oil in 71% isolated yield (40.8 mg, 0.18 mmol); The optical purity of **56y** was determined to be 83% *ee* by HPLC (CHIRALCEL® OD-H column, 95:5 hexanes/2-propanol at 210 nm, flow-rate: 1.0 mL/min); retention times: R_t = 9.6 min (minor enantiomer, *ent*-**56y**) and R_t = 11.9 min (major enantiomer, **56y**). Racemic product was prepared from reducing the ketone with sodium borohydride in methanol. Purification of the crude racemic product was the same as it for enantioenriched product. HPLC for racemic product was obtained. Each enantiomer was confirmed by comparing the retention time with racemic product under same HPLC conditions.

Spectral data for **56y**: R_f = 0.17 (CH_2Cl_2); $[\alpha]_D^{20}$ = +26.6 (*c*=1.0 in $CHCl_3$) 83% *ee* (*S*) (lit.[6] $[\alpha]_D^{23}$ = +36.7 (*c*=1.0 in $CHCl_3$) 98% *ee* (*S*)). ^{1}H NMR (500 MHz, $CDCl_3$) δ = 2.64 (s, 1H), 3.53 (dd, *J* = 10.4, 9.0, 1H), 3.60 (dd, *J* = 10.4, 3.5, 1H), 3.81 (s, 3H), 4.88 (dd, *J* = 9.0, 3.4, 1H), 6.88 – 6.93 (m, 2H), 7.28 – 7.34 (m, 2H);

^{13}C NMR (126 MHz, $CDCl_3$) δ = 40.29, 55.31, 73.46, 114.05, 127.23, 132.39, 159.65. These spectral data match those previously reported for this compound.[6]

4.2.2 General procedure for catalytic asymmetric MPV reduction of aliphatic ketones

Procedure B — illustrated for 1-adamantyl methyl ketone **57c**

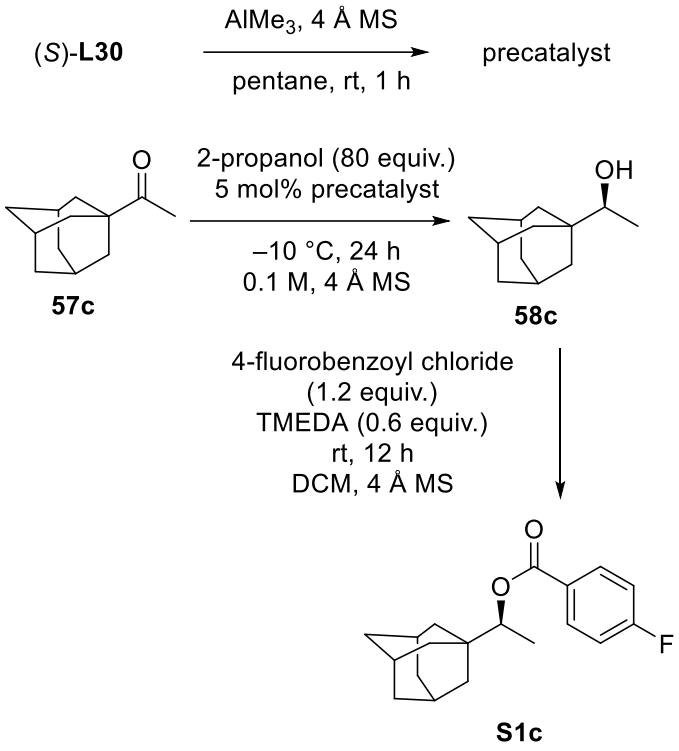

(S)-1-(1-adamantyl)ethyl 4-fluorobenzoate **S1c**: To a 5 mL flame-dried round bottom flask equipped with a stir bar was charged (*S*)-**L30** ((*S*)-**7,7'-*i*Pentyl$_2$VANOL**, 9.4 mg, 0.01625 mmol), 4 Å molecular sieves (25.0 mg, activated), and dry pentane (1 mL). Then a rubber septum stopper and argon balloon were attached. While stirring at room temperature, trimethylaluminum solution (6.2 µl, 0.0125 mmol, 2 M in toluene) was added to the reaction flask. After 1 hour, the flask containing the precatalyst was charged with dry 2-propanol (1.5

mL, 20 mmol) and chilled to –10 ˚C. To the mixture was added 1-adamantyl methyl ketone **57c** (44.6 mg, 0.25 mmol) and the resulting mixture was stirred for 24 hours at –10 ˚C. The reaction was quenched by the addition of 2 M HCl (1 mL) and then was warmed to room temperature. The mixture was transferred into a 60 mL separatory funnel and added 15 mL water before extracted with CH_2Cl_2 (15 mL × 3). Combined organic layer was concentrated under vacuum to afford the crude product. Purification of the crude product by silica gel chromatography (15 mm × 200 mm column, 5:1 hexanes/ EtOAc as eluent) afforded pure alcohol **58c**. Then to another 5 mL flame-dried round bottom flask equipped with a stir bar was charged **58c**, 4 Å molecular sieves (50.0 mg, activated), TMEDA ((22.5 µl, 0.15 mmol) and dry CH_2Cl_2 (2.5 mL). Then a rubber septum stopper and argon balloon were attached. While stirring at room temperature, 4-fluorobenzoyl chloride (35.5 µl, 0.3 mmol) was added to the reaction flask. The reaction mixture was stirred for 12 h at room temperature before quenched by 2 mL water. The mixture was transferred into a 60 mL separatory funnel and added 15 mL water before extracted with CH_2Cl_2 (15 mL × 3). Combined organic layer was concentrated under vacuum to afford the crude product. Purification of the crude product by silica gel chromatography (15 mm × 200 mm column, hexanes as eluent) afforded pure chiral ester **S1c** as a colorless oil in 84% yield over two steps (63.3 mg, 0.21 mmol). The optical purity of **S1c** was determined to be 94% *ee* by HPLC (CHIRALPAK® IA column, 100% hexanes at 220 nm, flow-rate: 1.0 mL/min); retention times: R_t = 12.7 min (minor enantiomer, *ent*-**S1c**) and R_t = 13.8 min (major enantiomer, **S1c**).

Each enantiomer was obtained and confirmed by reducing the ketone with sodium borohydride in methanol followed by making its 4-fluorobenzoate derivative.

Spectral data for **S1c**: R_f = 0.30 (hexanes); $[\alpha]_D^{20}$ = +38.9 (*c*=1.0 in $CHCl_3$) 94% *ee* (*S*); ^{1}H NMR (500 MHz, $CDCl_3$) δ = 1.23 (d, *J* = 6.5, 3H), 1.59 – 1.69 (m, 9H), 1.71 – 1.79 (m, 3H), 1.98 – 2.06 (m, 3H), 4.78 (d, *J* = 6.5, 1H), 7.10 – 7.15 (m, 2H), 8.03 – 8.12 (m, 2H); ^{13}C NMR (126 MHz, $CDCl_3$) δ = 13.51, 28.18, 36.15, 37.09, 38.05, 78.62, 115.43 (d, *J* = 21.9), 127.20 (d, *J* = 2.9), 132.01 (d, *J* = 9.1), 165.25, 165.60 (d, *J* = 253.26); IR (NaCl): $\tilde{\nu}$=2904 (s), 1715 (s), 1276 (s) cm^{-1}; HRMS (ESI-TOF) *m/z* 325.1581 [(M-Na^+); calcd. for $C_{19}H_{23}FNaO_2$: 325.1580].

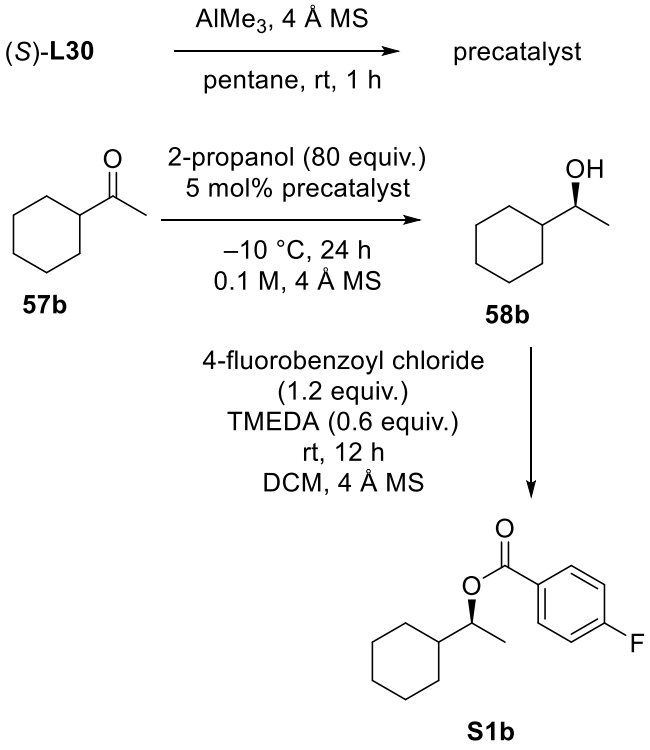

(S)-1-cyclohexylethyl 4-fluorobenzoate **S1b**: Crude chiral ester **S1b** was achieved according to procedure B. Purification of the crude product by silica gel chromatography (15 mm × 200 mm column, hexanes as eluent) afforded pure

chiral ester **S1b** as a colorless oil in 81% yield over two steps (50.4 mg, 0.20 mmol). The optical purity of **S1b** was determined to be 88% *ee* by HPLC (CHIRALPAK® IA column, 99.9:0.1 hexanes/2-propanol at 220 nm, flow-rate: 1.0 mL/min); retention times: R_t = 9.4 min (minor enantiomer, *ent*-**S1b**) and R_t = 10.0 min (major enantiomer, **S1b**). Each enantiomer was obtained and confirmed by reducing the ketone with sodium borohydride in methanol followed by making its 4-fluorobenzoate derivative.

Spectral data for **S1b**: R_f = 0.30 (hexanes); $[\alpha]_D^{20}$ = +21.5 (*c*=1.0 in $CHCl_3$) 88% *ee* (*S*); ^{1}H NMR (500 MHz, $CDCl_3$) δ = 0.99 – 1.25 (m, 5H), 1.27 (d, *J* = 6.4, 3H), 1.51 – 1.61 (m, 1H), 1.61 – 1.87 (m, 5H), 4.96 (t, *J* = 6.3, 1H), 7.04 – 7.13 (m, 2H), 8.01 – 8.08 (m, 2H); ^{13}C NMR (126 MHz, $CDCl_3$) δ = 17.07, 26.01, 26.04, 26.37, 28.44, 28.65, 42.74, 75.39, 115.31 (d, *J* = 21.9), 127.14 (d, *J* = 2.9), 131.97 (d, *J* = 9.4), 165.10, 165.58 (d, *J* = 253.26); IR (NaCl): $\tilde{\nu}$=2926 (s), 2852 (s), 1716 (s), 1603 (s), 1275 (s), 1237 (s) cm^{-1}; HRMS (ESI-TOF) *m/z* 273.1265 [(M-Na$^+$); calcd. for $C_{15}H_{13}FNaO_2$: 273.1267].

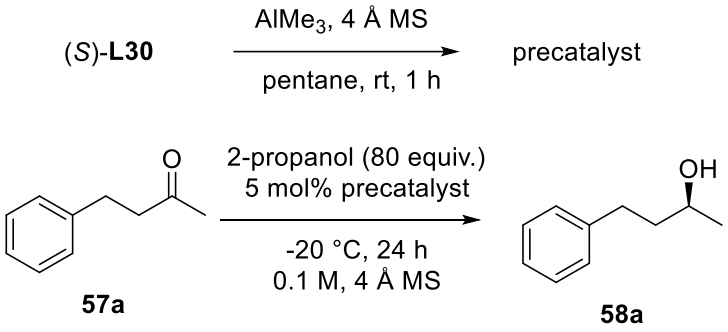

(S)-4-phenyl-butan-2-ol **58a**: Ketone **57a** was reduced according to procedure A at 0 ˚C with precatalyst made from (*S*)-**L30**. Purification of the crude product by silica gel chromatography (15 mm × 200 mm column, 5:1 hexanes/

EtOAc as eluent) afforded pure alcohol **58a** as a colorless oil in 91% isolated yield (34.0 mg, 0.23 mmol); The optical purity of **58a** was determined to be 82% *ee* by HPLC (CHIRALCEL® OD-H column, 97:3 hexanes/2-propanol at 210 nm, flow-rate: 1.0 mL/min); retention times: R_t = 8.8 min (minor enantiomer, *ent*-**58a**) and R_t = 13.8 min (major enantiomer, **58a**). Each enantiomer was obtained and confirmed by reducing the ketone with sodium borohydride in methanol.

Spectral data for **58a**: R_f = 0.16 (CH_2Cl_2); $[\alpha]_D^{20}$ = +20.4 (*c*=1.0 in $CHCl_3$) 82% *ee* (*S*) (lit.[18] $[\alpha]_D^{25}$ = +7.9 (*c*=1.0 in $CHCl_3$) 33% *ee* (*S*)). ^{1}H NMR (500 MHz, $CDCl_3$) δ = 1.25 (d, *J* = 6.2, 3H), 1.61 (s, 1H), 1.79 (m, 2H), 2.70 (dd, *J* = 9.4, 6.9, 1H), 2.76 (dd, *J* = 9.5, 6.1, 1H), 3.79 – 3.90 (m, 1H), 7.17 – 7.25 (m, 3H), 7.31 (td, *J* = 7.3, 1.4, 2H); ^{13}C NMR (126 MHz, $CDCl_3$) δ = 23.64, 32.15, 40.85, 67.53, 125.83, 128.41, 142.06 (one sp^2 carbon not located). These spectral data match those previously reported for this compound.[18]

4.2.3 Procedure for gram scale synthesis

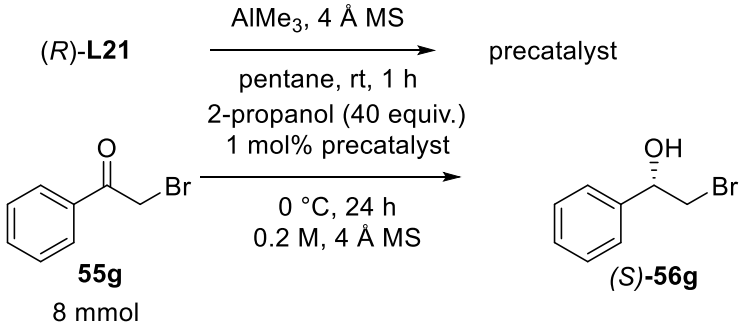

(S)-2-bromo-1-phenylethanol (S)-**56g**: To a 100 mL flame-dried round bottom flask equipped with a stir bar was charged (*R*)-**L21** ((*R*)-**7,7'-Cy$_2$VANOL**, 62.7 mg, 0.104 mmol), 4 Å molecular sieves (800 mg, activated), and dry pentane (16 mL). Then a rubber septum stopper and argon balloon were attached. While

stirring at room temperature, trimethylaluminum solution (40 µl, 0.08 mmol, 2 M in toluene) was added to the reaction flask. After 1 hour, the flask containing the precatalyst was charged with dry 2-propanol (24 mL, 320 mmol) and chilled to 0 ˚C. To the mixture was added 2-bromoacetophenone **55g** (1.59 g, 8 mmol) and the resulting mixture was stirred for 24 hours at 0 ˚C. The reaction was quenched by the addition of 2 M HCl (30 mL) and then was warmed to room temperature. The mixture was transferred into a 250 mL separatory funnel and added 30 mL water before extracted with CH_2Cl_2 (60 mL × 3). Combined organic layer was concentrated under vacuum to afford the crude product. Purification of the crude product by silica gel chromatography (30 mm × 200 mm column, 5:1 hexanes/ EtOAc as eluent) afforded pure alcohol (*S*)-**56g** as a pale yellow oil in 90% isolated yield (1.44 g, 7.2 mmol); The optical purity of (*S*)-**56g** was determined to be 97% *ee* by HPLC (CHIRALCEL® OD-H column, 98:2 hexanes/2-propanol at 210 nm, flow-rate: 1 mL/min); retention times: R_t = 12.9 min (major enantiomer, (*S*)-**56g**) and R_t = 16.1 min (minor enantiomer, (*R*)-**56g**). Spectral data for (*S*)-**56g**: $[\alpha]_D^{20}$ = +37.4 (*c*=1.0 in $CHCl_3$) 97% *ee* (*S*) (lit.[8] $[\alpha]_D^{20}$ = +42.3 (*c*=1.5 in CH_2Cl_2) 97% *ee* (*S*)); NMR spectra are the same as its enantiomer (*R*)-**56g**.

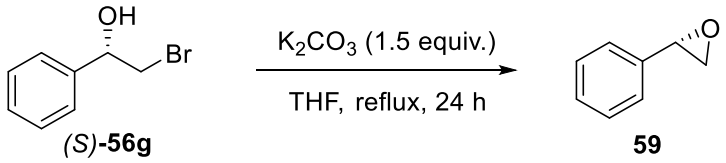

(S)-**56g** **59**

(S)-styrene oxide **59**: To a 100 mL flame-dried round bottom flask equipped with a stir bar was added *(S)*-**56g** (1.44 g, 7.2 mmol), anhydrous potassium carbonate (1.49 g, 10.8 mmol) and dry THF (40 mL). Then an oven-dried

condenser was attached and the mixture was refluxed and stirred for 24 hours in an oil bath that was set to 75˚C. Then the reaction was cooled to room temperature and added 50 mL water. The mixture was transferred into a 250 mL separatory funnel and was extracted with diethyl ether (60 mL × 3). Combined organic layer was concentrated under vacuum to afford the crude product. Purification of the crude product by silica gel chromatography (30 mm × 200 mm column, 10:1 hexanes/ EtOAc as eluent) afforded pure epoxide **59** as a colorless oil in 86% isolated yield (0.75 g, 6.2 mmol); The optical purity of **59** was determined to be 97% *ee* by HPLC (CHIRALCEL® OD-H column, 99.9:0.1 hexanes/2-propanol at 210 nm, flow-rate: 1 mL/min); retention times: R_t = 8.1 min (major enantiomer, **59**) and R_t = 8.9 min (minor enantiomer, *ent*-**59**).

Spectral data for **59**: R_f = 0.6 (CH_2Cl_2); $[\alpha]_D^{20}$ = +25.7 (*c*=1.0 in $CHCl_3$) 97% *ee* (*S*) (lit.[19] $[\alpha]_D^{21}$ = -24 (*c*=1.0 in $CHCl_3$) >99% *ee* (*R*)). ^{1}H NMR (500 MHz, $CDCl_3$) δ = 2.82 (dd, *J* = 5.5, 2.6, 1H), 3.15 (dd, *J* = 5.5, 4.1, 1H), 3.89 (dd, *J* = 4.1, 2.5, 1H), 7.31 – 7.43 (m, 5H); ^{13}C NMR (126 MHz, $CDCl_3$) δ = 51.23, 52.36, 125.58, 128.23, 128.56, 137.75. These spectral data match those previously reported for this compound.[19]

4.2.4 Procedure for resolution of racemic alcohols

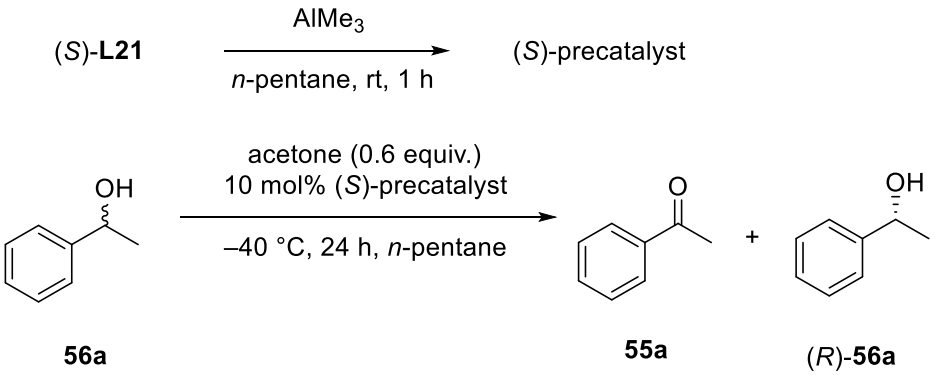

Procedure C — Oxidative kinetic resolution of racemic **56a**

(R)-1-phenylethanol **56a**: To a 5 mL flame-dried round bottom flask equipped with a stir bar was charged (*S*)-**L21** ((*S*)-**7,7'-Cy$_2$VANOL**, 19.6 mg, 0.0325 mmol), and dry pentane (2.5 mL). Then a rubber septum stopper and argon balloon were attached. While stirring at room temperature, trimethylaluminum solution (12.4 µl, 0.025 mmol, 2 M in toluene) was added to the reaction flask. After 1 hour, the flask containing the precatalyst was charged with racemic **56a** (0.25 mmol, 30.2 µl) and chilled to –40 ˚C. To the mixture was added acetone (11 µl, 0.15 mmol) via micro-syringe and the resulting mixture was stirred for 24 hours at –40 ˚C. The reaction was quenched by the addition of 2 M HCl (1 mL) and then was warmed to room temperature. The mixture was transferred into a 60 mL separatory funnel and added 15 mL water before extracted with CH_2Cl_2 (15 mL × 3). Combined organic layer was concentrated under vacuum to afford the crude product. Triphenylmethane was added as internal standard to determine NMR yield and 46% **56a** with 54% **55a** was observed. The optical purity of **56a** was determined to be 83% *ee* by HPLC (CHIRALCEL® OD-H column, 99:1 hexanes/2-propanol at 210 nm, flow-rate: 1 mL/min); retention times: R_t = 16.7 min (major enantiomer, **56a**) and R_t = 24.0 min (minor enantiomer, (*S*)-**56a**).

Procedure D — Formal dynamic kinetic resolution of racemic **56a**

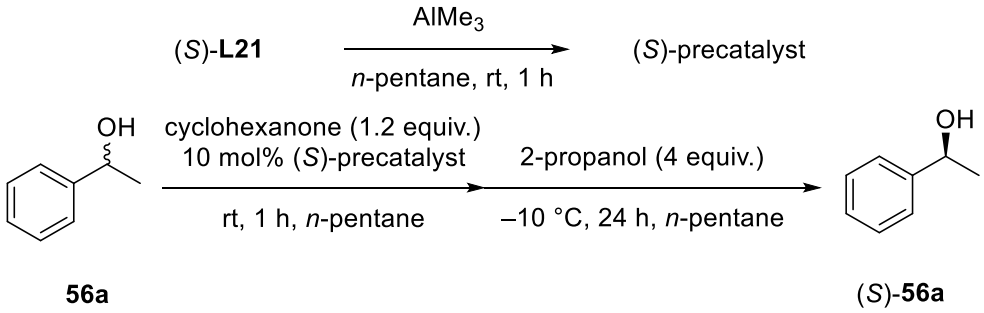

(S)-1-phenylethanol (*S*)-**56a**: To a 5 mL flame-dried round bottom flask equipped with a stir bar was charged (*S*)-**L21** ((*S*)-**7,7'-Cy$_2$VANOL**, 19.6 mg, 0.0325 mmol), and dry pentane (2.5 mL). Then a rubber septum stopper and argon balloon were attached. While stirring at room temperature, trimethylaluminum solution (12.4 µl, 0.025 mmol, 2 M in toluene) was added to the reaction flask. After 1 hour, the flask containing the precatalyst was charged with racemic **56a** (0.25 mmol, 30.2 µl). To the mixture was added cyclohexanone (31 µl, 0.3 mmol) via micro-syringe and the resulting mixture was stirred for 1 hour at room temperature. The reaction mixture was then chilled to –10 ˚C and charged with 2-propanol (1 mmol, 76.6 µl). After stirring for 24 hours the reaction was quenched by the addition of 2 M HCl (1 mL) and then was warmed to room temperature. The mixture was transferred into a 60 mL separatory funnel and added 15 mL water before extracted with CH_2Cl_2 (15 mL × 3). Combined organic layer was concentrated under vacuum to afford the crude product. Triphenylmethane was added as internal standard to determine NMR yield and 79% **56a** was observed. The optical purity of **56a** was determined to be 73% *ee* by HPLC (CHIRALCEL® OD-H column, 99:1 hexanes/2-propanol at 210 nm, flow-rate: 1 mL/min); retention times: R_t = 16.7 min (minor enantiomer, (*R*)-**56a**) and R_t = 24.0 min (major enantiomer, (*S*)-**56a**).

4.2.5 Computational study

Computations have been achieved with both Hartree-Fock and density functional theory in Gaussian 16[20]. Geometry optimizations were carried out at

HF/3-21G* or B3LYP/6-31G(d) level of theory in vacuum. Transition states of this asymmetric MPV reduction of acetophenone **55a** and 2-bromoacetophenone **55g** were simulated at HF/3-21G* or B3LYP/6-31G(d) level in vacuum and in three solvent: toluene, *n*-pentane and 2-propanol with CPCM as solvation method. The conformation of alkyl groups on ligands is considered. For example, two calculations (TS-R-Me and TS-S-Me) have been run for 7,7'-Me_2VANOL (**L17**), with each calculation shows the transition state towards R or S product. As for 7,7'-Et_2VANOL (**L18**), four calculations of different conformers (from the rotation of two ethyl groups) towards each product have been done. For each TS-S or TS-R, the one with lowest energy was chosen as real transition state. The free energy differences (ΔΔG) between TS-S and TS-R have been calculated (ΔΔG = ΔG(TS-R) – ΔG(TS-S)) and analyzed for 30 different ligands shown in Figure 2.3.

The simulations in the reduction of acetophenone **55a** have been achieved and analyzed in Table 4.1 to Table 4.5. Table 4.1 shows free energies calculated under HF/3-21G* level in vacuum. Table 4.2 shows free energies calculated under B3LYP/6-31G(d) level in vacuum. Table 4.3 shows free energies calculated under B3LYP/6-31G(d) level in toluene with CPCM as solvation method. Table 4.4 shows free energies calculated under B3LYP/6-31G(d) level in *n*-pentane with CPCM as solvation method. Table 4.5 shows free energies calculated under B3LYP/6-31G(d) level in 2-propanol with CPCM as solvation method. Results obtained in the reduction of 2-bromoacetophenone **55g** under HF/3-21G* level in vacuum are shown in Table 4.6.

Table 4.1 Free energy differences by HF/3-21G* in vacuum

Ligand	Product Chirality	Entry	ΔG(RHF)	ΔΔG(RHF)	ΔΔG(kcal/mol)
(*S*)-**L17**	R	TS-R-Me	-2255.211153	0.000605	0.380
	S	TS-S-Me	-2255.211758		
(*S*)-**L22**	R	TS-R-*t*Bu	-2487.951114	0.000835	0.524
	S	TS-S-*t*Bu	-2487.951949		
(*S*)-**L23**	R	TS-R-Ad	-2946.635443	0.000838	0.526
	S	TS-S-Ad	-2946.636281		
(*S*)-**L18**	R	TS-R-Et-1	-2332.792139	0.000710	0.446
		TS-R-Et-2	-2332.792139		
		TS-R-Et-3	-2332.792310		
		TS-R-Et-4	-2332.792327		
	S	TS-S-Et-1	-2332.792808		
		TS-S-Et-2	-2332.793037		
		TS-S-Et-3	-2332.792983		
		TS-S-Et-4	-2332.792761		
(*S*)-**L32**	R	TS-R-Bn-1	-2711.581502	0.000159	0.100
		TS-R-Bn-2	-2711.580483		
		TS-R-Bn-3	-2711.580790		
		TS-R-Bn-4	-2711.580155		
	S	TS-S-Bn-1	-2711.580670		
		TS-S-Bn-2	-2711.579780		
		TS-S-Bn-3	-2711.581661		
		TS-S-Bn-4	-2711.580179		
(*S*)-**L33**	R	TS-R-Ph	-2634.003988	-0.000579	-0.363
	S	TS-S-Ph	-2634.003409		
(*S*)-**L30**	R	TS-R-neoPentyl-1	-2565.535777	0.000456	0.286
		TS-R-neoPentyl-2	-2565.536868		
		TS-R-neoPentyl-3	-2565.538753		
		TS-R-neoPentyl-4	-2565.538788		
	S	TS-S-neoPentyl-1	-2565.538243		
		TS-S-neoPentyl-2	-2565.539066		
		TS-S-neoPentyl-3	-2565.539244		
		TS-S-neoPentyl-4	-2565.538515		
(*S*)-**L29**	R	TS-R-*i*Pr-1	-2410.374090	0.000900	0.565
		TS-R-*i*Pr-2	-2410.374162		
		TS-R-*i*Pr-3	-2410.373504		
		TS-R-*i*Pr-4	-2410.373289		
	S	TS-S-*i*Pr-1	-2410.374166		
		TS-S-*i*Pr-2	-2410.374991		

Table 4.1 (cont'd)

		TS-S-*i*Pr-3	-2410.375062		
		TS-S-*i*Pr-4	-2410.374707		
(*S*)-**L21**	R	TS-R-Cy-1	-2640.844051	0.001056	0.663
		TS-R-Cy-2	-2640.843954		
		TS-R-Cy-3	-2640.843195		
		TS-R-Cy-4	-2640.843615		
	S	TS-S-Cy-1	-2640.844959		
		TS-S-Cy-2	-2640.844085		
		TS-S-Cy-3	-2640.844198		
		TS-S-Cy-4	-2640.845107		
(*S*)-**L34**	R	TS-R-C1-Me-1	-2216.417358	0.000487	0.306
		TS-R-C1-Me-2	-2216.417464		
	S	TS-S-C1-Me-1	-2216.417875		
		TS-S-C1-Me-2	-2216.417951		
(*S*)-**L35**	R	TS-R-C1-*t*Bu-1	-2332.786816	0.000358	0.225
		TS-R-C1-*t*Bu-2	-2332.787942		
	S	TS-S-C1-*t*Bu-1	-2332.788300		
		TS-S-C1-*t*Bu-2	-2332.786524		
(*S*)-**L36**	R	TS-R-C1-Ph-1	-2405.814005	-0.000167	-0.105
		TS-R-C1-Ph-2	-2405.813572		
	S	TS-S-C1-Ph-1	-2405.813838		
		TS-S-C1-Ph-2	-2405.813603		
(*S*)-**L37**	R	TS-R-C1-Ad-1	-2562.129565	0.001682	1.055
		TS-R-C1-Ad-2	-2562.129534		
	S	TS-S-C1-Ad-1	-2562.131247		
		TS-S-C1-Ad-2	-2562.129082		
(*S*)-**L38**	R	TS-R-C1-MeOBu-1	-2445.997050	0.004531	2.843
		TS-R-C1-MeOBu-2	-2445.993660		
	S	TS-S-C1-MeOBu-1	-2446.001581		
		TS-S-C1-MeOBu-2	-2445.998230		
(*S*)-**L39**	R	TS-R-C1-MeOPr-1	-2407.207266	0.000264	0.166
		TS-R-C1-MeOPr-2	-2407.213316		
	S	TS-S-C1-MeOPr-1	-2407.213580		
		TS-S-C1-MeOPr-2	-2407.207851		
(*S*)-**L40**	R	TS-R-C1-CF_3Pr-1	-2627.813318	-0.000324	-0.203
		TS-R-C1-CF_3Pr-2	-2627.819638		
	S	TS-S-C1-CF_3Pr-1	-2627.819314		
		TS-S-C1-CF_3Pr-2	-2627.807782		
(*S*)-**L5**	R	TS-R-VANOL	-2177.623669	0.000393	0.247
	S	TS-S-VANOL	-2177.624062		

Table 4.1 (cont'd)

(*S*)-**L41**	R	TS-R-8-Me	-2255.192976	-0.000199	-0.125
	S	TS-S-8-Me	-2255.192777		
(*S*)-**L14**	R	TS-R-8-Ph	-2633.973695	-0.002046	-1.284
	S	TS-S-8-Ph	-2633.971649		
(*S*)-**L42**	R	TS-R-1-Naph-1	-2937.499686	-0.000148	-0.093
		TS-R-1-Naph-2	-2937.499136		
		TS-R-1-Naph-3	-2937.497921		
		TS-R-1-Naph-4	-2937.498702		
	S	TS-S-1-Naph-1	-2937.499538		
		TS-S-1-Naph-2	-2937.498318		
		TS-S-1-Naph-3	-2937.497828		
		TS-S-1-Naph-4	-2937.498406		
(*S*)-**L43**	R	TS-R-2-Naph-1	-2937.502854	-0.000421	-0.264
		TS-R-2-Naph-2	-2937.501899		
		TS-R-2-Naph-3	-2937.501969		
		TS-R-2-Naph-4	-2937.502212		
	S	TS-S-2-Naph-1	-2937.501140		
		TS-S-2-Naph-2	-2937.502301		
		TS-S-2-Naph-3	-2937.502433		
		TS-S-2-Naph-4	-2937.502310		
(*S*)-**L44**	R	TS-R-*n*Pr-1	-2410.374073	0.000718	0.451
		TS-R-*n*Pr-2	-2410.374357		
		TS-R-*n*Pr-3	-2410.374341		
		TS-R-*n*Pr-4	-2410.374103		
	S	TS-S-*n*Pr-1	-2410.374816		
		TS-S-*n*Pr-2	-2410.375075		
		TS-S-*n*Pr-3	-2410.375018		
		TS-S-*n*Pr-4	-2410.374767		
(*S*)-**L19**	R	TS-R-*n*Bu-1	-2487.954218	0.000623	0.391
		TS-R-*n*Bu-2	-2487.954330		
		TS-R-*n*Bu-3	-2487.954445		
		TS-R-*n*Bu-4	-2487.954558		
	S	TS-S-*n*Bu-1	-2487.955168		
		TS-S-*n*Bu-2	-2487.955181		
		TS-S-*n*Bu-3	-2487.955130		
		TS-S-*n*Bu-4	-2487.955128		
(*S*)-**L45**	R	TS-R-*n*Pentyl-1	-2565.530752	0.005462	3.427
		TS-R-*n*Pentyl-2	-2565.530992		
		TS-R-*n*Pentyl-3	-2565.531206		
		TS-R-*n*Pentyl-4	-2565.531119		

Table 4.1 (cont'd)

	S	TS-S-*n*Pentyl-1	-2565.536634		
		TS-S-*n*Pentyl-2	-2565.536668		
		TS-S-*n*Pentyl-3	-2565.536618		
		TS-S-*n*Pentyl-4	-2565.536595		
(*S*)-**L20**	R	TS-R-*n*Hexyl-1	-2643.117494	0.000596	0.374
		TS-R-*n*Hexyl-2	-2643.117235		
		TS-R-*n*Hexyl-3	-2643.117417		
		TS-R-*n*Hexyl-4	-2643.117556		
	S	TS-S-*n*Hexyl-1	-2643.117694		
		TS-S-*n*Hexyl-2	-2643.118152		
		TS-S-*n*Hexyl-3	-2643.118100		
		TS-S-*n*Hexyl-4	-2643.117722		
(*S*)-**L46**	R	TS-R-*n*Heptyl-1	-2720.698949	0.000593	0.372
		TS-R-*n*Heptyl-2	-2720.698666		
		TS-R-*n*Heptyl-3	-2720.698897		
		TS-R-*n*Heptyl-4	-2720.699037		
	S	TS-S-*n*Heptyl-1	-2720.699032		
		TS-S-*n*Heptyl-2	-2720.699630		
		TS-S-*n*Heptyl-3	-2720.699580		
		TS-S-*n*Heptyl-4	-2720.699058		
(*S*)-**L47**	R	TS-R-*n*Octyl-1	-2798.280444	0.000589	0.370
		TS-R-*n*Octyl-2	-2798.280151		
		TS-R-*n*Octyl-3	-2798.280372		
		TS-R-*n*Octyl-4	-2798.280519		
	S	TS-S-*n*Octyl-1	-2798.280564		
		TS-S-*n*Octyl-2	-2798.281108		
		TS-S-*n*Octyl-3	-2798.281056		
		TS-S-*n*Octyl-4	-2798.280587		
(*S*)-**L48**	R	TS-R-PhEt-1	-2789.161667	-0.000339	-0.213
		TS-R-PhEt-2	-2789.161863		
		TS-R-PhEt-3	-2789.164844		
		TS-R-PhEt-4	-2789.164933		
	S	TS-S-PhEt-1	-2789.164490		
		TS-S-PhEt-2	-2789.164594		
		TS-S-PhEt-3	-2789.164578		
		TS-S-PhEt-4	-2789.164480		
(*S*)-**L31**	R	TS-R-PhPr-1	-2866.743832	0.000680	0.427
		TS-R-PhPr-2	-2866.743860		
		TS-R-PhPr-3	-2866.744402		
		TS-R-PhPr-4	-2866.744197		

Table 4.1 (cont'd)

	S	TS-S-PhPr-1	-2866.744368		
		TS-S-PhPr-2	-2866.744995		
		TS-S-PhPr-3	-2866.745082		
		TS-S-PhPr-4	-2866.744662		
(*S*)-**L49**	R	TS-R-*t*BuPhPr-1	-3177.069583	0.000675	0.424
		TS-R-*t*BuPhPr-2	-3177.070588		
		TS-R-*t*BuPhPr-3	-3177.071290		
		TS-R-*t*BuPhPr-4	-3177.070564		
	S	TS-S-*t*BuPhPr-1	-3177.068697		
		TS-S-*t*BuPhPr-2	-3177.071532		
		TS-S-*t*BuPhPr-3	-3177.071965		
		TS-S-*t*BuPhPr-4	-3177.068747		

Table 4.2 Free energy differences by B3LYP/6-31G(d) in vacuum

Ligand	Product Chirality	Entry	ΔG(RHF)	ΔΔG(RHF)	ΔΔG(kcal/mol)
(*S*)-**L17**	R	TS-R-Me	-2281.201529	0.000247	0.155
	S	TS-S-Me	-2281.201776		
(*S*)-**L22**	R	TS-R-*t*Bu	-2516.912733	0.001385	0.869
	S	TS-S-*t*Bu	-2516.914118		
(*S*)-**L23**	R	TS-R-Ad	—	—	—
	S	TS-S-Ad	-2981.232716		
(*S*)-**L18**	R	TS-R-Et-1	-2359.774357	0.000448	0.281
		TS-R-Et-2	-2359.774073		
		TS-R-Et-3	-2359.774408		
		TS-R-Et-4	-2359.774402		
	S	TS-S-Et-1	-2359.774601		
		TS-S-Et-2	-2359.774562		
		TS-S-Et-3	-2359.774856		
		TS-S-Et-4	-2359.774424		
(*S*)-**L32**	R	TS-R-Bn-1	-2743.152328	-0.000145	-0.091
		TS-R-Bn-2	-2743.151889		
		TS-R-Bn-3	-2743.152163		
		TS-R-Bn-4	-2743.152686		
	S	TS-S-Bn-1	-2743.151767		
		TS-S-Bn-2	-2743.150755		
		TS-S-Bn-3	-2743.152541		
		TS-S-Bn-4	-2743.151657		
(*S*)-**L33**	R	TS-R-Ph	-2664.584329	-0.000124	-0.078

Table 4.2 (cont'd)

	S	TS-S-Ph	-2664.584205		
(*S*)-**L30**	R	TS-R-neoPentyl-1	-2595.491615	0.000238	0.149
		TS-R-neoPentyl-2	-2595.492577		
		TS-R-neoPentyl-3	-2595.493731		
		TS-R-neoPentyl-4	-2595.493901		
	S	TS-S-neoPentyl-1	-2595.493030		
		TS-S-neoPentyl-2	-2595.493757		
		TS-S-neoPentyl-3	-2595.494139		
		TS-S-neoPentyl-4	-2595.493535		
(*S*)-**L29**	R	TS-R-*i*Pr-1	-2438.346964	0.001842	1.156
		TS-R-*i*Pr-2	-2438.347032		
		TS-R-*i*Pr-3	-2438.346634		
		TS-R-*i*Pr-4	-2438.346342		
	S	TS-S-*i*Pr-1	-2438.347873		
		TS-S-*i*Pr-2	-2438.347543		
		TS-S-*i*Pr-3	-2438.347079		
		TS-S-*i*Pr-4	-2438.348874		
(*S*)-**L21**	R	TS-R-Cy-1	-2671.692652	0.000658	0.413
		TS-R-Cy-2	-2671.692763		
		TS-R-Cy-3	-2671.693277		
		TS-R-Cy-4	-2671.691920		
	S	TS-S-Cy-1	-2671.692805		
		TS-S-Cy-2	-2671.693935		
		TS-S-Cy-3	-2671.692821		
		TS-S-Cy-4	-2671.693351		
(*S*)-**L34**	R	TS-R-C1-Me-1	-2241.908744	0.000076	0.048
		TS-R-C1-Me-2	-2241.908921		
	S	TS-S-C1-Me-1	-2241.908997		
		TS-S-C1-Me-2	-2241.908860		
(*S*)-**L35**	R	TS-R-C1-*t*Bu-1	-2359.764156	-0.000511	-0.321
		TS-R-C1-*t*Bu-2	-2359.765355		
	S	TS-S-C1-*t*Bu-1	-2359.764844		
		TS-S-C1-*t*Bu-2	-2359.763987		
(*S*)-**L36**	R	TS-R-C1-Ph-1	-2433.600111	-0.000120	-0.075
		TS-R-C1-Ph-2	-2433.600327		
	S	TS-S-C1-Ph-1	-2433.600207		
		TS-S-C1-Ph-2	-2433.600177		
(*S*)-**L37**	R	TS-R-C1-Ad-1	-2591.923617	0.000728	0.457
		TS-R-C1-Ad-2	-2591.924444		
	S	TS-S-C1-Ad-1	-2591.925172		

Table 4.2 (cont'd)

		TS-S-C1-Ad-2	-2591.923758		
(*S*)-**L38**	R	TS-R-C1-MeOBu-1	-2474.246716	0.000622	0.390
		TS-R-C1-MeOBu-2	-2474.251720		
	S	TS-S-C1-MeOBu-1	-2474.252342		
		TS-S-C1-MeOBu-2	-2474.248315		
(*S*)-**L39**	R	TS-R-C1-MeOPr-1	-2434.965859	-0.000023	-0.014
		TS-R-C1-MeOPr-2	-2434.968218		
	S	TS-S-C1-MeOPr-1	-2434.968195		
		TS-S-C1-MeOPr-2	-2434.962808		
(*S*)-**L40**	R	TS-R-C1-CF_3Pr-1	-2657.518576	—	—
		TS-R-C1-CF_3Pr-2	—		
	S	TS-S-C1-CF_3Pr-1	-2657.521681		
		TS-S-C1-CF_3Pr-2	—		
(*S*)-**L5**	R	TS-R-VANOL	-2202.616218	-0.000047	-0.029
	S	TS-S-VANOL	-2202.616171		
(*S*)-**L41**	R	TS-R-8-Me	-2281.183497	-0.000166	-0.104
	S	TS-S-8-Me	-2281.183331		
(*S*)-**L14**	R	TS-R-8-Ph	-2664.558154	-0.000604	-0.379
	S	TS-S-8-Ph	-2664.557550		
(*S*)-**L42**	R	TS-R-1-Naph-1	-2971.777112	-0.000556	-0.349
		TS-R-1-Naph-2	-2971.777817		
		TS-R-1-Naph-3	-2971.777229		
		TS-R-1-Naph-4	-2971.777279		
	S	TS-S-1-Naph-1	-2971.777117		
		TS-S-1-Naph-2	-2971.776351		
		TS-S-1-Naph-3	-2971.777261		
		TS-S-1-Naph-4	-2971.776480		
(*S*)-**L43**	R	TS-R-2-Naph-1	-2971.786458	-0.000312	-0.196
		TS-R-2-Naph-2	-2971.785630		
		TS-R-2-Naph-3	-2971.785407		
		TS-R-2-Naph-4	-2971.785429		
	S	TS-S-2-Naph-1	-2971.784868		
		TS-S-2-Naph-2	-2971.785838		
		TS-S-2-Naph-3	-2971.785677		
		TS-S-2-Naph-4	-2971.786146		
(*S*)-**L44**	R	TS-R-*n*Pr-1	-2438.349950	-0.000069	-0.043
		TS-R-*n*Pr-2	-2438.349695		
		TS-R-*n*Pr-3	-2438.349579		
		TS-R-*n*Pr-4	-2438.349558		
	S	TS-S-*n*Pr-1	-2438.349842		

Table 4.2 (cont'd)

		TS-S-*n*Pr-2	-2438.349761		
		TS-S-*n*Pr-3	-2438.349881		
		TS-S-*n*Pr-4	-2438.349670		
(*S*)-**L19**	R	TS-R-*n*Bu-1	-2516.922875	-0.000115	-0.072
		TS-R-*n*Bu-2	-2516.923193		
		TS-R-*n*Bu-3	-2516.922852		
		TS-R-*n*Bu-4	-2516.922945		
	S	TS-S-*n*Bu-1	-2516.923043		
		TS-S-*n*Bu-2	-2516.923059		
		TS-S-*n*Bu-3	-2516.923078		
		TS-S-*n*Bu-4	-2516.922810		
(*S*)-**L45**	R	TS-R-*n*Pentyl-1	-2595.493095	0.004560	2.861
		TS-R-*n*Pentyl-2	-2595.493562		
		TS-R-*n*Pentyl-3	-2595.493583		
		TS-R-*n*Pentyl-4	-2595.493569		
	S	TS-S-*n*Pentyl-1	-2595.497737		
		TS-S-*n*Pentyl-2	-2595.498143		
		TS-S-*n*Pentyl-3	-2595.498058		
		TS-S-*n*Pentyl-4	-2595.498005		
(*S*)-**L20**	R	TS-R-*n*Hexyl-1	-2674.072315	0.000205	0.129
		TS-R-*n*Hexyl-2	-2674.072047		
		TS-R-*n*Hexyl-3	-2674.072651		
		TS-R-*n*Hexyl-4	-2674.072073		
	S	TS-S-*n*Hexyl-1	-2674.072202		
		TS-S-*n*Hexyl-2	-2674.072464		
		TS-S-*n*Hexyl-3	-2674.072856		
		TS-S-*n*Hexyl-4	-2674.072643		
(*S*)-**L46**	R	TS-R-*n*Heptyl-1	-2752.647207	0.000090	0.056
		TS-R-*n*Heptyl-2	-2752.646947		
		TS-R-*n*Heptyl-3	-2752.647350		
		TS-R-*n*Heptyl-4	-2752.647248		
	S	TS-S-*n*Heptyl-1	-2752.646894		
		TS-S-*n*Heptyl-2	-2752.646825		
		TS-S-*n*Heptyl-3	-2752.647440		
		TS-S-*n*Heptyl-4	-2752.647273		
(*S*)-**L47**	R	TS-R-*n*Octyl-1	-2831.221979	—	—
		TS-R-*n*Octyl-2	-2831.221727		
		TS-R-*n*Octyl-3	-2831.222047		
		TS-R-*n*Octyl-4	-2831.221489		
	S	TS-S-*n*Octyl-1	-2831.221846		

Table 4.2 (cont'd)

		TS-S-*n*Octyl-2	-2831.221079		
		TS-S-*n*Octyl-3	-2831.221669		
		TS-S-*n*Octyl-4	—		
(*S*)-**L48**	R	TS-R-PhEt-1	-2821.726901	-0.000169	-0.106
		TS-R-PhEt-2	-2821.726606		
		TS-R-PhEt-3	-2821.728665		
		TS-R-PhEt-4	-2821.729016		
	S	TS-S-PhEt-1	-2821.728486		
		TS-S-PhEt-2	-2821.728741		
		TS-S-PhEt-3	-2821.728847		
		TS-S-PhEt-4	-2821.728316		
(*S*)-**L31**	R	TS-R-PhPr-1	-2900.301239	0.000624	0.392
		TS-R-PhPr-2	-2900.301334		
		TS-R-PhPr-3	-2900.301972		
		TS-R-PhPr-4	-2900.301494		
	S	TS-S-PhPr-1	-2900.302049		
		TS-S-PhPr-2	-2900.302596		
		TS-S-PhPr-3	-2900.302308		
		TS-S-PhPr-4	-2900.301638		
(*S*)-**L49**	R	TS-R-*t*BuPhPr-1	-3214.597445	0.000957	0.601
		TS-R-*t*BuPhPr-2	-3214.597961		
		TS-R-*t*BuPhPr-3	-3214.599039		
		TS-R-*t*BuPhPr-4	-3214.598773		
	S	TS-S-*t*BuPhPr-1	-3214.597683		
		TS-S-*t*BuPhPr-2	-3214.599996		
		TS-S-*t*BuPhPr-3	-3214.598511		
		TS-S-*t*BuPhPr-4	-3214.597011		

Table 4.3 Free energy differences by B3LYP/6-31G(d) in toluene

Ligand	Product Chirality	Entry	ΔG(RHF)	ΔΔG(RHF)	ΔΔG(kcal/mol)
(*S*)-**L17**	R	TS-R-Me	2281.214230	-0.000783	-0.491
	S	TS-S-Me	2281.215013		
(*S*)-**L22**	R	TS-R-*t*Bu	-2516.925171	0.001366	0.857
	S	TS-S-*t*Bu	-2516.926537		
(*S*)-**L23**	R	TS-R-Ad	2981.244895	-0.000200	-0.126
	S	TS-S-Ad	2981.245095		
(*S*)-**L18**	R	TS-R-Et-1	-2359.784395	0.000146	0.092
		TS-R-Et-2	-2359.787568		

Table 4.3 (cont'd)

		TS-R-Et-3	-2359.786967		
		TS-R-Et-4	-2359.786967		
	S	TS-S-Et-1	-2359.787714		
		TS-S-Et-2	-2359.787446		
		TS-S-Et-3	-2359.787542		
		TS-S-Et-4	-2359.787616		
(*S*)-**L32**	R	TS-R-Bn-1	-2743.166417	0.001157	0.726
		TS-R-Bn-2	-2743.166285		
		TS-R-Bn-3	-2743.167294		
		TS-R-Bn-4	-2743.166047		
	S	TS-S-Bn-1	-2743.166614		
		TS-S-Bn-2	-2743.166074		
		TS-S-Bn-3	-2743.168451		
		TS-S-Bn-4	-2743.166706		
(*S*)-**L33**	R	TS-R-Ph	2664.598548	0.000430	0.270
	S	TS-S-Ph	2664.598118		
(*S*)-**L30**	R	TS-R-neoPentyl-1	-2595.504253	0.000614	0.385
		TS-R-neoPentyl-2	-2595.504924		
		TS-R-neoPentyl-3	-2595.506634		
		TS-R-neoPentyl-4	-2595.506316		
	S	TS-S-neoPentyl-1	-2595.505509		
		TS-S-neoPentyl-2	-2595.506467		
		TS-S-neoPentyl-3	-2595.507248		
		TS-S-neoPentyl-4	-2595.506603		
(*S*)-**L29**	R	TS-R-*i*Pr-1	-2438.359932	0.000301	0.189
		TS-R-*i*Pr-2	-2438.359932		
		TS-R-*i*Pr-3	-2438.359028		
		TS-R-*i*Pr-4	-2438.358369		
	S	TS-S-*i*Pr-1	-2438.360196		
		TS-S-*i*Pr-2	-2438.360141		
		TS-S-*i*Pr-3	-2438.360233		
		TS-S-*i*Pr-4	-2438.359995		
(*S*)-**L21**	R	TS-R-Cy-1	-2671.705470	0.000610	0.383
		TS-R-Cy-2	-2671.705616		
		TS-R-Cy-3	-2671.705532		
		TS-R-Cy-4	-2671.705173		
	S	TS-S-Cy-1	-2671.705854		
		TS-S-Cy-2	-2671.706062		
		TS-S-Cy-3	-2671.706226		
		TS-S-Cy-4	-2671.706212		

Table 4.3 (cont'd)

(*S*)-**L34**	R	TS-R-C1-Me-1	-2241.921576	-0.000213	-0.134
		TS-R-C1-Me-2	-2241.922093		
	S	TS-S-C1-Me-1	-2241.921558		
		TS-S-C1-Me-2	-2241.921880		
(*S*)-**L35**	R	TS-R-C1-*t*Bu-1	-2359.776397	0.000493	0.309
		TS-R-C1-*t*Bu-2	-2359.777719		
	S	TS-S-C1-*t*Bu-1	-2359.778212		
		TS-S-C1-*t*Bu-2	-2359.776746		
(*S*)-**L36**	R	TS-R-C1-Ph-1	-2433.613310	0.000087	0.055
		TS-R-C1-Ph-2	-2433.613765		
	S	TS-S-C1-Ph-1	-2433.613852		
		TS-S-C1-Ph-2	-2433.613556		
(*S*)-**L37**	R	TS-R-C1-Ad-1	-2591.936591	0.003476	2.181
		TS-R-C1-Ad-2	-2591.937242		
	S	TS-S-C1-Ad-1	-2591.940718		
		TS-S-C1-Ad-2	-2591.937375		
(*S*)-**L38**	R	TS-R-C1-MeOBu-1	-2474.258855	-0.000675	-0.424
		TS-R-C1-MeOBu-2	-2474.266229		
	S	TS-S-C1-MeOBu-1	-2474.265554		
		TS-S-C1-MeOBu-2	-2474.261828		
(*S*)-**L39**	R	TS-R-C1-MeOPr-1	-2434.980206	0.000386	0.242
		TS-R-C1-MeOPr-2	-2434.981761		
	S	TS-S-C1-MeOPr-1	-2434.982147		
		TS-S-C1-MeOPr-2	-2434.977076		
(*S*)-**L40**	R	TS-R-C1-CF_3Pr-1	-2657.530957	—	—
		TS-R-C1-CF_3Pr-2	-2657.533534		
	S	TS-S-C1-CF_3Pr-1	-2657.533040		
		TS-S-C1-CF_3Pr-2	—		
(*S*)-**L5**	R	TS-R-VANOL	-2202.628893	—	—
	S	TS-S-VANOL	—		
(*S*)-**L41**	R	TS-R-8-Me	-2281.195397	0.000171	0.107
	S	TS-S-8-Me	-2281.195568		
(*S*)-**L14**	R	TS-R-8-Ph	-2664.570620	-0.000579	-0.363
	S	TS-S-8-Ph	-2664.570041		
(*S*)-**L42**	R	TS-R-1-Naph-1	-2971.791061	-0.000667	-0.419
		TS-R-1-Naph-2	-2971.792600		
		TS-R-1-Naph-3	-2971.791322		
		TS-R-1-Naph-4	-2971.792132		
	S	TS-S-1-Naph-1	-2971.791028		
		TS-S-1-Naph-2	-2971.791121		

Table 4.3 (cont'd)

		TS-S-1-Naph-3	-2971.791884		
		TS-S-1-Naph-4	-2971.791933		
(*S*)-**L43**	R	TS-R-2-Naph-1	-2971.801158	0.000340	0.213
		TS-R-2-Naph-2	-2971.800279		
		TS-R-2-Naph-3	-2971.799874		
		TS-R-2-Naph-4	-2971.799915		
	S	TS-S-2-Naph-1	-2971.800295		
		TS-S-2-Naph-2	-2971.800595		
		TS-S-2-Naph-3	-2971.801498		
		TS-S-2-Naph-4	-2971.800655		
(*S*)-**L44**	R	TS-R-*n*Pr-1	-2438.362346	0.000042	0.026
		TS-R-*n*Pr-2	-2438.363215		
		TS-R-*n*Pr-3	-2438.362415		
		TS-R-*n*Pr-4	-2438.362525		
	S	TS-S-*n*Pr-1	-2438.363195		
		TS-S-*n*Pr-2	-2438.363257		
		TS-S-*n*Pr-3	-2438.363162		
		TS-S-*n*Pr-4	-2438.363146		
(*S*)-**L19**	R	TS-R-*n*Bu-1	-2516.935278	0.000515	0.323
		TS-R-*n*Bu-2	-2516.935900		
		TS-R-*n*Bu-3	-2516.936046		
		TS-R-*n*Bu-4	-2516.935683		
	S	TS-S-*n*Bu-1	-2516.933723		
		TS-S-*n*Bu-2	-2516.936345		
		TS-S-*n*Bu-3	-2516.936561		
		TS-S-*n*Bu-4	-2516.936145		
(*S*)-**L45**	R	TS-R-*n*Pentyl-1	-2595.506756	0.005509	3.457
		TS-R-*n*Pentyl-2	-2595.506956		
		TS-R-*n*Pentyl-3	-2595.506692		
		TS-R-*n*Pentyl-4	-2595.506985		
	S	TS-S-*n*Pentyl-1	-2595.512494		
		TS-S-*n*Pentyl-2	-2595.511453		
		TS-S-*n*Pentyl-3	-2595.511998		
		TS-S-*n*Pentyl-4	-2595.511596		
(*S*)-**L20**	R	TS-R-*n*Hexyl-1	-2674.085453	0.000360	0.226
		TS-R-*n*Hexyl-2	-2674.084394		
		TS-R-*n*Hexyl-3	-2674.085892		
		TS-R-*n*Hexyl-4	-2674.085167		
	S	TS-S-*n*Hexyl-1	-2674.085572		
		TS-S-*n*Hexyl-2	-2674.085775		

Table 4.3 (cont'd)

		TS-S-*n*Hexyl-3	-2674.086066		
		TS-S-*n*Hexyl-4	-2674.086252		
(*S*)-**L46**	R	TS-R-*n*Heptyl-1	-2752.659741	0.001243	0.780
		TS-R-*n*Heptyl-2	-2752.659533		
		TS-R-*n*Heptyl-3	-2752.660610		
		TS-R-*n*Heptyl-4	-2752.660160		
	S	TS-S-*n*Heptyl-1	-2752.661853		
		TS-S-*n*Heptyl-2	-2752.660294		
		TS-S-*n*Heptyl-3	-2752.660488		
		TS-S-*n*Heptyl-4	-2752.658273		
(*S*)-**L47**	R	TS-R-*n*Octyl-1	-2831.234149	0.000945	0.593
		TS-R-*n*Octyl-2	-2831.234715		
		TS-R-*n*Octyl-3	-2831.235061		
		TS-R-*n*Octyl-4	-2831.234757		
	S	TS-S-*n*Octyl-1	-2831.235453		
		TS-S-*n*Octyl-2	-2831.234796		
		TS-S-*n*Octyl-3	-2831.235031		
		TS-S-*n*Octyl-4	-2831.236006		
(*S*)-**L48**	R	TS-R-PhEt-1	-2821.741654	0.000562	0.353
		TS-R-PhEt-2	-2821.741272		
		TS-R-PhEt-3	-2821.743742		
		TS-R-PhEt-4	-2821.743753		
	S	TS-S-PhEt-1	-2821.743070		
		TS-S-PhEt-2	-2821.743902		
		TS-S-PhEt-3	-2821.744315		
		TS-S-PhEt-4	-2821.743465		
(*S*)-**L31**	R	TS-R-PhPr-1	-2900.315727	0.001110	0.697
		TS-R-PhPr-2	-2900.315540		
		TS-R-PhPr-3	-2900.317363		
		TS-R-PhPr-4	-2900.317012		
	S	TS-S-PhPr-1	-2900.316758		
		TS-S-PhPr-2	-2900.318473		
		TS-S-PhPr-3	-2900.317550		
		TS-S-PhPr-4	-2900.317031		
(*S*)-**L49**	R	TS-R-*t*BuPhPr-1	—	—	—
		TS-R-*t*BuPhPr-2	-3214.613030		
		TS-R-*t*BuPhPr-3	-3214.614380		
		TS-R-*t*BuPhPr-4	-3214.614488		
	S	TS-S-*t*BuPhPr-1	-3214.613414		
		TS-S-*t*BuPhPr-2	-3214.615371		

Table 4.3 (cont'd)

		TS-S-*t*BuPhPr-3	—		
		TS-S-*t*BuPhPr-4	-3214.612298		

Table 4.4 Free energy differences by B3LYP/6-31G(d) in *n*-pentane

Ligand	Product Chirality	Entry	ΔG(RHF)	ΔΔG(RHF)	ΔΔG(kcal/mol)
(*S*)-**L17**	R	TS-R-Me	-2281.211307	0.001128	0.708
	S	TS-S-Me	-2281.212435		
(*S*)-**L22**	R	TS-R-*t*Bu	-2516.922290	0.001320	0.828
	S	TS-S-*t*Bu	-2516.923610		
(*S*)-**L23**	R	TS-R-Ad	-2981.241963	0.000243	0.152
	S	TS-S-Ad	-2981.242206		
(*S*)-**L18**	R	TS-R-Et-1	-2359.784214	0.001191	0.747
		TS-R-Et-2	-2359.783843		
		TS-R-Et-3	-2359.783979		
		TS-R-Et-4	-2359.784047		
	S	TS-S-Et-1	-2359.782509		
		TS-S-Et-2	-2359.785048		
		TS-S-Et-3	-2359.784655		
		TS-S-Et-4	-2359.785405		
(*S*)-**L32**	R	TS-R-Bn-1	-2743.163129	0.001614	1.013
		TS-R-Bn-2	-2743.162897		
		TS-R-Bn-3	-2743.163753		
		TS-R-Bn-4	-2743.162839		
	S	TS-S-Bn-1	-2743.163599		
		TS-S-Bn-2	-2743.162649		
		TS-S-Bn-3	-2743.165367		
		TS-S-Bn-4	-2743.163283		
(*S*)-**L33**	R	TS-R-Ph	-2664.595120	-0.000184	-0.115
	S	TS-S-Ph	-2664.594936		
(*S*)-**L30**	R	TS-R-neoPentyl-1	-2595.501287	0.000589	0.370
		TS-R-neoPentyl-2	-2595.501800		
		TS-R-neoPentyl-3	-2595.503676		
		TS-R-neoPentyl-4	-2595.503325		
	S	TS-S-neoPentyl-1	-2595.502576		
		TS-S-neoPentyl-2	-2595.503550		
		TS-S-neoPentyl-3	-2595.504265		
		TS-S-neoPentyl-4	-2595.503545		
(*S*)-**L29**	R	TS-R-*i*Pr-1	-2438.356874	0.000427	0.268

Table 4.4 (cont'd)

		TS-R-*i*Pr-2	-2438.357049		
		TS-R-*i*Pr-3	-2438.356160		
		TS-R-*i*Pr-4	-2438.355560		
	S	TS-S-*i*Pr-1	-2438.357230		
		TS-S-*i*Pr-2	-2438.357476		
		TS-S-*i*Pr-3	-2438.357187		
		TS-S-*i*Pr-4	-2438.357051		
(*S*)-**L21**	R	TS-R-Cy-1	-2671.702286	0.000954	0.599
		TS-R-Cy-2	-2671.702725		
		TS-R-Cy-3	-2671.702466		
		TS-R-Cy-4	-2671.701913		
	S	TS-S-Cy-1	-2671.703169		
		TS-S-Cy-2	-2671.703228		
		TS-S-Cy-3	-2671.702841		
		TS-S-Cy-4	-2671.703679		
(*S*)-**L34**	R	TS-R-C1-Me-1	-2241.918541	0.000040	0.025
		TS-R-C1-Me-2	-2241.918822		
	S	TS-S-C1-Me-1	-2241.918625		
		TS-S-C1-Me-2	-2241.918862		
(*S*)-**L35**	R	TS-R-C1-*t*Bu-1	-2359.773554	0.000464	0.291
		TS-R-C1-*t*Bu-2	-2359.774688		
	S	TS-S-C1-*t*Bu-1	-2359.775152		
		TS-S-C1-*t*Bu-2	-2359.773970		
(*S*)-**L36**	R	TS-R-C1-Ph-1	-2433.610342	0.000080	0.050
		TS-R-C1-Ph-2	-2433.610972		
	S	TS-S-C1-Ph-1	-2433.610792		
		TS-S-C1-Ph-2	-2433.611052		
(*S*)-**L37**	R	TS-R-C1-Ad-1	-2591.933613	0.001705	1.070
		TS-R-C1-Ad-2	-2591.934365		
	S	TS-S-C1-Ad-1	-2591.936070		
		TS-S-C1-Ad-2	-2591.933854		
(*S*)-**L38**	R	TS-R-C1-MeOBu-1	-2474.256147	—	—
		TS-R-C1-MeOBu-2	—		
	S	TS-S-C1-MeOBu-1	-2474.262667		
		TS-S-C1-MeOBu-2	-2474.258592		
(*S*)-**L39**	R	TS-R-C1-MeOPr-1	-2434.976793	0.000420	0.264
		TS-R-C1-MeOPr-2	-2434.978707		
	S	TS-S-C1-MeOPr-1	-2434.979127		
		TS-S-C1-MeOPr-2	-2434.973842		
(*S*)-**L40**	R	TS-R-C1-CF_3Pr-1	-2657.528269	—	—

Table 4.4 (cont'd)

		TS-R-C1-CF_3Pr-2	—		
	S	TS-S-C1-CF_3Pr-1	-2657.530560		
		TS-S-C1-CF_3Pr-2	—		
(*S*)-**L5**	R	TS-R-VANOL	-2202.625972	—	—
	S	TS-S-VANOL	—		
(*S*)-**L41**	R	TS-R-8-Me	-2281.192693	0.000197	0.124
	S	TS-S-8-Me	-2281.192890		
(*S*)-**L14**	R	TS-R-8-Ph	-2664.567693	-0.000534	-0.335
	S	TS-S-8-Ph	-2664.567159		
(*S*)-**L42**	R	TS-R-1-Naph-1	-2971.787907	-0.000559	-0.351
		TS-R-1-Naph-2	-2971.789303		
		TS-R-1-Naph-3	-2971.788331		
		TS-R-1-Naph-4	-2971.787140		
	S	TS-S-1-Naph-1	-2971.788038		
		TS-S-1-Naph-2	-2971.787518		
		TS-S-1-Naph-3	-2971.788479		
		TS-S-1-Naph-4	-2971.788744		
(*S*)-**L43**	R	TS-R-2-Naph-1	-2971.797732	-0.000063	-0.040
		TS-R-2-Naph-2	-2971.796966		
		TS-R-2-Naph-3	-2971.796616		
		TS-R-2-Naph-4	-2971.796557		
	S	TS-S-2-Naph-1	-2971.796843		
		TS-S-2-Naph-2	-2971.797245		
		TS-S-2-Naph-3	-2971.797669		
		TS-S-2-Naph-4	-2971.797310		
(*S*)-**L44**	R	TS-R-*n*Pr-1	-2438.359713	0.000412	0.259
		TS-R-*n*Pr-2	-2438.359843		
		TS-R-*n*Pr-3	-2438.359426		
		TS-R-*n*Pr-4	-2438.359560		
	S	TS-S-*n*Pr-1	-2438.359817		
		TS-S-*n*Pr-2	-2438.360115		
		TS-S-*n*Pr-3	-2438.360255		
		TS-S-*n*Pr-4	-2438.360087		
(*S*)-**L19**	R	TS-R-*n*Bu-1	-2516.932575	-0.000015	-0.009
		TS-R-*n*Bu-2	-2516.933571		
		TS-R-*n*Bu-3	-2516.932947		
		TS-R-*n*Bu-4	-2516.932634		
	S	TS-S-*n*Bu-1	-2516.933298		
		TS-S-*n*Bu-2	-2516.933384		
		TS-S-*n*Bu-3	-2516.933556		

Table 4.4 (cont'd)

		TS-S-*n*Bu-4	-2516.933153		
(*S*)-**L45**	R	TS-R-*n*Pentyl-1	-2595.503904	0.005582	3.503
		TS-R-*n*Pentyl-2	-2595.503477		
		TS-R-*n*Pentyl-3	-2595.503635		
		TS-R-*n*Pentyl-4	-2595.503762		
	S	TS-S-*n*Pentyl-1	-2595.508312		
		TS-S-*n*Pentyl-2	-2595.508313		
		TS-S-*n*Pentyl-3	-2595.508643		
		TS-S-*n*Pentyl-4	-2595.509486		
(*S*)-**L20**	R	TS-R-*n*Hexyl-1	-2674.082401	0.000781	0.490
		TS-R-*n*Hexyl-2	-2674.081509		
		TS-R-*n*Hexyl-3	-2674.082803		
		TS-R-*n*Hexyl-4	-2674.082156		
	S	TS-S-*n*Hexyl-1	-2674.083332		
		TS-S-*n*Hexyl-2	-2674.082660		
		TS-S-*n*Hexyl-3	-2674.083584		
		TS-S-*n*Hexyl-4	-2674.083290		
(*S*)-**L46**	R	TS-R-*n*Heptyl-1	-2752.658109	0.000109	0.068
		TS-R-*n*Heptyl-2	-2752.656950		
		TS-R-*n*Heptyl-3	-2752.657481		
		TS-R-*n*Heptyl-4	-2752.657333		
	S	TS-S-*n*Heptyl-1	-2752.658218		
		TS-S-*n*Heptyl-2	-2752.657221		
		TS-S-*n*Heptyl-3	-2752.657890		
		TS-S-*n*Heptyl-4	-2752.658070		
(*S*)-**L47**	R	TS-R-*n*Octyl-1	-2831.231055	0.000759	0.476
		TS-R-*n*Octyl-2	-2831.231721		
		TS-R-*n*Octyl-3	-2831.232125		
		TS-R-*n*Octyl-4	-2831.231790		
	S	TS-S-*n*Octyl-1	-2831.232281		
		TS-S-*n*Octyl-2	-2831.231640		
		TS-S-*n*Octyl-3	-2831.232793		
		TS-S-*n*Octyl-4	-2831.232884		
(*S*)-**L48**	R	TS-R-PhEt-1	-2821.738030	0.000722	0.453
		TS-R-PhEt-2	-2821.737874		
		TS-R-PhEt-3	-2821.740124		
		TS-R-PhEt-4	-2821.740380		
	S	TS-S-PhEt-1	-2821.739705		
		TS-S-PhEt-2	-2821.740671		
		TS-S-PhEt-3	-2821.741102		

Table 4.4 (cont'd)

		TS-S-PhEt-4	-2821.739904		
(*S*)-**L31**	R	TS-R-PhPr-1	-2900.313067	—	—
		TS-R-PhPr-2	-2900.313124		
		TS-R-PhPr-3	-2900.313739		
		TS-R-PhPr-4	-2900.313276		
	S	TS-S-PhPr-1	-2900.313122		
		TS-S-PhPr-2	-2900.314589		
		TS-S-PhPr-3	-2900.314661		
		TS-S-PhPr-4	—		
(*S*)-**L49**	R	TS-R-*t*BuPhPr-1	—	—	—
		TS-R-*t*BuPhPr-2	-3214.609517		
		TS-R-*t*BuPhPr-3	-3214.610775		
		TS-R-*t*BuPhPr-4	-3214.610954		
	S	TS-S-*t*BuPhPr-1	—		
		TS-S-*t*BuPhPr-2	—		
		TS-S-*t*BuPhPr-3	—		
		TS-S-*t*BuPhPr-4	-3214.608910		

Table 4.5 Free energy differences by B3LYP/6-31G(d) in 2-propanol

Ligand	Product Chirality	Entry	ΔG(RHF)	ΔΔG(RHF)	ΔΔG(kcal/mol)
(*S*)-**L17**	R	TS-R-Me	-2281.224444	0.000058	0.036
	S	TS-S-Me	-2281.224502		
(*S*)-**L22**	R	TS-R-*t*Bu	-2516.935650	0.000460	0.289
	S	TS-S-*t*Bu	-2516.936110		
(*S*)-**L23**	R	TS-R-Ad	-2981.255023	0.000072	0.045
	S	TS-S-Ad	-2981.255095		
(*S*)-**L18**	R	TS-R-Et-1	-2359.796325	0.000557	0.350
		TS-R-Et-2	-2359.795807		
		TS-R-Et-3	-2359.797754		
		TS-R-Et-4	-2359.797029		
	S	TS-S-Et-1	-2359.797809		
		TS-S-Et-2	-2359.797069		
		TS-S-Et-3	-2359.797837		
		TS-S-Et-4	-2359.798311		
(*S*)-**L32**	R	TS-R-Bn-1	-2743.177049	-0.000201	-0.126
		TS-R-Bn-2	-2743.176942		
		TS-R-Bn-3	-2743.178766		
		TS-R-Bn-4	-2743.177610		

Table 4.5 (cont'd)

	S	TS-S-Bn-1	-2743.177906		
		TS-S-Bn-2	-2743.178565		
		TS-S-Bn-3	-2743.178406		
		TS-S-Bn-4	-2743.177572		
(*S*)-**L33**	R	TS-R-Ph	-2664.609277	-0.001563	-0.981
	S	TS-S-Ph	-2664.607714		
(*S*)-**L30**	R	TS-R-neoPentyl-1	-2595.513580	-0.000162	-0.102
		TS-R-neoPentyl-2	-2595.513639		
		TS-R-neoPentyl-3	-2595.517138		
		TS-R-neoPentyl-4	-2595.516517		
	S	TS-S-neoPentyl-1	-2595.515467		
		TS-S-neoPentyl-2	-2595.516449		
		TS-S-neoPentyl-3	-2595.516656		
		TS-S-neoPentyl-4	-2595.516976		
(*S*)-**L29**	R	TS-R-*i*Pr-1	-2438.370291	0.000140	0.088
		TS-R-*i*Pr-2	-2438.369476		
		TS-R-*i*Pr-3	-2438.368548		
		TS-R-*i*Pr-4	-2438.367890		
	S	TS-S-*i*Pr-1	-2438.370431		
		TS-S-*i*Pr-2	-2438.370277		
		TS-S-*i*Pr-3	-2438.370068		
		TS-S-*i*Pr-4	-2438.369607		
(*S*)-**L21**	R	TS-R-Cy-1	-2671.715225	0.001311	0.823
		TS-R-Cy-2	-2671.715347		
		TS-R-Cy-3	-2671.715026		
		TS-R-Cy-4	-2671.715268		
	S	TS-S-Cy-1	-2671.715861		
		TS-S-Cy-2	-2671.715950		
		TS-S-Cy-3	-2671.716220		
		TS-S-Cy-4	-2671.716658		
(*S*)-**L34**	R	TS-R-C1-Me-1	-2241.931534	-0.000168	-0.105
		TS-R-C1-Me-2	-2241.931381		
	S	TS-S-C1-Me-1	-2241.931113		
		TS-S-C1-Me-2	-2241.931366		
(*S*)-**L35**	R	TS-R-C1-*t*Bu-1	-2359.786400	0.000182	0.114
		TS-R-C1-*t*Bu-2	-2359.787574		
	S	TS-S-C1-*t*Bu-1	-2359.787756		
		TS-S-C1-*t*Bu-2	-2359.784005		
(*S*)-**L36**	R	TS-R-C1-Ph-1	-2433.622610	-0.000233	-0.146
		TS-R-C1-Ph-2	-2433.623484		

Table 4.5 (cont'd)

	S	TS-S-C1-Ph-1	-2433.622971		
		TS-S-C1-Ph-2	-2433.623251		
(*S*)-**L37**	R	TS-R-C1-Ad-1	-2591.946661	0.000998	0.626
		TS-R-C1-Ad-2	-2591.946118		
	S	TS-S-C1-Ad-1	-2591.947659		
		TS-S-C1-Ad-2	-2591.946328		
(*S*)-**L38**	R	TS-R-C1-MeOBu-1	-2474.268085	0.000173	0.109
		TS-R-C1-MeOBu-2	-2474.275571		
	S	TS-S-C1-MeOBu-1	-2474.275744		
		TS-S-C1-MeOBu-2	-2474.272188		
(*S*)-**L39**	R	TS-R-C1-MeOPr-1	-2434.990554	0.001055	0.662
		TS-R-C1-MeOPr-2	-2434.991728		
	S	TS-S-C1-MeOPr-1	-2434.992783		
		TS-S-C1-MeOPr-2	-2434.988287		
(*S*)-**L40**	R	TS-R-C1-CF_3Pr-1	-2657.540737	—	—
		TS-R-C1-CF_3Pr-2	—		
	S	TS-S-C1-CF_3Pr-1	-2657.542191		
		TS-S-C1-CF_3Pr-2	—		
(*S*)-**L5**	R	TS-R-VANOL	-2202.638596	0.000232	0.146
	S	TS-S-VANOL	-2202.638828		
(*S*)-**L41**	R	TS-R-8-Me	-2281.204503	-0.000159	-0.100
	S	TS-S-8-Me	-2281.204344		
(*S*)-**L14**	R	TS-R-8-Ph	-2664.580159	0.000004	0.003
	S	TS-S-8-Ph	-2664.580163		
(*S*)-**L42**	R	TS-R-1-Naph-1	-2971.801332	0.000307	0.193
		TS-R-1-Naph-2	-2971.802431		
		TS-R-1-Naph-3	-2971.802849		
		TS-R-1-Naph-4	-2971.802325		
	S	TS-S-1-Naph-1	-2971.801349		
		TS-S-1-Naph-2	-2971.801181		
		TS-S-1-Naph-3	-2971.802020		
		TS-S-1-Naph-4	-2971.803156		
(*S*)-**L43**	R	TS-R-2-Naph-1	-2971.810511	0.000594	0.373
		TS-R-2-Naph-2	-2971.811964		
		TS-R-2-Naph-3	-2971.811184		
		TS-R-2-Naph-4	-2971.811687		
	S	TS-S-2-Naph-1	-2971.811398		
		TS-S-2-Naph-2	-2971.812063		
		TS-S-2-Naph-3	-2971.811693		
		TS-S-2-Naph-4	-2971.812558		

Table 4.5 (cont'd)

(*S*)-**L44**	R	TS-R-*n*Pr-1	-2438.371576	0.001353	0.849
		TS-R-*n*Pr-2	-2438.372289		
		TS-R-*n*Pr-3	-2438.372754		
		TS-R-*n*Pr-4	-2438.372130		
	S	TS-S-*n*Pr-1	-2438.374107		
		TS-S-*n*Pr-2	-2438.374031		
		TS-S-*n*Pr-3	-2438.373190		
		TS-S-*n*Pr-4	-2438.372284		
(*S*)-**L19**	R	TS-R-*n*Bu-1	-2516.944993	0.000758	0.476
		TS-R-*n*Bu-2	-2516.945240		
		TS-R-*n*Bu-3	-2516.945529		
		TS-R-*n*Bu-4	-2516.946018		
	S	TS-S-*n*Bu-1	-2516.946087		
		TS-S-*n*Bu-2	-2516.946776		
		TS-S-*n*Bu-3	-2516.946558		
		TS-S-*n*Bu-4	-2516.945784		
(*S*)-**L45**	R	TS-R-*n*Pentyl-1	-2595.516286	0.004667	2.929
		TS-R-*n*Pentyl-2	-2595.515023		
		TS-R-*n*Pentyl-3	-2595.516854		
		TS-R-*n*Pentyl-4	-2595.515855		
	S	TS-S-*n*Pentyl-1	-2595.521521		
		TS-S-*n*Pentyl-2	-2595.521113		
		TS-S-*n*Pentyl-3	-2595.521018		
		TS-S-*n*Pentyl-4	-2595.520522		
(*S*)-**L20**	R	TS-R-*n*Hexyl-1	-2674.094825	0.001104	0.693
		TS-R-*n*Hexyl-2	-2674.094434		
		TS-R-*n*Hexyl-3	-2674.095763		
		TS-R-*n*Hexyl-4	-2674.095105		
	S	TS-S-*n*Hexyl-1	-2674.096043		
		TS-S-*n*Hexyl-2	-2674.096318		
		TS-S-*n*Hexyl-3	-2674.095743		
		TS-S-*n*Hexyl-4	-2674.096867		
(*S*)-**L46**	R	TS-R-*n*Heptyl-1	-2752.669497	0.001294	0.812
		TS-R-*n*Heptyl-2	-2752.670420		
		TS-R-*n*Heptyl-3	-2752.670617		
		TS-R-*n*Heptyl-4	-2752.669363		
	S	TS-S-*n*Heptyl-1	-2752.671911		
		TS-S-*n*Heptyl-2	-2752.670514		
		TS-S-*n*Heptyl-3	-2752.671018		
		TS-S-*n*Heptyl-4	-2752.671546		

Table 4.5 (cont'd)

(*S*)-**L47**	R	TS-R-*n*Octyl-1	-2831.244667	0.000189	0.119
		TS-R-*n*Octyl-2	-2831.244976		
		TS-R-*n*Octyl-3	-2831.246067		
		TS-R-*n*Octyl-4	-2831.244663		
	S	TS-S-*n*Octyl-1	-2831.245559		
		TS-S-*n*Octyl-2	-2831.245359		
		TS-S-*n*Octyl-3	-2831.245814		
		TS-S-*n*Octyl-4	-2831.246256		
(*S*)-**L48**	R	TS-R-PhEt-1	-2821.752212	-0.001061	-0.666
		TS-R-PhEt-2	-2821.753236		
		TS-R-PhEt-3	-2821.755531		
		TS-R-PhEt-4	-2821.756156		
	S	TS-S-PhEt-1	-2821.755095		
		TS-S-PhEt-2	-2821.754730		
		TS-S-PhEt-3	-2821.755069		
		TS-S-PhEt-4	-2821.754856		
(*S*)-**L31**	R	TS-R-PhPr-1	-2900.327387	0.000963	0.604
		TS-R-PhPr-2	-2900.327833		
		TS-R-PhPr-3	-2900.329549		
		TS-R-PhPr-4	-2900.327973		
	S	TS-S-PhPr-1	-2900.328895		
		TS-S-PhPr-2	-2900.330512		
		TS-S-PhPr-3	-2900.328856		
		TS-S-PhPr-4	-2900.328557		
(*S*)-**L49**	R	TS-R-*t*BuPhPr-1	-3214.624566	0.000264	0.166
		TS-R-*t*BuPhPr-2	-3214.624667		
		TS-R-*t*BuPhPr-3	-3214.626708		
		TS-R-*t*BuPhPr-4	-3214.625924		
	S	TS-S-*t*BuPhPr-1	-3214.624869		
		TS-S-*t*BuPhPr-2	-3214.626903		
		TS-S-*t*BuPhPr-3	-3214.626972		
		TS-S-*t*BuPhPr-4	-3214.624500		

Table 4.6 Calculated ΔΔG by HF/3-21G* in vacuum for 2-bromoacetophenone **55g**

Ligand	Product Chirality	Entry	ΔG(RHF)	ΔΔG(RHF)	ΔΔG(kcal/mol)
(*S*)-**L17**	R	TS-R-Me	-4814.909394	0.000971	0.609
	S	TS-S-Me	-4814.910365		
(*S*)-**L22**	R	TS-R-*t*Bu	-5047.648200	0.001266	0.794

Table 4.6 (cont'd)

	S	TS-S-*t*Bu	-5047.649466		
(*S*)-**L23**	R	TS-R-Ad	-5506.333231	0.000393	0.247
	S	TS-S-Ad	-5506.333624		
(*S*)-**L18**	R	TS-R-Et-1	-4892.489166	0.000868	0.545
		TS-R-Et-2	-4892.489050		
		TS-R-Et-3	-4892.490663		
		TS-R-Et-4	-4892.490694		
	S	TS-S-Et-1	-4892.490621		
		TS-S-Et-2	-4892.490842		
		TS-S-Et-3	-4892.491562		
		TS-S-Et-4	-4892.491247		
(*S*)-**L32**	R	TS-R-Bn-1	-5271.279064	0.000259	0.163
		TS-R-Bn-2	-5271.278504		
		TS-R-Bn-3	-5271.279032		
		TS-R-Bn-4	-5271.277300		
	S	TS-S-Bn-1	-5271.279112		
		TS-S-Bn-2	-5271.276791		
		TS-S-Bn-3	-5271.277585		
		TS-S-Bn-4	-5271.279323		
(*S*)-**L33**	R	TS-R-Ph	-5193.701766	-0.000083	-0.052
	S	TS-S-Ph	-5193.701683		
(*S*)-**L30**	R	TS-R-neoPentyl-1	-5125.230787	0.000276	0.173
		TS-R-neoPentyl-2	-5125.233505		
		TS-R-neoPentyl-3	-5125.237378		
		TS-R-neoPentyl-4	-5125.237048		
	S	TS-S-neoPentyl-1	-5125.233112		
		TS-S-neoPentyl-2	-5125.236316		
		TS-S-neoPentyl-3	-5125.237654		
		TS-S-neoPentyl-4	-5125.236051		
(*S*)-**L29**	R	TS-R-*i*Pr-1	-4970.072638	0.001198	0.752
		TS-R-*i*Pr-2	-4970.071776		
		TS-R-*i*Pr-3	-4970.069303		
		TS-R-*i*Pr-4	-4970.068837		
	S	TS-S-*i*Pr-1	-4970.071794		
		TS-S-*i*Pr-2	-4970.073836		
		TS-S-*i*Pr-3	-4970.071983		
		TS-S-*i*Pr-4	-4970.070724		
(*S*)-**L21**	R	TS-R-Cy-1	-5200.541651	0.001841	1.155
		TS-R-Cy-2	-5200.541837		
		TS-R-Cy-3	-5200.539640		

Table 4.6 (cont'd)

		TS-R-Cy-4	-5200.539789		
	S	TS-S-Cy-1	-5200.543678		
		TS-S-Cy-2	-5200.542310		
		TS-S-Cy-3	-5200.540998		
		TS-S-Cy-4	-5200.542226		
(*S*)-**L34**	R	TS-R-C1-Me-1	-4776.115543	0.000697	0.437
		TS-R-C1-Me-2	-4776.115956		
	S	TS-S-C1-Me-1	-4776.116653		
		TS-S-C1-Me-2	-4776.116084		
(*S*)-**L35**	R	TS-R-C1-*t*Bu-1	-4892.484186	-0.000557	-0.350
		TS-R-C1-*t*Bu-2	-4892.486412		
	S	TS-S-C1-*t*Bu-1	-4892.485628		
		TS-S-C1-*t*Bu-2	-4892.485855		
(*S*)-**L36**	R	TS-R-C1-Ph-1	-4965.512366	-0.000290	-0.182
		TS-R-C1-Ph-2	-4965.511566		
	S	TS-S-C1-Ph-1	-4965.511714		
		TS-S-C1-Ph-2	-4965.512076		
(*S*)-**L37**	R	TS-R-C1-Ad-1	-5121.827018	0.000343	0.215
		TS-R-C1-Ad-2	-5121.828512		
	S	TS-S-C1-Ad-1	-5121.828855		
		TS-S-C1-Ad-2	-5121.826754		
(*S*)-**L38**	R	TS-R-C1-MeOBu-1	-5005.693358	0.011136	6.988
		TS-R-C1-MeOBu-2	-5005.695033		
	S	TS-S-C1-MeOBu-1	-5005.706169		
		TS-S-C1-MeOBu-2	-5005.694963		
(*S*)-**L39**	R	TS-R-C1-MeOPr-1	-4966.905806	0.000900	0.565
		TS-R-C1-MeOPr-2	-4966.908733		
	S	TS-S-C1-MeOPr-1	-4966.909633		
		TS-S-C1-MeOPr-2	-4966.906129		
(*S*)-**L40**	R	TS-R-C1-CF_3Pr-1	-5187.508406	0.002286	1.434
		TS-R-C1-CF_3Pr-2	-5187.514823		
	S	TS-S-C1-CF_3Pr-1	-5187.509596		
		TS-S-C1-CF_3Pr-2	-5187.517109		
(*S*)-**L5**	R	TS-R-VANOL	-4737.322108	0.000202	0.127
	S	TS-S-VANOL	-4737.322310		
(*S*)-**L41**	R	TS-R-8-Me	-4814.889747	0.002585	-1.622
	S	TS-S-8-Me	-4814.887162		
(*S*)-**L14**	R	TS-R-8-Ph	-5193.665970	—	—
	S	TS-S-8-Ph	—		
(*S*)-**L42**	R	TS-R-1-Naph-1	-5497.198036	-0.001204	-0.756

Table 4.6 (cont'd)

		TS-R-1-Naph-2	-5497.197014		
		TS-R-1-Naph-3	-5497.195714		
		TS-R-1-Naph-4	-5497.196860		
	S	TS-S-1-Naph-1	-5497.196832		
		TS-S-1-Naph-2	-5497.195958		
		TS-S-1-Naph-3	-5497.195326		
		TS-S-1-Naph-4	-5497.196200		
(*S*)-**L43**	R	TS-R-2-Naph-1	-5497.201027	-0.000269	-0.169
		TS-R-2-Naph-2	-5497.200573		
		TS-R-2-Naph-3	-5497.200612		
		TS-R-2-Naph-4	-5497.200972		
	S	TS-S-2-Naph-1	-5497.199581		
		TS-S-2-Naph-2	-5497.200392		
		TS-S-2-Naph-3	-5497.200758		
		TS-S-2-Naph-4	-5497.200355		
(*S*)-**L44**	R	TS-R-*n*Pr-1	-4970.071001	0.000871	0.547
		TS-R-*n*Pr-2	-4970.072738		
		TS-R-*n*Pr-3	-4970.072706		
		TS-R-*n*Pr-4	-4970.070871		
	S	TS-S-*n*Pr-1	-4970.072762		
		TS-S-*n*Pr-2	-4970.072990		
		TS-S-*n*Pr-3	-4970.073609		
		TS-S-*n*Pr-4	-4970.073287		
(*S*)-**L19**	R	TS-R-*n*Bu-1	-5047.650688	0.000639	0.401
		TS-R-*n*Bu-2	-5047.650928		
		TS-R-*n*Bu-3	-5047.652811		
		TS-R-*n*Bu-4	-5047.653053		
	S	TS-S-*n*Bu-1	-5047.653124		
		TS-S-*n*Bu-2	-5047.653347		
		TS-S-*n*Bu-3	-5047.653692		
		TS-S-*n*Bu-4	-5047.653420		
(*S*)-**L45**	R	TS-R-*n*Pentyl-1	-5125.227321	0.005609	3.520
		TS-R-*n*Pentyl-2	-5125.227719		
		TS-R-*n*Pentyl-3	-5125.229567		
		TS-R-*n*Pentyl-4	-5125.229545		
	S	TS-S-*n*Pentyl-1	-5125.234628		
		TS-S-*n*Pentyl-2	-5125.234854		
		TS-S-*n*Pentyl-3	-5125.235176		
		TS-S-*n*Pentyl-4	-5125.234909		
(*S*)-**L20**	R	TS-R-*n*Hexyl-1	-5202.813695	0.000611	0.383

Table 4.6 (cont'd)

		TS-R-*n*Hexyl-2	-5202.813931		
		TS-R-*n*Hexyl-3	-5202.815784		
		TS-R-*n*Hexyl-4	-5202.816039		
	S	TS-S-*n*Hexyl-1	-5202.816203		
		TS-S-*n*Hexyl-2	-5202.816339		
		TS-S-*n*Hexyl-3	-5202.816650		
		TS-S-*n*Hexyl-4	-5202.816485		
(*S*)-**L46**	R	TS-R-*n*Heptyl-1	-5280.395174	0.000618	0.388
		TS-R-*n*Heptyl-2	-5280.395412		
		TS-R-*n*Heptyl-3	-5280.397264		
		TS-R-*n*Heptyl-4	-5280.397515		
	S	TS-S-*n*Heptyl-1	-5280.397677		
		TS-S-*n*Heptyl-2	-5280.397817		
		TS-S-*n*Heptyl-3	-5280.398133		
		TS-S-*n*Heptyl-4	-5280.397953		
(*S*)-**L47**	R	TS-R-*n*Octyl-1	-5357.976665	0.000618	0.388
		TS-R-*n*Octyl-2	-5357.976887		
		TS-R-*n*Octyl-3	-5357.978739		
		TS-R-*n*Octyl-4	-5357.978990		
	S	TS-S-*n*Octyl-1	-5357.979166		
		TS-S-*n*Octyl-2	-5357.979295		
		TS-S-*n*Octyl-3	-5357.979608		
		TS-S-*n*Octyl-4	-5357.979439		
(*S*)-**L48**	R	TS-R-PhEt-1	-5348.858666	0.000496	0.311
		TS-R-PhEt-2	-5348.859543		
		TS-R-PhEt-3	-5348.863294		
		TS-R-PhEt-4	-5348.862222		
	S	TS-S-PhEt-1	-5348.863370		
		TS-S-PhEt-2	-5348.863593		
		TS-S-PhEt-3	-5348.863790		
		TS-S-PhEt-4	-5348.863523		
(*S*)-**L31**	R	TS-R-PhPr-1	-5426.440229	0.001067	0.670
		TS-R-PhPr-2	-5426.440957		
		TS-R-PhPr-3	-5426.442773		
		TS-R-PhPr-4	-5426.442323		
	S	TS-S-PhPr-1	-5426.442360		
		TS-S-PhPr-2	-5426.442960		
		TS-S-PhPr-3	-5426.443840		
		TS-S-PhPr-4	-5426.443177		
(*S*)-**L49**	R	TS-R-*t*BuPhPr-1	-5736.765761	0.000998	0.626

Table 4.6 (cont'd)

		TS-R-*t*BuPhPr-2	-5736.767631		
		TS-R-*t*BuPhPr-3	-5736.769652		
		TS-R-*t*BuPhPr-4	-5736.767753		
	S	TS-S-*t*BuPhPr-1	-5736.768170		
		TS-S-*t*BuPhPr-2	-5736.769881		
		TS-S-*t*BuPhPr-3	-5736.770650		
		TS-S-*t*BuPhPr-4	-5736.767759		

In the reduction of acetophenone **55a** with catalyst prapared from (*S*)-**L21**, the transition state geometries calculated under DFT/B3LYP/6-31G(d) level with CPCM as solvation method in 2-propanol are shown in Figure 2.4.

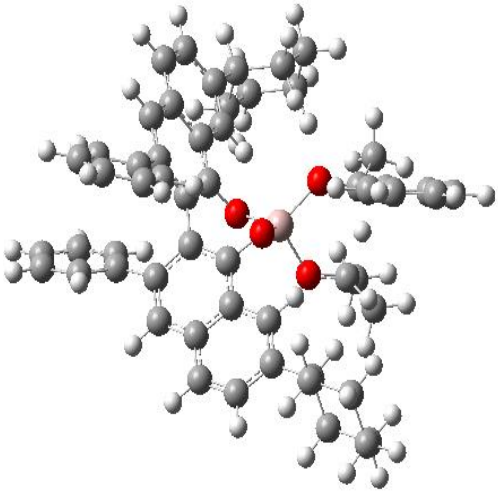

TS-S-L21-p

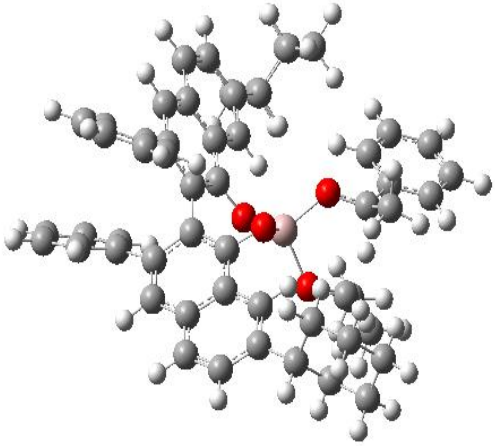

TS-R-L21-p

TS-R-L21-p Coordinate:

1	H	0.290	-3.977	-0.459	7	O	-0.532	-2.351	-1.542
2	C	-0.208	-3.622	-1.688	8	O	0.724	-2.376	0.811
3	C	0.729	-3.708	0.742	9	C	5.030	2.157	1.132
4	Al	-0.096	-1.200	-0.244	10	C	3.973	2.928	1.558
5	O	-1.456	-0.449	0.580	11	C	2.640	2.626	1.168
6	O	0.905	0.097	-0.877	12	C	2.421	1.493	0.330

13	C	3.533	0.712	-0.085
14	C	4.827	1.024	0.293
15	H	1.694	4.189	2.316
16	H	6.038	2.418	1.443
17	H	4.147	3.788	2.201
18	C	1.527	3.383	1.606
19	C	1.082	1.188	-0.081
20	C	0.006	2.002	0.281
21	C	0.238	3.088	1.201
22	C	-1.354	1.780	-0.310
23	C	-2.046	0.592	-0.071
24	C	-1.993	2.809	-1.094
25	C	-3.418	0.432	-0.462
26	C	-3.311	2.659	-1.483
27	C	-4.151	-0.744	-0.162
28	C	-4.059	1.499	-1.160
29	H	-3.780	3.426	-2.093
30	C	-5.481	-0.886	-0.523
31	C	-5.419	1.336	-1.535
32	C	-6.105	0.183	-1.223
33	H	-5.914	2.141	-2.073
34	H	-7.148	0.082	-1.516
35	C	-1.260	4.013	-1.584
36	C	-1.842	5.289	-1.499
37	C	-0.015	3.895	-2.229
38	C	-1.204	6.409	-2.033
39	H	-2.797	5.403	-0.994
40	C	0.624	5.014	-2.763
41	H	0.444	2.917	-2.328
42	C	0.034	6.277	-2.667
43	H	-1.673	7.386	-1.949
44	H	1.582	4.897	-3.263
45	H	0.533	7.149	-3.082
46	C	-0.875	3.872	1.812
47	C	-0.804	5.274	1.887
48	C	-1.975	3.232	2.411
49	C	-1.798	6.012	2.533
50	H	0.032	5.788	1.421
51	C	-2.969	3.969	3.056
52	H	-2.040	2.149	2.386
53	C	-2.886	5.362	3.119
54	H	-1.723	7.095	2.572
55	H	-3.805	3.451	3.518
56	C	-0.339	-4.379	1.600
57	H	-0.426	-5.449	1.408
58	H	-0.066	-4.236	2.652
59	H	-1.308	-3.902	1.431
60	C	2.095	-4.344	0.706
61	C	2.243	-5.739	0.625
62	C	3.241	-3.536	0.743
63	C	3.513	-6.312	0.593
64	H	1.370	-6.382	0.575
65	C	4.510	-4.113	0.717
66	H	3.129	-2.459	0.807
67	C	4.651	-5.501	0.643
68	H	3.615	-7.391	0.530
69	H	5.391	-3.478	0.758
70	H	5.640	-5.949	0.621
71	C	-1.373	-4.584	-1.802
72	H	-2.140	-4.357	-1.058
73	H	-1.818	-4.457	-2.798
74	H	-1.050	-5.623	-1.702

75	C	1.014	-3.904	-2.538
76	H	1.852	-3.267	-2.239
77	H	1.312	-4.953	-2.481
78	H	0.763	-3.669	-3.580
79	H	-3.661	5.935	3.620
80	H	3.347	-0.142	-0.728
81	H	-3.640	-1.536	0.376
82	C	6.002	0.187	-0.184
83	C	6.954	0.986	-1.105
84	C	6.795	-0.445	0.984
85	H	5.590	-0.640	-0.782
86	C	8.123	0.124	-1.605
87	H	7.351	1.850	-0.553
88	H	6.388	1.391	-1.954
89	C	7.963	-1.307	0.481
90	H	7.189	0.351	1.632
91	H	6.118	-1.045	1.607
92	C	8.898	-0.510	-0.440
93	H	8.795	0.730	-2.226
94	H	7.731	-0.674	-2.254
95	H	8.522	-1.713	1.334
96	H	7.565	-2.171	-0.071
97	H	9.698	-1.156	-0.822
98	H	9.388	0.285	0.143
99	C	-6.275	-2.139	-0.188
100	C	-5.694	-3.407	-0.855
101	C	-6.418	-2.356	1.337
102	H	-7.289	-2.000	-0.590
103	C	-6.527	-4.657	-0.530
104	H	-4.662	-3.558	-0.504
105	H	-5.636	-3.259	-1.941
106	C	-7.250	-3.606	1.661
107	H	-5.417	-2.461	1.781
108	H	-6.871	-1.468	1.794
109	C	-6.674	-4.860	0.985
110	H	-6.068	-5.541	-0.991
111	H	-7.525	-4.552	-0.981
112	H	-7.302	-3.749	2.748
113	H	-8.283	-3.452	1.316
114	H	-7.311	-5.730	1.192
115	H	-5.688	-5.082	1.417

END

TS-S-L21-p Coordinate:

1	H	-0.303	-3.991	-0.575
2	C	-0.731	-3.481	-1.786
3	C	0.174	-3.885	0.633
4	Al	0.138	-1.227	-0.315
5	O	-0.519	-2.185	-1.673
6	O	0.516	-2.599	0.747
7	O	-0.973	-0.127	0.492
8	O	1.494	-0.262	-0.878
9	C	5.957	0.338	1.347
10	C	5.175	1.384	1.784
11	C	3.833	1.525	1.342
12	C	3.313	0.551	0.438
13	C	4.143	-0.517	0.012
14	C	5.454	-0.639	0.445
15	H	3.360	3.253	2.547
16	H	6.983	0.252	1.697
17	H	5.578	2.119	2.477
18	C	2.985	2.568	1.791
19	C	1.961	0.690	-0.022
20	C	1.170	1.776	0.356
21	C	1.685	2.698	1.339
22	C	-0.169	2.002	-0.279
23	C	-1.195	1.068	-0.123
24	C	-0.438	3.207	-1.023
25	C	-2.530	1.340	-0.568
26	C	-1.723	3.474	-1.462
27	C	-3.594	0.423	-0.360
28	C	-2.794	2.576	-1.228
29	H	-1.915	4.372	-2.042
30	C	-4.885	0.694	-0.777
31	C	-4.123	2.839	-1.660
32	C	-5.133	1.930	-1.440
33	H	-4.331	3.777	-2.170
34	H	-6.139	2.163	-1.780
35	C	0.639	4.161	-1.422
36	C	0.456	5.547	-1.277
37	C	1.821	3.710	-2.036
38	C	1.420	6.451	-1.724
39	H	-0.445	5.915	-0.794
40	C	2.785	4.613	-2.484
41	H	1.974	2.645	-2.180
42	C	2.591	5.988	-2.328
43	H	1.257	7.518	-1.595
44	H	3.688	4.241	-2.962
45	H	3.343	6.691	-2.676
46	C	0.838	3.756	1.965
47	C	1.327	5.064	2.122
48	C	-0.428	3.454	2.498
49	C	0.578	6.039	2.782
50	H	2.298	5.320	1.707
51	C	-1.178	4.428	3.158
52	H	-2.151	4.169	3.568
53	H	-0.817	2.445	2.410
54	C	-0.680	5.725	3.302
55	H	-1.266	6.483	3.815
56	H	0.976	7.045	2.885
57	C	-2.180	-3.922	-1.745
58	H	-2.708	-3.449	-0.913
59	H	-2.655	-3.598	-2.680
60	H	-2.269	-5.008	-1.671

61	C	0.195	-4.218	-2.734
62	H	1.234	-3.916	-2.578
63	H	0.101	-5.301	-2.630
64	H	-0.087	-3.945	-3.759
65	C	1.374	-4.823	0.565
66	H	2.107	-4.432	-0.146
67	H	1.839	-4.856	1.557
68	H	1.101	-5.840	0.276
69	C	-1.011	-4.321	1.459
70	C	-1.413	-5.666	1.505
71	C	-1.740	-3.367	2.188
72	C	-2.511	-6.050	2.272
73	H	-0.876	-6.420	0.937
74	C	-2.837	-3.755	2.957
75	H	-1.436	-2.327	2.159
76	C	-3.226	-5.096	3.002
77	H	-2.810	-7.094	2.300
78	H	-3.387	-3.008	3.523
79	H	-4.080	-5.396	3.602
80	H	-3.375	-0.508	0.153
81	H	3.723	-1.241	-0.678
82	C	6.349	-1.778	-0.019
83	C	5.812	-3.165	0.407
84	C	6.600	-1.748	-1.545
85	H	7.325	-1.646	0.472
86	C	6.743	-4.301	-0.043
87	H	4.816	-3.316	-0.034
88	H	5.679	-3.189	1.496
89	C	7.531	-2.885	-1.993
90	H	5.638	-1.838	-2.070
91	H	7.022	-0.776	-1.829
92	C	6.998	-4.258	-1.557
93	H	6.317	-5.270	0.245
94	H	7.703	-4.212	0.488
95	H	7.660	-2.855	-3.083
96	H	8.529	-2.729	-1.556
97	H	7.701	-5.049	-1.847
98	H	6.056	-4.465	-2.087
99	C	-6.007	-0.299	-0.531
100	C	-7.105	0.271	0.398
101	C	-6.636	-0.820	-1.845
102	H	-5.566	-1.166	-0.017
103	C	-8.219	-0.754	0.662
104	H	-7.541	1.168	-0.063
105	H	-6.653	0.594	1.344
106	C	-7.751	-1.844	-1.578
107	H	-7.051	0.026	-2.411
108	H	-5.854	-1.264	-2.475
109	C	-8.831	-1.274	-0.647
110	H	-8.996	-0.306	1.295
111	H	-7.803	-1.601	1.228
112	H	-8.196	-2.166	-2.528
113	H	-7.313	-2.742	-1.117
114	H	-9.591	-2.037	-0.435
115	H	-9.349	-0.448	-1.157

END

In the reduction of acetophenone **55g** with catalyst prapared from (*S*)-**L21**, the transition state geometries calculated under HF/3-21G* level in vacuum are shown in Figure 2.5.

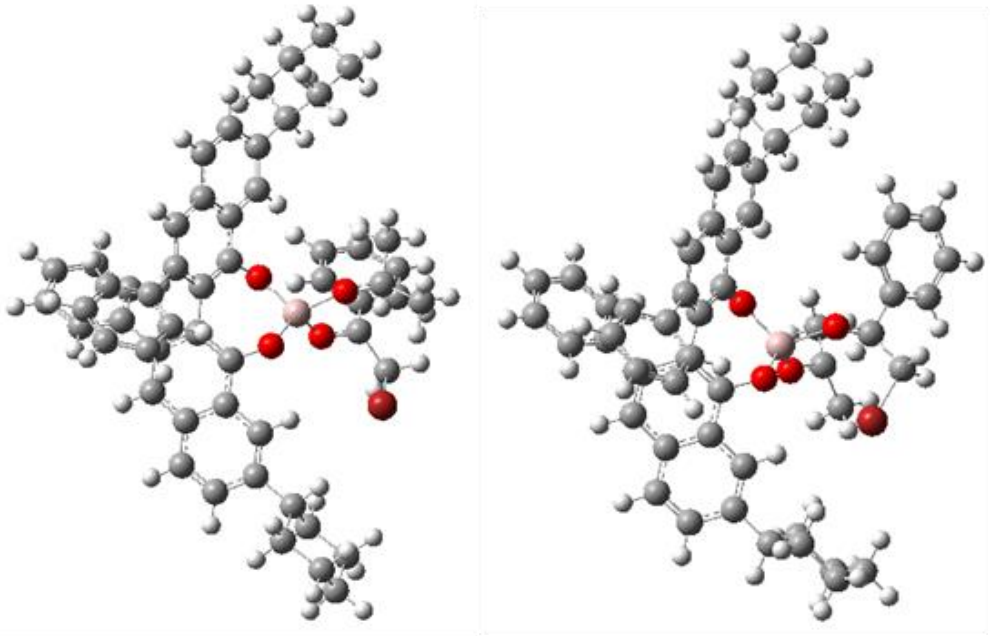

TS-S-L21-55g　　TS-R-L21-55g

TS-R-L21-55g Coordinate:

1	H	0.007	-3.767	0.784	13	C	-3.703	0.495	0.026
2	C	0.340	-3.248	1.905	14	C	-4.999	0.620	-0.373
3	C	-0.413	-3.578	-0.507	15	H	-2.291	4.094	-2.419
4	Al	0.177	-0.925	0.322	16	H	-6.356	1.800	-1.569
5	O	1.386	0.008	-0.490	17	H	-4.672	3.372	-2.333
6	O	-1.051	0.195	0.814	18	C	-2.045	3.347	-1.690
7	O	0.672	-1.983	1.631	19	C	-1.359	1.286	0.047
8	O	-0.451	-2.281	-0.654	20	C	-0.419	2.222	-0.292
9	C	-5.340	1.687	-1.246	21	C	-0.767	3.242	-1.235
10	C	-4.403	2.570	-1.673	22	C	0.944	2.211	0.328
11	C	-3.054	2.460	-1.253	23	C	1.797	1.165	0.126
12	C	-2.707	1.406	-0.399	24	C	1.390	3.323	1.119

25	C	3.149	1.213	0.570
26	C	2.675	3.373	1.563
27	C	4.036	0.149	0.306
28	C	3.597	2.339	1.272
29	H	2.992	4.191	2.180
30	C	5.334	0.189	0.717
31	C	4.946	2.367	1.700
32	C	5.782	1.330	1.429
33	H	5.299	3.222	2.243
34	H	6.802	1.368	1.758
35	C	0.446	4.386	1.579
36	C	0.753	5.729	1.407
37	C	-0.709	4.043	2.272
38	C	-0.080	6.712	1.914
39	H	1.631	5.999	0.856
40	C	-1.541	5.025	2.777
41	H	-0.948	3.010	2.417
42	C	-1.229	6.363	2.600
43	H	0.168	7.745	1.770
44	H	-2.428	4.746	3.310
45	H	-1.875	7.123	2.992
46	C	0.267	4.139	-1.837
47	C	0.086	5.515	-1.857
48	C	1.378	3.595	-2.471
49	C	1.001	6.335	-2.496
50	H	-0.757	5.940	-1.353
51	C	2.291	4.415	-3.107
52	H	1.519	2.534	-2.467
53	C	2.106	5.787	-3.122
54	H	0.852	7.397	-2.500
55	H	3.144	3.982	-3.593
56	C	0.686	-4.327	-1.255
57	H	0.821	-5.326	-0.886
58	H	0.401	-4.354	-2.297
59	C	-1.727	-4.295	-0.449
60	C	-1.814	-5.651	-0.152
61	C	-2.879	-3.570	-0.705
62	C	-3.044	-6.275	-0.123
63	H	-0.933	-6.220	0.071
64	C	-4.111	-4.201	-0.681
65	H	-2.804	-2.527	-0.929
66	C	-4.195	-5.550	-0.392
67	H	-3.108	-7.319	0.109
68	H	-4.998	-3.639	-0.889
69	H	-5.150	-6.036	-0.373
70	C	1.491	-4.143	2.328
71	H	2.296	-4.072	1.615
72	H	1.849	-3.786	3.289
73	H	1.169	-5.170	2.433
74	C	-0.946	-3.414	2.697
75	H	-1.749	-2.852	2.240
76	H	-1.230	-4.453	2.781
77	H	-0.774	-3.008	3.688
78	H	2.816	6.421	-3.616
79	H	-3.410	-0.286	0.696
80	H	3.651	-0.687	-0.237
81	C	-6.070	-0.335	0.127
82	C	-7.072	0.386	1.057
83	C	-6.830	-1.023	-1.029
84	H	-5.578	-1.110	0.709
85	C	-8.137	-0.589	1.594
86	H	-7.561	1.182	0.504

87	H	-6.531	0.844	1.878
88	C	-7.889	-2.005	-0.490
89	H	-7.324	-0.272	-1.635
90	H	-6.124	-1.540	-1.671
91	C	-8.883	-1.280	0.437
92	H	-8.840	-0.056	2.226
93	H	-7.654	-1.344	2.210
94	H	-8.419	-2.467	-1.317
95	H	-7.397	-2.798	0.068
96	H	-9.611	-1.983	0.828
97	H	-9.424	-0.532	-0.136
98	C	6.295	-0.957	0.437
99	C	5.849	-2.253	1.152
100	C	6.454	-1.216	-1.078
101	H	7.271	-0.683	0.829
102	C	6.829	-3.410	0.880
103	H	4.862	-2.529	0.795
104	H	5.769	-2.067	2.218
105	C	7.433	-2.375	-1.349
106	H	5.485	-1.463	-1.501
107	H	6.798	-0.310	-1.564
108	C	6.971	-3.659	-0.634
109	H	6.484	-4.311	1.377
110	H	7.803	-3.163	1.294
111	H	7.511	-2.549	-2.417
112	H	8.422	-2.103	-0.990
113	H	7.676	-4.464	-0.817
114	H	6.010	-3.966	-1.037
115	Br	2.397	-3.419	-1.173

END

TS-S-L21-55g Coordinate:

1	H	-0.203	-3.820	-0.584
2	C	-0.761	-3.389	-1.687
3	C	0.363	-3.540	0.610
4	Al	0.042	-0.954	-0.500
5	O	-0.486	-2.088	-1.733
6	O	0.566	-2.247	0.590
7	O	-1.200	-0.080	0.346
8	O	1.203	0.207	-1.031
9	C	5.523	1.338	1.177
10	C	4.625	2.232	1.661
11	C	3.277	2.219	1.223
12	C	2.895	1.256	0.281
13	C	3.851	0.336	-0.207
14	C	5.143	0.362	0.218
15	H	2.569	3.780	2.517
16	H	6.536	1.367	1.525
17	H	4.923	2.964	2.387
18	C	2.296	3.100	1.734
19	C	1.546	1.219	-0.166
20	C	0.626	2.130	0.273
21	C	1.011	3.065	1.289
22	C	-0.753	2.178	-0.311
23	C	-1.616	1.127	-0.161
24	C	-1.202	3.347	-1.007
25	C	-2.978	1.229	-0.560
26	C	-2.497	3.446	-1.412

27	C	-3.887	0.166	-0.343	58	H	-2.591	-3.195	-0.568
28	C	-3.425	2.408	-1.168	59	H	-2.785	-3.436	-2.294
29	H	-2.818	4.310	-1.960	60	H	-2.342	-4.800	-1.264
30	C	-5.193	0.260	-0.712	61	C	-0.063	-4.241	-2.732
31	C	-4.786	2.489	-1.556	62	H	0.997	-4.049	-2.724
32	C	-5.637	1.456	-1.335	63	H	-0.254	-5.292	-2.567
33	H	-5.134	3.388	-2.029	64	H	-0.460	-3.958	-3.701
34	H	-6.663	1.544	-1.635	65	C	1.615	-4.409	0.538
35	C	-0.254	4.427	-1.415	66	H	2.068	-4.415	1.518
36	C	-0.533	5.758	-1.136	67	H	1.403	-5.412	0.220
37	C	0.875	4.119	-2.166	68	C	-0.725	-4.031	1.521
38	C	0.302	6.763	-1.594	69	C	-0.968	-5.384	1.728
39	H	-1.390	6.000	-0.541	70	C	-1.513	-3.083	2.161
40	C	1.709	5.122	-2.621	71	C	-1.981	-5.784	2.577
41	H	1.091	3.095	-2.393	72	H	-0.380	-6.130	1.233
42	C	1.425	6.448	-2.337	73	C	-2.527	-3.490	3.009
43	H	0.077	7.787	-1.366	74	H	-1.338	-2.041	1.989
44	H	2.575	4.870	-3.200	75	C	-2.761	-4.837	3.221
45	H	2.073	7.225	-2.692	76	H	-2.161	-6.828	2.736
46	C	0.010	3.939	1.973	77	H	-3.130	-2.755	3.503
47	C	0.226	5.306	2.087	78	H	-3.545	-5.149	3.881
48	C	-1.105	3.381	2.588	79	H	-3.516	-0.716	0.134
49	C	-0.657	6.101	2.799	80	H	3.525	-0.388	-0.923
50	H	1.072	5.745	1.599	81	C	6.153	-0.647	-0.303
51	C	-1.987	4.176	3.296	82	C	7.380	0.031	-0.951
52	H	-2.842	3.732	3.766	83	C	6.605	-1.614	0.814
53	H	-1.273	2.327	2.512	84	H	5.661	-1.239	-1.070
54	C	-1.766	5.539	3.405	85	C	8.372	-1.017	-1.491
55	H	-2.450	6.154	3.955	86	H	7.885	0.646	-0.213
56	H	-0.479	7.156	2.875	87	H	7.049	0.685	-1.751
57	C	-2.214	-3.739	-1.422	88	C	7.604	-2.659	0.278

89	H	7.074	-1.046	1.612	103	H	-7.873	0.339	0.015
90	H	5.733	-2.107	1.230	104	H	-6.906	-0.105	1.405
91	C	8.822	-1.973	-0.369	105	C	-7.679	-2.632	-1.529
92	H	9.233	-0.521	-1.926	106	H	-7.265	-0.666	-2.312
93	H	7.893	-1.592	-2.280	107	H	-5.905	-1.761	-2.428
94	H	7.926	-3.309	1.085	108	C	-8.827	-2.211	-0.592
95	H	7.108	-3.280	-0.463	109	H	-9.083	-1.337	1.376
96	H	9.505	-2.718	-0.764	110	H	-7.731	-2.443	1.252
97	H	9.357	-1.407	0.388	111	H	-8.079	-2.998	-2.469
98	C	-6.159	-0.887	-0.467	112	H	-7.125	-3.447	-1.070
99	C	-7.316	-0.473	0.471	113	H	-9.480	-3.056	-0.397
100	C	-6.725	-1.450	-1.790	114	H	-9.423	-1.444	-1.079
101	H	-5.608	-1.686	0.023	115	Br	2.936	-3.671	-0.677
102	C	-8.270	-1.655	0.732	END				

4.3 Experimental information for chapter three

4.3.1 General procedure for preparing diene 93

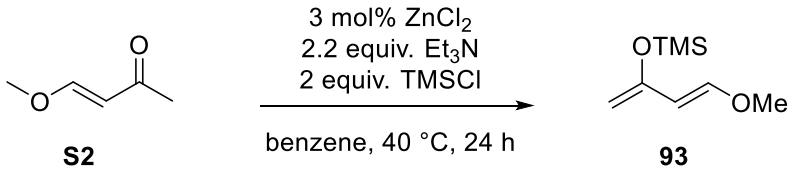

S2 **93**

4-Methoxy-2-trimethylsilyloxy-1,3-butadiene ***93*** (Danishefsky's diene): To a 250 mL oven-dried round bottomed flask was added anhydrous zinc chloride (163 mg, 1.20 mmol) to freshly distilled triethylamine (12.2 mL, 88.0 mmol), and a argon balloon with septum was attached and the mixture was stirred for 1 h at room temperature until the salt was suspended in the triethylamine. To this mixture was added (E)-4-methoxybut-3-en-2-one **S2** (4.07 mL, 40.0 mmol) in dry benzene (20 mL) in one portion. Then trimethylchlorosilane (10.2 mL, 80.0 mol) was injected

into the reaction dropwise over 30 minutes at room temperature while stirring. The reaction mixture was then heated at 40 ºC and stirred in oil bath for 24 hours. The reaction mixture was quenched by the addition of diethyl ether (150 mL) and filtered through a pad of Celite. The filtrate and combined ethereal washings were concentrated by rotavapor. Purification by vacuum distillation (9 mm Hg, 59 ºC) gave 4-methoxy-2-trimethylsilyloxy-1,3-butadiene **93** (3.81 g, 22.1 mmol) as a colorless liquid in 55% yield.

Spectral data for **93**: ^{1}H NMR (500 MHz, $CDCl_3$) δ = 0.24 (s, 9H), 3.59 (s, 3H), 3.96 – 4.21 (m, 2H), 5.36 (d, *J* = 12.4, 1H), 6.83 (d, *J* = 12.3, 1H). These spectral data match those previously reported for this compound[21].

4.3.2 General procedure for preparing aldehyde 231w

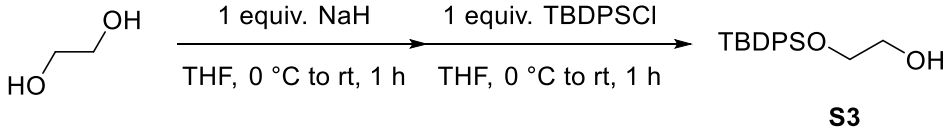

S3

*2-((tert-butyldiphenylsilyl)oxy)ethan-1-ol **S3**:* To a stirring mixture of sodium hydride (1.2 g, 30 mmol, 60% w/w in mineral oil) in 50 mL of freshly distilled THF at 0 ˚C was added ethylene glycol (1.7 mL, 30 mmol) and the resulting solution was warmed up to room temperature and stirred for 1 hour. Then a solution of *tert*-butyl(chloro)diphenylsilane (TBDPSCl, 30 mmol, 7.8 mL) in 20 mL THF was added to the stirring solution at 0 ˚C followed by warming up the reaction mixture to room temperature and stirring for another 1 h. The reaction was quenched by dilution of 100 mL diethyl ether and slow addition of 50 mL water. Then the separated organic layer was washed twice with 50 mL brine and dried over Na_2SO_4. After removing

the solvent under reduced pressure, the crude product was purified via column chromatography (30 x 250 mm, 10:1 hexane/ EtOAc as eluent) and the desired product **S3** (13.0 mmol, 3.91 g) was obtained as a light-yellow oil in 43% isolated yield.

Spectral data for **S3**: R_f = 0.15 (10:1 hexane: ethyl acetate); ^{1}H NMR (500 MHz, $CDCl_3$) δ = 1.14 (s, 9H), 3.71 – 3.74 (m, 2H), 3.79 - 3.84 (m, 2H), 7.40– 7.50 (m, 6H), 7.71 – 7.77 (m, 4H); ^{13}C NMR (126 MHz, $CDCl_3$) δ 19.28, 26.91, 63.73, 65.08, 127.82, 129.84, 133.32, 135.58. These spectral data match those previously reported for this compound[22].

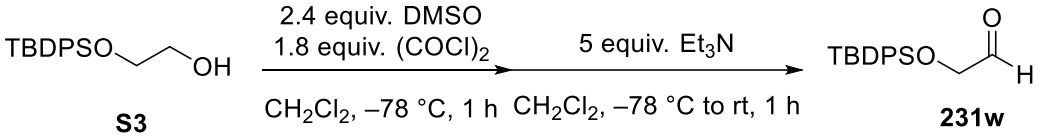

*2-((tert-butyldiphenylsilyl)oxy)acetaldehyde **231w**:* In an oven dried 250 mL round bottom flask under argon, oxalyl chloride ($(COCl)_2$, 23.4 mmol, 1.98 mL) and CH_2Cl_2 (50 mL) were added. Then the reaction flask was cooled down to -78 ˚C and a solution of DMSO (31.2 mmol, 2.22 mL) in 10 mL CH_2Cl_2 was added dropwise. After 10 minutes, alcohol **S3** (13.0 mmol, 3.91 g) solution in 20 mL of CH_2Cl_2 was added slowly and the reaction mixture was stirred at -78 ˚C for 1 h. The reaction was warmed up to room temperature and stirred for 1 h after the addition of Et_3N (65.0 mmol, 9.06 mL) and it was quenched by the slow addition of saturated aq NH_4Cl solution. The organic layer was separated and washed with brine and dried over Na_2SO_4. After removing the solvent under reduced pressure, the crude product was purified via column chromatography (30 x 250 mm, 10:1

hexane/ EtOAc as eluent) and the desired product **231w** (11.0 mmol, 3.29 g) was obtained as a light-yellow oil in 85% isolated yield.

Spectral data for **231w**: R_f = 0.2 (10:1 hexane: ethyl acetate); ^{1}H NMR (500 MHz, $CDCl_3$) δ = 1.12 (s, 9H), 4.23 (s, 2H), 7.39 – 7.43 (m, 4H), 7.44 – 7.48 (m, 2H), 7.65 – 7.69 (m, 4H), 9.74 (s, 1H); ^{13}C NMR (126 MHz, $CDCl_3$) δ 19.3, 26.8, 70.0, 127.7, 130.1, 132.5, 135.7, 201.7. These spectral data match those previously reported for this compound[22].

4.3.3 General procedure for preparing aldehyde 231y

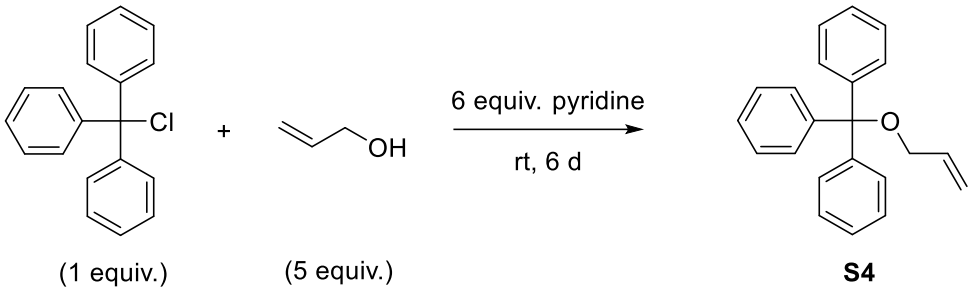

*allyl triphenylmethyl ether **S4**:* In an oven dried 100 mL round bottom flask was added triphenylmethyl chloride (5.58 g, 20.0 mmol), allyl alcohol (6.8 mL, 0.10 mol) and pyridine (9.7 mL, 0.12 mol). The reaction mixture was stirred for 6 days at room temperature before the precipitate was filtered off and washed with diethyl ether. The combined organic layer was washed with water and brine and was then dried over Na_2SO_4. After removing the solvent under reduced pressure, the crude product was purified via column chromatography (25 x 200 mm, 8:1 hexane/ CH_2Cl_2 as eluent) and the desired product **S4** (19.1 mmol, 5.74 g) was obtained as a white solid in 96% isolated yield.

Spectral data for **S4**: R_f = 0.25 (8:1 hexane: CH_2Cl_2); ^{1}H NMR (500 MHz, $CDCl_3$) δ = 3.63 (dt, *J* = 4.8, 1.7, 2H), 5.17 – 5.21 (m, 1H), 5.42 – 5.48 (m, 1H), 5.90 – 6.01 (m, 1H), 7.22 – 7.29 (m, 3H), 7.29 – 7.36 (m, 6H), 7.45 – 7.51 (m, 6H). These spectral data match those previously reported for this compound[23].

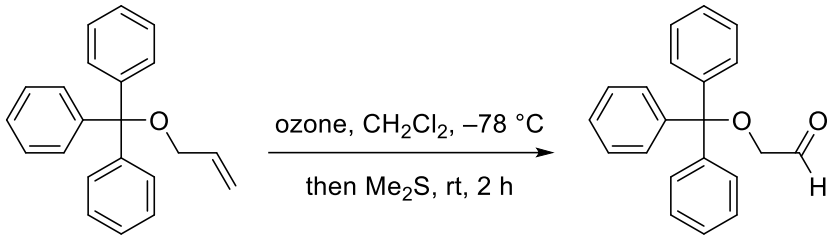

S4 **231y**

2-(trityloxy)acetaldehyde ***231y***: Ozone was bubbled through a pre-chilled solution at –78 °C of allyl triphenylmethyl ether **S4** (2.1 g, 7.0 mmol) in 50 mL CH_2Cl_2 containing $NaHCO_3$ (0.6 g, 7 mmol) until the pale blue color persisted. Excess ozone was flushed off with nitrogen gas and Me_2S (2.6 mL, 35 mmol) was added. The reaction mixture was warmed to room temperature and stirred for 2 h before the addition of 50 mL water. The organic layer was separated and washed with brine and dried over Na_2SO_4. After removing the solvent under reduced pressure, the crude product was purified via column chromatography (30 x 250 mm, 1:1 hexane/ CH_2Cl_2 as eluent) and the desired product **231y** (4.95 mmol, 1.50 g) was obtained as a colorless oil in 71% isolated yield.

Spectral data for **231y**: R_f = 0.2 (1:1 hexane: CH_2Cl_2); ^{1}H NMR (500 MHz, $CDCl_3$) δ = 3.90 (s, 2H), 7.27 – 7.40 (m, 9H), 7.49 – 7.55 (m, 6H), 9.53 (s, 1H). These spectral data match those previously reported for this compound[24].

4.3.4 General procedure for preparation of catalysts

Procedure E — preparation of the BINOL-propeller catalyst **216**:

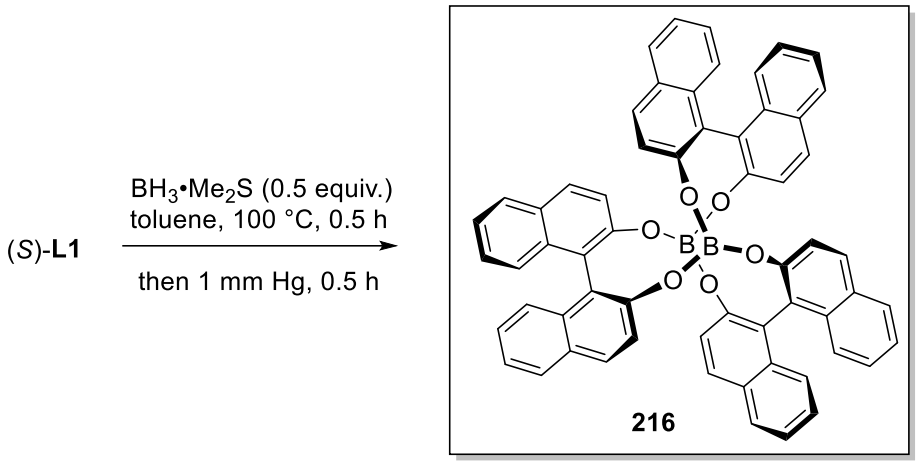

A 50 mL flamed dried Schlenk flask was equipped with a stir bar and connected to vacuum followed by flushing with nitrogen gas. To the flask was added (*S*)-BINOL (7.2 mg, 0.025 mmol) and freshly distilled toluene (1.5 mL) with nitrogen flow via the side arm. After all solids were dissolved, BH_3•Me_2S (6.3 μL, 0.013 mmol, as 2 M solution in toluene) was added via an oven-dried 50 μL syringe and the Schlenk flask was sealed and heated in an oil bath at 100 ºC. After 0.5 hour, the side arm of the Schlenk flask was connected to vacuum (1 mm Hg) and the Teflon cap was carefully loosened to apply vacuum to the solution in the flask. After the removal of solvent, white solids crashed out and the flask was kept in oil bath at 100 ºC for another 0.5 hours with vacuum. The flask containing BINOL-propeller catalyst **216** was allowed to cool to room temperature after 0.5 hours and flushed with nitrogen gas. NMR study revealed that the use of different equivalents of BH_3•Me_2S (6.3 to 50 μL, 0.0125 to 0.1 mmol, 0.5 to 4 equivalents, as 2 M solution in toluene) led to the same product **216**. The ^{1}H NMR spectrum of **216**

(with unreacted BINOL and toluene as impurity) is shown below. ^{1}H NMR (500 MHz, $CDCl_3$) δ = 6.62 – 6.68 (m, 12H), 7.03 (d, *J* = 8.2, 6H), 7.23 – 7.27 (m, 6H), 7.43 – 7.47 (m, 6H), 7.72 (d, *J* = 8.2, 6H). These spectral data match those previously reported for this compound[33].

^{1}H NMR Spectrum for 216

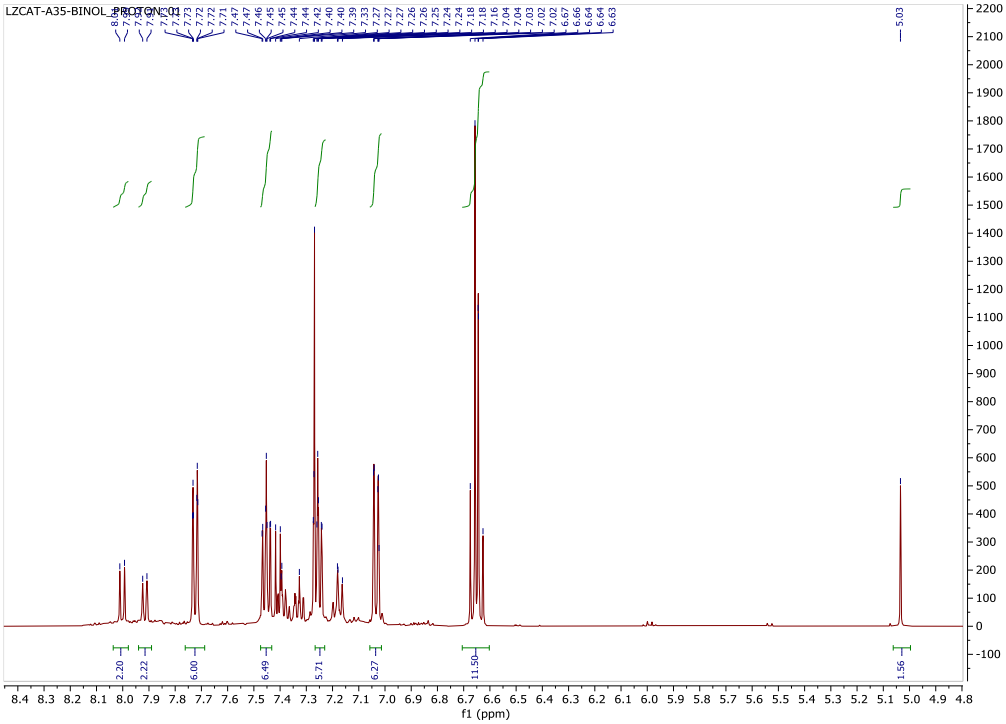

^{1}H NMR Spectrum for 216 (aromatic region)

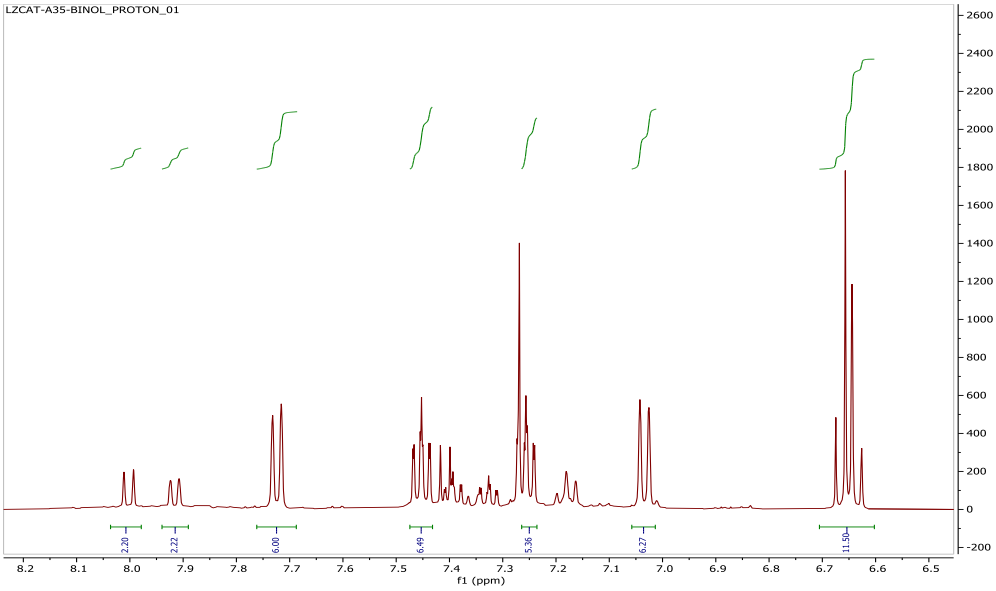

The ^{1}H NMR spectrum of **L1** (BINOL) is shown below.

^{1}H NMR Spectrum for BINOL

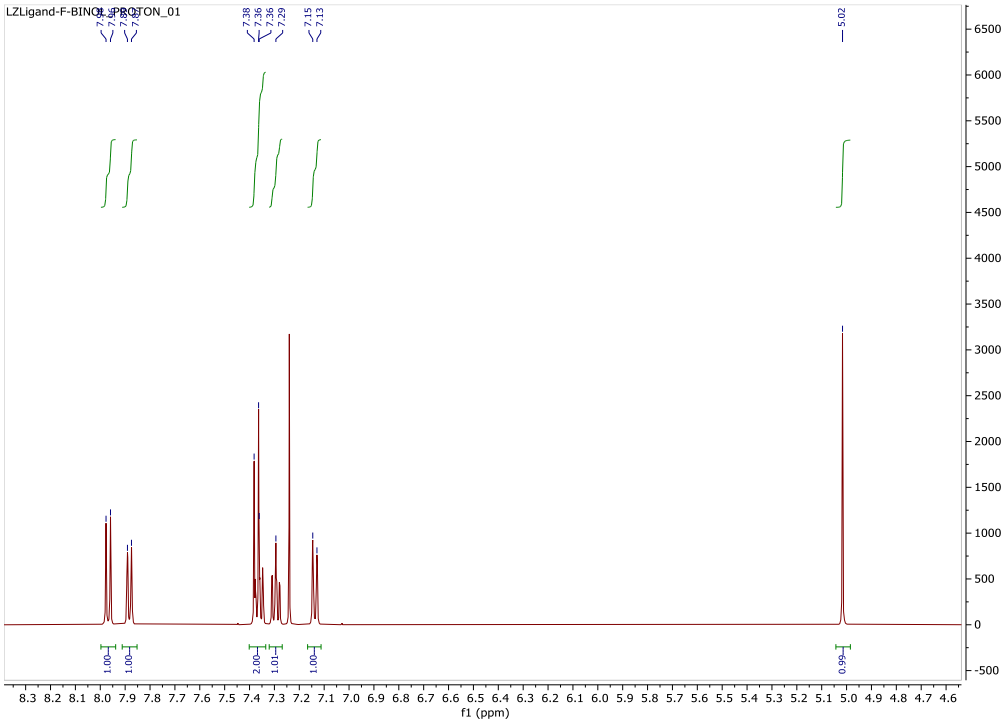

Procedure F — preparation of the borate ester catalyst **249**:

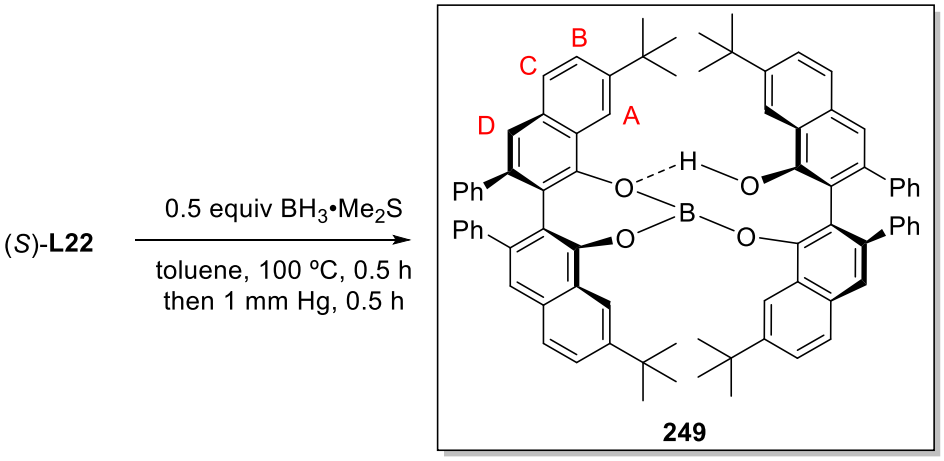

A 50 mL flame dried Schlenk flask was equipped with a stir bar and connected to vacuum followed by flushed with nitrogen gas. To the flask was added (*S*)-7,7'-*t*Bu$_2$VANOL (13.8 mg, 0.0250 mmol) and freshly distilled toluene (1.5 mL) with nitrogen flow via the side arm. After all solids were dissolved, BH_3•Me_2S (6.3 µL, 0.013 mmol, as 2 M solution in toluene) was added via an oven-dried 50 µL syringe and the Schlenk flask was sealed and heated in an oil bath at 100 ºC. After 0.5 hours, the side arm of the Schlenk flask was connected to vacuum (1 mm Hg) and the Teflon cap was carefully loosened to apply vacuum to the solution in the flask. After the removal of solvent, white solids crashed out and the flask was kept in oil bath at 100 ºC for another 0.5 hour with vacuum. The flask containing borate ester catalyst **249** was allowed to cool to room temperature after 0.5 hour and flushed with nitrogen gas.

The ^{1}H NMR spectrum of **249** (with unreacted **L22** as impurity) is shown below. The four *tert*-butyl groups of **249** shows the same signal as a singlet at 1.31 ppm, while the *tert*-butyl groups of the free ligand **L22** shows a singlet at 1.50 ppm.

^{1}H NMR (500 MHz, $CDCl_3$) δ = 1.31 (s, 36H, proton-*t*Bu), 6.58 – 6.61 (m, 8H, proton-Ph), 6.97 (dd, *J* = 8.7, 6.8, 8H, proton-Ph), 7.10 – 7.14 (m, 4H, proton-Ph), 7.39 (s, 4H, proton-D), 7.61 (dd, *J* = 8.6, 2.0, 4H, proton-B), 7.74 (d, *J* = 8.6, 4H, proton-C), 8.78 (d, *J* = 2.0, 4H, proton-A).

^{1}H NMR Spectrum for 249

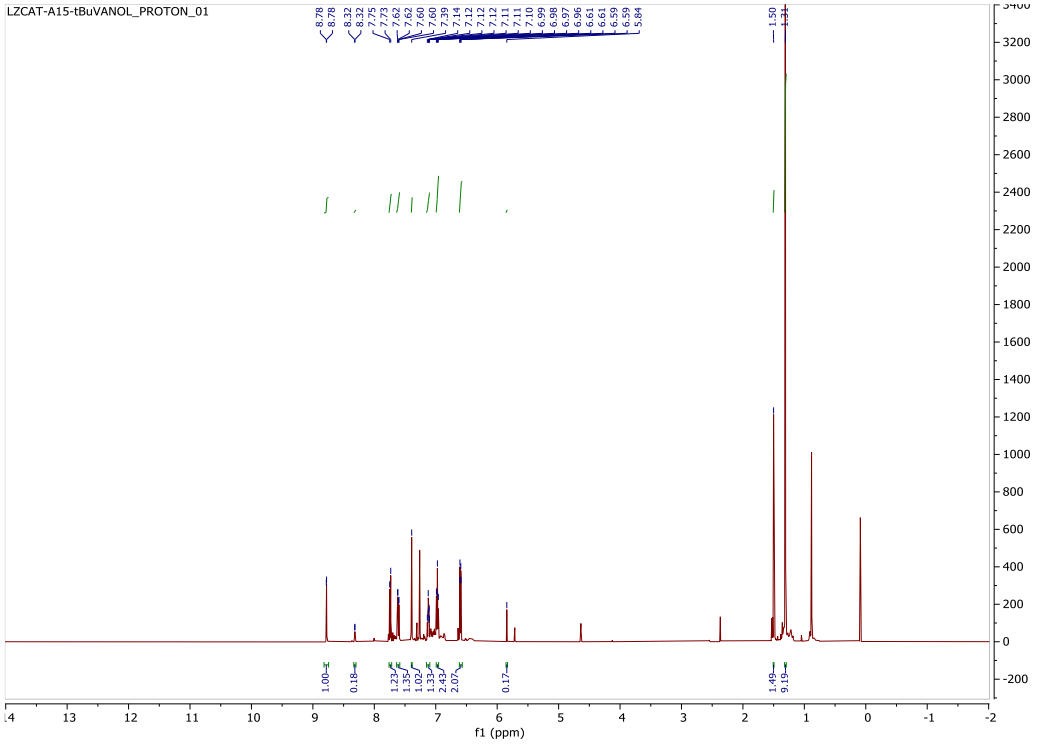

^{1}H NMR Spectrum for 249 (aromatic region)

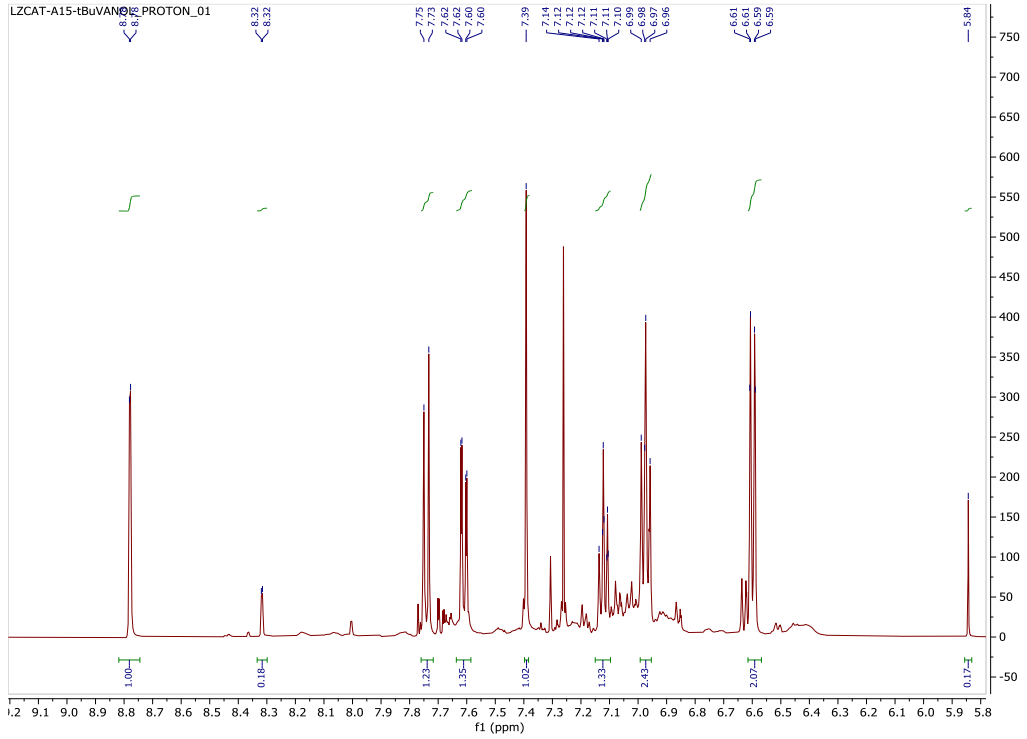

The ^{1}H NMR spectrum of **L22** (7,7'-*t*Bu$_2$VANOL) is shown below.

^{1}H NMR Spectrum for L22 (7,7'-*t*Bu$_2$VANOL)

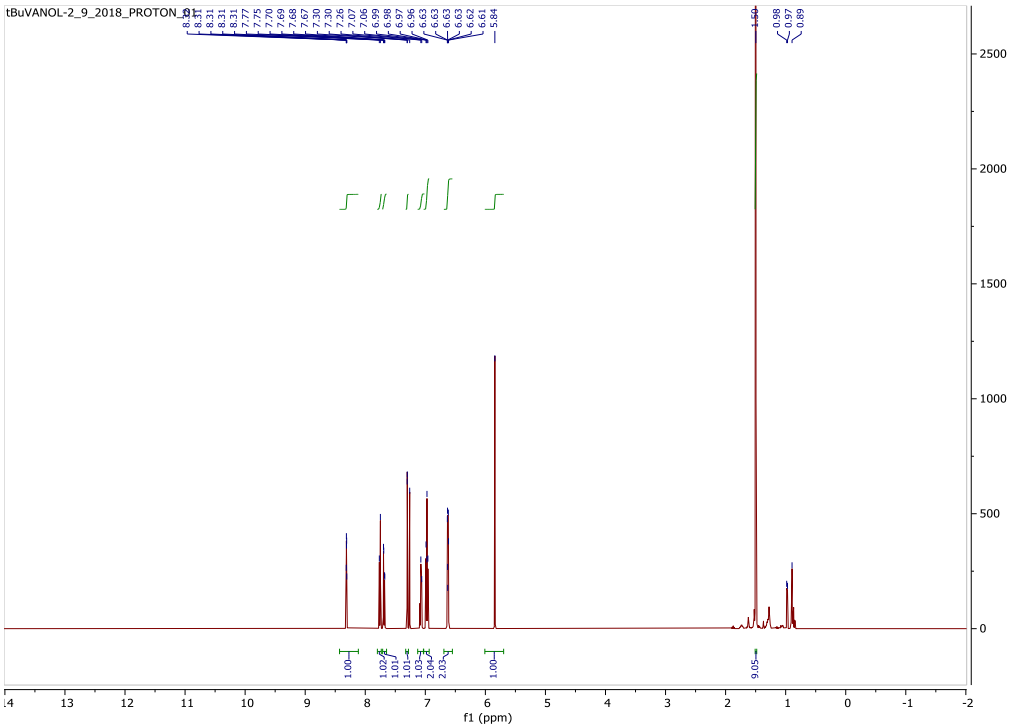

^{1}H NMR Spectrum for L22 (aromatic region)

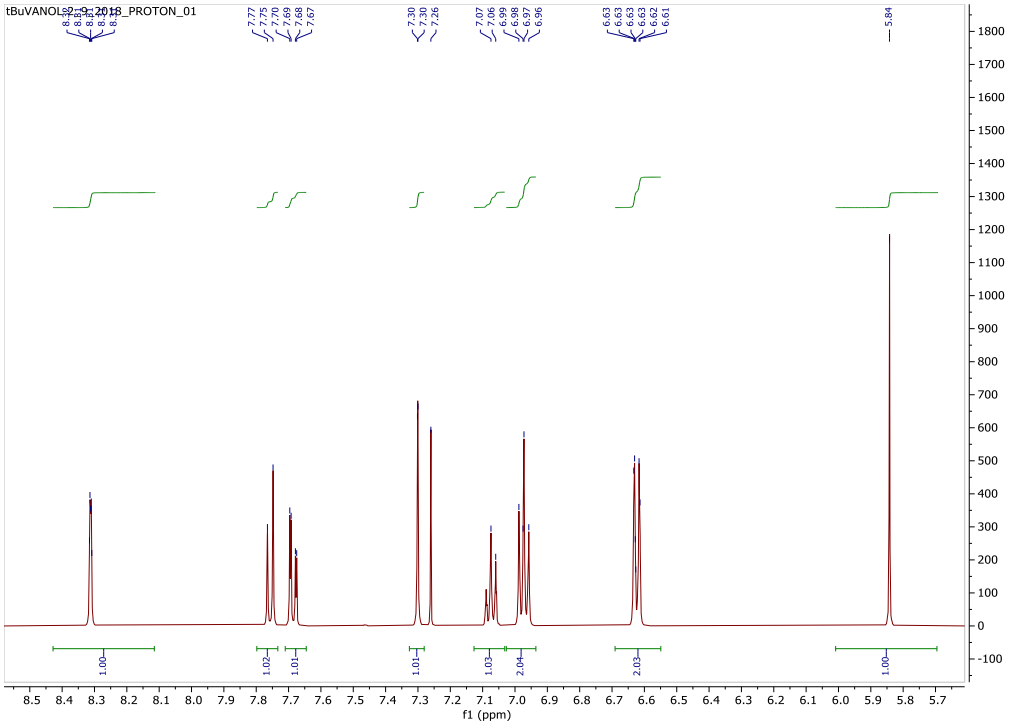

Procedure G — preparation of the VANOL-aluminum catalyst **253**:

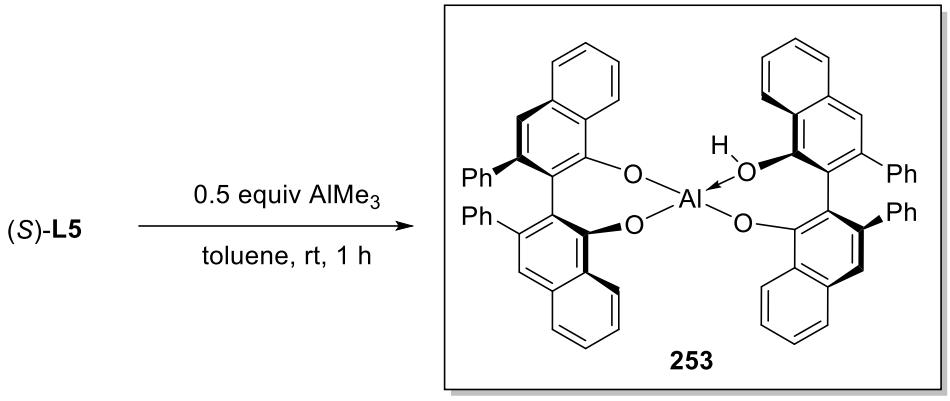

To a 10 mL oven-dried round bottom flask equipped with a stir bar was charged (*S*)-**L5** ((*S*)-**VANOL**, 22.0 mg, 0.050 mmol) and freshly distilled toluene (1 mL). Then a rubber septum stopper and argon balloon were attached. While stirring at room temperature, trimethylaluminum solution (13 μL, 0.025 mmol, 2 M in toluene) was added to the reaction flask. The stock solution of VANOL-aluminum catalyst **253** in toluene was achieved after stirring the mixture at room temperature for 1 hour.

4.3.5 General procedure for asymmetric HDA reaction

Procedure H — illustrated for the reaction of benzaldehyde **231a**:

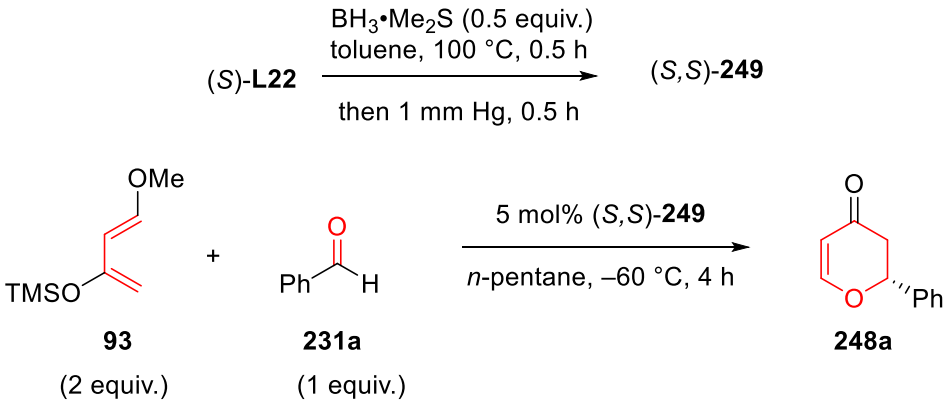

(R)-2-phenyl-2,3-dihydro-4H-pyran-4-one ***248a***: The catalyst **249** was prepared according to procedure F. To the Schlenk flask containing catalyst **249** with nitrogen flow was added 5 mL freshly distilled *n*-pentane and was swirled until all solids were dissolved. The flask was cooled to –60 °C for 10 minutes in a chiller with an ethanol cold bath followed by the addition of benzaldehyde **231a** (26 µL, 0.25 mmol) and diene **93** (97 µL, 0.50 mmol) with nitrogen flow through the side arm. The reaction was stirred at –60 °C for 4 hours before quenching with 2 mL 1 M HCl in MeOH/H_2O (1:1). The mixture was allowed to warm to room temperature and stirred for another 1 hour before the addition of 10 mL diethyl ether and 10 mL water, and then the layers were separated. The aqueous layer was extracted with diethyl ether (5 mL × 3). The combined organic layer was dried over Na_2SO_4 and concentrated under vacuum to afford the crude product. Purification of the crude product by silica gel chromatography (15 mm × 200 mm column, 4:1 hexanes/ EtOAc as eluent) afforded pure adduct **248a** as a colorless oil in 90% isolated yield (39.3 mg, 0.226 mmol); The optical purity of **248a** was determined to be 93% *ee* by HPLC (CHIRALCEL® OD column, 95:5 hexanes/2-propanol at 254 nm, flow-rate: 1 mL/min); retention times: R_t = 17.4 min (minor enantiomer, (*S*)-**248a**) and R_t = 20.7 min (major enantiomer, (*R*)-**248a**). The retention time for each enantiomer was confirmed by running the reaction with racemic **L22**.

Spectral data for **248a**: R_f = 0.28 (CH_2Cl_2); $[\alpha]_D^{20}$ = –112 (*c*=1.0 in $CHCl_3$) 93% *ee* (*R*) (lit.[25] $[\alpha]_D^{23}$ = +103.2 (*c*=0.5 in $CHCl_3$) 97% *ee* (*S*)); ^{1}H NMR (500 MHz, $CDCl_3$) δ = 2.68 (dd, *J* = 16.9, 3.5, 1H), 2.92 (dd, *J* = 16.9, 14.5, 1H), 5.44 (dd, *J* = 14.5, 3.4, 1H), 5.54 (d, *J* = 6.0, 1H), 7.38 – 7.45 (m, 5H), 7.49 (d, *J* = 6.0, 1H); ^{13}C

NMR (126 MHz, $CDCl_3$) δ 43.4, 81.1, 107.4, 126.1, 128.9, 129.0, 137.8, 163.3, 192.3. These spectral data match those previously reported for this compound.[25]

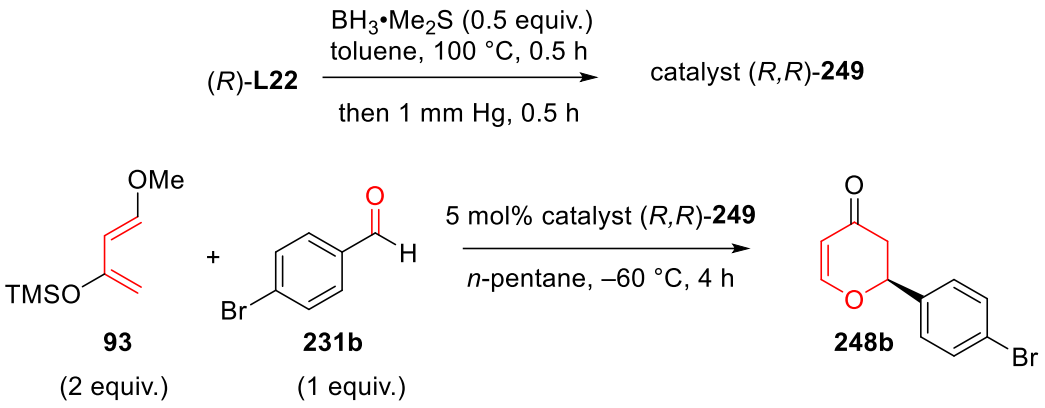

2-(4-bromophenyl)-2,3-dihydro-4H-pyran-4-one ***248b***: The catalyst *(R,R)*-**249** was prepared from (*R*)-**L22** according to procedure F and adduct **248b** was obtained according to procedure H with the use of aldehyde **231b** (46.3 mg, 0.250 mmol) and diene **93** (0.50 mmol, 97 µL). Purification of the crude product by silica gel chromatography (15 mm × 200 mm column, 4:1 hexanes/ EtOAc as eluent) afforded pure adduct **248b** as a yellow solid (m.p. 68-70 ˚C) in 94% isolated yield (59.2 mg, 0.234 mmol); The optical purity of **248b** was determined to be 91% *ee* by HPLC (CHIRALCEL® OD column, 95:5 hexanes/2-propanol at 254 nm, flow-rate: 1 mL/min); retention times: R_t = 18.3 min (major enantiomer) and R_t = 22.2 min (minor enantiomer). The retention time for each enantiomer was confirmed by running the reaction with racemic **L22**. The absolute configuration of **248b** was assumed to be S, homochiral with other products from same procedure, which configurations have been confirmed.

Spectral data for **248b**: R_f = 0.25 (CH_2Cl_2); $[\alpha]_D^{20}$ = +131 (*c*=1.0 in $CHCl_3$) 91% *ee*; ^{1}H NMR (500 MHz, $CDCl_3$) δ = 2.65 (dd, *J* = 16.8, 3.5, 1H), 2.85 (dd, *J* =

16.8, 14.4, 1H), 5.40 (dd, *J* = 14.4, 3.5, 1H), 5.54 (d, *J* = 6.0, 1H), 7.24 – 7.32 (m, 2H), 7.47 (d, *J* = 6.0, 1H), 7.53 – 7.57 (m, 2H); ^{13}C NMR (126 MHz, $CDCl_3$) δ 43.3, 80.3, 107.5, 122.9, 127.7, 132.0, 136.9, 163.0, 191.7. These spectral data match those previously reported for this compound.[26]

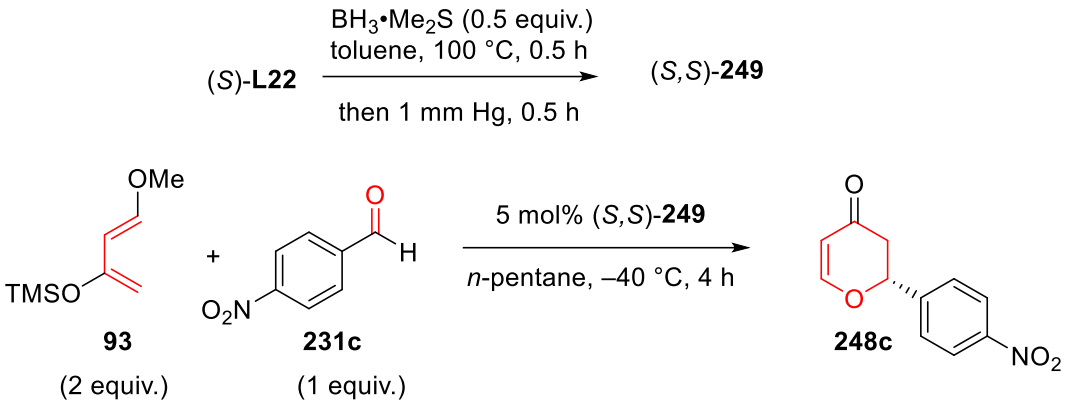

(R)-2-(4-nitrophenyl)-2,3-dihydro-4H-pyran-4-one ***248c***: The catalyst **249** was prepared from (*S*)-**L22** according to procedure F and adduct **248c** was obtained according to procedure H with the use of aldehyde **231c** (37.8 mg, 0.250 mmol) and diene **93** (0.50 mmol, 97 µL). Purification of the crude product by silica gel chromatography (10 mm × 150 mm column, 5:1 hexanes/ EtOAc as eluent) afforded pure adduct **248c** as a yellow solid (m.p. 96-98 ˚C) in 93% isolated yield (51.1 mg, 0.233 mmol); The optical purity of **248c** was determined to be 92% *ee* by HPLC (CHIRALCEL® OD-H column, 80:20 hexanes/2-propanol at 254 nm, flow-rate: 1 mL/min); retention times: R_t = 13.7 min (major enantiomer) and R_t = 16.5 min (minor enantiomer).

Spectral data for **248c**: R_f = 0.21 (CH_2Cl_2); $[\alpha]_D^{20}$ = –71 (*c*=1.0 in $CHCl_3$) 92% *ee*;) (lit.[25] $[\alpha]_D^{24}$ = +58.3 (*c*=1.0 in CH_2Cl_2) 94% *ee* (*S*)); ^{1}H NMR (500 MHz, $CDCl_3$) δ = 2.73 (dd, *J* = 16.9, 3.7, 1H), 2.85 (dd, *J* = 16.8, 14.2, 1H), 5.53 – 5.62 (m, 2H), 7.53 (d, *J* = 6.0, 1H), 7.57 – 7.64 (m, 2H), 8.28 – 8.34 (m, 2H); ^{13}C NMR (126 MHz, $CDCl_3$) δ 43.4, 79.7, 107.9, 124.2, 126.7, 144.9, 148.1, 162.6, 190.7. These spectral data match those previously reported for this compound.[33]

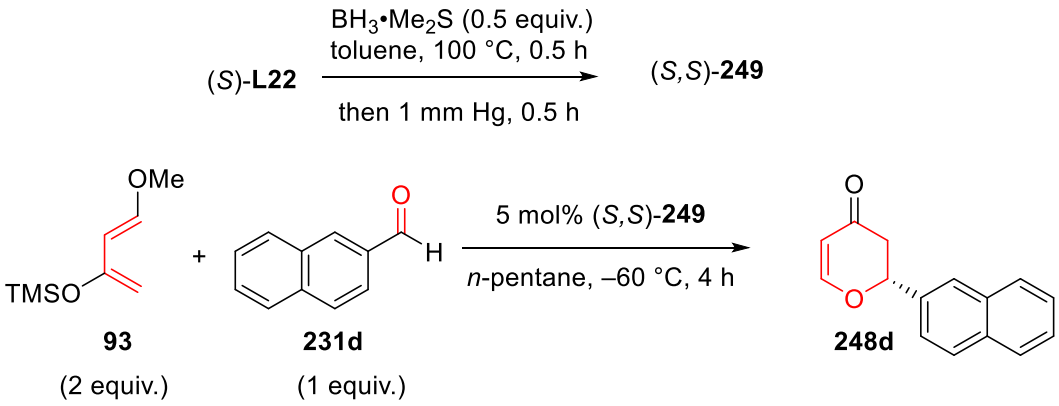

(R)-2-(2-naphthyl)-2,3-dihydro-4H-pyran-4-one ***248d***: The catalyst **249** was prepared from (*S*)-**L22** according to procedure F and adduct **248d** was obtained according to procedure H with the use of aldehyde **231d** (39.0 mg, 0.250 mmol) and diene **93** (0.50 mmol, 97 µL). Purification of the crude product by silica gel chromatography (10 mm × 150 mm column, 5:1 hexanes/ EtOAc as eluent) afforded pure adduct **248d** as a white solid (m.p. 57-59 ˚C) in 89% isolated yield (49.7 mg, 0.222 mmol); The optical purity of **248d** was determined to be 90% *ee* by HPLC (CHIRALCEL® OD column, 80:20 hexanes/2-propanol at 254 nm, flow-rate: 1 mL/min); retention times: R_t = 15.7 min (minor enantiomer) and R_t = 23.5 min (major enantiomer). The retention time for each enantiomer was confirmed by running the reaction with racemic **L22**.

Spectral data for **248d**: R_f = 0.12 (4:1 hexane/ EtOAc); $[\alpha]_D^{20}$ = –164 (*c*=1.0 in $CHCl_3$) 90% *ee*;) (lit.[27] $[\alpha]_D^{21}$ = +95.8 (*c*=1.03 in $CHCl_3$) 96% *ee* (*S*)); ^{1}H NMR (500 MHz, $CDCl_3$) δ = 2.76 (dd, *J* = 16.9, 3.5, 1H), 3.02 (dd, *J* = 16.9, 14.4, 1H), 5.57 (d, *J* = 6.0, 1H), 5.60 (dd, *J* = 14.4, 3.5, 1H), 7.47 – 7.57 (m, 4H), 7.84 – 7.89 (m, 3H), 7.91 (d, *J* = 8.5, 1H); ^{13}C NMR (126 MHz, $CDCl_3$) δ 42.8, 81.2, 107.1, 123.5, 125.4, 126.6, 126.7, 127.8, 128.2, 128.8, 133.1, 133.4, 135.7, 164.1, 192.9. These spectral data match those previously reported for this compound.[28]

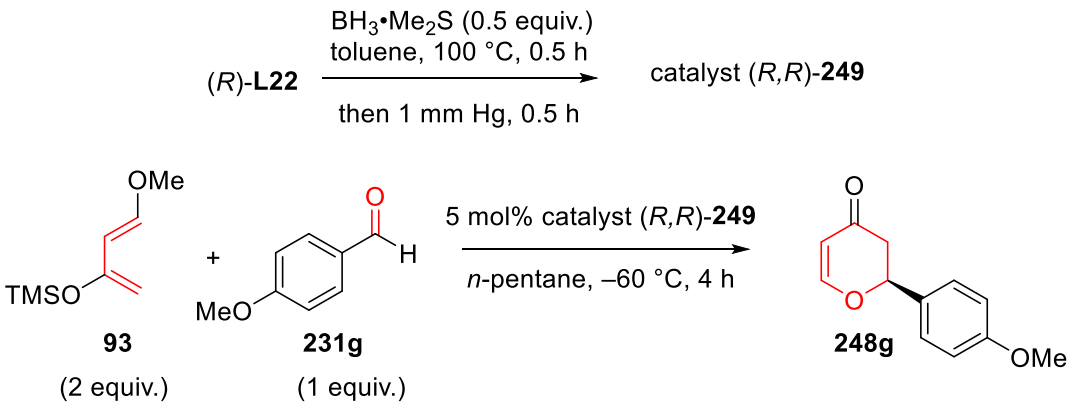

(S)-2-(4-methoxyphenyl)-2,3-dihydro-4H-pyran-4-one ***248g***: The catalyst *(R,R)*-**249** was prepared from (*R*)-**L22** according to procedure F and adduct **248g** was obtained according to procedure H with the use of aldehyde **231g** (30.4 µL, 0.250 mmol) and diene **93** (0.50 mmol, 97 µL). Purification of the crude product by silica gel chromatography (10 mm × 150 mm column, 5:1 hexanes/ EtOAc as eluent) afforded pure adduct **248g** as a yellow oil in 78% isolated yield (40.0 mg, 0.196 mmol); The optical purity of **248g** was determined to be 92% *ee* by HPLC (CHIRALCEL® OD-H column, 95:5 hexanes/2-propanol at 254 nm, flow-rate: 1 mL/min); retention times: R_t = 16.1 min (major enantiomer) and R_t = 18.3 min

(minor enantiomer). The retention time for each enantiomer was confirmed by running the reaction with racemic **L22**.

Spectral data for **248g**: R_f = 0.13 (4:1 hexane/ EtOAc); $[\alpha]_D^{20}$ = +95 (*c*=1.0 in $CHCl_3$) 92% *ee*;) (lit.[27] $[\alpha]_D^{23}$ = +121 (*c*=1.04 in $CHCl_3$) 99% *ee* (*S*)); ^{1}H NMR (500 MHz, $CDCl_3$) δ = 2.57 – 2.67 (m, 1H), 2.93 (dd, *J* = 16.9, 14.5, 1H), 3.83 (s, 3H), 5.38 (dd, *J* = 14.5, 3.4, 1H), 5.52 (d, *J* = 6.0, 1H), 6.87 – 6.98 (m, 2H), 7.29 – 7.37 (m, 2H), 7.46 (d, *J* = 6.0, 1H); ^{13}C NMR (126 MHz, $CDCl_3$) δ 43.2, 55.4, 80.9, 107.3, 114.2, 127.8, 129.8, 160.1, 163.3, 192.5. These spectral data match those previously reported for this compound.[28]

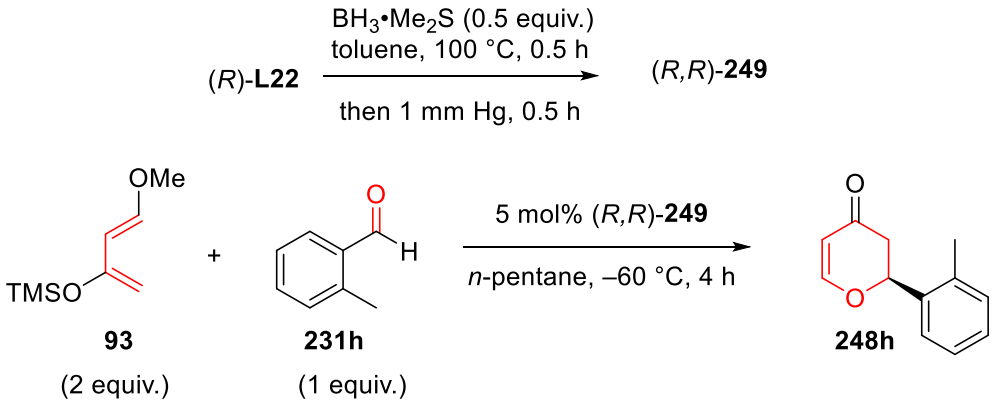

(S)-2-(2-methylphenyl)-2,3-dihydro-4H-pyran-4-one ***248h***: The catalyst *(R,R)*-**249** was prepared from (*R*)-**L22** according to procedure F and adduct **248h** was obtained according to procedure H with the use of aldehyde **231h** (28.9 µL, 0.250 mmol) and diene **93** (0.50 mmol, 97 µL). Purification of the crude product by silica gel chromatography (15 mm × 200 mm column, 4:1 hexanes/ EtOAc as eluent) afforded pure adduct **248h** as a colorless oil in 91% isolated yield (42.8 mg, 0.227 mmol); The optical purity of **248h** was determined to be 93% *ee* by HPLC

(CHIRALCEL® OD column, 95:5 hexanes/2-propanol at 254 nm, flow-rate: 1 mL/min); retention times: R_t = 15.2 min (major enantiomer) and R_t = 22.1 min (minor enantiomer). The retention time for each enantiomer was confirmed by running the reaction with racemic **L22**.

Spectral data for **248h**: R_f = 0.28 (CH_2Cl_2); $[\alpha]_D^{20}$ = +34 (*c*=1.0 in $CHCl_3$) 93% *ee*;) (lit.[25] $[\alpha]_D^{16}$ = +40.6 (*c*=0.5 in $CHCl_3$) 92% *ee* (*S*)); ^{1}H NMR (500 MHz, $CDCl_3$) δ = 2.36 (s, 3H), 2.61 (dd, *J* = 17.0, 3.3, 1H), 2.89 (dd, *J* = 16.9, 14.7, 1H), 5.54 (d, *J* = 6.0, 1H), 5.64 (dd, *J* = 14.7, 3.2, 1H), 7.19 – 7.24 (m, 1H), 7.27 – 7.31 (m, 2H), 7.45 – 7.49 (m, 1H), 7.51 (d, *J* = 6.0, 1H); ^{13}C NMR (126 MHz, $CDCl_3$) δ 18.9, 42.4, 78.5, 107.3, 125.7, 126.5, 128.8, 130.9, 135.1, 135.9, 163.5, 192.4. These spectral data match those previously reported for this compound.[25]

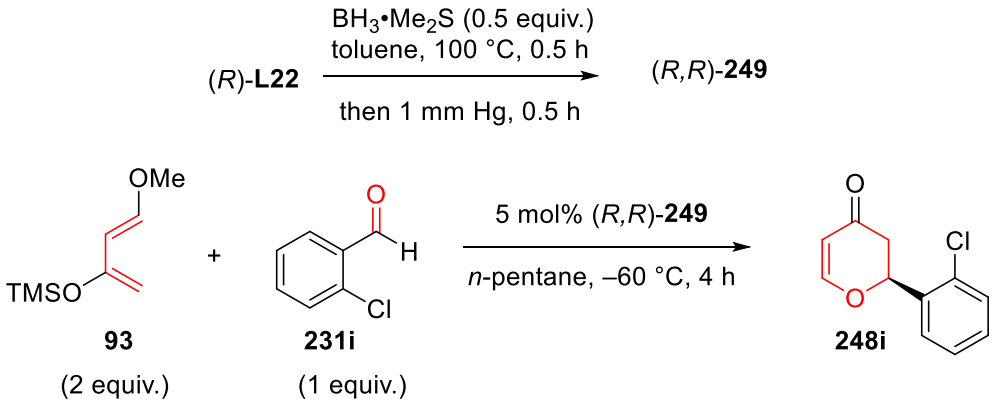

(S)-2-(2-chlorophenyl)-2,3-dihydro-4H-pyran-4-one ***248i***: The catalyst *(R,R)*-**249** was prepared from (*R*)-**L22** according to procedure F and adduct **248i** was obtained according to procedure H with the use of aldehyde **231i** (28.2 µL, 0.250 mmol) and diene **93** (0.50 mmol, 97 µL). Purification of the crude product by silica gel chromatography (15 mm × 200 mm column, 4:1 hexanes/ EtOAc as eluent) afforded pure adduct **248i** as a colorless oil in 94% isolated yield (49.2 mg,

0.236 mmol); The optical purity of **248i** was determined to be 93% *ee* by HPLC (CHIRALCEL® OD column, 97:3 hexanes/2-propanol at 254 nm, flow-rate: 1 mL/min); retention times: R_t = 25.6 min (major enantiomer) and R_t = 31.7 min (minor enantiomer). The retention time for each enantiomer was confirmed by running the reaction with racemic **L22**.

Spectral data for **248i**: R_f = 0.27 (CH_2Cl_2); $[\alpha]_D^{20}$ = –68 (*c*=1.0 in $CHCl_3$) 90% *ee*;) (lit.[29] $[\alpha]_D^{25}$ = –127 (*c*=0.24 in $CHCl_3$) 98% *ee* (*S*)); ^{1}H NMR (500 MHz, $CDCl_3$) δ = 2.72 (dd, *J* = 16.9, 14.1, 1H), 2.80 (dd, *J* = 16.9, 3.8, 1H), 5.56 (d, *J* = 6.0, 1H), 5.83 (dd, *J* = 14.1, 3.8, 1H), 7.32 (td, *J* = 7.6, 1.8, 1H), 7.36 (td, *J* = 7.5, 1.5, 1H), 7.40 (dd, *J* = 7.8, 1.5, 1H), 7.52 (d, *J* = 6.1, 1H), 7.60 (dd, *J* = 7.7, 1.8, 1H); ^{13}C NMR (126 MHz, $CDCl_3$) δ 42.1, 78.1, 107.6, 127.1, 127.4, 129.8(x2), 131.7, 136.7, 162.6, 191.7. These spectral data match those previously reported for this compound.[34]

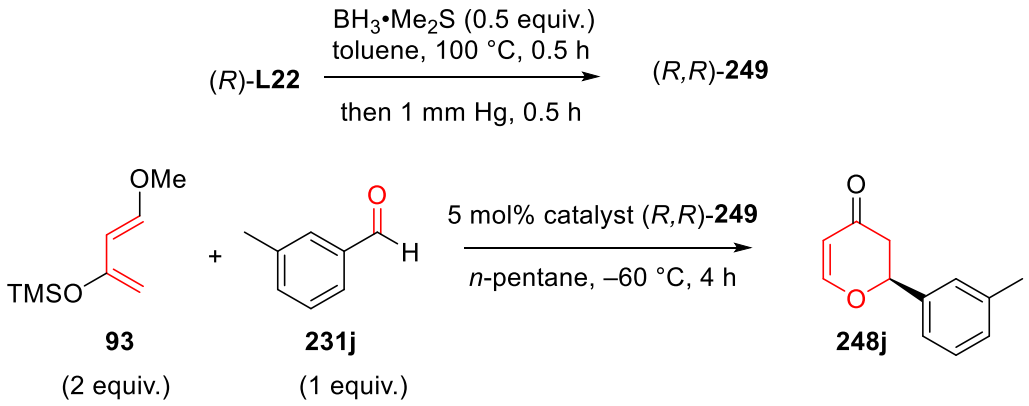

(S)-2-(3-methylphenyl)-2,3-dihydro-4H-pyran-4-one ***248j***: The catalyst *(R,R)*-**249** was prepared from (*R*)-**L22** according to procedure F and adduct **248j** was obtained according to procedure H with the use of aldehyde **231j** (29.5 µL, 0.250 mmol) and diene **93** (0.50 mmol, 97 µL). Purification of the crude product by

silica gel chromatography (15 mm × 200 mm column, 4:1 hexanes/ EtOAc as eluent) afforded pure adduct **248j** as a colorless oil in 96% isolated yield (45.0 mg, 0.239 mmol); The optical purity of **248j** was determined to be 95% *ee* by HPLC (CHIRALCEL® OD column, 95:5 hexanes/2-propanol at 254 nm, flow-rate: 1 mL/min); retention times: R_t = 14.6 min (major enantiomer) and R_t = 18.2 min (minor enantiomer). The retention time for each enantiomer was confirmed by running the reaction with racemic **L22**.

Spectral data for **248j**: R_f = 0.28 (CH_2Cl_2); $[\alpha]_D^{20}$ = +69 (*c*=1.0 in $CHCl_3$) 95% *ee*;) (lit.[25] $[\alpha]_D^{16}$ = +89.8 (*c*=0.45 in $CHCl_3$) 92% *ee* (*S*)); ^{1}H NMR (500 MHz, $CDCl_3$) δ = 2.40 (s, 3H), 2.65 (dd, *J* = 16.9, 3.4, 1H), 2.92 (dd, *J* = 16.9, 14.5, 1H), 5.39 (dd, *J* = 14.5, 3.4, 1H), 5.53 (d, *J* = 6.0, 1H), 7.17 – 7.25 (m, 3H), 7.32 (t, *J* = 7.6, 1H), 7.48 (d, *J* = 6.0, 1H); ^{13}C NMR (126 MHz, $CDCl_3$) δ 21.5, 43.4, 81.2, 107.3, 123.2, 126.8, 128.8, 129.7, 137.8, 138.7, 163.2, 192.3. These spectral data match those previously reported for this compound.[25]

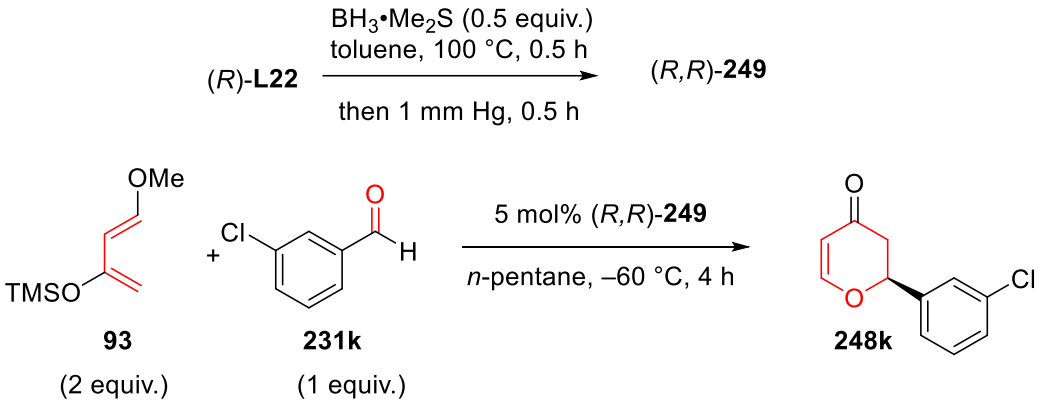

2-(3-chlorophenyl)-2,3-dihydro-4H-pyran-4-one ***248k***: The catalyst *(R,R)*-**249** was prepared from (*R*)-**L22** according to procedure F and adduct **248k** was

obtained according to procedure H with the use of aldehyde **231k** (28.3 µL, 0.250 mmol) and diene **93** (0.50 mmol, 97 µL). Purification of the crude product by silica gel chromatography (15 mm × 200 mm column, 4:1 hexanes/ EtOAc as eluent) afforded pure adduct **248k** as a colorless oil in 88% isolated yield (46.1 mg, 0.221 mmol); The optical purity of **248k** was determined to be 90% *ee* by HPLC (CHIRALCEL® OD column, 98:2 hexanes/2-propanol at 254 nm, flow-rate: 1 mL/min); retention times: R_t = 26.5 min (major enantiomer) and R_t = 37.9 min (minor enantiomer). The retention time for each enantiomer was confirmed by running the reaction with racemic **L22**. The absolute configuration of **248k** was assumed to be S, homochiral with other products from same procedure, which configurations have been confirmed.

Spectral data for **248k**: R_f = 0.26 (CH_2Cl_2); $[\alpha]_D^{20}$ = +52 (*c*=1.0 in $CHCl_3$) 90% *ee*); ^{1}H NMR (500 MHz, $CDCl_3$) δ = 2.66 (dd, *J* = 16.8, 3.5, 1H), 2.86 (dd, *J* = 16.8, 14.4, 1H), 5.41 (dd, *J* = 14.4, 3.5, 1H), 5.54 (d, *J* = 6.0, 1H), 7.24 – 7.29 (m, 1H), 7.33 – 7.38 (m, 2H), 7.40 – 7.45 (m, 1H), 7.48 (d, *J* = 6.0, 1H); ^{13}C NMR (126 MHz, $CDCl_3$) δ 43.4, 80.7, 107.6, 124.1, 126.3, 129.0, 130.2, 134.8, 139.9, 162.9, 191.5. These spectral data match those previously reported for this compound.[30]

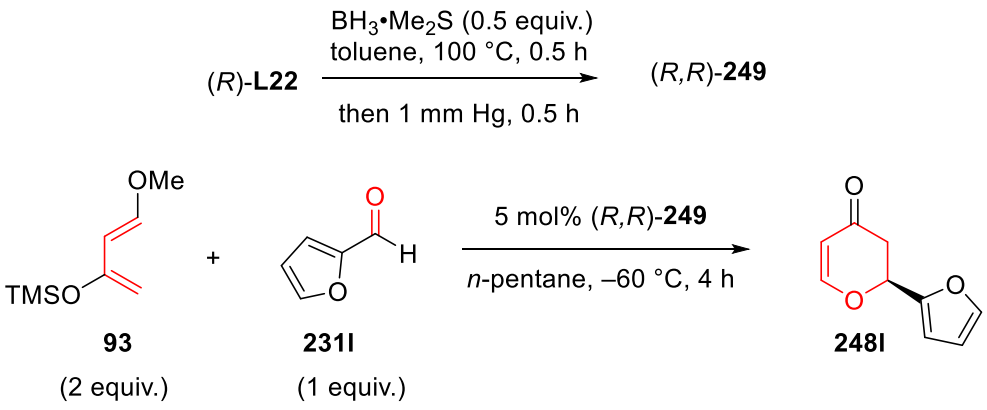

(S)-2-(2-furyl)-2,3-dihydro-4H-pyran-4-one ***248l***: The catalyst *(R,R)*-**249** was prepared from (*R*)-**L22** according to procedure F and adduct **248l** was obtained according to procedure H with the use of aldehyde **231l** (20.7 µL, 0.250 mmol) and diene **93** (0.50 mmol, 97 µL). Purification of the crude product by silica gel chromatography (15 mm × 200 mm column, 4:1 hexanes/ EtOAc as eluent) afforded pure adduct **248l** as a yellow solid (m.p. 66-67 ˚C) in 86% isolated yield (35.4 mg, 0.216 mmol); The optical purity of **248l** was determined to be 94% *ee* by HPLC (CHIRALCEL® OD column, 95:5 hexanes/2-propanol at 254 nm, flow-rate: 1 mL/min); retention times: R_t = 16.4 min (minor enantiomer) and R_t = 17.9 min (major enantiomer). The retention time for each enantiomer was confirmed by running the reaction with racemic **L22**.

Spectral data for **248l**: R_f = 0.26 (CH_2Cl_2); $[\alpha]_D^{20}$ = +126 (*c*=1.0 in $CHCl_3$) 94% *ee*;) (lit.[25] $[\alpha]_D^{23}$ = +255.4 (*c*=0.5 in $CHCl_3$) 67% *ee* (*S*)); ^{1}H NMR (500 MHz, $CDCl_3$) δ = 2.73 (dd, *J* = 16.9, 3.9, 1H), 3.09 (dd, *J* = 16.9, 12.9, 1H), 5.45 – 5.49 (m, 1H), 5.50 (d, *J* = 6.1, 1H), 6.41 (dd, *J* = 3.4, 1.8, 1H), 6.44 – 6.46 (m, 1H), 7.37 (d, *J* = 6.0, 1H), 7.47 – 7.48 (m, 1H); ^{13}C NMR (126 MHz, $CDCl_3$) δ 39.5, 73.5, 107.4, 109.7, 110.6, 143.6, 150.0, 162.4, 191.3. These spectral data match those previously reported for this compound.[25]

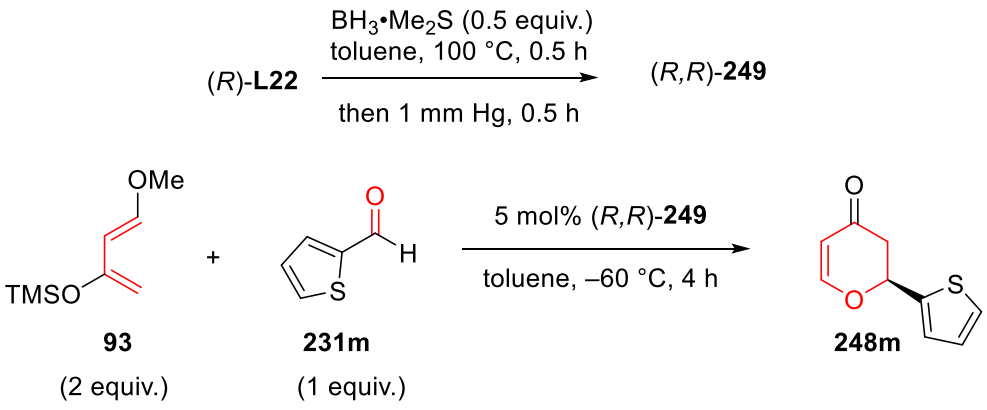

2-(2-thiophenyl)-2,3-dihydro-4H-pyran-4-one ***248m***: The catalyst *(R,R)*-**249** was prepared from (*R*)-**L22** according to procedure F and adduct **248m** was obtained according to procedure H with the use of aldehyde **231m** (23.4 µL, 0.250 mmol) and diene **93** (0.50 mmol, 97 µL). Toluene as solvent instead of *n*-pentane was employed. Purification of the crude product by silica gel chromatography (15 mm × 200 mm column, 4:1 hexanes/ EtOAc as eluent) afforded pure adduct **248m** as a yellow oil in 72% isolated yield (32.6 mg, 0.181 mmol); The optical purity of **248m** was determined to be 85% *ee* by HPLC (CHIRALPAK® AD column, 99:1 hexanes/2-propanol at 254 nm, flow-rate: 1 mL/min); retention times: R_t = 39.9 min (minor enantiomer) and R_t = 46.4 min (major enantiomer). The retention time for each enantiomer was confirmed by running the reaction with racemic **L22**. The absolute configuration of **248m** was assumed to be S, homochiral with other products from same procedure, which configurations have been confirmed.

Spectral data for **248m**: R_f = 0.25 (CH_2Cl_2); $[\alpha]_D^{20}$ = +125 (*c*=1.0 in $CHCl_3$) 85% *ee*); ^{1}H NMR (500 MHz, $CDCl_3$) δ = 2.83 (dd, *J* = 16.8, 3.7, 1H), 3.03 (dd, *J* = 16.8, 13.3, 1H), 5.53 (d, *J* = 6.1, 1H), 5.68 (dd, *J* = 13.2, 3.7, 1H), 7.04 (dd, *J* = 5.1, 3.5, 1H), 7.12 (d, *J* = 3.7, 1H), 7.37 – 7.45 (m, 2H); ^{13}C NMR (126 MHz, $CDCl_3$) δ 43.1, 76.5, 107.6, 126.3, 126.7, 126.9, 140.3, 162.7, 191.4. These spectral data match those previously reported for this compound.[27]

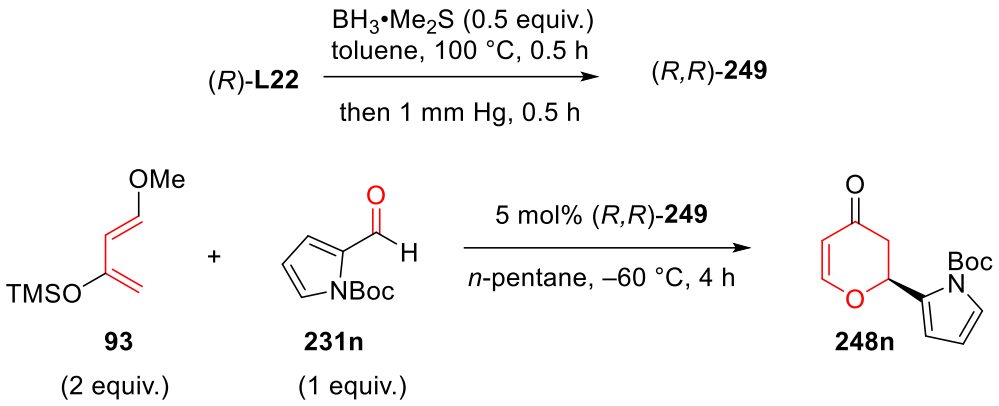

N-Boc-2-(2-pyrrol)-2,3-dihydro-4H-pyran-4-one ***248n***: The catalyst *(R,R)*-**249** was prepared from (*R*)-**L22** according to procedure F and adduct **248n** was obtained according to procedure H with the use of aldehyde **231n** (48.8 mg, 0.250 mmol) and diene **93** (0.50 mmol, 97 µL). Purification of the crude product by silica gel chromatography (15 mm × 200 mm column, 4:1 hexanes/ EtOAc as eluent) afforded pure adduct **248n** as a yellow oil in 92% isolated yield (60.4 mg, 0.229 mmol); The optical purity of **248n** was determined to be 93% *ee* by HPLC (CHIRALCEL® OJ-H column, 95:5 hexanes/2-propanol at 254 nm, flow-rate: 1 mL/min); retention times: R_t = 16.6 min (minor enantiomer) and R_t = 21.5 min (major enantiomer). The retention time for each enantiomer was confirmed by running the reaction with racemic **L22**. The absolute configuration of **248n** was assumed to be S, homochiral with other products from same procedure, which configurations have been confirmed.

Spectral data for **248n**: R_f = 0.27 (CH_2Cl_2); $[\alpha]_D^{20}$ = +114 (*c*=1.0 in $CHCl_3$) 93% *ee*); ^{1}H NMR (500 MHz, $CDCl_3$) δ = 1.60 (s, 9H), 2.84 (dd, *J* = 16.7, 4.1, 1H), 2.93 (dd, *J* = 16.6, 12.4, 1H), 5.49 (d, *J* = 6.0, 1H), 6.10 (dd, *J* = 12.4, 4.1, 1H), 6.19 (t, *J* = 3.4, 1H), 6.39 (dd, *J* = 3.5, 1.8, 1H), 7.32 (dd, *J* = 3.3, 1.7, 1H), 7.40 (d, *J* = 6.0, 1H); ^{13}C NMR (126 MHz, $CDCl_3$) δ 28.0, 41.2, 73.8, 84.6, 107.2, 110.3, 113.6, 123.3, 130.6, 148.7, 162.9, 192.4; HRMS (ESI-TOF) *m/z* 264.1236 [(M-H$^+$); calcd. for $C_{14}H_{18}NO_4$: 264.1236].

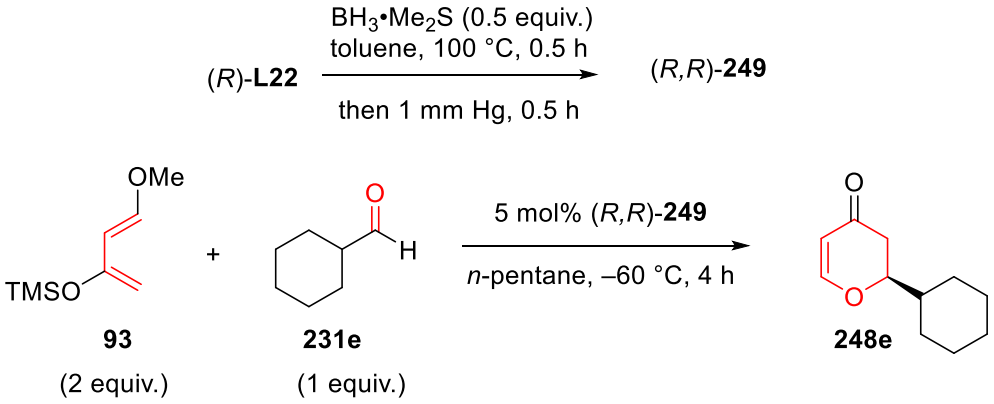

(S)-2-cyclohexyl-2,3-dihydro-4H-pyran-4-one ***248e***: The catalyst *(R,R)*-**249** was prepared from (*R*)-**L22** according to procedure F and adduct **248e** was obtained according to procedure H with the use of aldehyde **231e** (30.3 µL, 0.250 mmol) and diene **93** (0.50 mmol, 97 µL). Purification of the crude product by silica gel chromatography (15 mm × 200 mm column, 5:1 hexanes/ EtOAc as eluent) afforded pure adduct **248e** as a colorless oil in 97% isolated yield (43.6 mg, 0.242 mmol); The optical purity of **248e** was determined to be 98% *ee* by HPLC (CHIRALCEL® OD column, 99:1 hexanes/2-propanol at 254 nm, flow-rate: 1 mL/min); retention times: R_t = 14.6 min (major enantiomer) and R_t = 16.4 min

(minor enantiomer). The retention time for each enantiomer was confirmed by running the reaction with racemic **L22**.

Spectral data for **248e**: R_f = 0.19 (4:1 hexane/ EtOAc); $[\alpha]_D^{20}$ = +130 (*c*=1.0 in $CHCl_3$) 98% *ee*;) (lit.[25] $[\alpha]_D^{16}$ = +112 (*c*=0.1 in $CHCl_3$) 68% *ee* (*S*)); ^{1}H NMR (500 MHz, $CDCl_3$) δ = 1.00 – 1.91 (m, 11H), 2.38 (dd, *J* = 16.7, 3.3, 1H), 2.55 (dd, *J* = 16.7, 14.5, 1H), 4.16 (ddd, *J* = 14.5, 5.8, 3.3, 1H), 5.39 (d, *J* = 5.9, 1H), 7.37 (d, *J* = 5.9, 1H); ^{13}C NMR (126 MHz, $CDCl_3$) δ 25.8, 25.9, 26.2, 28.0, 28.1, 39.1, 41.4, 84.2, 106.8, 164.8, 193.9. These spectral data match those previously reported for this compound.[25]

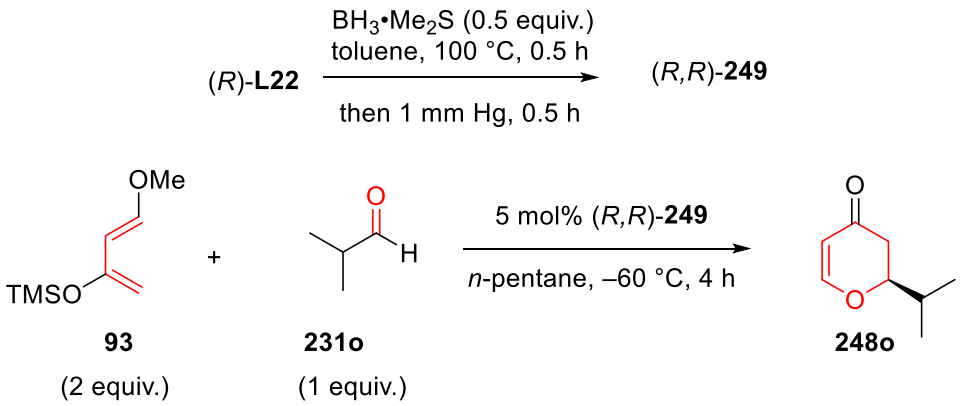

2-(iso-propyl)-2,3-dihydro-4H-pyran-4-one ***248o***: The catalyst *(R,R)*-**249** was prepared from (*R*)-**L22** according to procedure F and adduct **248o** was obtained according to procedure H with the use of aldehyde **231o** (23.0 µL, 0.250 mmol) and diene **93** (0.50 mmol, 97 µL). Toluene as solvent instead of *n*-pentane was employed. Purification of the crude product by silica gel chromatography (10 mm × 250 mm column, 4:1 hexanes/ EtOAc as eluent) afforded pure adduct **248o** as a colorless oil in 81% isolated yield (28.3 mg, 0.202 mmol); The optical purity of **248o** was determined to be 89% *ee* by HPLC (CHIRALCEL® OD-H column,

99.5:0.5 hexanes/2-propanol at 254 nm, flow-rate: 1 mL/min); retention times: R_t = 10.3 min (major enantiomer) and R_t = 11.4 min (minor enantiomer). The retention time for each enantiomer was confirmed by running the reaction with racemic **L22**. The absolute configuration of **248b** was assumed to be S, homochiral with other products from same procedure, which configurations have been confirmed.

Spectral data for **248o**: R_f = 0.25 (CH_2Cl_2); $[\alpha]_D^{20}$ = +82 (*c*=1.0 in $CHCl_3$) 89% *ee*); ^{1}H NMR (500 MHz, $CDCl_3$) δ = 1.01 (dd, *J* = 11.4, 6.8, 6H), 1.94 – 2.03 (m, 1H), 2.39 (dd, *J* = 16.7, 3.3, 1H), 2.54 (dd, *J* = 16.6, 14.6, 1H), 4.12 – 4.19 (m, 1H), 5.37 – 5.42 (m, 1H), 7.38 (d, *J* = 6.0, 1H). These spectral data match those previously reported for this compound.[35]

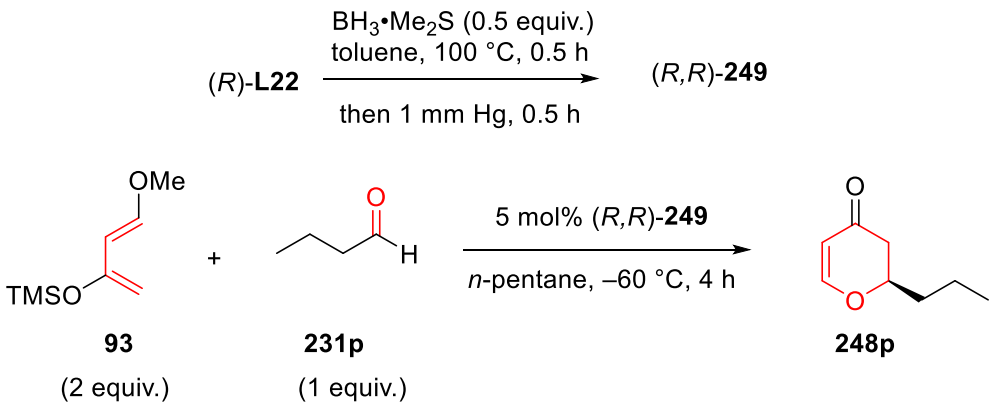

(R)-2-(n-propyl)-2,3-dihydro-4H-pyran-4-one ***248p***: The catalyst *(R,R)*-**249** was prepared from (*R*)-**L22** according to procedure F and adduct **248p** was obtained according to procedure H with the use of aldehyde **231p** (22.5 µL, 0.250 mmol) and diene **93** (0.50 mmol, 97 µL). Purification of the crude product by silica gel chromatography (15 mm × 200 mm column, 5:1 hexanes/ EtOAc as eluent) afforded pure adduct **248p** as a colorless oil in 95% isolated yield (33.2 mg, 0.237 mmol); The optical purity of **248p** was determined to be 90% *ee* by HPLC

(CHIRALCEL® OD column, 99:1 hexanes/2-propanol at 254 nm, flow-rate: 1 mL/min); retention times: R_t = 14.1 min (major enantiomer) and R_t = 15.3 min (minor enantiomer). The retention time for each enantiomer was confirmed by running the reaction with racemic **L22**.

Spectral data for **248p**: R_f = 0.25 (CH_2Cl_2); $[\alpha]_D^{20}$ = +75 (*c*=1.0 in $CHCl_3$) 90% *ee*;) (lit.[32] $[\alpha]_D^{28}$ =– 78.4 (*c*=0.1 in $CHCl_3$) 94% *ee* (*S*)); ^{1}H NMR (500 MHz, $CDCl_3$) δ = 0.96 – 0.99 (m, 3H), 1.43 – 1.69 (m, 4H), 2.43 (dd, *J* = 16.8, 3.8, 1H), 2.52 (dd, *J* = 16.7, 13.5, 1H), 4.37 – 4.44 (m, 1H), 5.38 – 5.42 (m, 1H), 7.36 (d, *J* = 5.8, 1H). These spectral data match those previously reported for this compound.[32]

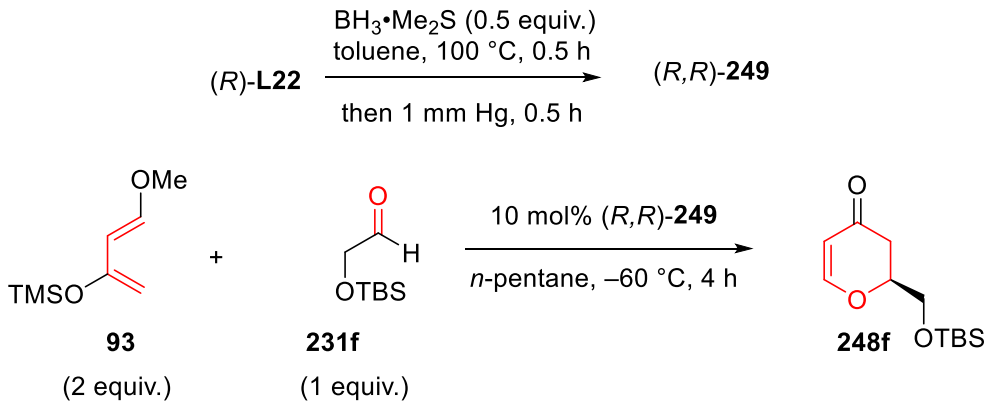

2-(tert-butyldimethylsiloxymethyl)-2,3-dihydro-4H-pyran-4-one ***248f***: The catalyst *(R,R)*-**249** was prepared from (*R*)-**L22** according to procedure F and adduct **248f** was obtained according to procedure H with the use of aldehyde **231f** (48.0 µL, 0.250 mmol) and diene **93** (0.50 mmol, 97 µL). Catalyst loading was 10 mol%. Purification of the crude product by silica gel chromatography (15 mm × 200 mm column, 5:1 hexanes/ EtOAc as eluent) afforded pure adduct **248f** as a colorless oil in 81% isolated yield (49.3 mg, 0.203 mmol); The optical purity of **248f** was determined to be 87% *ee* by HPLC (CHIRALCEL® OD column, 99.5:0.5

hexanes/2-propanol at 254 nm, flow-rate: 1 mL/min); retention times: R_t = 14.8 min (major enantiomer) and R_t = 17.3 min (minor enantiomer). The absolute configuration of **248f** was assumed to be S, homochiral with other products from same procedure, which configurations have been confirmed.

Spectral data for **248f**: R_f = 0.20 (4:1 hexane/ EtOAc); $[\alpha]_D^{20}$ = +26 (*c*=1.0 in $CHCl_3$) 87% *ee*); ^{1}H NMR (500 MHz, $CDCl_3$) δ = 0.09 (s, 6H), 0.90 (s, 9H), 2.41 (dd, *J* = 16.9, 3.7, 1H), 2.73 (dd, *J* = 16.9, 14.0, 1H), 3.81 (dd, *J* = 11.4, 4.6, 1H), 3.90 (dd, *J* = 11.4, 3.9, 1H), 4.46 (ddt, *J* = 14.1, 4.6, 3.8, 1H), 5.40 (d, *J* = 6.1, 1H), 7.36 (d, *J* = 6.0, 1H); ^{13}C NMR (126 MHz, $CDCl_3$) δ –5.4, 18.8, 25.8, 38.1, 64.2, 80.9, 106.9, 163.0, 191.8; HRMS (ESI-TOF) *m/z* 243.1422 [(M-H$^+$); calcd. for $C_{12}H_{23}O_3Si$: 243.1416].

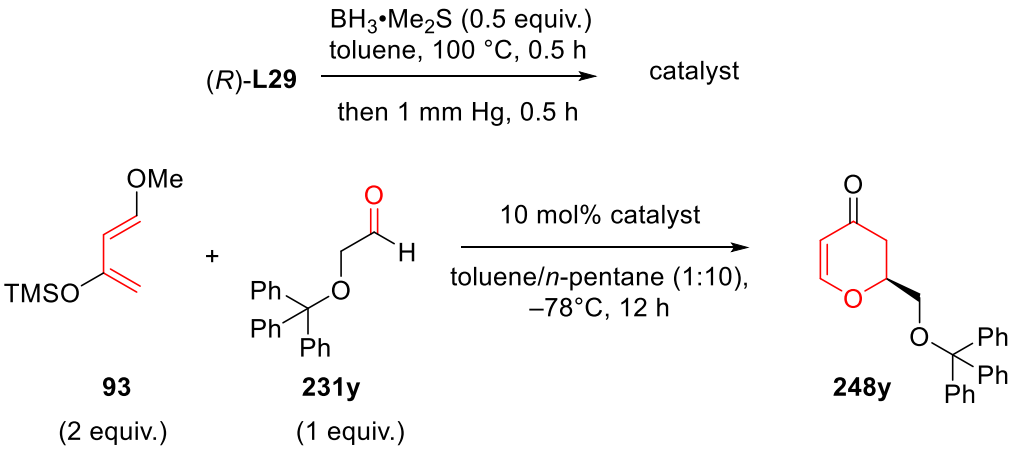

2-(triphenylmethoxymethyl)-2,3-dihydro-4H-pyran-4-one ***248y***: The catalyst was prepared from (*R*)-**L29** according to procedure F and adduct **248y** was obtained according to procedure H with the use of aldehyde **231y** (75.6 mg, 0.250 mmol) and diene **93** (0.50 mmol, 97 µL). Catalyst loading was 10 mol% and solvent was toluene/*n*-pentane (1:10). Purification of the crude product by silica gel

chromatography (15 mm × 200 mm column, 5:1 hexanes/ EtOAc as eluent) afforded pure adduct **248y** as a colorless oil in 92% isolated yield (85.0 mg, 0.229 mmol); The optical purity of **248y** was determined to be 93% *ee* by HPLC (CHIRALCEL® OD-H column, 95:5 hexanes/2-propanol at 254 nm, flow-rate: 1 mL/min); retention times: R_t = 8.6 min (major enantiomer) and R_t = 13.2 min (minor enantiomer). The absolute configuration of **248y** was assumed to be S, homochiral with other products from same procedure, which configurations have been confirmed.

Spectral data for **248y**: R_f = 0.18 (4:1 hexane/ EtOAc); $[\alpha]_D^{20}$ = +57 (*c*=1.0 in $CHCl_3$) 93% *ee*); ^{1}H NMR (500 MHz, $CDCl_3$) δ = 2.41 (dd, *J* = 16.9, 3.6, 1H), 2.79 (dd, *J* = 16.9, 14.1, 1H), 3.30 – 3.46 (m, 2H), 4.56 (ddt, *J* = 13.9, 5.0, 3.8, 1H), 5.44 (d, *J* = 6.0, 1H), 7.24 – 7.29 (m, 3H), 7.30 – 7.36 (m, 6H), 7.42 (d, *J* = 6.0, 1H), 7.44 – 7.49 (m, 6H); ^{13}C NMR (126 MHz, $CDCl_3$) δ 37.0, 64.0, 77.8, 88.3, 107.7, 127.3, 127.9, 128.6, 143.5, 162.0, 193.0; HRMS (ESI-TOF) *m/z* 371.1645 [(M-H^+); calcd. for $C_{25}H_{23}O_3$: 371.1647].

4.3.6 Computational study

Computations have been achieved with density functional theory in Gaussian 16[20]. Geometry optimizations of boron catalyst **222** and aluminum catalyst **253** were carried out at B3LYP/6-31G(d) level of theory in vacuum.

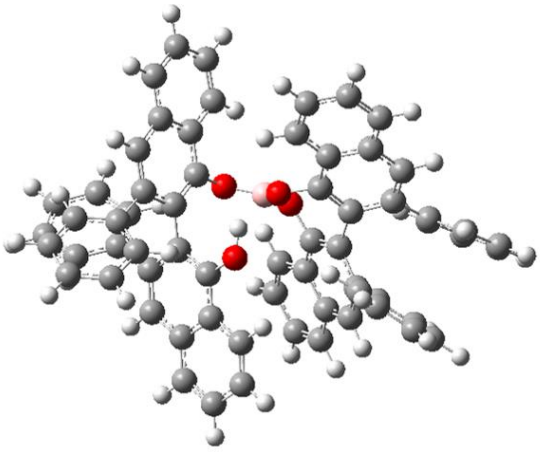

VANOL$_2$-Boron
222

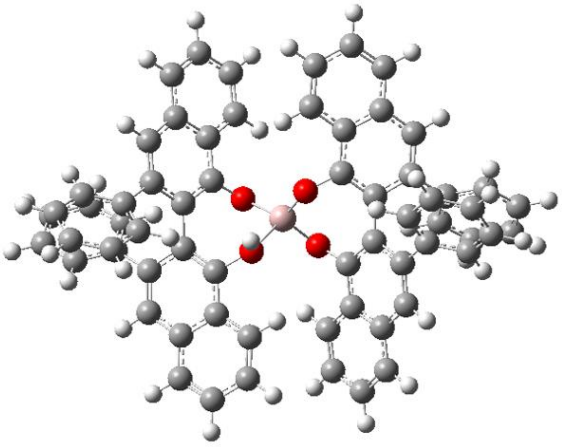

VANOL$_2$-Aluminum
253

222 Coordinate:

1	C	2.140	5.770	1.606	15	C	2.654	-0.361	-0.654
2	C	3.257	5.026	1.296	16	C	1.819	-0.678	-1.713
3	C	3.131	3.716	0.761	17	C	3.358	-1.438	-0.002
4	C	1.825	3.183	0.546	18	C	1.768	-1.971	-2.305
5	C	0.689	3.974	0.862	19	C	3.324	-2.701	-0.559
6	C	0.847	5.239	1.385	20	C	0.963	-2.267	-3.435
7	H	5.240	3.394	0.455	21	C	2.581	-2.995	-1.730
8	H	2.249	6.770	2.017	22	H	3.836	-3.515	-0.053
9	H	4.253	5.431	1.454	23	C	0.978	-3.531	-3.984
10	C	4.255	2.940	0.386	24	H	0.346	-1.483	-3.858
11	C	1.731	1.862	0.024	25	C	2.564	-4.288	-2.317
12	H	-0.303	3.574	0.685	26	C	1.785	-4.549	-3.422
13	C	2.830	1.065	-0.246	27	H	3.177	-5.070	-1.875
14	C	4.140	1.662	-0.125	28	H	1.782	-5.542	-3.863

29	O	0.963	0.276	-2.256
30	O	0.436	1.397	-0.178
31	C	4.020	-1.266	1.321
32	C	5.286	-1.821	1.572
33	C	3.348	-0.631	2.380
34	C	5.864	-1.740	2.838
35	H	5.827	-2.295	0.758
36	C	3.927	-0.550	3.645
37	H	2.354	-0.225	2.215
38	C	5.188	-1.102	3.880
39	H	6.848	-2.170	3.008
40	H	3.387	-0.061	4.452
41	H	5.639	-1.039	4.867
42	C	5.382	1.001	-0.620
43	C	6.557	1.029	0.150
44	C	5.439	0.424	-1.900
45	C	7.749	0.500	-0.342
46	H	6.524	1.448	1.151
47	C	6.631	-0.107	-2.391
48	H	4.549	0.408	-2.520
49	C	7.791	-0.072	-1.615
50	H	8.644	0.527	0.275
51	H	6.654	-0.542	-3.387
52	H	8.720	-0.486	-1.999
53	O	-1.261	0.794	-1.706
54	O	-0.763	-0.210	1.842
55	C	-2.242	1.390	-0.923
56	C	-1.515	-1.143	1.176
57	C	-2.874	0.649	0.062
58	C	-2.613	2.724	-1.256
59	C	-1.240	-2.502	1.517
60	C	-2.527	-0.795	0.290
61	C	-3.936	1.275	0.808
62	C	-1.988	3.465	-2.294
63	C	-3.673	3.325	-0.509
64	C	-2.043	-3.523	0.924
65	C	-0.208	-2.863	2.421
66	C	-3.308	-1.837	-0.318
67	C	-4.305	2.572	0.511
68	C	-4.671	0.562	1.895
69	C	-2.387	4.755	-2.568
70	H	-1.203	3.000	-2.881
71	C	-4.054	4.658	-0.816
72	C	-1.783	-4.877	1.264
73	C	-3.064	-3.156	0.012
74	C	0.017	-4.187	2.730
75	H	0.404	-2.082	2.858
76	C	-4.404	-1.540	-1.287
77	H	-5.100	3.041	1.086
78	C	-6.068	0.445	1.827
79	C	-4.007	0.056	3.024
80	C	-3.426	5.359	-1.820
81	H	-4.858	5.114	-0.242
82	C	-0.779	-5.203	2.149
83	H	-2.394	-5.654	0.811
84	H	-3.655	-3.939	-0.455
85	C	-5.709	-1.985	-1.023
86	C	-4.157	-0.870	-2.497
87	C	-6.784	-0.168	2.856
88	H	-6.589	0.820	0.951
89	C	-4.725	-0.553	4.053
90	H	-2.929	0.153	3.103

91	H	-3.729	6.378	-2.046
92	H	-0.592	-6.243	2.400
93	C	-6.740	-1.762	-1.937
94	H	-5.914	-2.494	-0.085
95	C	-5.188	-0.650	-3.410
96	H	-3.149	-0.541	-2.729
97	C	-6.114	-0.669	3.973
98	H	-7.865	-0.255	2.782
99	H	-4.195	-0.936	4.921
100	C	-6.483	-1.093	-3.134
101	H	-7.745	-2.111	-1.711
102	H	-4.976	-0.136	-4.344
103	H	-6.670	-1.147	4.776
104	H	-7.284	-0.919	-3.847
105	B	0.060	0.822	-1.373
106	H	-0.758	0.624	1.340
107	H	-0.028	5.836	1.626
108	H	0.363	-3.750	-4.852
109	H	-1.904	5.312	-3.366
110	H	0.812	-4.454	3.421

END

253 Coordinate:

1	C	2.538	5.817	0.669
2	C	3.575	5.062	0.167
3	C	3.453	3.652	0.037
4	C	2.230	3.029	0.429
5	C	1.175	3.831	0.936
6	C	1.328	5.195	1.057
7	H	5.380	3.338	-0.885
8	H	2.646	6.894	0.765
9	H	4.506	5.534	-0.137
10	C	4.487	2.850	-0.503
11	C	2.116	1.608	0.307
12	H	0.249	3.350	1.230
13	C	3.179	0.820	-0.131
14	C	4.371	1.477	-0.608
15	C	3.131	-0.680	-0.055
16	C	2.223	-1.422	-0.810
17	C	4.086	-1.390	0.761
18	C	2.327	-2.846	-0.925
19	C	4.173	-2.767	0.682
20	C	1.472	-3.595	-1.774
21	C	3.336	-3.523	-0.175
22	H	4.878	-3.293	1.319
23	C	1.611	-4.963	-1.877
24	H	0.720	-3.068	-2.349
25	C	3.440	-4.935	-0.290
26	C	2.600	-5.640	-1.124
27	H	4.205	-5.450	0.287
28	H	2.699	-6.719	-1.210
29	O	1.212	-0.821	-1.509
30	O	0.922	1.042	0.673
31	C	4.949	-0.698	1.763
32	C	6.317	-1.004	1.858
33	C	4.405	0.204	2.693
34	C	7.115	-0.427	2.845

35	H	6.757	-1.683	1.133
36	C	5.202	0.781	3.680
37	H	3.347	0.442	2.649
38	C	6.561	0.469	3.761
39	H	8.172	-0.674	2.894
40	H	4.759	1.474	4.391
41	H	7.182	0.922	4.529
42	C	5.470	0.737	-1.293
43	C	6.811	0.969	-0.944
44	C	5.203	-0.139	-2.358
45	C	7.850	0.345	-1.634
46	H	7.034	1.629	-0.110
47	C	6.241	-0.763	-3.048
48	H	4.175	-0.315	-2.659
49	C	7.570	-0.526	-2.688
50	H	8.880	0.535	-1.342
51	H	6.011	-1.433	-3.872
52	H	8.378	-1.014	-3.226
53	O	-1.241	0.765	-1.480
54	O	-0.899	-0.906	0.716
55	C	-2.237	1.405	-0.815
56	C	-2.122	-1.563	0.362
57	C	-3.161	0.698	-0.043
58	C	-2.338	2.826	-0.974
59	C	-2.111	-2.975	0.478
60	C	-3.183	-0.799	-0.080
61	C	-4.149	1.425	0.715
62	C	-1.455	3.549	-1.816
63	C	-3.364	3.525	-0.270
64	C	-3.309	-3.653	0.094
65	C	-1.006	-3.726	0.958
66	C	-4.344	-1.517	-0.553
67	C	-4.230	2.797	0.585
68	C	-5.051	0.765	1.703
69	C	-1.584	4.914	-1.955
70	H	-0.686	3.007	-2.354
71	C	-3.463	4.933	-0.427
72	C	-3.364	-5.067	0.216
73	C	-4.381	-2.894	-0.435
74	C	-1.097	-5.096	1.065
75	H	-0.085	-3.219	1.223
76	C	-5.481	-0.840	-1.239
77	H	-4.953	3.346	1.182
78	C	-6.421	1.078	1.732
79	C	-4.556	-0.116	2.678
80	C	-2.594	5.612	-1.253
81	H	-4.241	5.465	0.115
82	C	-2.284	-5.773	0.696
83	H	-4.275	-5.580	-0.081
84	H	-5.252	-3.427	-0.805
85	C	-6.806	-1.147	-0.888
86	C	-5.259	0.045	-2.307
87	C	-7.263	0.529	2.699
88	H	-6.827	1.739	0.973
89	C	-5.396	-0.667	3.645
90	H	-3.497	-0.356	2.694
91	H	-2.683	6.689	-1.368
92	H	-2.337	-6.854	0.786
93	C	-7.877	-0.584	-1.582
94	H	-6.993	-1.812	-0.051
95	C	-6.330	0.607	-2.999
96	H	-4.242	0.276	-2.609

97	C	-6.755	-0.347	3.659
98	H	-8.320	0.783	2.697
99	H	-4.986	-1.341	4.393
100	C	-7.643	0.296	-2.639
101	H	-8.895	-0.830	-1.290
102	H	-6.137	1.284	-3.827
103	H	-7.410	-0.776	4.413
104	H	-8.477	0.735	-3.180
105	Al	0.102	0.127	-0.569
106	H	-0.874	-0.557	1.626
107	H	0.512	5.799	1.447
108	H	0.956	-5.526	-2.536
109	H	-0.903	5.458	-2.603
110	H	-0.242	-5.663	1.423

END

REFERENCES

REFERENCES

1. Ding, Z.; Osminski, W. E. G.; Ren, H.; Wulff, W. D. Scalable Syntheses of the Vaulted Biaryl Ligands VAPOL and VANOL via the Cycloaddition/Electrocyclization Cascade. *Org. Proc. Res. & Dev.* **2011**, *15*, 1089-1107.

2. Guan, Y.; Ding, Z.; Wulff, W. D. Vaulted Biaryls in Catalysis: A Structure–Activity Relationship Guided Tour of the Immanent Domain of the VANOL Ligand. *Chem. Eur. J.* **2013**, *19*, 15565-15571.

3. Guan, Y.; Wulff, W. D. Construction of a vaulted biaryl ligand library for the aziridination reaction. Ph.D thesis. Michigan State University, **2012**.

4. Yin, X.; Wulff, W. D. Application of Chiral Borates in Asymmetric Catalysis and Chiral Resolution. Ph.D thesis. Michigan State University, **2018**.

5. Cheung, F. K.; Lin, C.; Minissi, F.; Crivillé, A. L.; Graham, M. A.; Fox, D. J.; Wills, M. An Investigation into the Tether Length and Substitution Pattern of Arene-Substituted Complexes for Asymmetric Transfer Hydrogenation of Ketones. *Org. Lett.* **2007,** *9*, 4659-4662.

6. Wang, F.; Liu, H.; Cun, L.; Zhu, J.; Deng, J.; Jiang, Y. Asymmetric Transfer Hydrogenation of Ketones Catalyzed by Hydrophobic Metal−Amido Complexes in Aqueous Micelles and Vesicles. *J. Org. Chem.* **2005**, *70*, 9424-9429.

7. Inagaki, T.; Phong, L. T.; Furuta, A.; Ito, J.; Nishiyama, H. Iron- and Cobalt-Catalyzed Asymmetric Hydrosilylation of Ketones and Enones with Bis(oxazolinylphenyl)amine Ligands. *Chem. Eur. J.* **2010,** *16*, 3090-3096.

8. Du, D.-M.; Fang, T.; Xu, J.; Zhang, S.-W. Structurally Well-Defined, Recoverable C_3-Symmetric Tris(β-hydroxy phosphoramide)-Catalyzed Enantioselective Borane Reduction of Ketones. *Org. Lett.* **2006**, *8*, 1327-1330.

9. Touge, T.; Hakamata, T.; Nara, H.; Kobayashi, T.; Sayo, N.; Saito, T.; Kayaki, Y.; Ikariya, T. Oxo-Tethered Ruthenium(II) Complex as a Bifunctional Catalyst for Asymmetric Transfer Hydrogenation and H2 Hydrogenation. *J. Am. Chem. Soc.* **2011**, *133*, 14960-14963.

10. Kędziora, K.; Bisogno, F.; Lavandera, I.; Gotor-Fernández, V.; Montejo-Bernardo, J.; García-Granda, S.; Kroutil, W.; Gotor, V. Expanding the Scope of Alcohol Dehydrogenases towards Bulkier Substrates: Stereo- and Enantiopreference for α,α-Dihalogenated Ketones. *ChemCatChem* **2014**, *6*, 1066-1072.

11. Singh, R. P.; TwamLey, B.; Fabry-Asztalos, L.; Matteson, D. S.; Shreeve, J. M. Efficient Syntheses of Fluorinated Aryl Alcohols of High Enantiomeric Purity via Boronic Esters. *J. Org. Chem.* **2000**, *65*, 8123-8125.

12. Xu, Y.; Clarkson, G. C.; Docherty, G.; North, C. L.; Woodward, G.; Wills, M. Ruthenium(II) Complexes of Monodonor Ligands: Efficient Reagents for Asymmetric Ketone Hydrogenation. *J. Org. Chem.* **2005**, *70*, 8079-8087.

13. Darwish, M. O.; Wallace, A.; Clarkson, G. J.; Wills, M. Use of tridentate TsDPEN/pyridine ligands in ruthenium-catalysed asymmetric reduction of ketones. *Tetrahedron Lett.* **2013**, *54*, 4250-4253.

14. Cozzi, P. G.; Kotrusz, P. Highly Enantioselective Addition of Me2Zn to Aldehydes Catalyzed by ClCr(Salen). *J. Am. Chem. Soc.* **2006**, *128*, 4940-4941.

15. Kantam, M. L.; Yadav, J.; Laha, S.; Srinivas, P.; Sreedhar, B.; Figueras, F. Asymmetric Hydrosilylation of Ketones Catalyzed by Magnetically Recoverable and Reusable Copper Ferrite Nanoparticles. *J. Org. Chem.* **2009**, *74*, 4608-4611.

16. Szőllősi, G.; Kolcsár, V. Highly Enantioselective Transfer Hydrogenation of Prochiral Ketones Using Ru(II)-Chitosan Catalyst in Aqueous Media. *ChemCatChem* **2019**, *11*, 820-830.

17. Lu, C.; Luo, Z.; Huang, L.; Li, X. The Ru-catalyzed enantioselective preparation of chiral halohydrins and their application in the synthesis of (*R*)-clorprenaline and (*S*)-sotalol. *Tetrahedron: Asymmetry* **2011**, *22*, 722-727.

18. Inagaki, T.; Ito, A.; Ito, J.; Nishiyama, H. Asymmetric Iron-Catalyzed Hydrosilane Reduction of Ketones: Effect of Zinc Metal upon the Absolute Configuration. *Angew. Chem. Int. Ed.* **2010**, *49*, 9384-9387.

19. Forbes, D. C.; Bettigeri, S. V.; Patrawala, S. A.; Pischek, S. C.; Standen, M. C. S-Methylidene agents: preparation of chiral non-racemic heterocycles. *Tetrahedron* **2009**, *65*, 70-76.

20. Gaussian 16, Revision A.03, Frisch, M. J.; Trucks, G. W.; Schlegel, H. B.; Scuseria, G. E.; Robb, M. A.; Cheeseman, J. R.; Scalmani, G.; Barone, V.; Petersson, G. A.; Nakatsuji, H.; Li, X.; Caricato, M.; Marenich, A. V.; Bloino, J.; Janesko, B. G.; Gomperts, R.; Mennucci, B.; Hratchian, H. P.; Ortiz, J. V.; Izmaylov, A. F.; Sonnenberg, J. L.; Williams-Young, D.; Ding, F.; Lipparini, F.; Egidi, F.; Goings, J.; Peng, B.; Petrone, A.; Henderson, T.; Ranasinghe, D.; Zakrzewski, V. G.; Gao, J.; Rega, N.; Zheng, G.; Liang, W.; Hada, M.; Ehara, M.; Toyota, K.; Fukuda, R.; Hasegawa, J.; Ishida, M.; Nakajima, T.; Honda, Y.; Kitao, O.; Nakai, H.; Vreven, T.; Throssell, K.; Montgomery, J. A., Jr.; Peralta, J. E.; Ogliaro, F.; Bearpark, M. J.; Heyd, J. J.; Brothers, E. N.; Kudin, K. N.; Staroverov, V. N.; Keith, T. A.; Kobayashi, R.; Normand, J.; Raghavachari, K.; Rendell, A. P.; Burant, J. C.; Iyengar, S. S.; Tomasi, J.; Cossi, M.; Millam, J. M.; Klene, M.; Adamo,

C.; Cammi, R.; Ochterski, J. W.; Martin, R. L.; Morokuma, K.; Farkas, O.; Foresman, J. B.; Fox, D. J. Gaussian, Inc., Wallingford CT, 2016.

21. Cui, Y.; Jiang, H.; Li, Z.; Wu, N.; Yang, Z.; Quan, J. Unexpected Regioselectivity in the Synthesis of Pyranonaphthoquinone via the Diels−Alder Reaction. *Org. Lett.* **2009**, *11*, 4628-4631.

22. Krompiec, S.; Kuźnik, N.; Urbala, M.; Rzepa, J. Isomerization of alkyl allyl and allyl silyl ethers catalyzed by ruthenium complexes. *J. Mol. Catal. A: Chem.* **2006**, *248*, 198-209.

23. Kleinbeck, F.; Fettes, G. J.; Fader, L. D.; Carreira, E. M. Total Synthesis of Bafilomycin A_1. *Chem. Eur. J.* **2012**, *18*, 3598-3610.

24. White, J. D.; Shaw, S. *cis*-2,5-Diaminobicyclo[2.2.2]octane, a New Scaffold for Asymmetric Catalysis via Salen−Metal Complexes. *Org. Lett.* **2011**, *13*, 2488-2491.

25. Long, J.; Hu, J.; Shen, X.; Ji, B.; Ding, K. Discovery of Exceptionally Efficient Catalysts for Solvent-Free Enantioselective Hetero-Diels−Alder Reaction. *J. Am. Chem. Soc.* **2002,** *124,* 10-11.

26. Watanabe, Y.; Washio, T.; Shimada, N.; Anada, M.; Hashimoto, S. Highly enantioselective hetero-Diels–Alder reactions between Rawal's diene and aldehydes catalyzed by chiral dirhodium(ii) carboxamidates. *Chem. Commun.* **2009**, 7294-7296.

27. Kitazawa, T.; Mukaiyama, T. Hetero Diels-Alder Type Reactions Between Danishefsky's Dienes in the Presence of Lewis Base Catalysts. An Efficient Method for the Synthesis of Substituted 2,3-Dihydropyran-4-ones. *Heterocycles* **2006**, *69*, 417-427.

28. Baldoli, C.; Maiorana, S.; Licandro, E.; Zinzalla, G.; Lanfranchi, M.; Tiripicchio, A. Stereoselective hetero Diels–Alder reactions of chiral tricarbonyl (η^6-benzaldehyde) chromium complexes. *Tetrahedron: Asymmetry*, **2001**, *12*, 2159-2167.

29. Du, H.; Zhang, X.; Wang, Z.; Bao, H.; You, T.; Ding, K. BINOLate–Magnesium Catalysts for Enantioselective Hetero-Diels–Alder Reaction of Danishefsky's Diene with Aldehydes. *Eur. J. Org. Chem.* **2008**, 2248-2254.

30. Beemelmanns, C.; Husmann, R.; Whelligan, D. K.; Özçubukçu, S.; Bolm, C. Planar-Chiral Bis-silanols and Diols as H-Bonding Asymmetric Organocatalysts. *Eur. J. Org. Chem.* **2012**, 3373-3376.

31. Unni, A. K.; Takenaka, N.; Yamamoto, H.; Rawal, V. H. Axially Chiral Biaryl Diols Catalyze Highly Enantioselective Hetero-Diels−Alder Reactions through Hydrogen Bonding. *J. Am. Chem. Soc.* **2005**, 127, 1336-1337.

32. Zhuang, W., Poulsen, T. B., and Jørgensen, A. K. A versatile catalyst for asymmetric reactions of carbonyl groups working purely by activation through hydrogen bonding: Mukaiyama-aldol, hetero Diels–Alder and Friedel–Crafts reactions. *Org. Biomol. Chem.* **2005**, 3, 3284-3289.

33. Hu, G.; Gupta, A. K.; Huang, L.; Zhao, W.; Yin, X.; Osminski, W. E. G.; Huang, R. H.; Wulff, W. D.; Izzo, J. A.; Vetticatt, M. J. *Pyro*-Borates, *Spiro*-Borates, and Boroxinates of BINOL—Assembly, Structures, and Reactivity. *J. Am. Chem. Soc.* **2017**, *139*, 10267-10285.

34. Zulauf, A.; Mellah, M.; Guillot, R.; Schulz, E. Chromium‐Thiophene‐salen‐Based Polymers for Heterogeneous Asymmetric Hetero‐Diels–Alder Reactions. *Eur. J. Org. Chem.* **2008**, 2118-2129.

35. Danishefsky, S.; Kerwin, J. F.; Kobayashi, S. Lewis acid catalyzed cyclocondensations of functionalized dienes with aldehydes. *J. Am. Chem. Soc.* **1982**, *104*, 358-360.